

Functional Polyolefins Prepared by Group 4 Diamide Complexes Through Tandem Ring-Opening Metathesis/Vinyl Insertion Polymerization

Von der Fakultät Chemie der Universität Stuttgart
zur Erlangung der Würde eines
Doktors der Naturwissenschaften (Dr. rer. nat.) genehmigte Abhandlung

Vorgelegt von
Guangjuan Xu, MSc
aus Jilin/China

Hauptberichter:	Prof. Dr. Michael R. Buchmeiser
1. Mitberichter:	Prof. Dr. Bernd Plietker
2. Mitberichter:	Prof. Dr.-Ing. Elias Klemm
Tag der mündlichen Prüfung:	19. Mai 2014

Institut für Polymerchemie
der Universität Stuttgart

2014

Victory belongs to the most persevering.

Napoleon Bonaparte (1769-1852)

This PhD work was carried out from August 2010 to March 2014 under the supervision of Prof. Dr. Michael R. Buchmeiser, at the Institute of Polymer Chemistry, University of Stuttgart.

Acknowledgements

First and foremost, I'd like to express my thanks to Prof. Dr. Michael R. Buchmeiser for offering me a doctoral position in his well-established group and his motivation, encouragement and generous support during my PhD program. Many thanks to the China Scholarship Counsel (CSC) for financial support during my education.

It is an honor to me to have Prof. Dr. Bernd Plietker and Prof. Dr.-Ing. Elias Klemm as my examiners in the examination board.

My sincere thanks to Dr. Dongren Wang for his advises and generous help on the development of my experiments. Thanks to Herrn Jan Pigorsch for assisting me in ordering chemicals and building the equipment. Frau Dagmar Schuhmacher and Frau Rita Stiehle also help to make my life easier in the university.

Many thanks to Dr. Wolfgang Frey for single crystal X-ray measurement, Frau Barbara Förtsch for elemental analysis, and my colleague Maria Speiser for TGA and DSC measurements.

I would like to thank all my colleagues at the Institute of Polymer Chemistry, University of Stuttgart. Hannah Winter, Guram Venkata Narayana, Benjamin Autenrieth, Stefan Nauman, Jörg Unold, Katharina Herz, Roman Schowner, Laura Widmann, Christina Lienert, Sarah Deh, Iris Elser, Johanna Spörl, Vijay Taori, Melita van der Ende, Min Wang, Jing Zhao, Suman Sen, Bernhard Sandig, Abhishek Narayan Mondal, Rebekka Klaas, Dominik Imbrich please accept my cordial thanks for the harmony atmosphere and entertainment in the group.

My special thanks to my dear friends here in Stuttgart, Yingchun Huang, Chengxiang Zhu, Yaohua Xiong, Lingling Chen, Shenghua Chen, Meng Wu, Qiang Chen, Chenyu Zhou. Thanks for your support and help during the time I spent in Germany. I also

convey my thanks to my close friends Haibin Li, Lei Chen, Linlin Yu, Lina Wang, thanks for their trust and support.

My deepest gratitude goes to my father, my mother, my younger sister, younger brother for their love and support in my life. Without all of these, this dissertation would not have been finished.

Thanks to all of you.

Table of Contents

Table of Contents	I
List of Abbreviations and Symbols	III
Zusammenfassung	VI
Abstract	X
Goal/Aim	XIV
1. General Introduction	1
1.1 History of Polyethylene	3
1.2 Heterogeneous Ziegler-Natta Catalysis	5
1.3 Homogeneous Ziegler-Natta Catalysis.....	6
1.3.1 Metallocene catalysts	6
1.3.2 Post-metallocene catalysts	7
1.4 Coordination Addition Polymerization	7
1.5 Ring-opening Metathesis Polymerization	9
1.6 Functional Polyolefins	14
1.6.1 Direct copolymerization	15
1.6.2 Post-polymerization modification	16
1.7 References.....	17
2. Functional Polyolefins by Post-polymerization Modification	25
2.1 Introduction	27
2.2 Results and Discussion.....	28
2.2.1 Synthesis of poly(COE)	28
2.2.2 Epoxidation of poly(COE)	29
2.2.3 Hydroxylation of poly(COE)	30
2.2.4 Hydrobromination of poly(COE).....	31
2.2.5 Poly(ethylene)- <i>graft</i> -poly(tert-butyl acrylate) via ATRP.....	33
2.3 Conclusions	41
2.4 References.....	41
3. Bis(diamido)silylene Zirconium^{IV} Complexes Containing the Bromoborane Motifs in Vinyl Insertion Polymerization: On the Role of Cyclopentene	45
3.1 Introduction	47
3.2 Results and Discussion.....	48
3.2.1 Syntheses of ligands and complexes.....	48

3.2.2 Homopolymerization of ethylene.....	51
3.2.3 Copolymerization of ethylene (E) with cyclopentene (CPE) (E-CPE)	53
3.2.4 Copolymerization of ethylene (E) with norborn-2-ene (NBE) (E-NBE)....	59
3.3 Conclusions	67
3.4 References.....	67
4. On the Mechanism of Tandem Ring-Opening Metathesis/Vinyl Insertion	
Copolymerization of Ethylene With Norborn-2-ene	71
4.1 Introduction	73
4.2 Results and Discussion.....	73
4.2.1 Homopolymerization of NBE and copolymerization of E with NBE	73
4.2.2 Activation process of MAO on 1	74
4.2.3 Reaction of 1 /MAO with NBE.....	78
4.3 Conclusions	82
4.4 References.....	82
5. Experimental and Spectroscopic Data	85
5.1 General Remarks	87
5.2 Functional Polyolefins by Post-polymerization Modification	88
5.3 Bis(diamido)silylene Zirconium ^{IV} Complexes Containing the Bromoborane Motifs in Vinyl Insertion Polymerization: On the Role of Cyclopentene.....	90
5.4 On the Mechanism of Tandem Ring-Opening Metathesis/Vinyl Insertion Copolymerization of Ethylene With Norborn-2-ene.....	96
5.5 References.....	98
6. Appendix	99
6.1 Functional Polyolefins by Post-polymerization Modification	101
6.2 Bis(diamido)silylene Zirconium ^{IV} Complexes Containing the Bromoborane Motifs in Vinyl Insertion Polymerization: On the Role of Cyclopentene.....	105
6.3 On the Mechanism of Tandem Ring-Opening Metathesis/Vinyl Insertion Copolymerization of Ethylene With Norborn-2-ene.....	125
7. Curriculum Vitae.....	131
Declaration of Authorship.....	133

List of Abbreviations and Symbols

Å	Angstrom
Ad	Adamantyl
ATR	Attenuated total reflection
Bu	Butyl
calcd.	Calculated
CGCs	Constrained geometry complexes
COE	<i>cis</i> -Cyclooctene
CPE	Cyclopentene
CTA	Chain transfer agent
DCM	Dichloromethane
°C	Degree Celcius
DSC	Differential scanning calorimetry
DME	1,2-Dimethoxyethane
δ	Chemical shift
E	Ethylene
equiv.	Equivalents
EPA	Environmental Protection Agency
ESI-MS	Electrospray ionisation mass spectrometry
Et	Ethyl
et al.	And others
Et ₂ O	Diethyl ether
EtOAc	Ethyl acetate
EVE	Ethyl vinyl ether
FT-IR	Fourier transform infrared
g	Gram
GC-MS	Gas chromatography mass spectrometry
GPC	Gel permeation chromatography
h	Hours
HDPE	High density polyethylene
HT-GPC	High temperature gel permeation chromatography
Hz	Hertz
ISEC	Inverse size exclusion chromatography

<i>J</i>	Coupling constants in Hertz
LDPE	Low density polyethylene
LLDPE	Linear low density polyethylene
M	Molar
m	Multiplet
MAO	Methylaluminoxane
m/z	mass/charge
MDPE	Medium density polyethylene
M ⁺	Molecular ion
MeOH	Methanol
mg	Milligram
MHz	Megahertz (10 ⁶ Hz)
min	Minute
mL	Milliliter
mmol	Millimol
mol-%	Molar percentage
<i>M_n</i>	Number-average molecular weight
<i>M_w</i>	Weight-average molecular weight
MS	Mass spectroscopy
MWD	Molecular weight distribution
NBE	Norborn-2-ene
NHC	N-Heterocyclic carbene
NMR	Nuclear magnetic resonance
<i>P</i>	Pressure
PB-1	Polybutene-1
PCy ₃	Tricyclohexylphosphine
PDI	Poly dispersity index
PE	Polyethylene
Ph	Phenyl
PMP	Polymethylpentene
ROMP	Ring-opening metathesis polymerization
PP	Polypropylene
ppm	Parts per million
PS	Polystyrene

R_t	Retention time
rt	Room temperature
S	Singlet
SEC	Size exclusion chromatography
SPI	The Society of the Plastics Industry
SPS	Solvent purification system
t	Time
T	Temperature
TEA	Triethylamine
T_g	Glass transition temperature
TGA	Thermal gravimetric analysis
THF	Tetrahydrofuran
T_m	Melting temperature
TMS	Tetramethylsilane
UV-Vis	Ultra violet-visible
VIP	Vinyl insertion polymerization
VLDPE	Very low density polyethylene
vol.-%	Volume percentage
wt.-%	Weight percentage
Z.-N.	Ziegler-Natta
μL	Microliter
μmol	Micromol

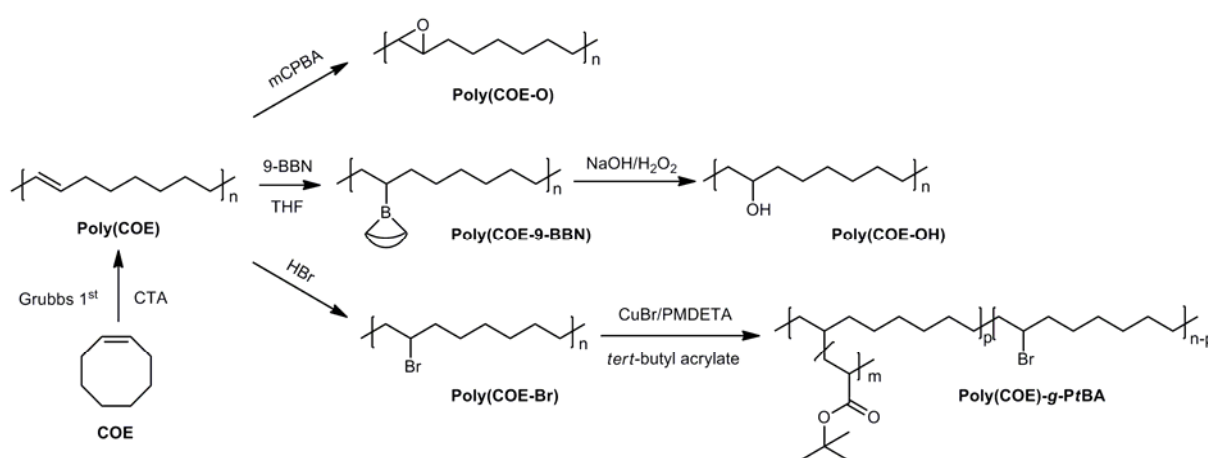
Zusammenfassung

Seit der intensiven Erforschung und Kommerzialisierung neuer, auf single-site und Metallocen-Katalysatoren basierenden Polymerisationstechnologien, werden Polyolefine mit neuen und innovativen Eigenschaften in einem Millionen Tonnen Maßstab pro Jahr hergestellt. Obwohl die gesättigte Struktur der Polyolefine viele Vorteile bietet schränkt ihre unpolare Natur ihre Anwendungsmöglichkeiten ein. Ungesättigte Copolymere besitzen großes Potenzial für die Materialwissenschaften, da sich aus ihnen funktionalisierte Polyolefine herstellen lassen, ohne das dafür polare Monomere copolymerisiert werden müssen. Die anschließende Einführung funktioneller polarer Gruppen in ungesättigte Polyolefine führt zu einer beachtlichen Veränderung der chemischen und physikalischen Eigenschaften der Polymere, wie der Permeabilität oder der Adhäsionsfähigkeit. Mithilfe von Tandem-Ringöffnungsmethatase-polymerisation/Vynylinsertionspolymerisation (ROMP/VIP) lassen sich Copolymere herstellen, die sowohl gesättigte und ungesättigte cyclische Olefin abgeleitete Einheiten in derselben Polymerkette enthalten. Falls sich die olefinischen Doppelbindungen durch chemische Modifikation funktionalisieren lassen, werden funktionale Polyolefine erhalten. Das Ziel dieser Arbeit war die Herstellung von ROMP/VIP-abgeleiteten Copolymeren und ihre anschließende Funktionalisierung.

Das erste Kapitel dieser Arbeit befasst sich mit dem historischen Hintergrund der Polyolefinsynthese.

Im zweiten Kapitel wird die Polymerisation von *cis*-Cycloocten (COE) durch Grubbs-Initiatoren der ersten Generation beschrieben. Poly(COE) dient als Modellverbindung für andere ungesättigte ROMP/VIP-abgeleitete Copolymere. Durch Verwendung eines Kettentransfer-Reagenzes (*cis*-4-Okten) wurde Poly(COE) mit einem durchschnittlichen Molekulargewicht von $41000 \text{ g}\cdot\text{mol}^{-1}$ (PDI 1,48) hergestellt, bei einem Verhältnis Katalysator zu Monomer von 1:800 (M_n theoretisch $88000 \text{ g}\cdot\text{mol}^{-1}$). Das bedeutet, dass im Vergleich zu einer Polymerisation ohne Kettentransfer-Reagenz mehr als 50 mol-% Initiator eingespart werden können um das gewünschte Molekulargewicht zu erreichen. Durch die nachfolgenden Epoxidierungen, Hydroxylierungen und Hydrobromierungen konnte das ungesättigte Polymer

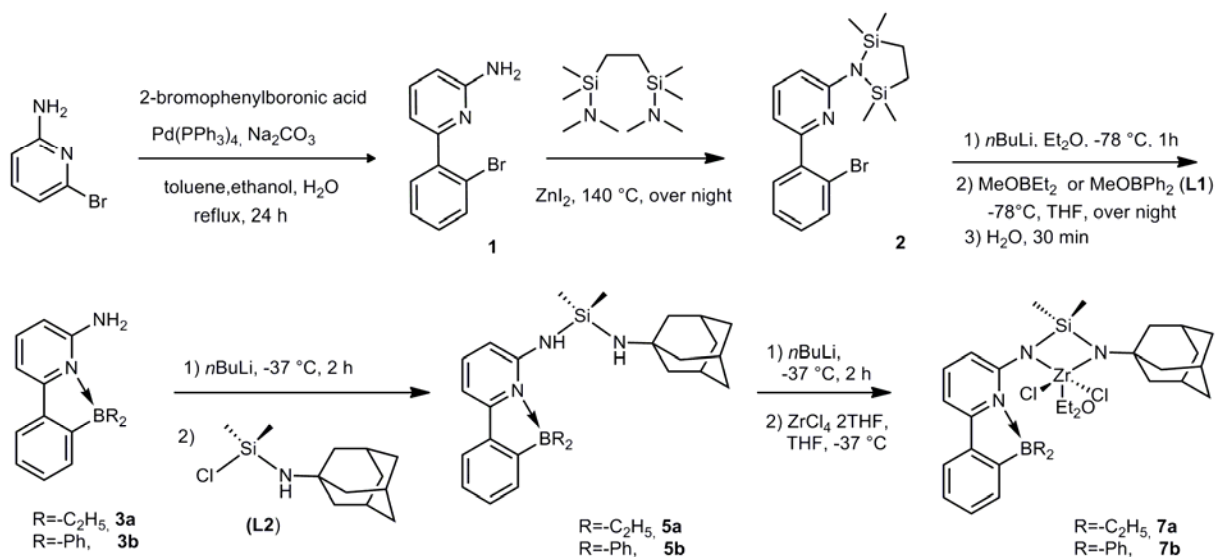
quantitativ in das korrespondierende funktionalisierte Polymer konvertiert werden. Interessanterweise kann das nicht-aktivierte hydrobromierte Poly(COE) als Makroinitiator für die Atom Transfer Radical Polymerization (ATRP) oder für die durch sichtbares Licht induzierte Pfropfpolymerisation von *tert*-Butylacrylat verwendet werden. Durch Variation der Reaktionsbedingungen konnte eine Serie von genau definierten Pfropfcopolymeren mit verschiedenen Pfropflängen und Pfropfdichten hergestellt werden. Der maximale Anteil an Verpfropfung betrug 80 mol-%. Alle Polymere wurden vollständig durch ^1H - und ^{13}C -NMR Spektroskopie sowie GPC, FT-IR und DSC charakterisiert (Schema 1).



Schema 1 Synthese von Poly(COE) und die korrespondierenden nachfolgenden Modifikationen.

Das dritte Kapitel dieser Arbeit befasst sich mit der Copolymerisation von Ethylen mit cyclischen Olefinen. Ein neuer Zirkoniumdiamid-Komplex (**7b**) wurde mit 6-[2-(Diphenylboryl)phenyl]pyridin-2-amin (**3b**) als Ligand hergestellt. Dieser Ligand wurde entwickelt und hergestellt da er ein Lewis-Säure-Base Paar (B-N) enthält und sterisch anspruchsvoller ist als 6[2-(Diethylboryl)phenyl]pyridin-2-amin (**3a**), welcher potenziell aktiv ist bezüglich der Tandem-Ringöffnungsmethatesepolymerisation/Vinylinserionspolymerisation. Sowohl der Ligand **3b** als auch der Komplex **7b** wurden durch ^1H -NMR-, ^{13}C -NMR-Spektroskopie, FT-IR und Elementaranalyse charakterisiert. Die Polymerisation von Katalysator **7b** wurde mit der des sterisch weniger anspruchsvollen Katalysators **7a** verglichen. Nach der Aktivierung mit MAO zeigte Komplex **7b** eine Produktivität von 90 kg/mol·h·bar in der Polymerisation von Ethylen, 1265 kg/mol·h·bar in der Copolymerisation von Ethylen/Cyclopenten (E-CPE) und 50 kg/mol·h·bar in der

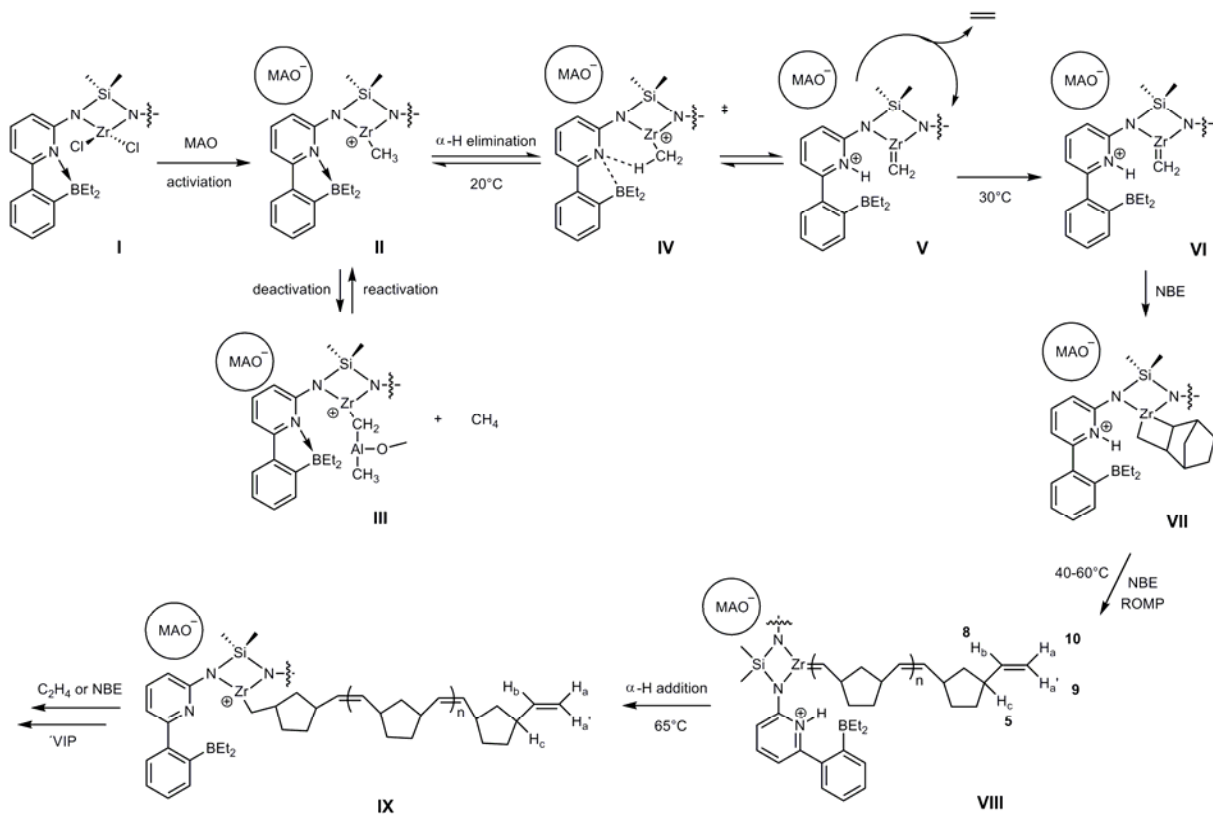
Copolymerisation von Ethylen/Bicyclo[2.2.1]hept-2-en (E-NBE). Der Einbau von 1 bis 18 mol-% CPE oder NBE konnte mittels ^{13}C -NMR-Spektroskopie nachgewiesen werden. Der Grund für den Anstieg der Produktivität an PE in Anwesenheit von CPE bei geringem Anteil (etwa 1 mol-%) von eingebautem CPE wurde mittels Copolymerisation von Ethylen und Cyclopenten-1- ^{13}C aufgeklärt. Unglücklicherweise waren sowohl Komplex **7a**/MAO als auch **7b**/MAO nicht aktiv in der reversiblen ROMP/VIP Copolymerisation. Durch ^{13}C -NMR-Spektroskopie konnte gezeigt werden, dass nur durch Vinylinsertionspolymerisation gebildetes Poly(E)-*co*-Poly(NBE)_{VIP} erhalten wurde. Die Taktizität des Poly(E)-*co*-Poly(NBE)_{VIP} wurde bestimmt (Schema 2).



Schema 2 Synthese der Komplexe **7a** und **7b**.

Im vierten Kapitel wurde eine Serie von NMR-Experimenten durchgeführt, mit denen der Mechanismus der Tandem-ROMP/VIP Copolymerisation untersucht wurde. Der Zirkonium-Komplex **1** wurde für diese klassische Reaktion ausgewählt. Das Reaktionssystem wurde mittels ^1H -NMR- und ^{11}B -NMR-Spektroskopie in einem Temperaturbereich von -60°C bis 70°C untersucht. Nach der Addition von MAO bei -60°C wurden beide Chloratome im Komplex **1** sofort durch Methylgruppen substituiert, bei -20°C fing das kationische Zentrum (**II**) an, eine schlafende Spezies (**III**) zu bilden, die nicht polymerisationsaktiv war und stattdessen Methan freisetzte. Eine Erhöhung der Temperatur auf 20°C resultierte in einer α -H-Eliminierung und es bildete sich ein ROMP-aktiver Zirkonium-Alkyliden-Komplex (**V**) der ein Signal bei $\delta = 8.6$ ppm im ^1H -NMR-Spektrum zeigte. Leider durchlief diese aktive Spezies eine

bimolekulare Zersetzung und setzte Ethylen frei. Das ^{11}B -NMR-Spektrum zeigte, dass das anfangs vierfach koordinierte Boratom bei 30 °C dreifach koordiniert ist (Bindungsspaltung der N-B-Bindung) und dadurch die ROMP startet. Die olefinischen Endgruppen (**VIII**) konnten im ^1H -NMR-Spektrum beobachtet werden und die entsprechenden Kopplungskonstanten wurden zugeordnet und waren konstant. Über 65 °C konnte eine α -H-Addition beobachtet werden, eine neue dreifach koordinierte Borspezies erschien im ^{11}B -NMR-Spektrum und die Vinylinsertionspolymerisation begann. Basierend auf diesen Studien konnten sowohl der Aktivierungsprozess als auch die aktive Spezies während der Homopolymerisation von Norborn-2-en und der Copolymerisation von Ethylen mit Norborn-2-en aufgeklärt werden. Die entscheidende Rolle des (N-(6-(2-(Diethylboryl)phenyl)pyrid-2-yl)-Liganden für den α -H-Abstraktionsprozess konnte nachgewiesen werden. Die Erkenntnisse die durch diese Studien gewonnen wurden, werden zusammen mit dem bereits basierenden Wissen hilfreich für das Design eines neuen, für die Tandem-ROMP/VIP Copolymerisation passenden, Katalysators sein (Schema 3).



Schema 3 Vorgeschlagener Mechanismus für die Polymerisation von NBE aktiviert durch 1/MAO.

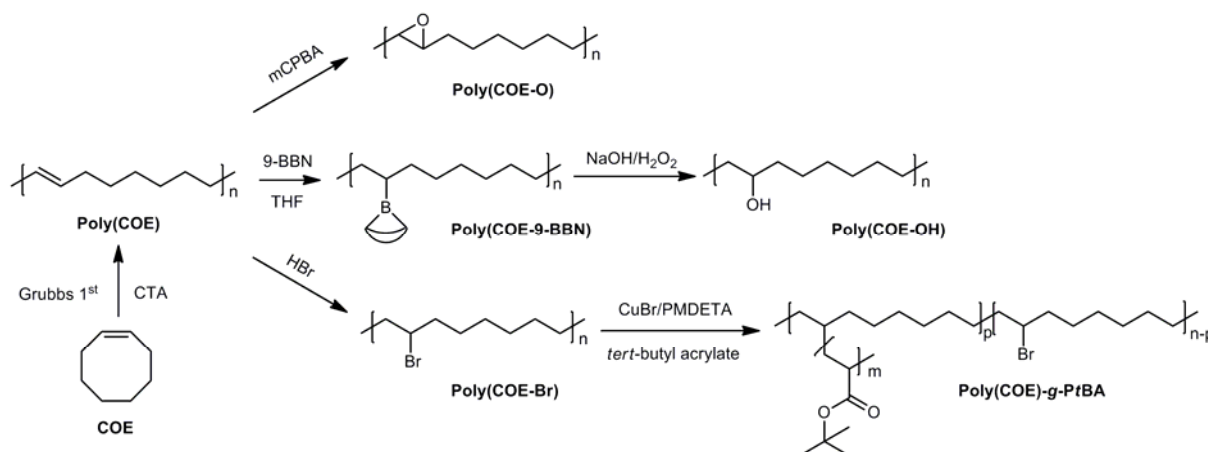
Abstract

Since the intense exploration and commercialization of new polymerization technologies based on single-site and metallocene catalysts, polyolefins with new and innovative properties are produced on a multibillion pound scale per year. Although the saturated structure of polyolefins offers many merits, the non-polar nature of polyolefins limits their applications. Unsaturated copolymers hold great potential in materials chemistry, as they allow for the synthesis of functional polyolefins without the need of copolymerizing polar monomers. Subsequent introduction of functional polar groups into unsaturated polyolefins will substantially alter the physical and chemical properties of the polymers such as permeability, dyeability and adhesion. Tandem ring-opening metathesis/vinyl insertion polymerization (ROMP/VIP) produces copolymers containing both cyclic olefin-derived saturated and unsaturated moieties within the same polymer chain. In case the olefinic double bonds can be functionalized by chemical modification, functional polyolefins would be obtained. The objective of this research was to prepare ROMP/VIP-derived copolymers and to functionalize the corresponding polyolefins by post-modification reactions.

The first chapter introduces the historical background in the field of polyolefin synthesis.

In the second chapter the polymerization of *cis*-cyclooctene (COE) by the 1st generation Grubbs initiator was described. Poly(COE) served as a model polymer for other unsaturated ROMP/VIP-derived copolymers. By employing a chain transfer agent (CTA) (*cis*-4-octene), poly(COE) with a number-average molecular weight of 41000 g·mol⁻¹ (PDI 1.48) was obtained using a catalyst to monomer ratio of 1:800 (M_n 88000 g·mol⁻¹ in theory for CTA-free reaction). This means to obtain the target molecular weight poly(COE), more than 50 mol-% of the initiator was saved compared to a CTA-free polymerization. The following epoxidation, hydroxylation and hydrobromination reactions quantitatively converted the unsaturated polymer to the corresponding functional polymers. Interestingly, the *non-activated* hydrobrominated poly(COE) can be used as a macroinitiator for atom transfer radical polymerization (ATRP) or visible light-induced graft polymerization of *tert*-butyl acrylate. By varying

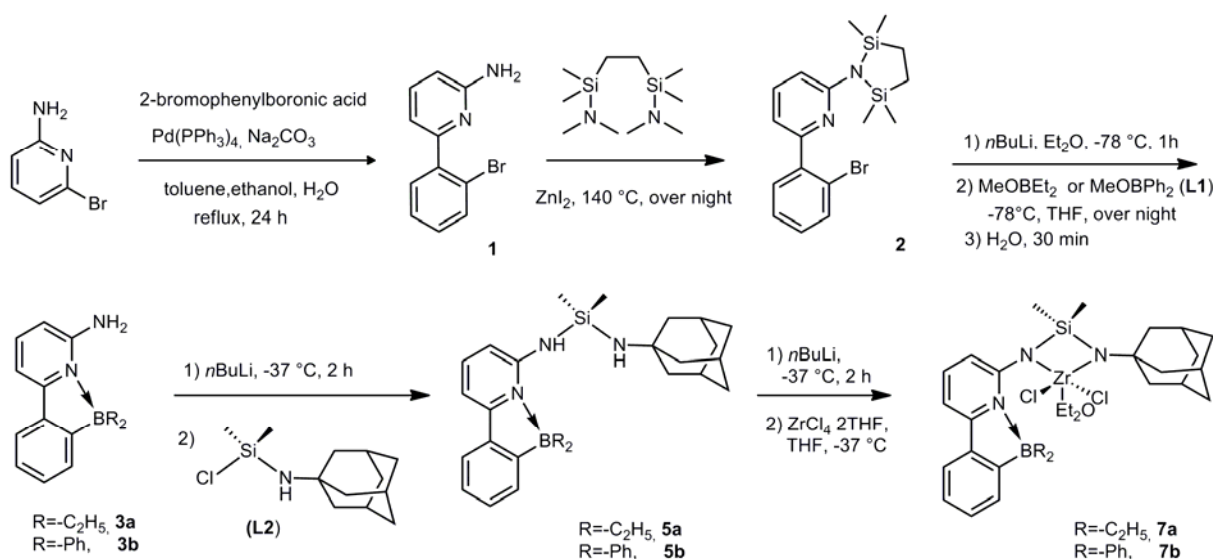
the reaction conditions, a series of well-defined graft copolymers with different graft densities and graft lengths were prepared. The maximum extent of grafting was approximately 80 mol-%. All polymers were fully characterized by ^1H NMR, ^{13}C NMR, GPC, FT-IR and DSC (Scheme 1).



Scheme 1 Synthesis of poly(COE) and the corresponding post-modification synthesis.

The third chapter deals with the copolymerization of ethylene with cyclic olefins. A new zirconium diamide complex (**7b**) based on the ligand 6-[2-(diphenylboryl)phenyl]pyridine-2-amine (**3b**) was synthesized. This ligand was designed and synthesized as it contains a Lewis-acid and Lewis-base pair (B-N) and is more bulky than 6-[2-(diethylboryl)phenyl]pyridin-2-amine (**3a**), which proved to be potentially active to produce tandem ring-opening metathesis/vinyl insertion copolymers. Both the ligand **3b** and the complex **7b** were characterized by ^1H NMR, ^{13}C NMR, FT-IR and elemental analyses. Polymerization of **7b** was compared with its less bulky analogue **7a**. Upon activation with methylaluminoxane (MAO), complex **7b** showed a productivity of 90 kg/mol·h·bar in ethylene polymerization, 1265 kg/mol·h·bar in ethylene/cyclopentene (E-CPE) copolymerization and 50 kg/mol·h·bar in ethylene/bicyclo[2.2.1]hept-2-ene (E-NBE) copolymerization. About 1 or 18 mol-% of CPE or NBE incorporation was evidenced by ^{13}C NMR analyses. The reason for the boost in productivity of PE in the presence of CPE at low (about 1 mol-%) CPE incorporation was elucidated by E/cyclopentene- ^{13}C copolymerization reactions. Unfortunately, both complexes **7a**/MAO and **7b**/MAO were not active in the reversible ROMP/VIP copolymerization. ^{13}C NMR spectra revealed that only vinyl-insertion

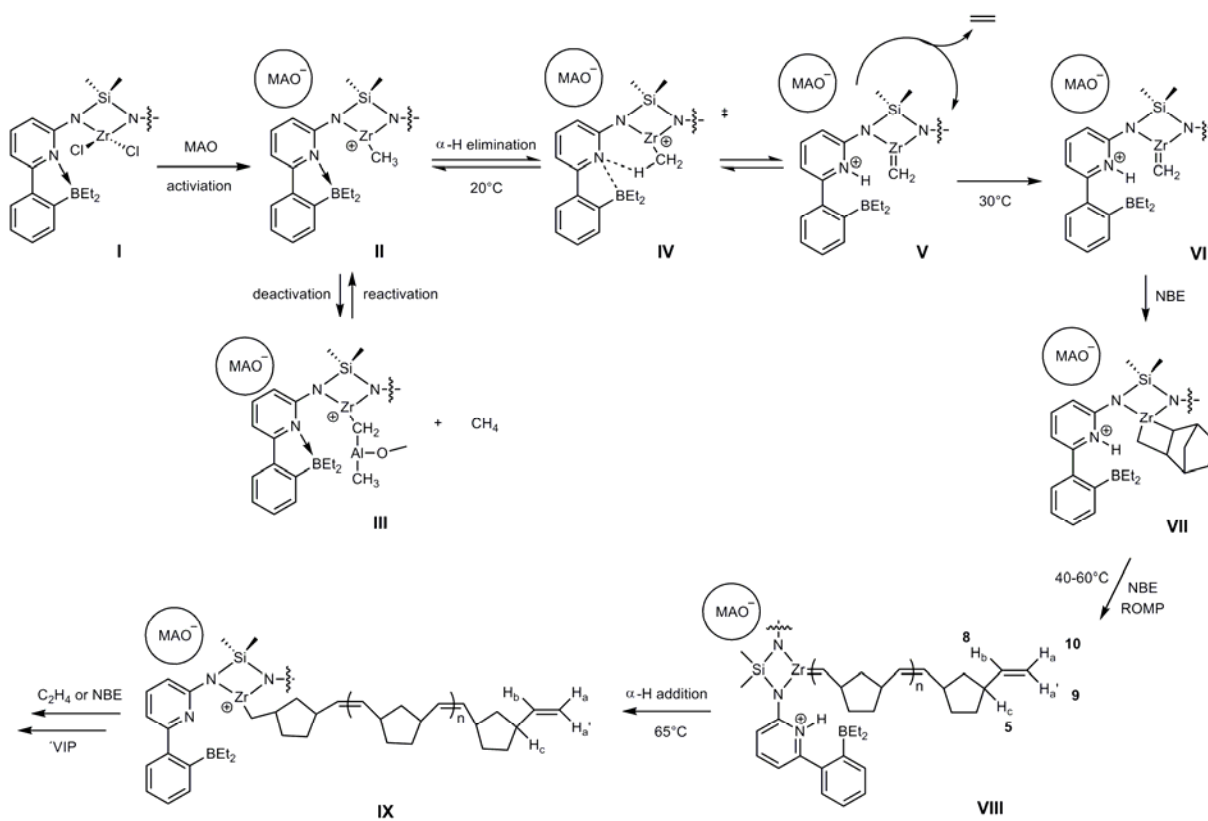
derived poly(E)-co-poly(NBE)_{VIP} was obtained. The tacticity of the poly(E)-co-poly(NBE)_{VIP} copolymer was assigned (Scheme 2).



Scheme 2 Syntheses of complexes **7a** and **7b**.

In the fourth chapter, a series NMR reactions was carried out to study the mechanism of the tandem ROMP/VIP copolymerization reaction. Zirconium complex **1** was chosen to perform this typical reaction. The reaction system was monitored by ¹H NMR, ¹¹B NMR in the temperature range of -60 °C to 70 °C in toluene-*d*₈. Upon addition of MAO at -60 °C, both chlorides in **1** were immediately substituted by methyl groups, at -20 °C the cationic center (**II**) started to give a dormant species (**III**) which was inactive in polymerization and started to produce methane. An increase in temperature to 20 °C resulted in α-H elimination and a ROMP-active zirconium alkylidene (**V**) formed that gave a signal at δ = 8.6 ppm in the ¹H NMR. Unfortunately, this active species undergoes bimolecular decomposition and produces ethylene. ¹¹B NMR showed that the originally tetra-coordinated B atom became tri-coordinated (the N-B bonds cleaved) at 30 °C, then ROMP started. The end olefinic group (**VIII**) were clearly observed in ¹H NMR and the corresponding coupling constant could be assigned and were consistent. Above 65 °C, an α-H addition must occur, as a new tri-coordinated B species appears in ¹¹B NMR and increases its resonance sharply. It was proposed that vinyl insertion polymerization occurs since then. Based on this study, both the activation process and active species in the homopolymerization of NBE as well as in the copolymerization of E-NBE became clear. The pivotal role of the (N-(6-(2-(diethylboryl)phenyl)pyrid-2-yl)-ligand in the α-H abstraction process has

been verified. The insights gained in this study, together with existing knowledge will be helpful for the design of new catalysts suitable for tandem ROMP/VIP copolymerization (Scheme 3).



Scheme 3 Proposed mechanism of NBE polymerization activated by 1/MAO.

Goal/Aim

Functional polyolefins with improved compatibility and adhesion can act as an interfacial agent between non-polar and polar materials, which will dramatically expand its applications. The basic point is that the structural and compositional parameters of polyolefins should retain during functionalization. Current functionalization technologies are basically focusing on direct polymerization of polar comonomers or post-modification of a saturated polymer, such as a free radical reaction. The drawback of these two approaches are either with reduced catalyst activity and polymer molecular weight or induce multiple free radical species which inevitably produce many undesirable impurities, not only reduce the overall grafting efficiency, but also trigger degradation of the polymer backbone and/or cross-link between the polymer chains. Other than radical method in post-modification, the functionalization could also be carried out by selectively and conveniently converting a reactive group in a polymer to its desired ultimate functional groups under mild reaction conditions. The goal of this research was to prepare functional polyolefins. The ultimate objective was to synthesize ring-opening metathesis polymerization-derived and vinyl insertion polymerization-derived (ROMP/VIP-derived) copolymers and to functionalize the corresponding cyclic olefin copolymers (COCs) by post-modification reactions.

The work started by functionalization of a model polymer. In this case, poly(*cis*-cyclooctene) (poly(COE)) was chosen as it contains unsaturated double bonds which offers a possibility for further modification. Poly(COE) in a molecular weight of 41000 g·mol⁻¹ (PDI 1.48) was synthesized by using 1st Grubbs initiator and a chain transfer agent. The following epoxidation, hydroxylation and hydrobromination reactions quantitatively converted the unsaturated polymer to the corresponding functional polymers. Interestingly, the *non-activated* hydrobrominated poly(COE) can be used as a macroinitiator for atom transfer radical polymerization (ATRP) or visible light-induced graft polymerization of *tert*-butyl acrylate (*t*BA). By varying the reaction conditions, a series of well-defined graft copolymers with different graft densities and graft lengths were prepared. The maximum extent of grafting was approximately 80 mol-%.

Consecutively two Group 4 complexes containing 6-[2-(diethylboryl)phenyl]pyridine-2-amine ligand or 6-[2-(diphenylboryl)phenyl]pyridine-2-amine ligand were synthesized. These complexes were designed and synthesized as the ligands contained a Lewis-acid and Lewis-base pair (B-N), which proved to be potentially active to produce tandem ROMP/VIP-derived copolymers. The former work by other colleagues such as Sebnem and Zou had already proved this point, that group IV complexes containing aminoborane ligand are active to produce COCs, such as ethylene (E) with norborn-2-ene (NBE) copolymer or E with *cis*-cyclooctene (COE) copolymer, which contains both saturated and unsaturated moieties in the same polymer chain, though with a low catalyst activity. The copolymerizations of E with cyclopentene (CPE) and E with NBE were carried out by employing these two new complexes (upon activation with MAO). However they were not active for tandem ROMP/VIP copolymerization. ^{13}C NMR spectra revealed that only VIP-derived poly(E)-*co*-poly(NBE)_{VIP} was obtained and the maximum NBE incorporation was 18 mol-%. The tacticity of the poly(E)-*co*-poly(NBE)_{VIP} copolymer was assigned. All the VIP-derived poly(E)-*co*-poly(NBE) sequences show predominantly isolated/alternating-syndiotactic E-NBE, as well as alternating-isotactic E-NBE sequences. An interesting phenomenon was found for the copolymerization of E-CPE that with a minimum amount of CPE (0.8 vol.-%) in the polymerization mixture, the catalyst activity was boosted by a factor of 31 (compared to ethylene homopolymerization). The reason for the boosted productivity of PE in the presence of CPE (CPE incorporation about 1 mol-%) was elucidated by E/cyclopentene-1- ^{13}C copolymerization reactions.

The final work was focusing on the mechanism study of the tandem ROMP/VIP copolymerization reaction. Zirconium complex **1** was chosen to perform this typical reaction. A series of NMR reactions were carried out. The reaction system was monitored by ^1H NMR, ^{11}B NMR in the temperature range of -60 °C to 70 °C in toluene-*d*₈. The activation and deactivation processes of MAO on complex **1** were captured by ^1H NMR. An increase in temperature must have resulted in α -H elimination as a ROMP-active zirconium alkylidene gave a signal at $\delta = 8.6$ ppm in the ^1H NMR. Unfortunately, this active species undergone bimolecular decomposition and produced ethylene. ^{11}B NMR showed that the originally tetra-coordinated B atom became tri-coordinated (the N-B bonds cleaved) at 30 °C, which proved the

formation of zirconium alkylidene. When NBE was added to the system ROMP reaction started. The starting olefinic groups were clearly observed in ^1H NMR and the corresponding coupling constant could be assigned and were consistent. Above $65\text{ }^\circ\text{C}$, an $\alpha\text{-H}$ addition must have occurred, as a new tri-coordinated B species appeared in ^{11}B NMR and increased its resonance sharply. It was proposed that vinyl insertion polymerization occurs since then. Based on this study, both the activation process and active species in the homopolymerization of NBE as well as in the copolymerization of E-NBE became clear. The pivotal role of the (N-(6-(2-(diethylboryl)phenyl)pyrid-2-yl)-ligand in the $\alpha\text{-H}$ abstraction process has been verified. The insights gained in this study, together with existing knowledge will be most helpful for the design of new catalysts suitable for tandem ROMP/VIP copolymerization.

1. General Introduction

This chapter is a general historic review over polyolefins, mainly focusing on polyethylene (PE), i.e. polymerization and functionalization. Other polyolefins, such as polypropylene (PP), polybutene-1 (PB-1), polymethylpentene (PMP) are considered to be outside the scope of this chapter.

1.1 History of Polyethylene

Polyethylene (PE), a polymer of ethylene ($\text{CH}_2=\text{CH}_2$), is a thermoplastic material.^[1-3] That is, it can be melted and shaped into a form which can be subsequently remolded into other forms. As PE is usually processed above 190 °C, where it is completely amorphous, melting ranges (120 to 180 °C) are less important than flow characteristics of the molten polymer.^[4-6] Depending on the desired PE properties, the most common production approaches are Ziegler-Natta catalysis,^[7-11] Phillips catalysis (supported chromium catalysts)^[12-15] and free radical polymerization.^[16-18]

Modern PE has its origins starting in the 1930s. Nowadays, PE can find its major use as a commodity polymer and is used in a wider range of applications than any other polymer. The primary use is in packaging, such as plastic bags, plastic films and bottles. Descriptions of early work on PE have been provided by McMillan, Kiefer and Seymour.^[19-21] The noteworthy milestones in the evolution of PE include the following:

- In the 1930s, Eric Fawcett, Rignald Gibson and Michael Perrin (chemists in Imperial Chemical Industries) produced low density PE (LDPE) under high temperature and pressure (142 MPa and 170 °C).
- In the early 1950s, transition metal catalysts that produce high molecular weight linear PE were independently discovered by Hogan and Banks in the US (silica-supported chromium catalyst) and by Ziegler in Germany (combining titanium compounds and aluminum alkyls).
- In the late 1960s and 1970s, gas phase process, medium density PE (MDPE) and supported catalysts on magnesium compounds emerged.
- In the late 1970s, Kaminsky, Sinn and coworkers discovered that the catalyst activity increased enormously when methylaluminoxane (MAO) is used as cocatalyst for metallocene single-site catalysts.

- In the 1990s, Exxon and Dow commercialized metallocene single-site catalysts to produce linear low density PE (LLDPE) and very low density PE (VLDPE); later Brookhart and coworkers discovered non-metallocene single-site catalysts based on chelated late transition metals.

The Society of the Plastics Industry (SPI) identifies three main categories of PE based on density: low density (0.910-0.925 g·cm⁻³), medium density (0.926-0.940 g·cm⁻³), high density (0.941-0.965 g·cm⁻³). In a few cases, copolymers are named using abbreviations for the comonomer employed. Apparently, these classifications are far from sufficient to describe the wide range of PE available. In industry, PE is commonly classified and named using acronyms that incorporate resin density or molecular weight. An overview of various classifications of PE in common use in industry is provided below:

- *Ultra-High-Molecular-Weight Polyethylene (UHMWPE)*
- *High Density Polyethylene (HDPE)*
- *Medium Density Polyethylene (MDPE)*
- *Linear Low Density Polyethylene (LLDPE)*
- *Low Density Polyethylene (LDPE)*
- *Very Low Density Polyethylene (VLDPE)*
- *Cross-linked Polyethylene (PEX or XLPE)*
- *Copolymers of Ethylene with Polar Comonomers*
- *Cyclic Olefin Copolymers (COCs)*

In 2013, the global consumption of PE was approximately 150 million metric tons.^[22] To aid recycling, the SPI has issued numeric codes to identify the plastic used in fabricated articles. Each article should have an imprint of a triangle which encloses a number identifying the plastic used in its fabrication. HDPE is indicated by the number 2 and PP by the number 5. Codes for PE and other plastics are shown in Figure 1.1.^[23] According to the United State Environmental Protection Agency (EPA) figures, only about 12.1 % of total municipal waste in 2007 was contributed by plastics, following paper (32.7 %), yard waste (12.8 %) and food (12.5 %).^[24] Nowadays, items made from plastics with improved mechanical strength result in lower weights per unit.^[25-27]

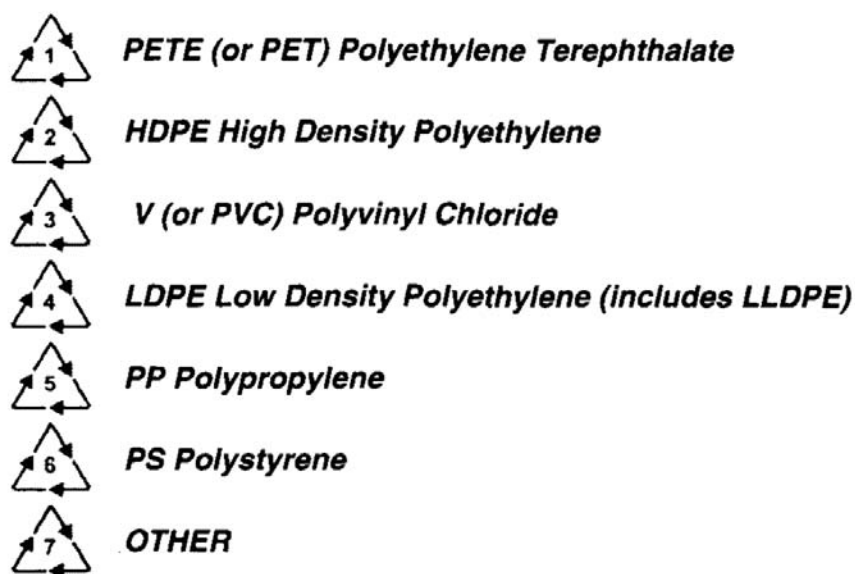


Figure 1.1 SPI coding of plastics.^[23]

1.2 Heterogeneous Ziegler-Natta Catalysis

The Ziegler-Natta catalyst is so named in recognition of the pioneering work by Karl Ziegler and Giulio Natta, who separately synthesized and characterized PE and polypropylene (PP). Now, most commercial Ziegler-Natta catalysts are heterogeneous inorganic solids, essentially insoluble in common organic solvents, but some are homogeneous, primarily those derived from vanadium compounds. As Ziegler-Natta catalysts may be poisoned even by traces of oxygen and water, they must be handled under an inert atmosphere (usually nitrogen). The origins of Ziegler-Natta polyolefin catalysts can be found in several books authorized by McMillan, Seymour, Boor, Vandenberg and Repka.^[19, 21, 28-29]

Commercial Ziegler-Natta catalysts are supported, i.e. bound to a solid with a high surface area. All modern supported Ziegler-Natta catalysts designed for olefin polymerization are $MgCl_2$ -supported titanium tetrachloride and silica with a diameter of 30-40 μm as a carrier. During the catalyst synthesis, both the Ti compounds and $MgCl_2$ are packed into the silica pores. By exposing the catalyst system to organoaluminum compounds such as $Al(C_2H_5)_3$, $TiCl_4$ was reduced to active $TiCl_3$, which starts the polymerization. Supported catalysts result in dispersed active centers which are highly accessible. Catalyst activity can reach up to 5000 $g_{PE}/g_{catalyst}$

and the molecular weight is controlled primarily by the use of hydrogen as a chain transfer agent (CTA). Transition metal residues in PE produced with modern supported catalysts are very low, typically less than 5 ppm.^[30-33] The Cossee-Arman mechanism is the most accepted route for olefin polymerization.^[34-35]

1.3 Homogeneous Ziegler-Natta Catalysis

1.3.1 Metallocene catalysts

Metallocene catalysts are homogeneous and the metal center acts as the sole polymerization site for what it is often referred to as a single-site catalysts (SSC). They act in combination with group 13 organometallics such as methylaluminoxane (MAO) or fluoroarylboranes.^[36-42] As most Ziegler-Natta catalysts are heterogeneous, metallocenes are considered as a subset of Ziegler-Natta catalysts. The active center for SSCs is believed to be cationic, while active centers for Ziegler-Natta catalysts are thought to involve neutral octahedral complexes having open coordination sites. Though important technology, metallocenes only contribute less than 4 % of the global industrial production of PE.^[43] Ziegler-Natta, Phillips and free radical polymerizations still dominate the market of PE.

In the 1970s, enormous progress was made by Kaminsky, Sinn and coworkers. The discovery of MAO instead of diethylaluminum chloride or other conventional cocatalysts dramatically increased the polymerization activity.^[44-46] Commercial use of metallocene catalysts began in 1990s. Stereoregular PP or other α -olefin copolymers were realized by selecting a suitable metallocene catalyst. Some important metallocene catalysts display C_{2v} , C_2 , C_s , or C_1 symmetry. The tacticity of resulting polymer follows Ewen's symmetry rules.^[47-51]

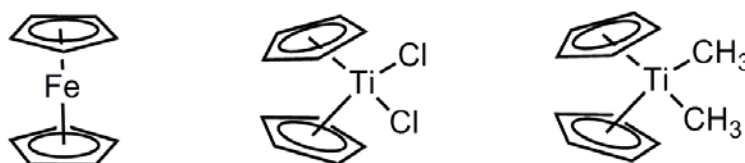


Figure 1.2 Structure of metallocenes.

1.3.2 Post-metallocene catalysts

Post-metallocene (or non-metallocene) catalysts were discovered in the 1990s and are mostly based on late transition metals (primarily Pd, Ni and Fe) with chelating ligands (containing oxygen, nitrogen, phosphorus, and sulphur).^[52-58] Owing to a mechanism called “chain-walking”, certain non-metallocene catalysts induce chain branching. Both short chain and long chain branchings were observed in the polymers produced by these catalysts. PE in various structures that range from high density PE to hydrocarbon plastomers and elastomers are produced. The development of coordination polymerization also enables copolymerization with polar monomers such as methyl vinyl ketones, methyl acrylate, acrylonitrile though with low monomer incorporation and/or molecular weights.^[59-64]

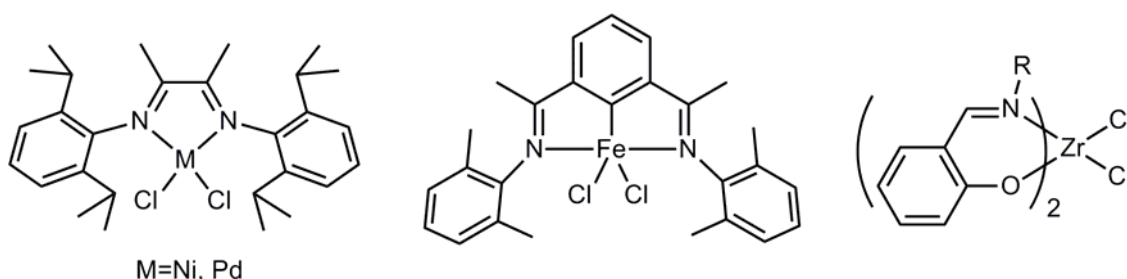


Figure 1.3 Non-metallocene single-site catalysts (SSCs).

1.4 Coordination Addition Polymerization

Coordination polymerization is a form of addition polymerization in which the monomer adds to a growing macromolecule through an organometallic active center.^[65-70] The development of this polymerization technique started in the 1950s with heterogeneous Ziegler-Natta catalysts, which were based on titanium tetrachloride and an aluminum cocatalyst. Coordination polymerization has a great impact on the physical properties of vinyl polymers such as PE and PP compared to the same polymers prepared by other techniques, such as free radical polymerization. The polymers tend to be linear and not branched and have much higher molar mass. Coordination type polymers are also stereoregular and can be isotactic or syndiotactic instead of just atactic.^[71-76] This tacticity introduces crystallinity in otherwise amorphous polymers. The active site for SSC is usually cationic and follows the Cossee-Arlman mechanism. Depending on the polymerization conditions

and catalyst property, chain termination methods can be β -hydrogen transfer, β -hydrogen elimination, β -methyl elimination or chain transfer to aluminum. Under the usual experimental conditions β -hydrogen transfer dominates chain termination mechanisms.^[77-82]

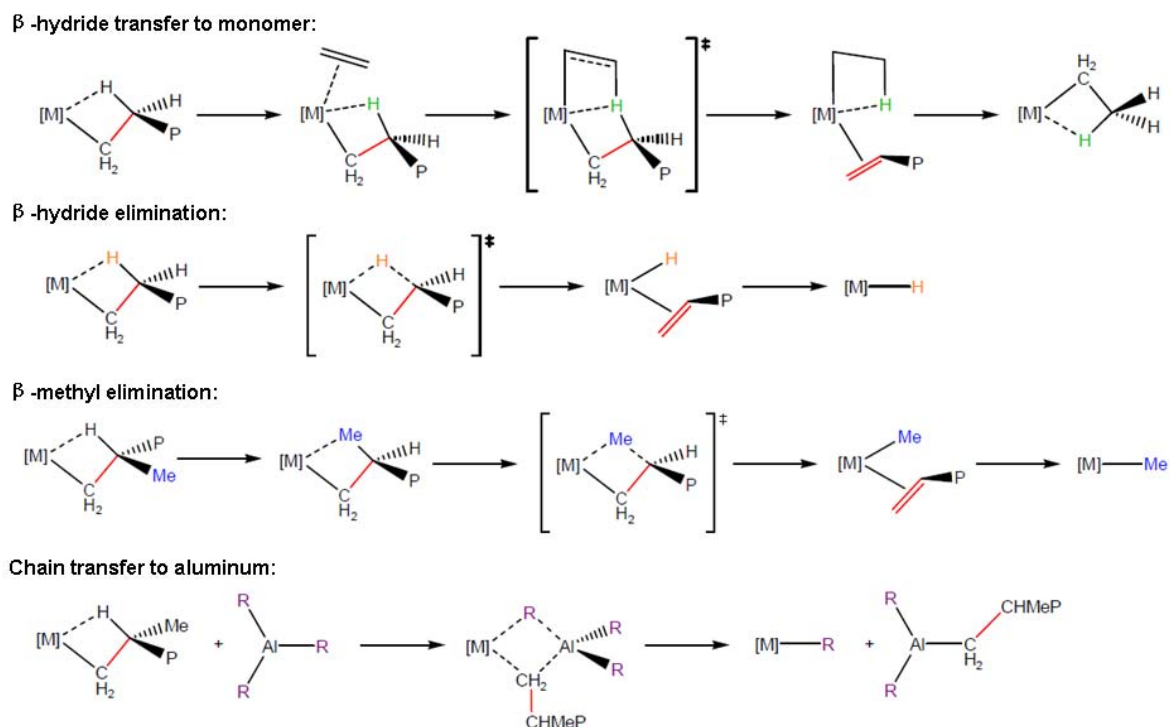


Figure 1.4 Chain termination for olefin polymerization. ^[77-82]

Cyclic olefin copolymers (COCs) prepared via coordination polymerization are shown in Figure 1.5.^[83-93] COC is a relatively new family of thermoplastic amorphous as compared to commodities such as PE and PP. Their excellent optical transparency, high glass transition temperature, and good heat resistance make them interesting materials for optical applications.

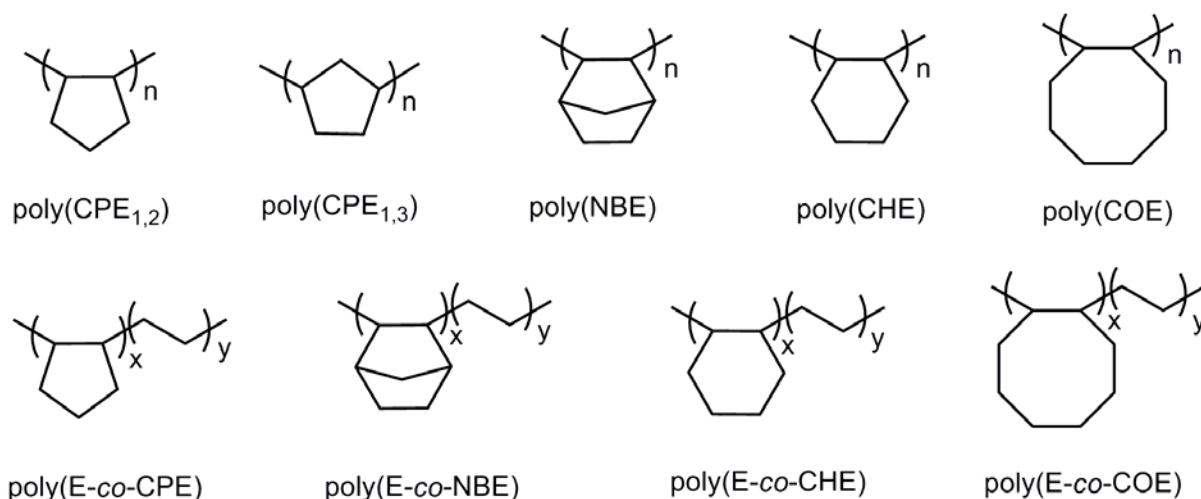


Figure 1.5 Cyclic olefin copolymers via vinyl insertion polymerization.

1.5 Ring-opening Metathesis Polymerization

The phenomenon of olefin metathesis can be traced back to 1950s in the polymer industry where chemists reported that propene was converted to ethylene and 2-butene when heated with molybdenum (in the form of the molybdenum oxide or $\text{Mo}(\text{CO})_6$ on alumina).^[94] Since the very beginning, olefin metathesis has attracted remarkable attentions. A number of researchers, such as Eleuterio, Truett, Calderon, Chauvin have devoted their studies to the development of mechanism and catalytic systems.^[95-102] In 1971, Chauvin and his student Hérisson elucidated the transition metal alkene metathesis mechanism which remains the generally accepted mechanism until today (Figure 1.6). Consecutive work was made by Schrock and Grubbs *et al.* A variety of highly active and well-defined catalysts were developed.^[103-113] There is a vivid metaphor about olefin metathesis that it is a change of partners dance in which the ‘catalyst pair’ and the ‘alkene pair’ dance around and change partners with one another. To honour their contribution, Yves Chauvin, Robert Grubbs and Richard Schrock were collectively awarded the 2005 Nobel Prize in Chemistry. Now olefin metathesis is widely used in organic synthesis, polymer and material science.

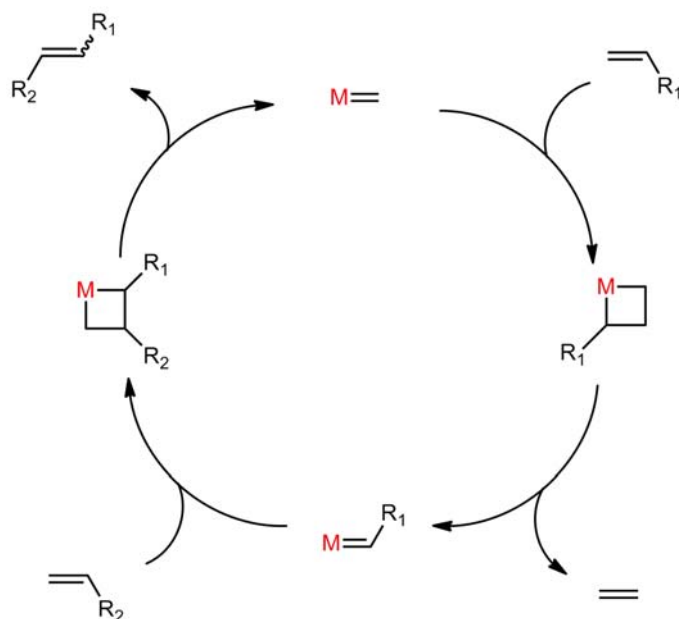


Figure 1.6 The Chauvin mechanism of transition metal alkene metathesis.

Ring-opening metathesis polymerization (ROMP) is a type of olefin metathesis chain growth polymerization process where cyclic olefins are converted to a polymeric material. This important feature distinguishes ROMP from typical olefin addition polymerization. The reaction in ROMP was driven by the relief of ring strain in cyclic olefins that occurs during incorporation of the monomer into the growing polymer chain. The most common monomers possess a considerable degree of strain (>5 kcal/mol). One notable exception is cyclohexene. With low ring strain, this cyclic olefin has very little enthalpic driving force to be polymerized using ROMP (Figure 1.7).^[114-120]

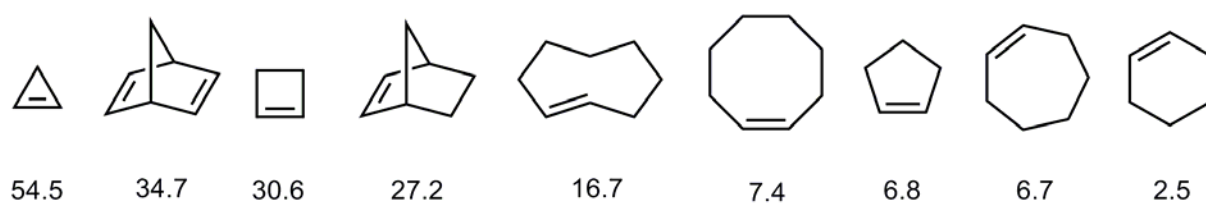


Figure 1.7 Relative ring strain for selected cyclic olefins (kcal/mol).^[115]

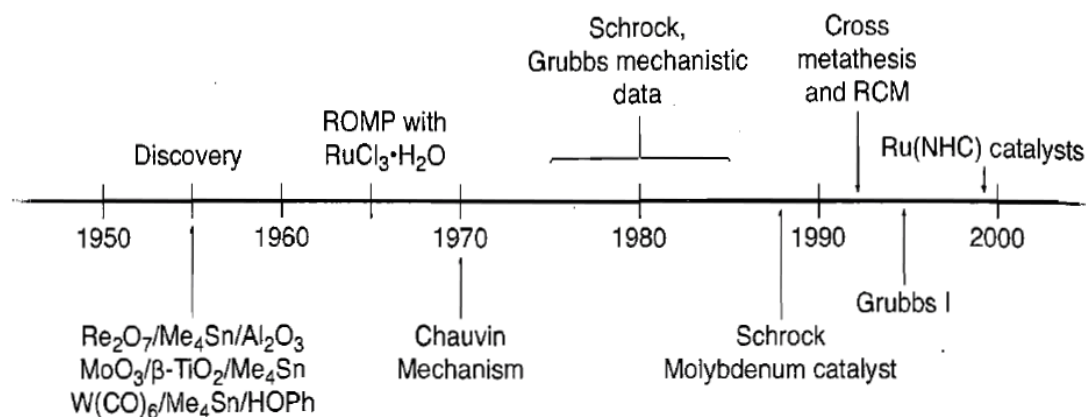


Figure 1.8 Timeline of olefin metathesis.^[121]

A timeline for the development of olefin metathesis, adapted from a review by Grubbs, is shown in Figure 1.8. It shows that early catalyst systems were often heterogeneous mixtures that were sensitive toward air and moisture, such as WCl₆, WOCl₄ and MoO₃ which were enhanced with strongly Lewis acidic alkyl aluminum cocatalyst. Recently, the catalysts used in the ROMP reaction are mainly Schrock-type catalysts (Mo^{IV}, W^{IV}) and/or Grubbs-type catalyst (Ru^{II}) (Figure 1.9). Though Mo-based Schrock catalysts are air sensitive, they hold an outstanding position in olefin metathesis. The complex [Mo(N-2,6-Pr₂C₆H₃)(CHCMe₂Ph)(OTf)₂(DME)] represents as a universal precursor, out of which all commonly used Schrock-type catalysts can be prepared. The 1st generation of Grubbs catalyst (**G1**) was well-defined in 1995. Replacing the phosphines by a saturated N-heterocyclic carbene (NHC) (1,3-bis(2,4,6-trimethylphenyl)dihydroimidazole), the 2nd generation Grubbs initiator (**G2**) was produced. As the NHC is a better electro-donating ligand compared to phosphine, higher activity was observed. The Grubbs-Hoveyda catalysts (**GH**) are more thermally stable than the other ruthenium metathesis catalysts and therefore have been useful for reactions requiring higher temperatures. Both the 1st and 2nd generation catalysts (**G1**, **G2**, **GH1** and **GH2**) are now commercially available. With their simple synthesis, tolerance towards functional groups in the alkene and air-tolerance, Grubbs catalysts are often more compatible in synthetic organic chemistry.

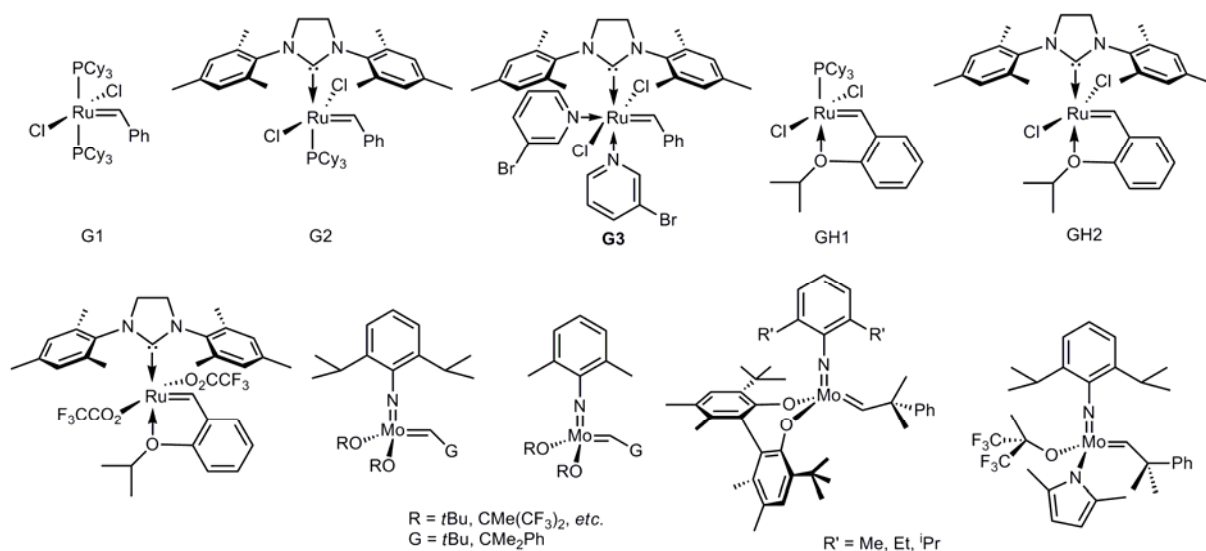


Figure 1.9 Representative Grubbs-type and Schrock-type initiators.

Transition metal carbene moieties, normally described as $M=CR_2$, are essential in a ROMP catalyst. There are basically two types of metal carbene complexes, **Fischer carbenes** and **Schrock carbenes** (Figure 1.10).^[122-125] **Fischer carbenes** possess an electronegative substituent and are often stable in the singlet spin state. The metal-carbon bonds in complexes are not strongly polarized. This property of the metal-ligand bond and the presence of an electrophilic substituent at the carbon make these complexes electrophilic. Cyclic olefin therefore cannot coordinate to this type of metal alkylidene complex and form the beginning of a growing polymer chain. **Schrock carbenes** on the other hand with only hydrogen or alkyl groups are characterized by a more nucleophilic carbene carbon. Transition metal carbene complexes resulting from the coupling of a triplet state carbene and a triplet state metal can be applied for the alkene metathesis process. The transition metal alkylidene mechanism on ROMP reaction are shown in Figure 1.11.^[126-130]

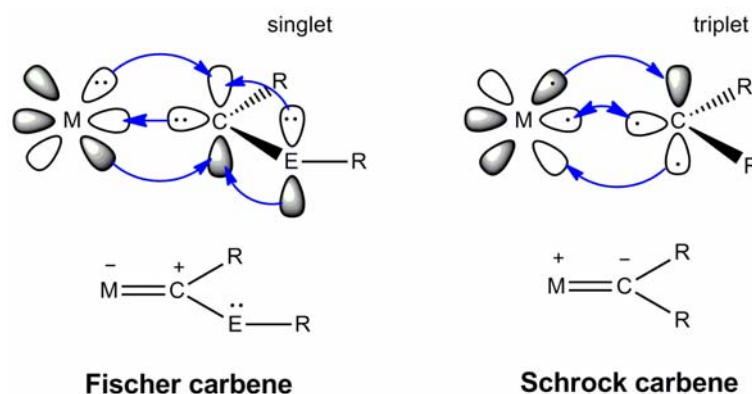


Figure 1.10 Orbital interactions in transition metal carbene complexes.^[126]

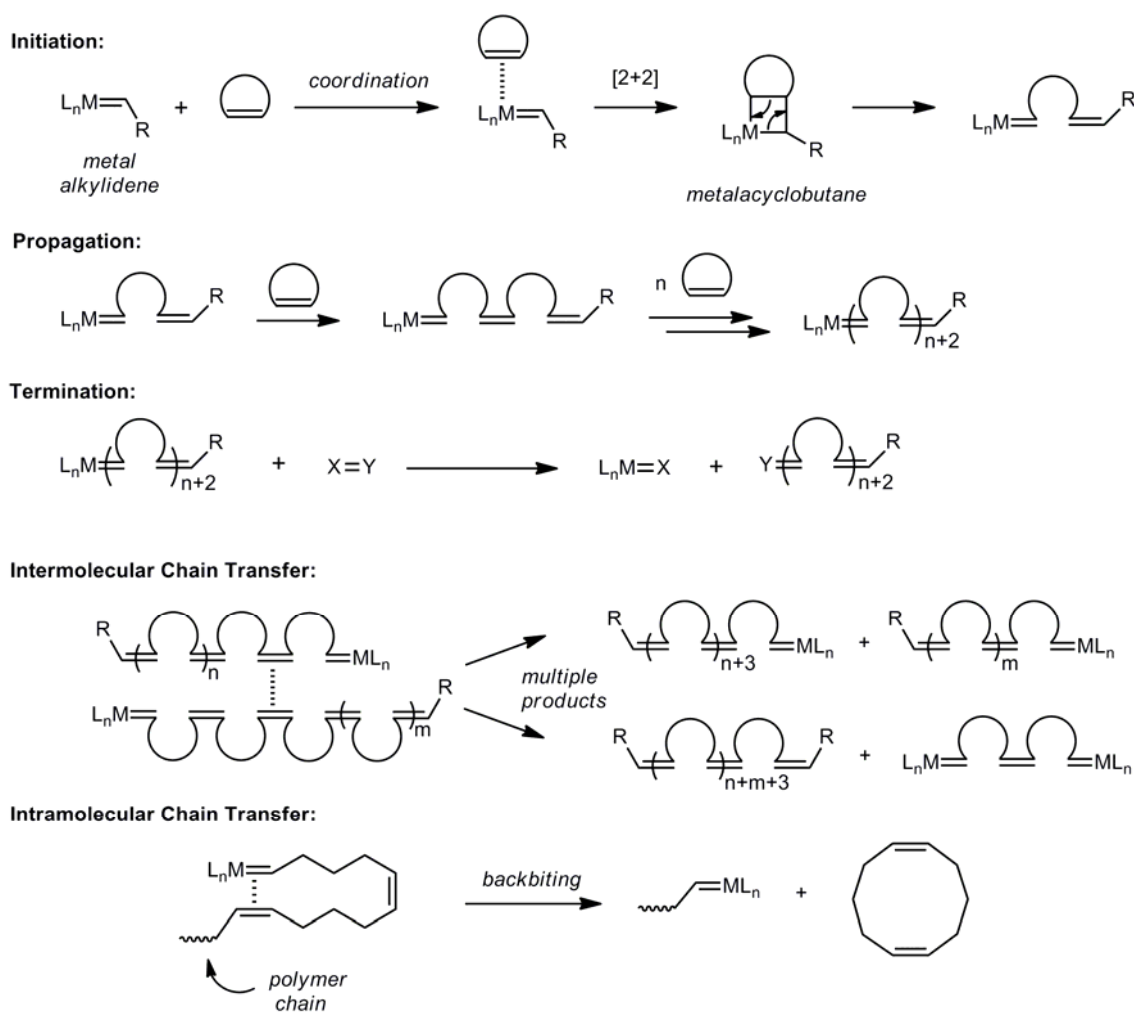


Figure 1.11 A general mechanism to a typical ROMP reaction and the secondary metathesis reactions.^[127]

In addition to the general mechanism for ROMP reaction (including initiation, propagation and termination) illustrated in Figure 1.11, the equilibrium can also be reached via intermolecular chain-transfer and/or intramolecular chain-transfer (a backbiting process) reactions. Examples of the secondary metathesis in ROMP reactions are also shown in Figure 1.11. In an intermolecular chain-transfer reaction, a polymer chain with an active metal alkylidene on its terminus can go for metathesis reaction with any olefin along the backbone in the same reaction vessel. Although the total number of polymer chains and active species remains unchanged, the molecular weights of the individual polymers will increase or decrease accordingly. In an intramolecular chain-transfer reaction, the active terminus of a growing polymer chain reacts with itself, leading to a polymer chain of reduced molecular weight and a cyclic oligomer. Collectively, these secondary metathesis reactions effectively

broaden molecular weight distribution (or polydispersity) of the system. The extent of these processes depends on the temperature, monomer concentration, solvent, and reaction time.

Recent progress was made by precise control of polymer tacticity and regiochemistry which can have dramatic influence on the thermal, rheological and crystallization properties. Schrock and colleagues reported the utilization of monoaryloxide-pyrrolido-imidoalkylidene (MAP) complexes of Mo(VI) for the synthesis of *cis*-syndiotactic polymers of several norbornadiene monomers. Grubbs also reported that Ru-mediated ROMP reaction can generate highly *cis*-, highly tacticity (>95 %) polymers.^[131-133]

1.6 Functional Polyolefins

Polyolefins comprise the least expensive and most commercially produced polymers available and they can find their applications in various packaging films, plastic bags, bottles and pipes as their outstanding chemical resistance and broad-ranging mechanical properties. However, the poor compatibility of polyolefins with oxygen- and nitrogen-containing polymers, polar pigments, and additives has limited the usage of these polymers in applications that require, for example, good coating/adhesion characteristics. These practical restrictions can result from the lack of polar functional groups or other active groups along the polymer backbone. The introduction of functional groups to polyolefins can be sufficient to alter the properties of these plastics for speciality applications and is of considerable interest for researchers and industries. With improved compatibility and adhesion, polyolefins can act as an interfacial agent between non-polar and polar materials which subsequently expands its application profile.^[134-135]

The superior properties of polyolefins must be retained during functionalization. This requires that the functionalization should be conducted in a controlled manner that renders all the polyolefin structural and compositional parameters and without compromising the desired features characteristic of the parent materials, such as processability, chemical robustness, and mechanical strength. Current functionalization methodologies (chemical functionality and reactivity) are limited.

Basically, there are two approaches to the functionalized PE and both have advantages and shortcomings. They are i) direct copolymerization of α -olefin with a polar functional comonomer, ii) chemical modification of the preformed polymer.

1.6.1 Direct copolymerization

Technically, direct polymerization of an α -olefin with a functional monomer via coordination polymerization process is an effective and straightforward way to obtain functional polyolefins. However, Ziegler-Natta and metallocene catalysts, usually early transition metals (Ti, Zr, Hf), are oxophilic. Functional monomers (N, O, or halides containing ligands) are more preferred to complex with active polymerization centers which significantly deactivate the catalysts, and suspend the polymerization. Though neutral and acidic heteroatoms (Si and B) are introduced to functional monomers and protecting sensitive functional groups are applied to avoid the catalysts poison, the polymers are suffering from low yield and low molecular weight.^[136-139] More recently Brookhart and co-workers employed late transition metals (Fe, Ni, Pd) complexes for olefin polymerization which tend to be less oxophilic and more stable to the heteroatoms.^[52-64] Copolymers of ethylene with polar monomers such as methyl acrylate are produced though with reduced activity and polymer molecular weight. Generally, new characteristic features are observed for the PEs obtained from such late-transition metal catalytic systems. Highly linear PE is usually obtained using the iron or cobalt complexes, whereas highly branched PE is commonly formed by the nickel or palladium complexes.

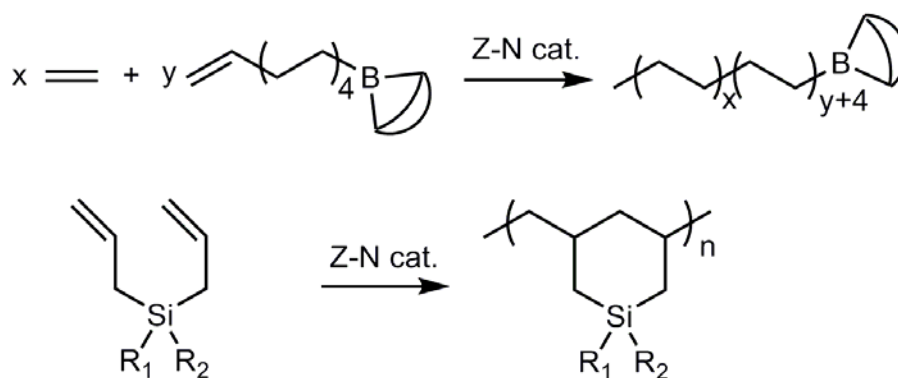


Figure 1.12 Examples of functional polyolefins by direct polymerization.^[134]

1.6.2 Post-polymerization modification

Chemical modification of the preformed polymers (PE, PP) offers a very attractive opportunity to access functional polymers. So far, the most favoured functionalization processes are based on post-modification. However, only very limited chemistry is available to activate the completely saturated aliphatic molecular structure. The current functionalization approach is based on a free radical reaction.^[140-142] Hydrogen abstraction from a completely saturated polymer backbone requires severe reaction conditions, such as high temperature, radiation and plasma. Multiple free radical species usually coexist in the system and inevitably produce many undesirable impurities, which not only reduce the overall grafting efficiency, but also trigger degradation of the polymer backbone and/or cross linking between the polymer chains. Surface modification through free radical activation improves only surface properties but not the bulk properties of the polymer. It also faces chemical and physical difficulties, which makes it very hard to understand each reaction in detail.

On the other hand, the reactive polyolefin intermediate approach provides an attractive alternative. This approach is to synthesize a reactive group containing polymer and then selectively and conveniently interconverted the reactive sites to the desired ultimate functional groups under mild reaction conditions.^[143-150] The research group of Chung has worked extensively on the reactive polyolefin intermediate (precursor) approach. Borane-containing polyolefins have been prepared by hydroboration reactions of the unsaturated polymers (Figure 1.13). New progress made by his group is the functional polyolefins for energy applications. Notably, Mecking and coworkers reported that monofunctional highly branched ethylene oligomers in essentially quantitative yield can be achieved by functionalization of the unsaturated end group of the oligomer chains via cross metathesis or epoxidation, respectively (Figure 1.14).

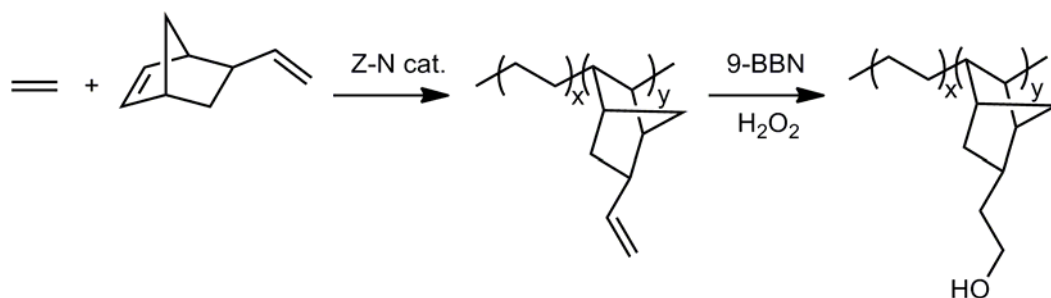


Figure 1.13 Examples of functional polyolefins by post-polymerization.^[149]

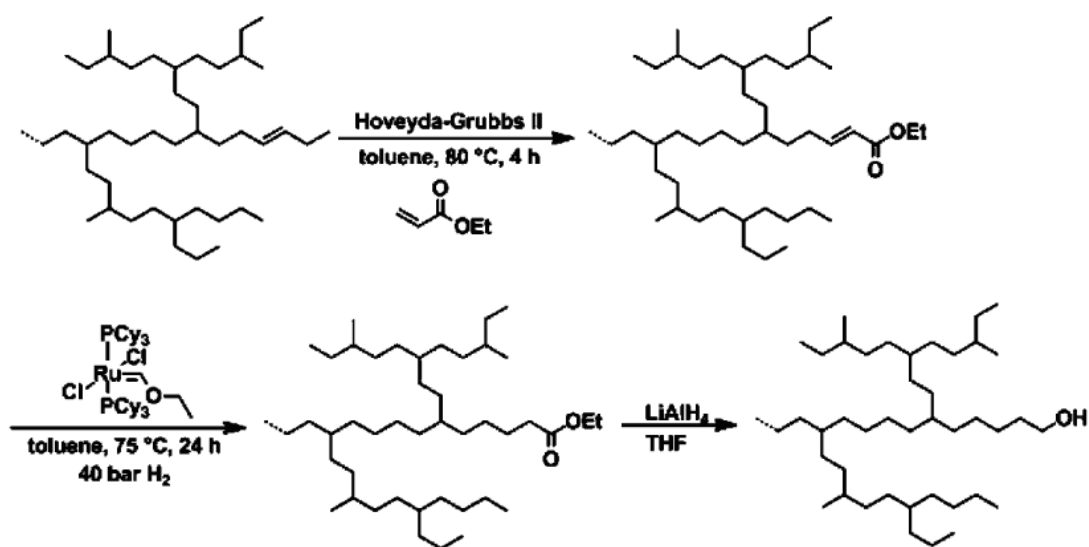


Figure 1.14 Monofunctionalization of hyperbranched PE via cross metathesis.^[150]

1.7 References

- [1] J. M. Deitzel, J. Kleinmeyer, D. Harris, N. C. Beck Tan, *Polymer* **2001**, *42*, 261-272.
- [2] S. A. Baurle, A. Hotta, A. A. Gusev, *Polymer* **2006**, *47*, 6243-6253.
- [3] R. F. Boyer, *Macromolecules* **1973**, *6*, 288-299.
- [4] R. Hiss, S. Hobeika, C. Lynn, G. Strobl, *Macromolecules* **1999**, *32*, 4390-4403.
- [5] B. I. Voit, A. Lederer, *Chem. Rev.* **2009**, *109*, 5924-5973.
- [6] G. Matsuba, S. Sakamoto, Y. Ogino, K. Nishida, T. Kanaya, *Macromolecules* **2007**, *40*, 7270-7275.
- [7] K. Ziegler, E. Holzkamp, H. Breil, H. Martin, *Angew.chem.* **1955**, *67*, 541-547.
- [8] V. C. Gibson, S. K. Spitzmesser, *Chem. Rev.* **2003**, *103*, 283-315.

- [9] G. Natta, *Angew.chem.* **1956**, 68, 393-403.
- [10] G. Natta, *Angew.chem.* **1964**, 76, 553-566.
- [11] P. Pino, R. Mulhaupt, *Angew. Chem.* **1980**, 92, 869-887; *Angew. Chem. Int. Ed.* **1980**, 19, 857-875.
- [12] B. M. Weckhuysen, I. E. Wachs, R. A. Schoonheydt, *Chem. Rev.* **1996**, 96, 3327-3349.
- [13] A. Jabri, C. Temple, P. Crewdson, S. Gambarotta, I. Korobkov, R. Duchateau, *J. Am. Chem. Soc.* **2006**, 128, 9238-9247.
- [14] C. Barzan, D. Gianolio, E. Groppo, C. Lamberti, V. Monteil, E. A. Quadrelli, S. Bordiga, *Chem. Eur. J.* **2013**, 19, 17277-17282.
- [15] E. Groppo, C. Lamberti, S. Bordiga, G. Spoto, A. Zecchina, *Chem. Rev.* **2005**, 105, 115-183.
- [16] M. Ouchi, T. Terashima, M. Sawamoto, *Chem. Rev.* **2009**, 109, 4963-5050.
- [17] K. E. Russell, *Prog. Polym. Sci.* **2002**, 27, 1007-1038.
- [18] K. Matyjaszewski, J. H. Xia, *Chem. Rev.* **2001**, 101, 2921-2990.
- [19] F. M. McMillan, *The Chain Straighteners*, MacMillan Publishing Company, London, **1979**.
- [20] D. M. Kiefer, *Today's Chemist at Work*, June **1997**, p51.
- [21] R. B. Seymour, *Advances in Polyolefins*, Plenum Press, New York, **1985**.
- [22] Source:
http://www.academia.edu/4066905/POLYETHYLENE_PRODUCTION_TECHNOLOGIES
- [23] D. B. Malpass, *Introduction to Industrial Polyethylene: Properties, Catalysts, Processes*, Wiley-Scrivener, **2010**.
- [24] Source: <http://www.epa.gov/epawaste/nonhaz/municipal/index.htm>.
- [25] C. Booker, *The Real Global Warming Disaster*, Continuum, London, **2009**.
- [26] E. Yashima, K. Maeda, H. Iida, Y. Furusho, K. Nagai, *Chem. Rev.* **2009**, 109, 6102-6211.
- [27] S. R. Forrest, *Nature* **2004**, 428, 911-918.
- [28] J. Boor, *Ziegler-Natta Catalysts and Polymerizations*, Academic Press Inc., **1979**.
- [29] R. B. Seymour, T. Cheng, *History of Polyolefins*, D. Reidel Publishing Co., Dordrecht, Holland, **1986**.
- [30] G. G. Hlatky, *Chem. Rev.* **2000**, 100, 1347-1376.

- [31] A. F. Hill, *Organotransition Metal Chemistry*, Wiley-Interscience, New York, **2002**.
- [32] Y. V. Kissin, *Alkene Polymerization Reactions with Transition Metal Catalysts*, Elsevier: Amsterdam, **2008**.
- [33] G. Fink, B. Steinmetz, J. Zechlin, C. Przybyla, B. Tesche, *Chem. Rev.* **2000**, *100*, 1377-1390.
- [34] G. Allegra, *Makromol. Chem.* **1971**, *145*, 235-246.
- [35] E. J. Arlman, P. Cossee, *J. Catal.* **1964**, *3*, 99-104.
- [36] L. Resconi, L. Cavallo, A. Fait, F. Piemontesi, *Chem. Rev.* **2000**, *100*, 1253-1345.
- [37] W. Kaminsky, *Adv. Catal.* **2001**, *46*, 89-159.
- [38] A. L. McKnight, R. M. Waymouth, *Chem. Rev.* **1998**, *98*, 2587-2598.
- [39] W. Kaminsky, *Macromol. Chem. Phys.* **1996**, *197*, 3907-3945.
- [40] X. M. Yang, C. L. Stern, T. J. Marks, *J. Am. Chem. Soc.* **1994**, *116*, 10015-10031.
- [41] T. K. Woo, L. Fan, T. Ziegler, *Organometallics* **1994**, *13*, 2252-2261.
- [42] B. Lippert, *Coord. Chem. Rev.* **2000**, *200-202*, 487-516.
- [43] R. H. Crabtree, *The organometallic chemistry of the Transition Metals 3rd Ed.*, Wiley-Interscience, New York, **2001**.
- [44] W. Kaminsky, *J. Chem. Soc. Dalton Trans.* **1998**, 1413-1418.
- [45] W. Kaminsky, *J Polym. Sci. A: Polym. Chem.* **2004**, *42*, 3911-3921.
- [46] W. Kaminsky, *Macromolecules* **2012**, *45*, 3289-3297.
- [47] G. W. Coates, *Chem. Rev.* **2000**, *100*, 1223-1252.
- [48] H. H. Brintzinger, D. Fischer, R. Mülhaupt, B. Rieger, R. M. Waymouth, *Angew. Chem.* **1995**, *107*, 1255-1283; *Angew. Chem. Int. Ed.* **1995**, *34*, 1143-1170.
- [49] J. A. Ewen, L. Haspeslagh, J. L. Atwood, H. M. Zhang, *J. Am. Chem. Soc.* **1987**, *109*, 6544-6545.
- [50] A. R. Lavoie, M. H. Ho, R. M. Waymouth, *Chem. Commun.* **2003**, 864-865.
- [51] V. Busicom, V. Castelli, P. Aprea, R. Cipullo, A. Segre, G. Talarico, M. Vacatello, *J. Am. Chem. Soc.* **2003**, *125*, 5451-5460.
- [52] S. D. Ittel, L. K. Johnson, M. Brookhart, *Chem. Rev.* **2000**, *100*, 1169-1203.
- [53] D. P. Gates, S. A. Svejda, E. Oñate, C. M. Killian, L. K. Johnson, P. S. White, M. Brookhart, *Macromolecules* **2000**, *33*, 2320-2334.

- [54] V. M. Möhring, G. Fink, *Angew. Chem.* **1985**, *97*, 982-984; *Angew. Chem. Int. Ed.* **1985**, *24*, 1001-1003.
- [55] Z. Guan, *Chem. Eur. J.* **2002**, *8*, 3087-3092.
- [56] M. Ouchi, T. Terashima, M. Sawamoto, *Chem. Rev.* **2009**, *109*, 4963-5050.
- [57] G. J. P. Britovsek, M. Bruce, V. C. Gibson, B. S. Kimberley, P. J. Maddox, S. Mastroianni, S. J. McTavish, C. Redshaw, G. A. Solan, S. Stromberg, A. J. P. White, D. J. Williams, *J. Am. Chem. Soc.* **1999**, *121*, 8728-8740.
- [58] K. Nomura, S. Zhang, *Chem. Rev.* **2011**, *111*, 2342-2362 .
- [59] L. S. Boffa, B. M. Novak, *Chem. Rev.* **2000**, *100*, 1479-1493.
- [60] A. Nakamura, S. Ito, K. Nozaki, *Chem. Rev.* **2009**, *109*, 5215-5244.
- [61] D. H. Camacho, Z. B. Guan, *Chem. Commun.* **2010**, *46*, 7879-7893.
- [62] C. M. Roland, R. Casalini, *Macromolecules* **2003**, *36*, 1361-1367.
- [63] Y. X. Chen, *Chem. Rev.* **2009**, *109*, 5157-5214.
- [64] M. Zaheer, T. Schmalz, G. Motz, R. Kempe, *Chem. Soc. Rev.* **2012**, *41*, 5102-5116.
- [65] J. D. Scollard, D. H. McConville, *J. Am. Chem. Soc.* **1996**, *118*, 10008-10009.
- [66] G. W. Coates, P. D. Hustad, S. Reinartz, *Angew. Chem.* **2002**, *114*, 2340-2361; *Angew. Chem. Int. Ed.* **2002**, *41*, 2236-2257.
- [67] S. Matsui, M. Mitani, J. Saito, Y. Tohi, H. Makio, N. Matsukawa, Y. Takagi, K. Tsuru, M. Nitabaru, T. Nakano, H. Tanaka, N. Kashiwa, T. Fujita, *J. Am. Chem. Soc.* **2001**, *123*, 6847-6856.
- [68] H. C. Aspinall, *Chem. Rev.* **2002**, *102*, 1807-1850.
- [69] S. Mecking, *Angew. Chem.* **2001**, *113*, 550-557; *Angew. Chem. Int. Ed.* **2001**, *40*, 534-540.
- [70] L. Jia, X. M. Yang, C. L. Stern, T. J. Marks, *Organometallics* **1997**, *16*, 842-857.
- [71] E. Y. Tshuva, I. Goldberg, M. Kol, *J. Am. Chem. Soc.* **2000**, *122*, 10706-10707.
- [72] R. Paukkeri, *Polymer* **1993**, *34*, 2488-2494.
- [73] T. K. Wu, M. L. Sheer, *Macromolecules* **1977**, *10*, 529-531.
- [74] J. Dybal, S. Krimm, *Macromolecules* **1990**, *23*, 1301-1308.
- [75] A. Gitsas, G. Floudas, *Macromolecules* **2008**, *41*, 9423-9429.
- [76] F. C. Schilling, F. A. Bovey, M. D. Bruch, S. A. Kozlowski, *Macromolecules* **1985**, *18*, 1418-1422.

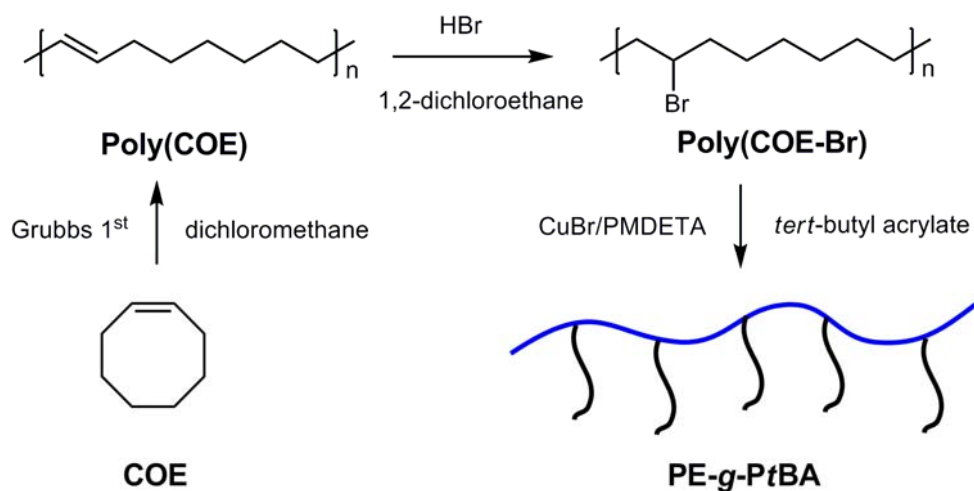
- [77] L. Resconi, F. Piemontesi, G. Franciscano, L. Abis, T. Fiorani, *J. Am. Chem. Soc.* **1992**, *114*, 1025-1032.
- [78] P. Margl, L. Q. Deng, T. Ziegler, *J. Am. Chem. Soc.* **1999**, *121*, 154-162.
- [79] L. Resconi, F. Piemontesi, G. Franciscano, L. Abis, T. Fiorani, *J. Am. Chem. Soc.* **1992**, *114*, 1025-1032.
- [80] S. Hajela, J. E. Bercaw, *Organometallics* **1994**, *13*, 1147-1154.
- [81] Z. Y. Guo, D. C. Swenson, R. F. Jordan, *Organometallics* **1994**, *13*, 1424-1432.
- [82] L. Resconi, S. Bossi, L. Abis, *Macromolecules* **1990**, *23*, 4489-4491.
- [83] H. G. Alt, A. Köppl, *Chem. Rev.* **2000**, *100*, 1205-1221.
- [84] X. F. Li, Z. M. Hou, *Coord. Chem. Rev.* **2008**, *252*, 1842-1869.
- [85] W. Spaleck, M. Antberg, J. Rohrmann, A. Winter, B. Bachmann, P. Kiprof, J. Behm, W. A. Herrmann, *Angew. Chem.* **1992**, *104*, 1373-1376; *Angew. Chem. Int. Ed.* **1992**, *31*, 1347-1350.
- [86] C. Karafilidis, K. Angermund, B. Gabor, A. Rufinska, R. J. Mynott, G. Breitenbruch, W. Thiel, G. Fink, *Angew. Chem.* **2007**, *119*, 3819-3823; *Angew. Chem. Int. Ed.* **2007**, *46*, 3745-3749.
- [87] N. Naga, *J. Polym. Sci. A: Polym. Chem.* **2005**, *43*, 1285-1291.
- [88] W. Wang, K. Nomura, *Macromolecules* **2005**, *38*, 5905-5913.
- [89] I. Tritto, L. Boggioni, D. R. Ferro, *Coord. Chem. Rev.* **2006**, *250*, 212-241.
- [90] M. L. Gao, X. L. Sun, Y. F. Gu, X. L. Yao, C. F. Li, J. Y. Bai, C. Wang, Z. Ma, Y. Tang, Z. W. Xie, S. Z. Bu, C. T. Qian, *J. Polym. Sci. A: Polym. Chem.* **2008**, *46*, 2807-2819.
- [91] X. Y. Tang, Y. X. Wang, B. X. Li, J. Y. Liu, Y. S. Li, *J. Polym. Sci. A: Polym. Chem.* **2013**, *51*, 1585-1594.
- [92] J. Y. Liu, K. Nomura, *Adv. Synth. Catal.* **2007**, *349*, 2235-2240.
- [93] M. Fujita, G. W. Coates, *Macromolecules* **2002**, *35*, 9640-9647.
- [94] I. Ojima, *Catalytic Asymmetric Synthesis 2nd ed.*, Wiley-VCH, New York, **2000**.
- [95] R. R. Schrock, G. W. Parshall, *Chem. Rev.* **1976**, *76*, 243-268.
- [96] J. D. Scollard, D. H. McConville, *J. Am. Chem. Soc.* **1996**, *118*, 10008-10009.
- [97] R. Baumann, W. M. Davis, R. R. Schrock, *J. Am. Chem. Soc.* **1997**, *119*, 3830-3831.
- [98] R. H. Grubbs, W. Tumas, *Science* **1989**, *243*, 907-915.
- [99] H. S. Eleuterio, *J. Mol. Catal.* **1991**, *65*, 55-61.

- [100] W. L. Truett, D. R. Johnson, I. M. Robinson, B. A. Montague, *J. Am. Chem. Soc.* **1960**, *82*, 2337-2340.
- [101] J. L. Hérisson, Y. Chauvin, *Makromol. Chem.* **1971**, *141*, 161-176.
- [102] N. Calderon, H. Y. Chen, K. W. Scott, *Tetrahedron Lett.* **1967**, *8*, 3327-3329.
- [103] M. R. Churchill, H. J. Wasserman, H. W. Turner, R. R. Schrock, *J. Am. Chem. Soc.* **1982**, *104*, 1710-1716
- [104] D. H. McConville, J. R. Wolf, R. R. Schrock, *J. Am. Chem. Soc.* **1993**, *115*, 4413-4414.
- [105] R. R. Schrock, P. Meakin, *J. Am. Chem. Soc.* **1974**, *96*, 5288-5290.
- [106] R. R. Schrock, A. H. Hoveyda, *Angew. Chem.* **2003**, *115*, 4740-4782; *Angew. Chem. Int. Ed.* **2003**, *42*, 4592-4633.
- [107] T. M. Trnka, R. H. Grubbs, *Chem. Rev.* **2007**, *107*, 5813-5840.
- [108] R. R. Schrock, *Acc. Chem. Res.* **1986**, *19*, 342-348.
- [109] P. Schwab, M. B. France, J. W. Ziller, R. H. Grubbs, *Angew. Chem.* **1995**, *107*, 2179-2181; *Angew. Chem. Int. Ed.* **1995**, *34*, 2039-2041.
- [110] M. Scholl, S. Qing, C. W. Lee, R. H. Grubbs, *Org. Lett.* **1999**, *1*, 953-956.
- [111] S. Kobayashi, L. M. Pitet, M. A. Hillmyer, *J. Am. Chem. Soc.* **2011**, *133*, 5794-5797.
- [112] J. A. Love, J. P. Morgan, T. M. Trnka, R. H. Grubbs, *Angew. Chem.* **2002**, *114*, 4207-4209; *Angew. Chem. Int. Ed.* **2002**, *41*, 4035-4037.
- [113] A. Leitgeb, J. Wappel, C. Slugovc, *Polymer* **2010**, *51*, 2927-2946.
- [114] R. C. Pratt, B. G. G. Lohmeijer, J. L. Hedrick, *Chem. Rev.* **2007**, *107*, 5813-5840.
- [115] R. Walker, R. M. Conrad, R. H. Grubbs, *Macromolecules* **2009**, *42*, 599-605.
- [116] S. T. Nguyen, L. K. Johnson, R. H. Grubbs, *J. Am. Chem. Soc.* **1992**, *114*, 3974-3975.
- [117] K. B. Wiberg, *Angew. Chem.* **1986**, *98*, 312-322; *Angew. Chem. Int. Ed.* **1986**, *25*, 312-322.
- [118] M. Lichtenheldt, D. R. Wang, K. Vehlow, I. Reihardt, C. Kuhnel, U. Decker, S. Blechert, M. R. Buchmeiser, *Chem. Eur. J.* **2009**, *15*, 9451-9457.
- [119] K. Vehlow, D. R. Wang, M. R. Buchmeiser, S. Blechert, *Angew. Chem.* **2008**, *120*, 2655-2658; *Angew. Chem. Int. Ed.* **2008**, *47*, 2615-2618.
- [120] M. B. Smith, J. March, *Advanced Organic Chemistry: Reactions, Mechanisms, and Structure 6th ed.*, Wiley-Interscience, New York, **2007**.

- [121] T. M. Trnka, R. H. Grubbs, *Acc. Chem. Res.* **2001**, *34*, 18-29.
- [122] F. W. Hartner, J. Schwartz, S. M. Clift, *J. Am. Chem. Soc.* **1983**, *105*, 640-641.
- [123] E. O. Fischer, A. Maasböl, *Angew. Chem.* **1964**, *76*, 645-646; *Angew. Chem. Int. Ed.* **1964**, *3*, 580-581.
- [124] M. D. Fryzuk, S. S. H. Mao, M. J. Zaworotko, L. R. MacGillivray, *J. Am. Chem. Soc.* **1993**, *115*, 5336-5337.
- [125] R. H. Crabtree, *The Organometallic Chemistry of the Transition Metals 4th ed.*, New Wiley-Interscience, Jersey, **2005**.
- [126] J. F. Hartwig, *Organotransition Metal Chemistry: From Bonding to Catalysis*, University Science Books, California, **2010**.
- [127] C. W. Bielawski, R. H. Grubbs, *Prog. Polym. Sci.* **2007**, *32*, 1-29.
- [128] R. H. Grubbs, W. Tumas, *Nature* **1989**, *128*, 907-915.
- [129] A. Mutch, M. Leconte, F. Lefebvre, J. Basset, *J Mol. Cat.* **1998**, *133*, 191-199.
- [130] R. H. Grubbs, S. Chang, *Tetrahedron* **1998**, *54*, 4413-4450.
- [131] B. L. Quigley, R. H. Grubbs, *Chem. Sci.* **2014**, *5*, 501-506.
- [132] H. A. Brown, R. M. Waymouth, *Acc. Chem. Res.* **2013**, *46*, 2585-2596.
- [133] L. E. Rosebrugh, V. M. Marx, B. K. Keitz, R. H. Grubbs, *J. Am. Chem. Soc.* **2013**, *135*, 10032-10035.
- [134] T. C. Chung, *Functionalization of Polyolefins*, Academic Press, London, **2002**.
- [135] N. K. Boen, M. A. Hillmyer, *Chem. Soc. Rev.* **2005**, *34*, 267-275.
- [136] H. C. Brown, R. Liotta, G. W. Kramer, *J. Org. Chem.* **1978**, *43*, 1058-1063.
- [137] G. Natta, G. Mazzanti, P. Longi, F. Bernardini, *J Polym. Sci.* **1958**, *31*, 181-183.
- [138] T. C. Chung, D. Rhubright, *Macromolecules* **1993**, *26*, 3019-3025.
- [139] T. C. Chung, *Macromolecules* **1988**, *21*, 865-869.
- [140] Y. Uyama, K. Kato, Y. Ikada, *Adv. Polym. Sci.* **1998**, *137*, 1-39.
- [141] P. E. Gloor, Y. Tang, A. E. Kostanska, A. E. Hamielec, *Polymer* **1994**, *35*, 1012-1030.
- [142] M. Aglietto, R. Bertani, G. Ruggeri, F. Ciardelli, *Makromol. Chem.* **1992**, *193*, 179-186.
- [143] S. Ramakrishnan, E. Berluce, T. C. Chung, *Macromolecules* **1990**, *23*, 378-382.
- [144] W. Kaminsky, *Polyolefins: 50 years after Ziegler and Natta II*, Springer, Heidelberg, **2013**.

- [145] M. Atiqullah, M. Tinkl, R. Pfaendner, M. N. Akhtar, I. Hussain, *Polym. Rev.* **2010**, *50*, 178-230.
- [146] T. C. Chung, *Macromolecules* **2013**, *46*, 6671–6698.
- [147] G. Xu, D. Wang, M. R. Buchmeiser, *Macromol. Rapid Commun.* **2012**, *33*, 75-79.
- [148] K. Herz, D. A. Imbrich, J. Unold, G. Xu, M. Speiser, M. R. Buchmeiser, *Macromol. Chem. Phys.* **2013**, *214*, 1522-1527.
- [149] S. Marathe, S. Sivaram, *Macromolecules* **1994**, *27*, 1083-1086.
- [150] T. Wiedemann, G. Voit, A. Tchernook, P. Roesle, I. Goettker-Schnetmann, S. Mecking, *J. Am. Chem. Soc.* **2014**, *136*, 2078-2085.

2. Functional Polyolefins by Post-polymerization Modification



Synthetic route to the poly(COE)-g-PtBA.

The material covered in this chapter has appeared in

G. Xu, D. Wang, M. R. Buchmeiser, *Macromol. Rapid Commun.* **2012**, *33*, 75-79;

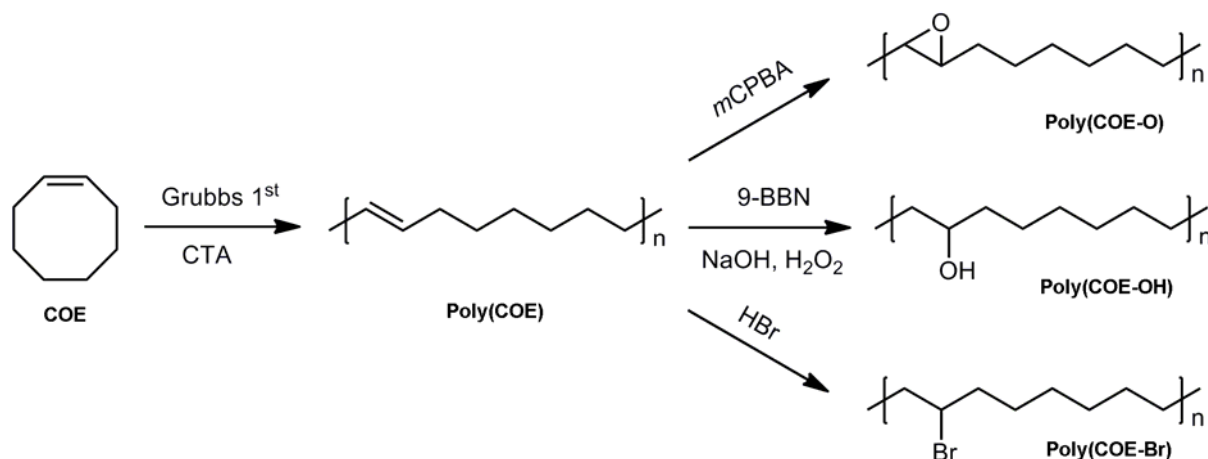
M. Ciftci, P. Batat, A. Demirel. G. J. Xu, M. R. Buchmeiser, Y. Yagci, *Macromolecules* **2013**, *46*, 6395-6401.

2.1 Introduction

Atom transfer radical polymerization (ATRP), one of the most common pseudo-living and controlled radical polymerization (CRP) techniques allows for the synthesis of macromolecules with controlled molecular weights and narrow molecular weight distributions. ATRP is also characterized by a great tolerance vs. functional groups, thereby allowing for the copolymerization of a variety of functional monomers.^[1-5] Most commonly, copper complexes are used and the underlying polymerization mechanism is well understood.^[6] A wide range of multidentate nitrogen-based ligands^[7-10] allows for the (co-)polymerization of various monomers including (meth)acrylates,^[11-13] styrenes,^[14-16] (meth)acrylamides,^[17-19] and acrylonitrile.^[20-22] Each of these monomers contains substituents that are able to stabilize propagating radicals. The initiator itself is typically an *activated* alkyl halide (RX). In order to obtain a controlled polymerization, the initiation rate must be faster than or equal to the propagation rate.^[23-24] Furthermore, the reformation of the 'dormant species' must be faster than propagation in order to guarantee for a low concentration of free radicals.

Brush- as well as graft-copolymers have been prepared *via* 'grafting to'^[25-28] and 'grafting through'^[29-30] methods, the 'grafting from' method is certainly the best one in terms of brush density.^[31-34] What all methods have in common is the use of *activated* alkyl halides, e.g., of α -bromocarboxylic esters. Such activated halogen-alkyl bonds are weaker than standard alkyl-halide bonds and thus more susceptible to homolytic cleavage by the Cu(I) complex. Vice versa, there are no reports on the ATRP of *non-activated* alkyl halides. Nonetheless, particularly the functionalization of such *non-activated* alkyl halides would offer a highly useful access to functionalized alkanes. Here, a simple one-step modification of ring-opening metathesis polymerization (ROMP) derived poly(*cis*-cyclooctene) (poly(COE)) is reported. The epoxidation, hydroxylation and hydrobromination reactions quantitatively converted the unsaturated polymer to the corresponding functional polymers. As determined by ¹H and ¹³C NMR, the hydrobrominated poly(COE), (poly(COE-Br)), has no apparent structural defects. Interestingly, the *non-activated* hydrobrominated poly(COE) can be used as a macroinitiator for ATRP or visible light-induced graft polymerization of *tert*-butyl acrylate (*t*BA). By varying the reaction conditions, a series of well-defined graft copolymers with different graft densities and graft lengths were prepared. The

maximum extent of grafting was approximately 80 mol-%. All polymers were fully characterized by ^1H NMR, ^{13}C NMR, gel permeation chromatography (GPC), FT-IR and differential scanning calorimetry (DSC).



Scheme 2.1 Synthesis of poly(COE) and the corresponding post-modification.

2.2 Results and Discussion

2.2.1 Synthesis of poly(COE)

Cis-cyclooctene (COE) was polymerized by using the 1st-generation Grubbs initiator (**G1**). In a ratio of **G1**:COE = 1:800, poly(COE) (*cis*:*trans*- = 15:85) with a number-average molecular weight (M_n) of 118,400 g·mol⁻¹ and a polydispersity index (PDI) of 1.56 was obtained. As the solubility of the further modified polymers is affected by polymer molecular weight, this high molecular weight poly(COE) was determined not to be a good choice for post-modification reactions. Poly(COE) with a relatively lower molecular weight can be produced either by increase the ratio of initiator to monomer or in the original initiator to monomer ratio but employing a chain transfer agent (CTA). Considering a minimum amount of **G1**, *cis*-4-octene was used as a CTA for the synthesis of lower molecular weight poly(COE). By employing a ratio of **G1**:COE:CTA = 1:800:6, a white powder poly(COE) (*cis*:*trans*- = 15:85) with a M_n of 41,000 g·mol⁻¹ and a PDI of 1.48 was successfully obtained. This way, the molecular weight of poly(COE) was significantly reduced and more than 50 mol-% of the initiator necessary under standard, CTA-free polymerization conditions could be saved. Both poly(COE)s with different molecular weight were used for the following modification reaction.

2.2.2 Epoxidation of poly(COE)



Scheme 2.2 Epoxidation of poly(COE).

Epoxidation of poly(COE) was carried out in dichloromethane in a Schlenk flask by the addition of *m*CPBA at 0 °C. The reaction was gradually warmed to room temperature and stirred overnight. After precipitating and drying, 0.51 g of poly(COE-O) was collected. The quantitative epoxidation of poly(COE) was confirmed by FT-IR spectroscopy. Figure 2.1 shows that the peaks at 2917 and 2850 cm⁻¹ belonging to the -CH₂- stretch vibration and the peaks at 1462 and 720 cm⁻¹ belonging to the C-H bend (or rock) vibration overlap for both poly(COE) and poly(COE-O). The signal for the =C-H stretch vibration at 3003 cm⁻¹, the peak of the C-C stretch vibration at 1070 cm⁻¹, and of the =C-H out-of-plane vibration at 964 cm⁻¹ of poly(COE) were completely replaced by the peak of the C-O stretch vibration at 1203, 1072 cm⁻¹ and the peak of the C-O-C vibration at 883 cm⁻¹ of poly(COE-O). After drying, the epoxidated poly(COE) was no longer soluble in toluene, 1,2,4-trichlorobenzene, xylene and chloroform even above 50 °C. This may be caused by inter- or intra-molecular hydrogen bonds. Differential scanning calorimetry (DSC) measurements didn't give any information about *T_g*, *T_c* or *T_m*.

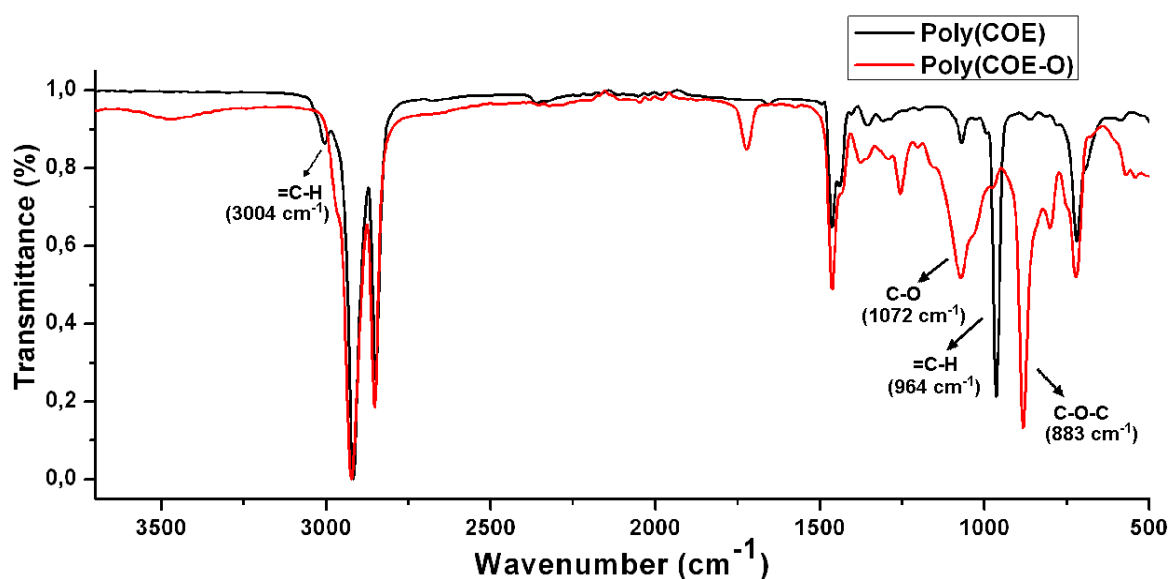
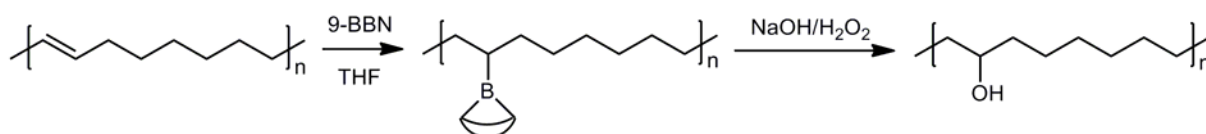


Figure 2.1 Comparison of IR spectra of poly(COE) to poly(COE-O).

2.2.3 Hydroxylation of poly(COE)



Scheme 2.3 Hydroxylation of poly(COE) based on hydroboration-oxidation reaction.

Hydroboration of poly(COE) was carried out in a THF solution by the dropwise addition of 9-BBN at 0 °C. The reaction was then kept at 50 °C for 16 h. The reaction intermediate of poly(COE-9-BBN) was captured to make sure that hydroboration was completed. The following oxidation was carried out by the addition of sodium hydroxide and hydrogen peroxide at 0 °C to the reaction solution. After the addition, the reaction was kept at 60 °C for 16 h. A white powder was at last collected. The FT-IR spectra show bands at 3324 and 1341 cm^{-1} are characteristic for the -OH groups. By comparing the IR spectra of poly(COE) and poly(COE-OH), except for the typical peaks that belonging to the -CH₂- stretch vibration (2917 and 2850 cm^{-1}) and the C-H bend (or rock) vibration (1462 and 720 cm^{-1}), the new signals at 1121 and 1032 cm^{-1} that belonging to the C-O stretch vibration of poly(COE-OH) were observed (Figure 2.2). This poly(COE-OH) was also insoluble in regular organic solvents after drying. DSC measurements revealed a T_m value of 133.7 °C for poly(COE-OH) (Figure 2.3), which is much higher than the T_m value of poly(COE) (*cis*:-*trans*- = 15:85) (T_m = 39 °C).

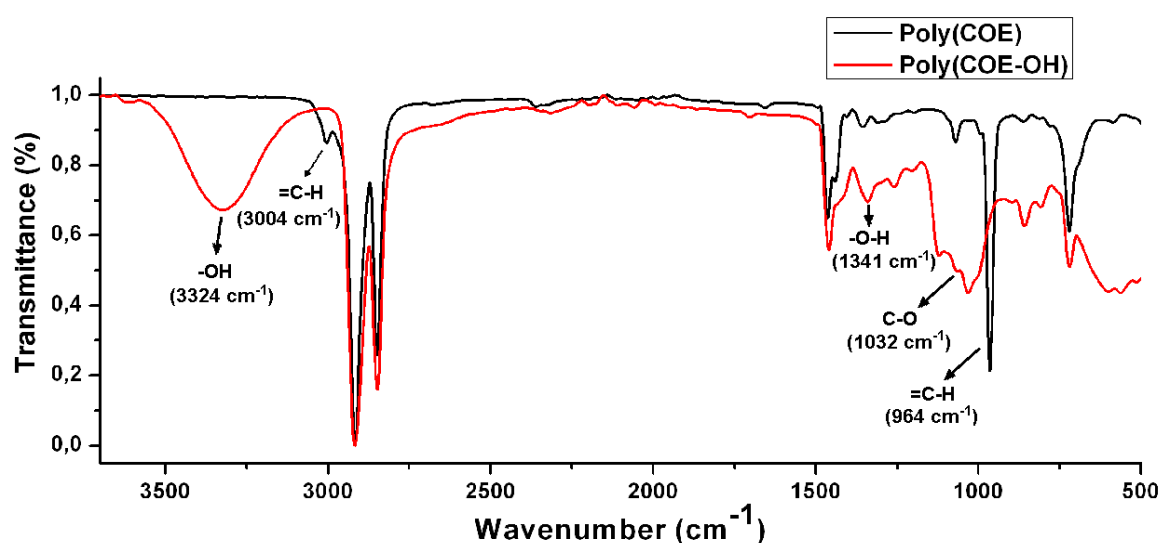


Figure 2.2 Comparison of IR spectra of poly(COE) to poly(COE-OH).

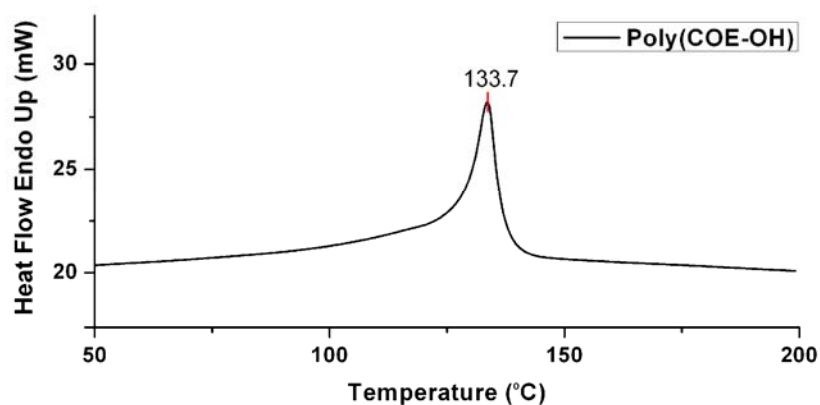


Figure 2.3 DSC plot of poly(COE-OH).

2.2.4 Hydrobromination of poly(COE)

Hydrobromination of poly(COE) was accomplished by treating a solution of poly(COE) in 1,2-dichloroethane with HBr (33 wt.-% solution in acetic acid) at 100 °C. Under these conditions, the conversion of the vinyl group to the alkyl bromide was quantitative as evidenced by ^1H NMR spectrum and without detectable polymer chain degradation. The complete disappearance of the $-\text{CH}=\text{CH}-$ resonance ($\delta = 5.38$ ppm) and the appearance of the resonance of $-\text{CHBr}-$ ($\delta = 4.02$ ppm) are shown in Figure 2.4. Complete conversion of the vinyl group to the alkyl bromide was also confirmed by ^{13}C NMR spectrum. As shown in Figure 2.5, the quantitative disappearance of the resonances at $\delta = 130.0$ and 130.04 ppm corresponding to the double bonds and the appearance of resonance at $\delta = 59.12$ ppm corresponding to the alkyl bromide group were also observed.

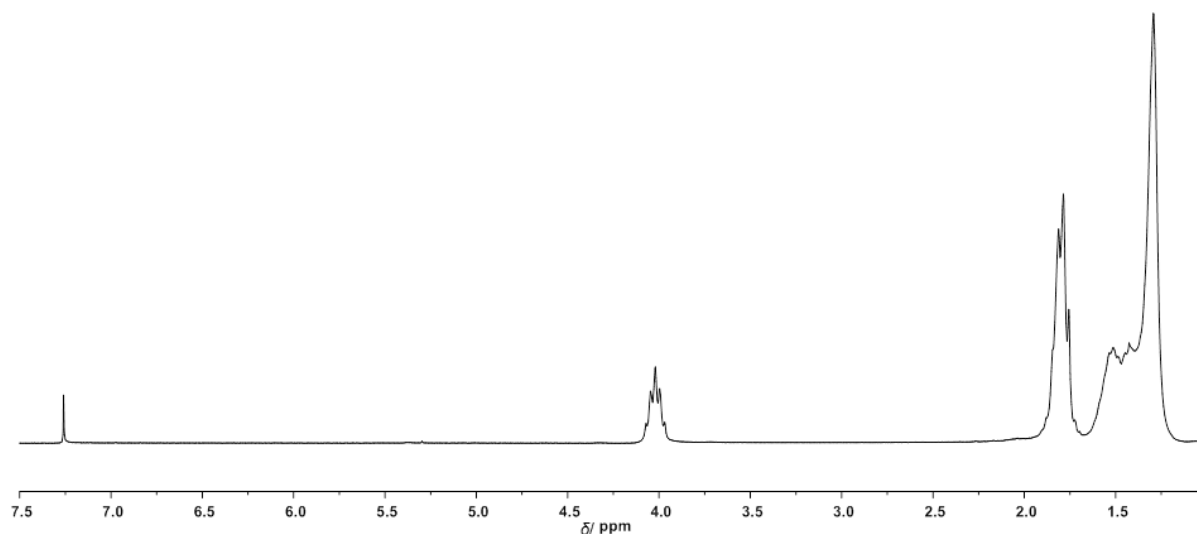


Figure 2.4 ^1H NMR spectrum of poly(COE-Br) (CDCl_3).

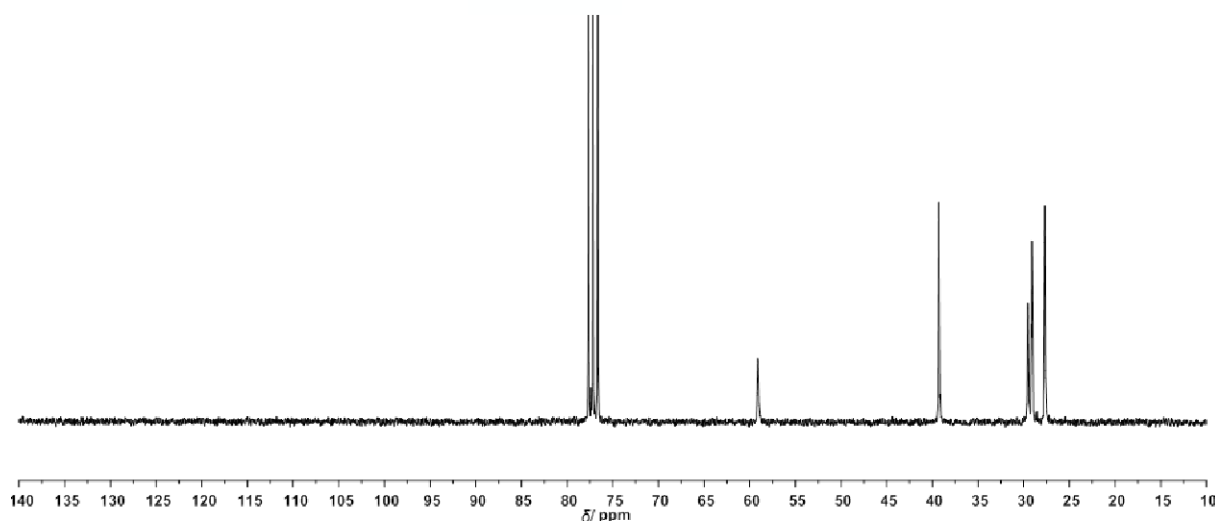


Figure 2.5 ^{13}C NMR spectrum of poly(COE-Br) (CDCl_3).

The quantitative hydrobromination of poly(COE) was also confirmed by FT-IR spectroscopy. Figure 2.6 shows that the peaks at 2917 and 2850 cm^{-1} belonging to the $-\text{CH}_2-$ stretch vibration and the peaks at 1462 and 720 cm^{-1} belonging to the C-H bend (or rock) vibration overlap for both poly(COE) and poly(COE-Br). Instead, the peak of the $=\text{C}-\text{H}$ stretch vibration at 3003 cm^{-1} , the peak of the C-C stretch vibration at 1070 cm^{-1} , and the $=\text{C}-\text{H}$ out-of-plane vibration at 963 cm^{-1} of poly(COE) were completely replaced by the peak of the C-Br stretch vibration of poly(COE-Br) at 613 and 530 cm^{-1} . GPC measurements vs. PS revealed that the poly(COE-Br), possessed a M_n of $54,000\text{ g}\cdot\text{mol}^{-1}$ and a PDI of 1.58 .

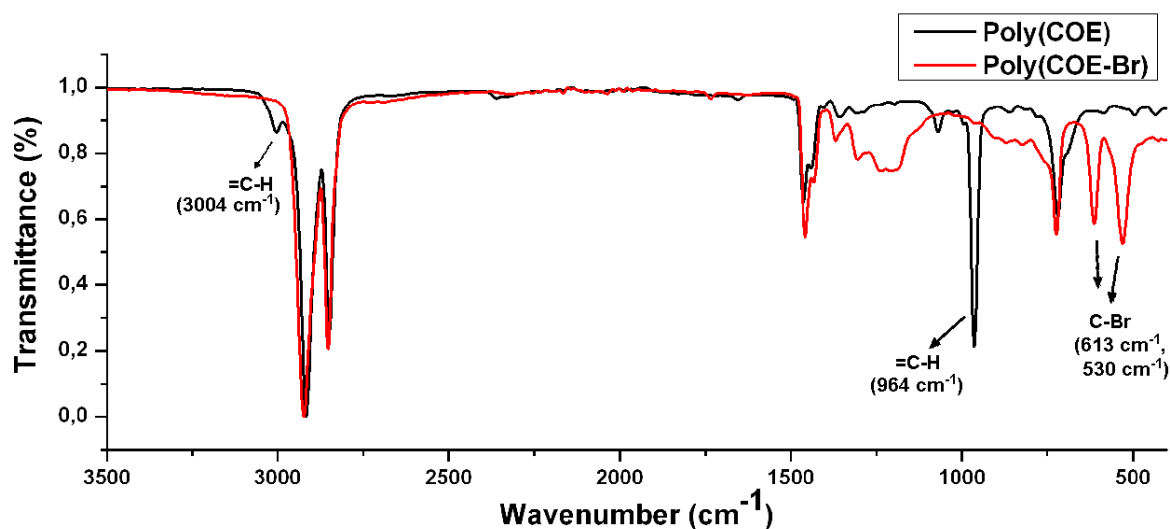
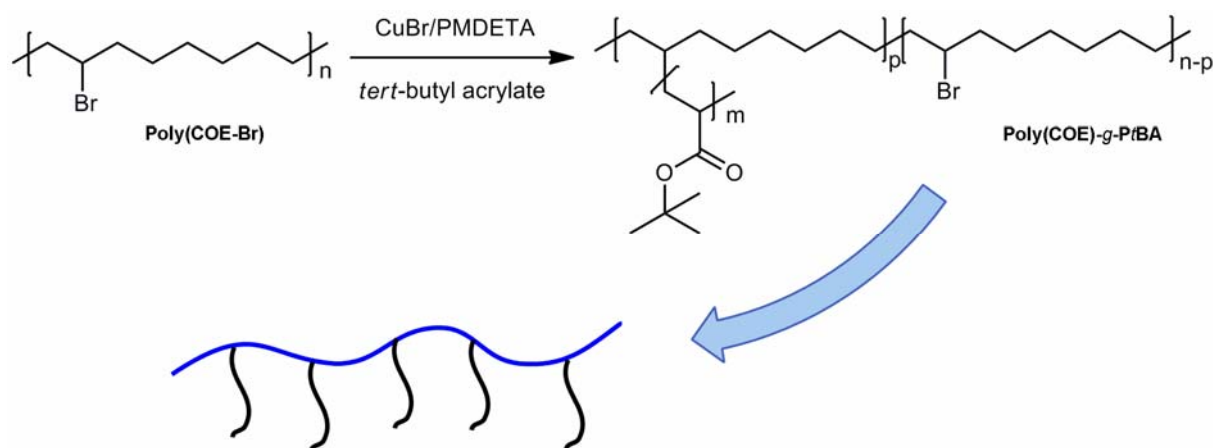


Figure 2.6 Comparison of IR spectra of poly(COE) to poly(COE-OH).

2.2.5 Poly(ethylene)-graft-poly(*tert*-butyl acrylate) via ATRP



Scheme 2.4 Synthetic route to the poly(COE)-*g*-PtBA = PE-*g*-PtBA copolymer.

Atom-transfer radical graft polymerization of *tert*-butyl acrylate (*t*BA) on poly(COE-Br) was carried out in toluene at elevated temperature using Cu(I)Br and pentamethyldiethylenetriamine (PMDETA) (Scheme 2.4). The graft-polymerization results are summarized in Table 1. With increasing amounts of *t*BA, the fraction of the bromo-groups from where a graft chain can be started can be adjusted between 25-80 mol-% (Table 2.1, entries 1-4). In contrast, increasing amounts of catalyst did not increase the number of graft chains (Table 2.1, entries 5-6). Increasing the reaction temperature to 100°C or the reaction time to 130 h (Table 2.1, entries 7-10) did not significantly increase the number of grafted PtBA chains but slightly

increased the overall molecular weight of the *g*-copolymer. Noteworthy, all *g*-copolymers possessed unimodal molecular weight distributions ($1.54 < \text{PDI} < 2.4$) indicating a fairly homogeneous distribution of the *t*BA *g*-chains (Figure 2.7).

Table 2.1 Graft copolymerization of *t*BA^a from poly(COE-Br)^b.

#	poly[COE-Br] ₀ : <i>t</i> BA ₀ : [CuBr] ₀ :[PMDETA] ₀	<i>t</i> (h)	T (°C)	<i>M</i> _n (g·mol ⁻¹)	PDI	Grafting (%) ^c	DP _(<i>t</i>BA) ^d
1	1:20:1:1	110	90	57,000	1.55	25	1
2	1:50:1:1	110	90	93,000	1.78	58	3
3	1:100:1:1	110	90	105,000	2.10	69	2
4	1:200:1:1	110	90	230,000	1.54	80	14
5	1:50:2:2	110	90	101,000	1.80	51	4
6	1:200:2:2	110	90	133,000	2.04	76	3
7	1:50:1:1	110	100	59,000	2.36	58	1
8	1:100:1:1	110	100	107,000	1.98	77	2
9	1:50:1:1	130	100	64,000	2.26	65	1
10	1:100:1:1	130	100	121,000	1.96	79	3

^a Graft copolymerization was carried out at T = 90 °C, poly(COE-Br) = 3 % (w/v) in toluene; ^b *M*_n of (polyCOE-Br) = 54,000 g·mol⁻¹, PDI = 1.58; ^c percentage of bromoalkyl groups that started a *g*-polymer chain; ^d degree of polymerization of the *g*-chains.

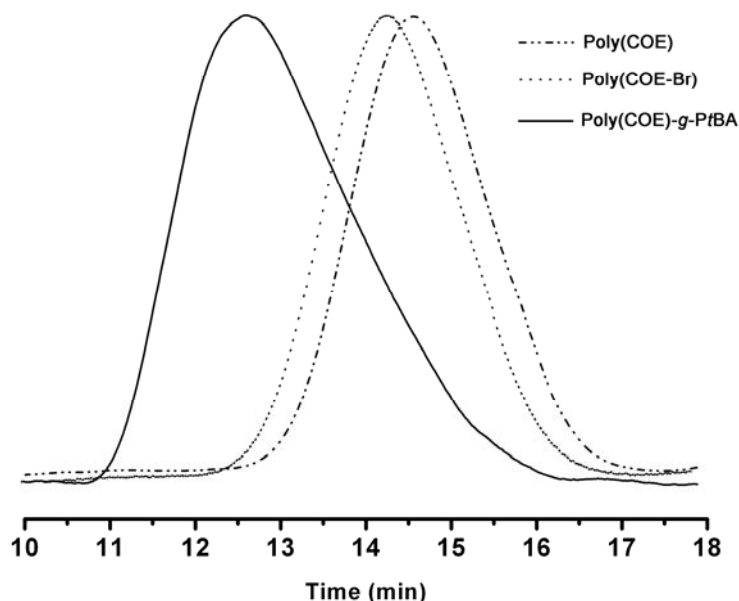


Figure 2.7 GPC profiles of poly(COE), Poly(COE-Br) and PE-*g*-PtBA (Table 2.1, entry 4).

Compared to the ^1H NMR spectra of poly(COE-Br) (Figure 8), the one of PE-*g*-PtBA show residual signals of the CHBr moieties around $3.9 < \delta < 4.1$ ppm, confirming an initiation efficiency $< 100\%$. The emergence of a new resonance at $\delta = 2.22$ ppm is attributed to the $-\text{CH}_2\text{CH}-$ protons of the grafted PtBA. In the ^{13}C NMR spectra (Figure 2.9), the appearance of the carbonyl and tertiary carbon signals at $\delta = 174.3$ and 80.5 ppm and a weak resonance of the alkyl halide at $\delta = 59.0$ ppm confirm the grafting of PtBA from poly(COE-Br).

FT-IR spectra (Figure 2.10) show that the peaks at 2929 and 2856 cm^{-1} belonging to the $-\text{CH}_2-$ stretch vibration and the peaks at 1451 and 752 cm^{-1} belonging to the C-H bend (or rock) vibration overlap for poly(COE-Br) and PE-*g*-PtBA. The peak of the CH_3 stretch (and scissoring) vibration at 2976 , 1391 , and 1367 cm^{-1} , the peak of the C=O stretch vibration at 1724 cm^{-1} , the peak of the C-O stretch vibration at 1254 and 1142 cm^{-1} , and of the C-O-C vibration at 845 and 801 cm^{-1} of PE-*g*-PtBA replace the peak of the C-Br stretch vibration of poly(COE-Br) at 613 and 530 cm^{-1} .

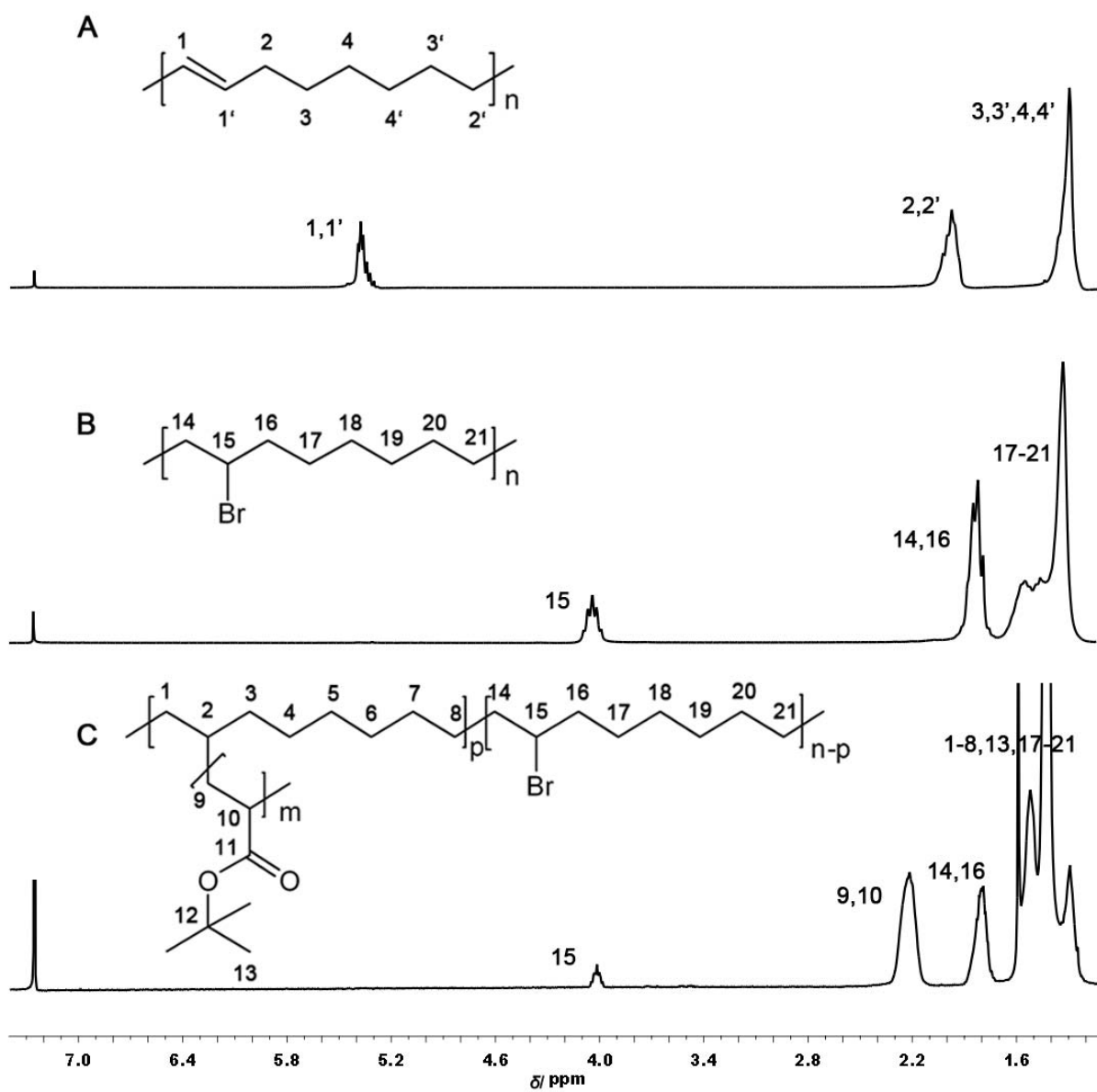


Figure 2.8 ^1H NMR spectra of A) poly(COE), B) poly(COE-Br) and C) PE-*g*-PtBA (CDCl_3).

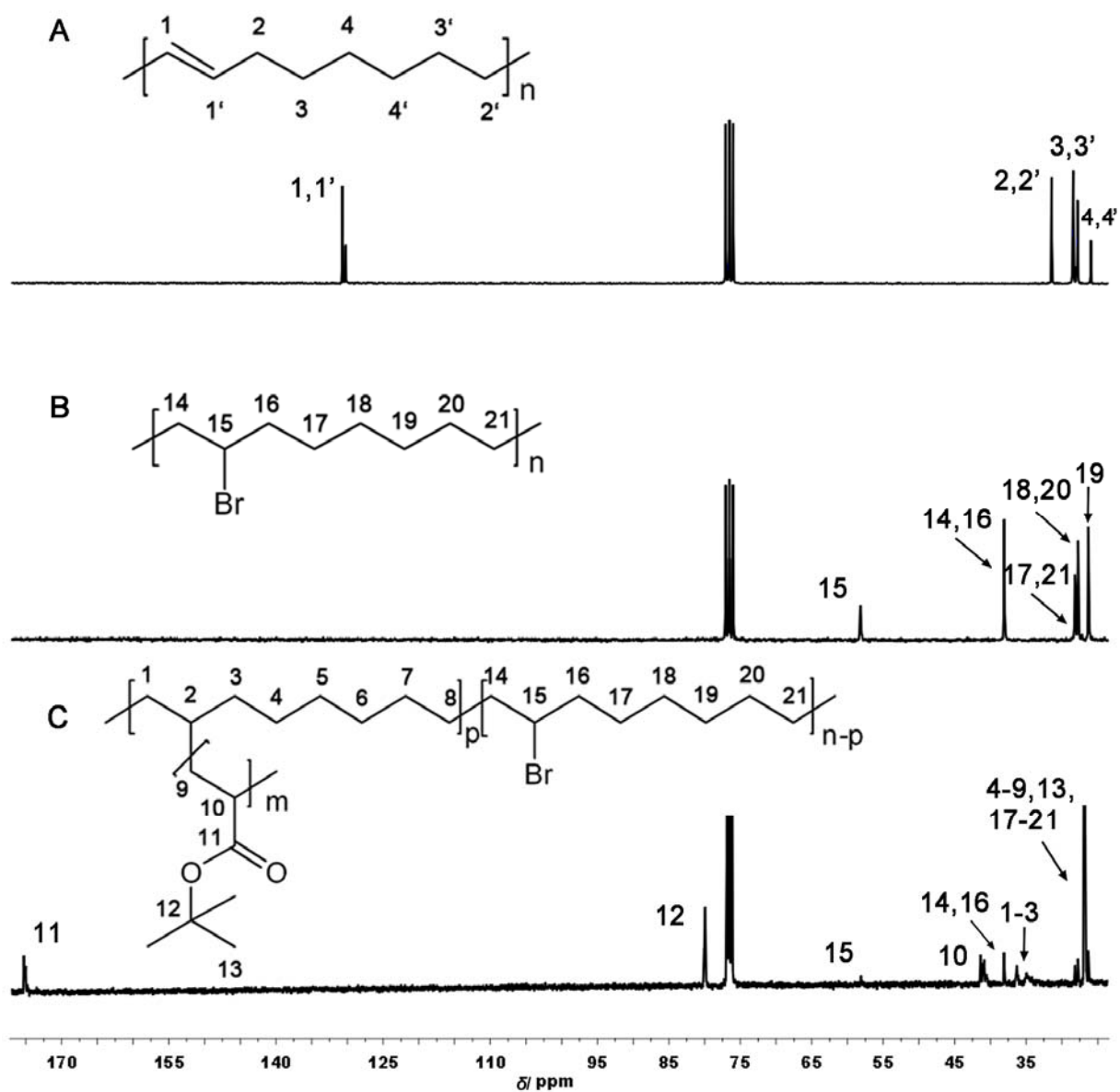


Figure 2.9 ^{13}C NMR spectra of A) poly(COE), B) poly(COE-Br) and C) PE-g-PtBA (CDCl_3).

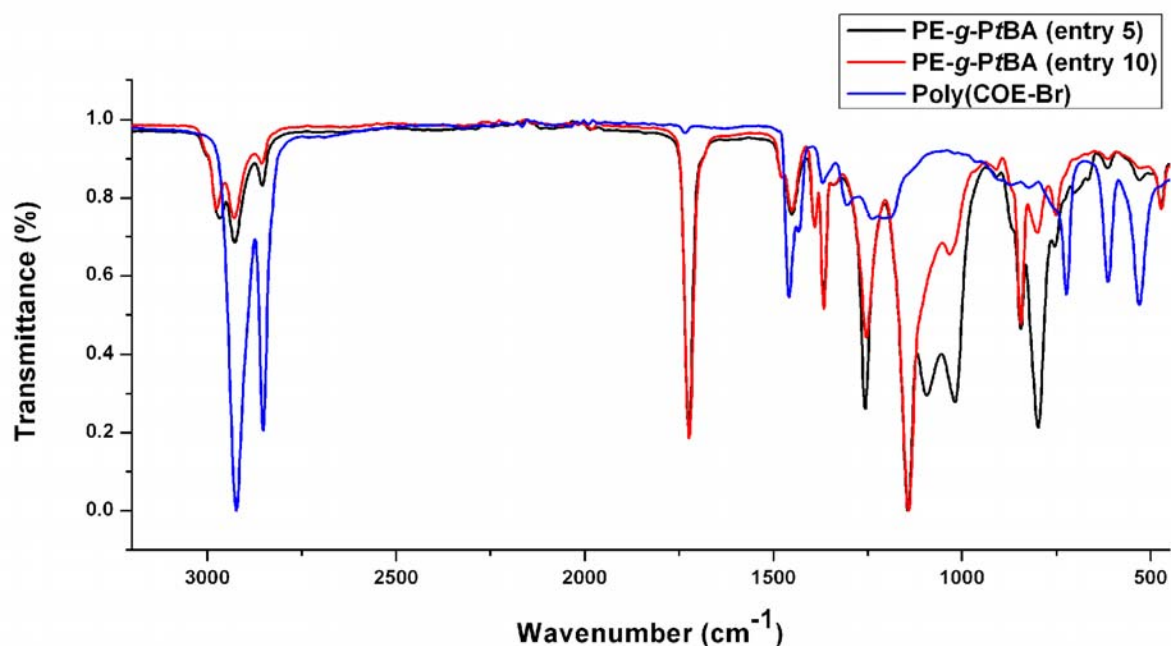


Figure 2.10 FT-IR spectra of poly(COE-Br) and PE-*g*-PtBA (Table 2.1, entries 5 and 10).

The *t*BA content in the graft copolymer can be calculated based on the ^1H NMR spectrum by using equation (1),^[35]

$$t\text{BA/mol-}\% = \left[\frac{b+c}{3a+b+c} \right] \times 100 \% \quad (1)$$

where a represents the integrated peak area at $\delta = 4.02$ ppm for the CHBr proton of the poly(COE-Br) part, b and c represent the total integrated peak area at $\delta = 2.22$ ppm corresponding to the three protons in the $-\text{CH}_2-$ and $-\text{CH}-$ moieties of the grafted PtBA. The grafting-% of these polymers is shown in Table 2.1. The number of *t*BA repeat units in each brush chain ranged from 1 to 14. All GPC traces of poly(COE), poly(COE-Br) and PE-*g*-PtBA showed a unimodal molecular weight distribution and a significant shift of the maximum value towards higher molecular weights. This strongly suggests that the entire graft copolymerization occurred without any detectable amounts ($< 5\%$) of free homopolymer, i.e. of PtBA. All copolymers displayed a single melting point (T_m) in DSC, further supporting the formation of one copolymer (Figure 2.11). With increasing monomer incorporation,

the T_m values of the *g*-copolymers decreased from 51 to 42°C. This lowering in T_m is attributed to the increasingly disturbed packing of the linear PE chains.

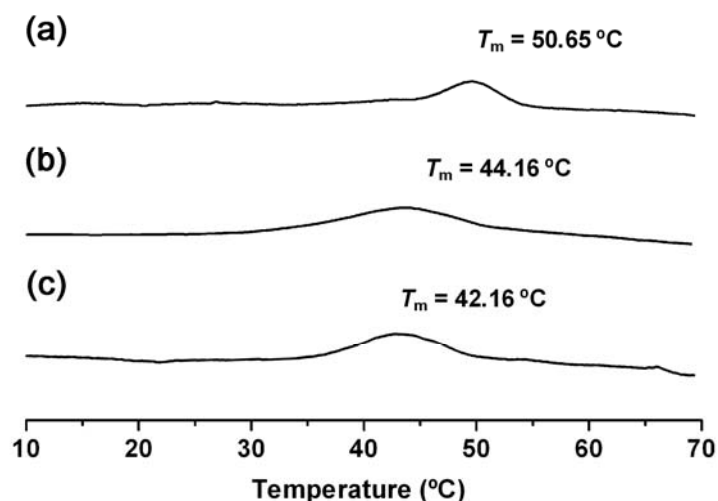
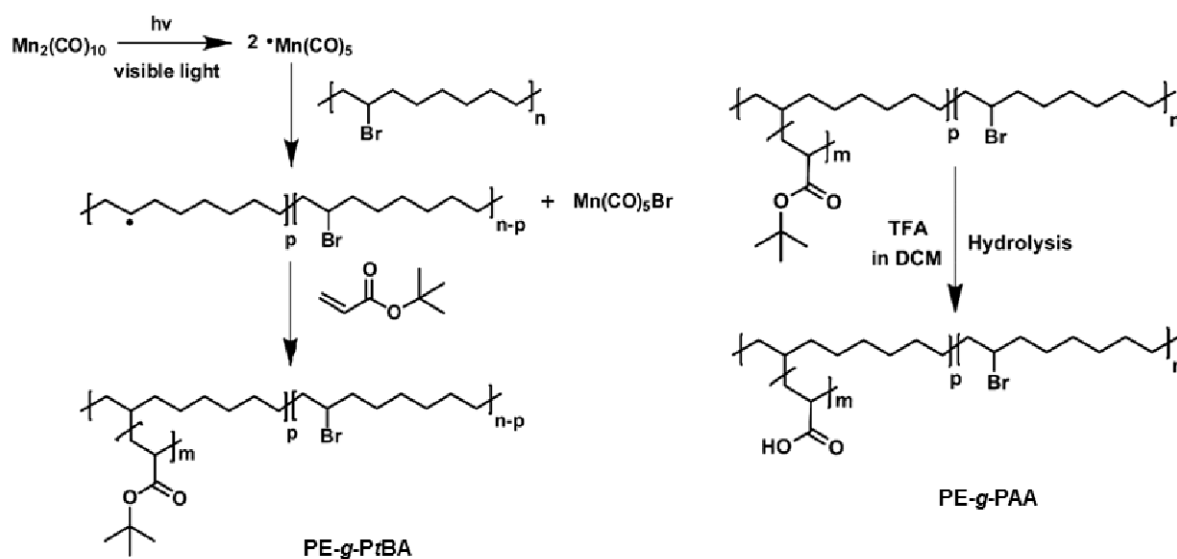


Figure 2.11 DSC plots of poly(COE)-*g*-PtBA copolymers (a) entry 2, (b) entry 3, (c) entry 4, Table 2.1.

2.2.6 Visible light-induced grafting of polyolefins

Visible light-induced free radical polymerization of *tert*-butyl acrylate (*t*BA) using $\text{Mn}_2(\text{CO})_{10}$ in the presence of poly(COE-Br) was carried out by the group of Professor Yagci of the Istanbul Technical University.^[36] As shown in Scheme 2.5, *tert*-butyl acrylate was successfully grafted to the macroinitiator poly(COE-Br) under UV light in the presence of $\text{Mn}_2(\text{CO})_{10}$. Depending on the dimanganese decacarbonyl $\text{Mn}_2(\text{CO})_{10}$ concentration and irradiation time, the grafting density and efficiency were in the range of 68-73 mol-% based on the bromoalkyl groups. Next, the *t*BA moieties of PE-*g*-PtBA were converted into acrylic acid units through acidic hydrolysis to generate PE-*g*-PAA copolymers.



Scheme 2.5 Visible light-induced graft copolymerization of *t*BA from poly(COE-Br) by using $\text{Mn}_2(\text{CO})_{10}$ followed by the hydrolysis of PE-*g*-PtBA to PE-*g*-PAA.

Table 2.2 Visible light-induced graft copolymerization of *t*BA from poly(COE-Br)^a by using $\text{Mn}_2(\text{CO})_{10}$.

run	Poly(COE-Br)/ <i>t</i> BA/ $\text{Mn}_2(\text{CO})_{10}$	<i>t</i> (h)	Conv. (%) ^b	M_n (g·mol ⁻¹)	PDI	Grafting (%) ^c
1	1/50/0.5	4	27	570,000	3.26	68
2	1/50/0.25	4	24	634,000	2.79	72
3	1/50/0.125	4	34	628,000	3.40	73
4	1/50/0.125	2	33	300,000	2.60	69
5	1/100/0.0125	2	31	265,900	1.46	71

^a $M_n(\text{poly}(\text{COE-Br})) = 41,000 \text{ g}\cdot\text{mol}^{-1}$, PDI = 2.11; ^b Conversion of the monomer was determined gravimetrically; ^c Degree of grafting: percentage of bromoalkyl groups that started a *g*-polymer chain.

As can be seen from Table 2.2, neither the amount of $\text{Mn}_2(\text{CO})_{10}$ nor the irradiation time significantly affected the conversion of *t*BA or the degree of grafting. However, at low $\text{Mn}_2(\text{CO})_{10}$ concentrations, comparably low molecular weight polymers with narrow polydispersity were obtained. Notably, compared to the ATRP route, the overall polydispersities of the graft copolymers obtained by photochemical means were broader. This can be expected because in the photochemical route, the

initiating free radicals are continuously formed by irradiation; growing polymer chains with large differences in chain lengths are present at the same time.

2.3 Conclusions

In summary, unsaturated poly(COE) was effectively converted to epoxidized poly(COE-O). Alternatively, hydroxyl- and bromo- groups could be introduced. A facile chemical modification of poly(COE) via quantitative hydrobromination and the corresponding graft copolymerization of *tert*-butyl acrylate by ATRP or visible light-induced from *non-activated alkyl* bromide moieties has been elucidated. Overall, a series of well-defined functional poly(ethylene) graft copolymers with high molecular weight have been successfully synthesized. This approach thus presents a straightforward access to functional polyolefins.

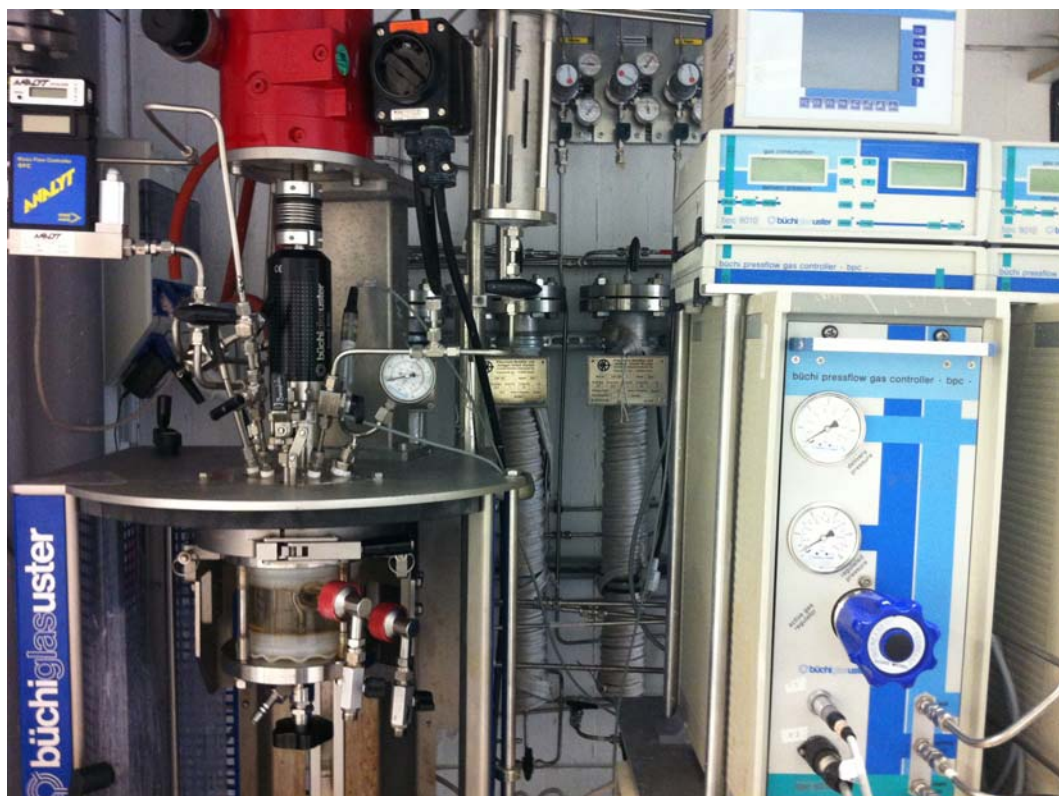
2.4 References

- [1] M. Kamigaito, T. Ando, M. Sawamoto, *Chem. Rev.* **2001**, *101*, 3689-3745.
- [2] A. Limer, D. M. Haddleton, *Macromolecules* **2006**, *39*, 1353-1358.
- [3] A. J. D. Magenau, N. C. Strandwitz, A. Gennaro, K. Matyjaszewski, *Science* **2011**, *332*, 81-84.
- [4] K. Matyjaszewski, J. Xia, *Chem. Rev.* **2001**, *101*, 2921-2990.
- [5] V. Percec, A. V. Popov, E. Ramirez-Castillo, M. Monteiro, B. Barboiu, O. Weichold, A. D. Asandei, C. M. Mitchell, *J. Am. Chem. Soc.* **2002**, *124*, 4940-4941.
- [6] J. S. Wang, K. Matyjaszewski, *J. Am. Chem. Soc.* **1995**, *117*, 5614-5615.
- [7] D. M. Haddleton, C. B. Jasieczek, M. J. Hannon, A. J. Shooter, *Macromolecules* **1997**, *30*, 2190-2193.
- [8] A. A. Kavitha, N. K. Singha, *Macromolecules* **2010**, *43*, 3193-3205.
- [9] M. Ouchi, T. Terashima, M. Sawamoto, *Chem. Rev.* **2009**, *109*, 4963-5050.
- [10] W. Tang, A. K. Nanda, K. Matyjaszewski, *Macromol. Chem. Phys.* **2005**, *206*, 1171-1177.
- [11] C. R. Becer, R. Hoogenboom, D. Fournier, U. S. Schubert, *Macromol. Rapid Commun.* **2007**, *28*, 1161-1166.

- [12] V. Percec, F. Asgarzadeh, *J. Polym. Sci. A: Polym. Chem.* **2001**, *39*, 1120-1135.
- [13] X. S. Wang, S. F. Lascelles, R. A. Jackson, S. P. Armes, *Chem. Commun.* **1999**, 1817-1818.
- [14] Y. Kotani, M. Kamigaito, M. Sawamoto, *Macromolecules* **2000**, *33*, 6746-6751.
- [15] R. Liu, Z. Li, D. Yuan, C. Meng, Q. Wu, F. Zhu, *Polymer* **2011**, *52*, 356-362.
- [16] L. Sauguet, C. Boyer, B. Ameduri, B. Boutevin, *Macromolecules* **2006**, *39*, 9087-9101.
- [17] O. J. Cayre, N. Chagneux, S. Biggs, *Soft Matter*. **2011**, *7*, 2211-2234.
- [18] J. Raynaud, N. Liu, M. Fevre, Y. Gnanou, D. Taton, *Polym. Chem.* **2011**, *2*, 1706-1712.
- [19] G. Zheng, C. Pan, *Polymer* **2005**, *46*, 2802-2810.
- [20] A. Berkefeld, S. Mecking, *Angew. Chem.* **2008**, *120*, 2572-2576; *Angew. Chem. Int. Ed.* **2008**, *47*, 2538-2542.
- [21] A. Debuigne, J. Warnant, R. Jérôme, I. Voets, A. de Keizer, M. A. Cohen Stuart, C. Detrembleur, *Macromolecules* **2008**, *41*, 2353-2360.
- [22] X. H. Liu, Y. G. Li, Y. Lin, Y. S. Li, *J. Polym. Sci. A: Polym. Chem.* **2007**, *45*, 1272-1281.
- [23] R. N. Y. Kwak, K. Matyjaszewski, *Macromolecules* **2008**, *41*, 4585-4596.
- [24] K. Matyjaszewski, J. L. Wang, T. Grimaud, D. A. Shipp, *Macromolecules* **1998**, *31*, 1527-1534.
- [25] H. Gao, K. Matyjaszewski, *J. Am. Chem. Soc.* **2007**, *129*, 6633-6639.
- [26] U. Schulze, T. Fónagy, H. Komber, G. Pompe, J. Pionteck, B. Iván, *Macromolecules* **2003**, *36*, 4719-4726.
- [27] C. Boyer, B. Boutevin, J. J. Robin, *Polymer Degradation and Stability* **2005**, *90*, 326-339.
- [28] J. J. Robin, C. Boyer, B. Boutevin, C. Loubat, *Polymer* **2008**, *49*, 4519-4528.
- [29] D. Le, V. Montembault, J. C. Soutif, M. Rutnakornpituk, L. Fontaine, *Macromolecules* **2010**, *43*, 5611-5617.
- [30] Y. Xia, B. D. Olsen, J. A. Kornfield, R. H. Grubbs, *J. Am. Chem. Soc.* **2009**, *131*, 18525-18532.
- [31] C. Boyer, A. H. Soeriyadi, P. J. Roth, M. R. Whittaker, T. P. Davis, *Chem. Commun.* **2011**, *47*, 1318-1320.
- [32] W. Ma, H. Otsuka, A. Takahara, *Chem. Commun.* **2011**, *47*, 5813-5815.

- [33] K. Matyjaszewski, T. E. Patten, J. Xia, *J. Am. Chem. Soc.* **1997**, *119*, 674-680.
- [34] K. Matyjaszewski, N. V. Tsarevsky, *Nature Chem.* **2009**, *1*, 276-288.
- [35] D. J. Haloi, K. Naskar, N. K. Singha, *Macromol. Chem. Phys.* **2011**, *212*, 478-484.
- [36] M. Ciftci, P. Batat, A. Demirel, G. J. Xu, M. R. Buchmeiser, Y. Yagci, *Macromolecules* **2013**, *46*, 6395-6401.

3. Bis(diamido)silylene Zirconium^{IV} Complexes Containing the Bromoborane Motifs in Vinyl Insertion Polymerization: On the Role of Cyclopentene



The material covered in this chapter has appeared in

G. V. Narayana, G. J. Xu, D. R. Wang, W. Frey, M. R. Buchmeiser, *ChemPlusChem* **2014**, 79, 151-162;

G. J. Xu, G. V. Narayana, M. Speiser, D. R. Wang, M. R. Buchmeiser, *Macromol. Chem. Phys.* **2014**, DOI: 10.1002/macp.201400032.

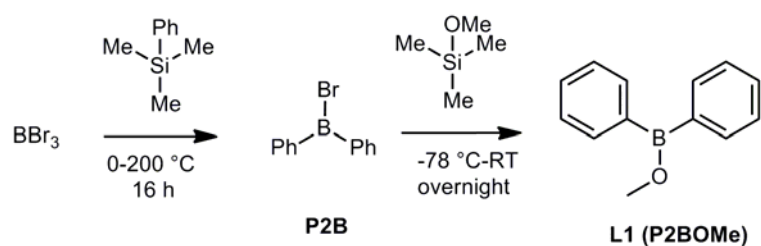
3.1 Introduction

Polyolefins can be prepared either via vinyl insertion polymerization (VIP)^[1-4] or ring-opening metathesis polymerization (ROMP).^[5-8] Cyclic olefin copolymers (COCs), i.e. copolymers of ethylene (E) or α -olefins with cyclic olefins such as norborn-2-ene (NBE) or cyclopentene (CPE), are an important family of thermoplastic amorphous polymers.^[9-11] Among these, ethylene-norborn-2-ene (E-NBE) copolymers are of substantial interest because of their excellent optical transparency, high glass transition temperature, and good heat resistance. Their stability against hydrolysis and chemical degradation combined with their stiffness make them interesting materials for optical applications, for example in compact discs, lenses, optical fibers or films.^[12-14]

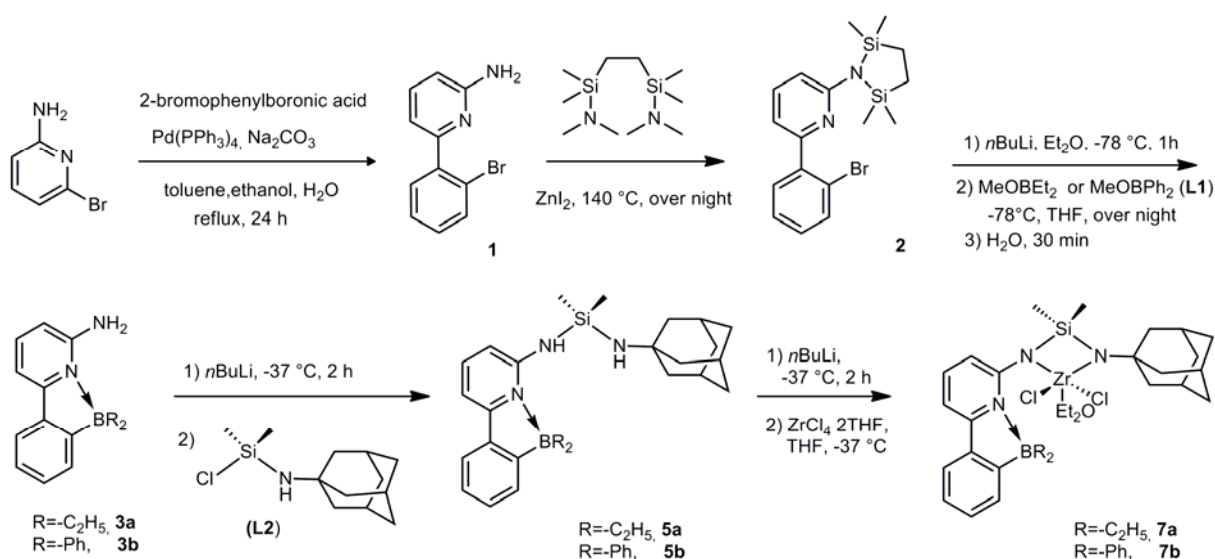
During the past twenty years, group IV metal complexes containing amide ligands emerged as promising pre-catalysts for olefin polymerization. Compared to the 14-electrons in Zr-biscyclopentadienyl $[\text{Cp}_2\text{ZrR}]^+$ complexes, 10-electrons in Zr-bisamido complexes $[(\text{R}_2\text{N})_2\text{ZrR}]^+$ formally have a lower electron count. This formal lower electron count results in a more electrophilic and therefore potentially more active catalyst fragment.^[3, 15-16] Inspired by earlier reports, we prepared two group IV complexes **Zr-1** and **Ti-1**, that is $[\text{Me}_2\text{Si}(\text{DbppN})_2\text{ZrCl}_2 \cdot (\text{THF})]$ (DbppN=6-(2-(diethylboryl)phenyl)pyrid-2-ylamido) and $[\text{Me}_2\text{Si}(\eta^5\text{-Me}_4\text{C}_5)(6\text{-(2-(diethylboryl)phenyl)pyrid-2-ylamido)TiCl}_2]$. These two complexes bear the aminoborane motif and can undergo α -H elimination process after activation by methylalumoxane (MAO) at high cyclic olefin concentration.^[17-18] Therefore, these catalysts can be used for the synthesis of COCs that contain both VIP- and ROMP-derived units, allowing for the synthesis of, e.g., poly(NBE)_{ROMP-co}-poly(NBE)_{VIP-co}-poly(E) or poly(COE)_{ROMP-co}-poly(COE)_{VIP-co}-poly(E). The obtained COCs are prone to functionalization through polymer analogous reactions, such as hydrogenation, epoxidation or hydrobromination, thereby granting access to functional polyolefins as already demonstrated for analogous polymers.^[19-22]

This particular reactivity of the above mentioned group IV complexes **Zr-1** and **Ti-1** made it necessary to identify additional specific structural characteristics apart from the aminoborane motif that are responsible for the unique reactivity of both **Zr-1** and

Ti-1. For these purposes, two ligands were designed and synthesized (**3a** and **3b**). The corresponding diamido Zr^{IV}-based complexes **7a** and **7b** (Scheme 1 and 2) were applied for homopolymerization of ethylene and copolymerization of ethylene with cyclopentene (E-CPE) and ethylene with NBE (E-NBE). Here, the polymerization conditions, catalyst activity, microstructure of the copolymers, ligand effects on olefin polymerization and the dramatic effect of high concentrations of CPE on polymerization activity were investigated.



Scheme 3.1 Synthesis of ligand **L1**.



Scheme 3.2 Syntheses of complexes **7a** and **7b**.

3.2 Results and Discussion

3.2.1 Syntheses of ligands and complexes

The aminoborane ligand **3a** and complex **7a** were synthesized according to the literature.^[18-19] To study the influence of the ligand on catalyst activity, the more bulky analog **3b** was designed and synthesized.^[24-25] Deprotonation of **3b** with *n*-

butyllithium in diethyl ether and reaction with **L2** yielded the diamino ligand **5b**. By deprotonation of **5b** with *n*-butyllithium and reaction with $\text{ZrCl}_4 \cdot 2\text{THF}$, complex **7b** was obtained in 30 % yield. The synthetic routes are shown in Scheme 1 and 2. The ligands and complexes were fully characterized by ^1H NMR, ^{13}C NMR, MS, elemental analysis and FT-IR. In addition, the structure of complex **7b** was determined by X-ray crystallography (Figure 3.1). Crystal information and selected bond lengths and angles are listed in Table 3.1 and 3.2. As boron is a highly electron-deficient atom, the lone pair of the neighbouring pyridine-N occupies its *p* orbital with a B-N bond distance of 1.59 Å.

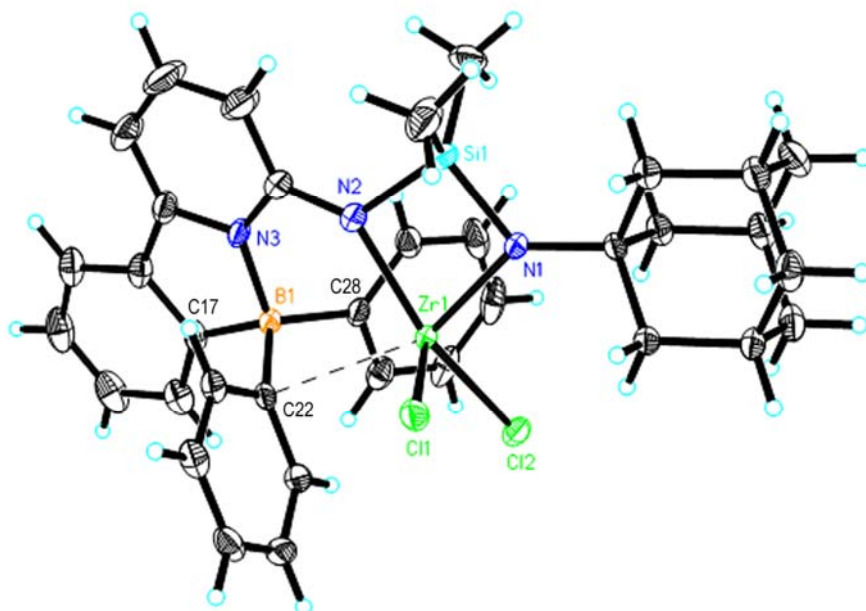


Figure 3.1 ORTEP drawing of complex **7b** (50 % thermal ellipsoids).

Table 3.1 Crystal data and structure refinement for complex **7b**.

Empirical formula	$\text{C}_{35}\text{H}_{38}\text{BCl}_2\text{N}_3\text{SiZr}$
Formula weight	701.70
Temperature	110(2) K
Crystal system, space group	Tetragonal, I -4
Unit cell dimensions	$a = 18.7084(6) \text{ \AA}$, $\alpha = 90^\circ$ $b = 18.7084(6) \text{ \AA}$, $\beta = 90^\circ$ $c = 22.1438(7) \text{ \AA}$, $\gamma = 90^\circ$
Volume	$7750.4(4) \text{ \AA}^3$
Z, Calculated density	8, 1.203 mg/m^3

Absorption coefficient	0.478 mm ⁻¹
F(000)	2896
Crystal size	0.68 x 0.21 x 0.12 mm
Theta range for data collection	1.84° to 28.27°
Limiting indices	-24<=h<=22, -17<=k<=24, -29<=l<=29
Reflections collected / unique	35211 / 9588 [R(int) = 0.0333]
Completeness to theta = 28.27	100.0 %
Absorption correction	Semi-empirical from equivalents
Max. and min. transmission	0.7457 and 0.6815
Refinement method	Full-matrix least-squares on F ²
Data / restraints / parameters	9588 / 0 / 390
Goodness-of-fit on F²	1.046
Final R indices [I>2sigma(I)]	R ₁ = 0.0261, wR ₂ = 0.0637
R indices (all data)	R ₁ = 0.0296, wR ₂ = 0.0650
Absolute structure parameter	-0.01(2)
Largest diff. peak and hole	0.302 and -0.228 e·Å ⁻³

Table 3.2 Bond lengths [Å] and angles [°] for **7b**.

Bond Distances			
Zr(1)-N(1)	2.0178(16)	Zr(1)-N(2)	2.1341(16)
Zr(1)-Cl(1)	2.4075(5)	Zr(1)-Cl(2)	2.4197(5)
Zr(1)-C(22)	2.7161(17)	Zr(1)-Si(1)	2.8714(5)
Si(1)-N(1)	1.7484(16)	Si(1)-N(2)	1.7668(17)
Si(1)-C(34)	1.859(3)	Si(1)-C(35)	1.862(2)
B(1)-N(3)	1.591(3)	B(1)-C(17)	1.621(3)
B(1)-C(28)	1.642(3)	B(1)-C(22)	1.654(3)
Bond Angles			
N(1)-Zr(1)-N(2)	74.52(6)	Cl(1)-Zr(1)-Cl(2)	102.731(18)
N(1)-Zr(1)-Cl(1)	94.59(5)	N(1)-Zr(1)-C(22)	154.96(6)
N(2)-Zr(1)-Cl(1)	104.66(5)	N(2)-Zr(1)-C(22)	80.63(6)
N(1)-Zr(1)-Cl(2)	101.11(5)	Cl(1)-Zr(1)-C(22)	88.74(4)
N(2)-Zr(1)-Cl(2)	152.51(5)	Cl(2)-Zr(1)-C(22)	102.32(4)
N(1)-Zr(1)-Si(1)	36.96(4)	Cl(1)-Zr(1)-Si(1)	98.496(19)
N(2)-Zr(1)-Si(1)	37.85(5)	Cl(2)-Zr(1)-Si(1)	134.514(17)

C(22)-Zr(1)-Si(1)	118.01(4)	N(3)-B(1)-C(22)	109.28(16)
N(3)-B(1)-C(17)	97.80(14)	C(17)-B(1)-C(22)	108.67(15)
N(3)-B(1)-C(28)	111.38(15)	C(28)-B(1)-C(22)	116.24(14)
C(17)-B(1)-C(28)	111.88(16)		

3.2.2 Homopolymerization of ethylene

Group IV bisamido-complexes are known to present active pre-catalysts for olefin homo- and copolymerization.^[26-28] While non-bridged bisamido complexes showed only low activities ($< 20 \text{ kg}_{\text{polymer}}/\text{mol}_{\text{cat.}} \cdot \text{h} \cdot \text{bar}$), the bridged analogues allowed for high activities in the polymerization of α -olefins with typical values for polyethylene (PE) in the range of 3.5-5300 $\text{kg}_{\text{polymer}}/\text{mol}_{\text{cat.}} \cdot \text{h} \cdot \text{bar}$ and polypropylene (PP) in the range of 7-320 $\text{kg}_{\text{polymer}}/\text{mol}_{\text{cat.}} \cdot \text{h} \cdot \text{bar}$.^[29-34] In all these polymerizations, both the polymerization kinetics and the activity are strongly influenced by the chelate ring size.

With this background, the homopolymerization of ethylene by the action of complexes **7a** and **7b** activated by methylaluminoxane (MAO) was carried out in a ratio of catalyst:MAO = 1:2000 at $p = 4$ bar of ethylene gas. Moderate activities up to 128 $\text{kg} \cdot \text{mol}^{-1} \cdot \text{h}^{-1} \cdot \text{bar}^{-1}$ were observed. Linear PE with melting points in the range of $123 < T_m < 135$ °C measured by differential scanning calorimetry (DSC) was found. Molecular weights (M_n) were in the range of $102,000 < M_n < 630,000 \text{ g} \cdot \text{mol}^{-1}$. The polydispersity indexes (PDI) of PE produced by complexes **7a**/MAO and **7b**/MAO were relatively broad ($2.3 < \text{PDI} < 11$). As shown in Table 3.3, while keeping the ethylene pressure constant at 4 bar, an increase in temperature results in an increase in catalyst activity and in the M_n of resultant PE (Table 3.3, entries 1-3, entries 4-6). **7a**/MAO shows higher productivity than **7b**/MAO. This can be explained by the increasing steric bulk at the borane atom, i.e. switching from ethyl-substituted in **7a** to phenyl-substituted in **7b**, results in lower catalyst activity and lower molecular weights.

Table 3.3 Ethylene homopolymerization with **7a** and **7b** activated by MAO.

# ^a	Catalyst	<i>T</i> (°C)	Activity ^b	<i>M_n</i> ^c (g/mol)	<i>M_w</i> / <i>M_n</i> ^c	<i>T_m</i> ^d (°C)
1		50	93	325,000	11	133
2	7a	65	105	630,000	3.4	134
3		80	128	551,000	4.2	135
4		50	10	102,000	9	122
5	7b	65	14	121,000	7.7	124
6		80	90	340,000	2.3	125

^a Polymerization conditions: 500 mL autoclave, total volume of the reaction mixture 250 mL, catalyst:MAO = 1:2000, [catalyst] = 2×10^{-5} mol·L⁻¹, *p* = 4 bar of ethylene unless stated otherwise, toluene, *t* = 1 h; ^b kg·mol⁻¹·h⁻¹·bar⁻¹; ^c Determined by HT-GPC in 1,2,4-trichlorobenzene vs. PS; ^d Measured by DSC.

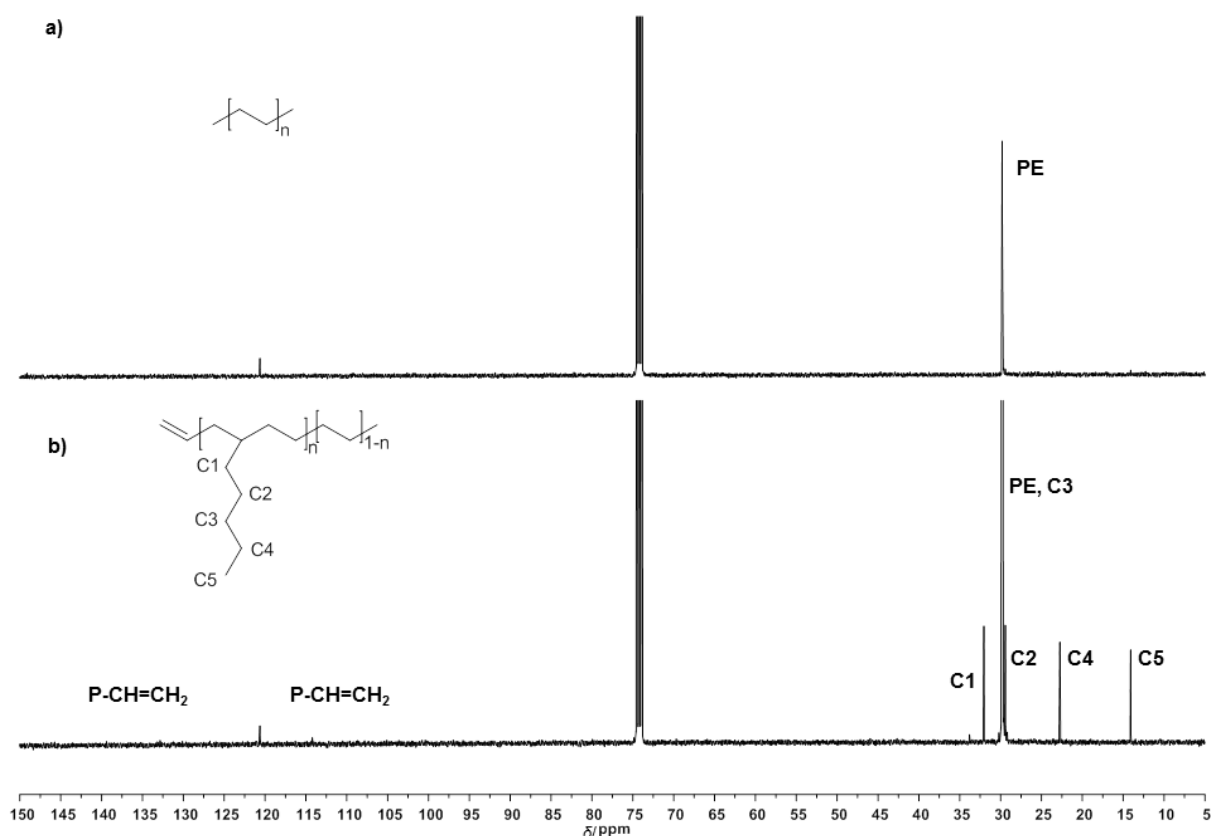


Figure 3.2 ¹³C NMR spectra of PE produced by the action of a) **7a**/MAO, b) **7b**/MAO (Table 3.3, entry 2 and entry 6) (1,1,2,2-[D₂]tetrachloroethane). The signal at $\delta = 120.64$ ppm is a solvent impurity. P = polymer chain.

It is worth to mention that PE produced by **7a**/MAO is a high-density polyethylene (HDPE), which confirmed by the relatively high melting points (T_m 133-135 °C) and less amount of branches (shown in the ^{13}C NMR). As depicted in Figure 3.2a, PE produced by **7a**/MAO shows a characteristic resonance at $\delta = 29.8$ ppm, no other side-chain branches were observed. While for PE produced by **7b**/MAO (Figure 3.2b), C1-C5 short-chain branches (63 branches per 1000 C-atoms) were clearly seen at $\delta = 14.1, 22.8, 29.4, 29.7$ and 32.1 ppm, terminal olefinic resonances at $\delta = 114$ and 139 ppm implicated that β -hydrogen transfer from the growing polymer chain to an upcoming olefin is at least one source of chain termination in **7b**/MAO. Chain transfer to the aluminium cocatalyst was implicated as the lone source of termination since olefinic resonances were absent in the NMR spectrum of PE produced by **7a**/MAO. Selected HT-GPC profiles of PE derived from **7a**/MAO and **7b**/MAO are shown in Figure 3.3.

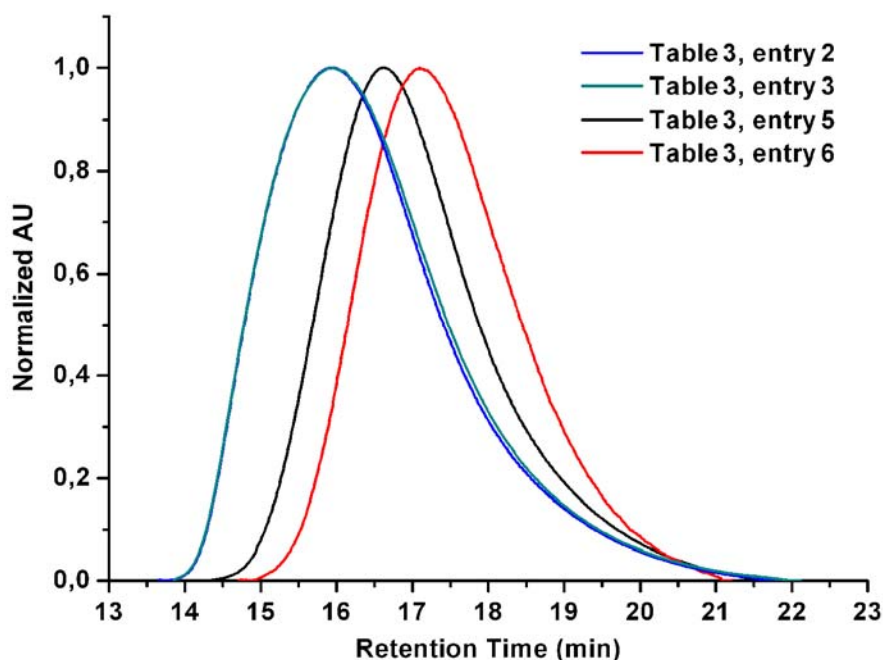


Figure 3.3 HT-GPC traces of PE produced by **7a**/MAO and **7b**/MAO.

3.2.3 Copolymerization of ethylene (E) with cyclopentene (CPE) (E-CPE)

Copolymerization of ethylene with CPE was conducted at 50 °C, 65 °C and 80 °C by using **7a**/MAO and **7b**/MAO. For entry 2 Table 3.4, about 3.5 vol.-% CPE (8.8 mL) was used with respect to the total reaction solution for copolymerization (250 mL). Catalyst activity was about $1050 \text{ kg}\cdot\text{mol}^{-1}\cdot\text{h}^{-1}\cdot\text{bar}^{-1}$ which is about 11 times compared

to ethylene homopolymerization (entry 1, Table 3.4). With the same CPE amount, an increase in temperature from 50 °C to 80 °C resulted in a further increase in catalyst activity up to 4000 kg·mol⁻¹·h⁻¹·bar⁻¹ but in a decrease in the molecular weight 443,000 < M_n < 92,000 g·mol⁻¹ (Table 3.4, entries 2 to 4). By decreasing the CPE amount from 3.5 vol.-% to 0.8 vol.-%, the catalyst activity slightly decreased but was still high as 3750 kg·mol⁻¹·h⁻¹·bar⁻¹ (Table 3.4, entries 4 and 5). Upon reducing the CPE amount to 0.1 vol.-%, catalyst activity dropped sharply to 250 kg·mol⁻¹·h⁻¹·bar⁻¹, which is about the same as the one found for ethylene homopolymerization at the same temperature 130 kg·mol⁻¹·h⁻¹·bar⁻¹ (Table 3.4, entries 6-7). It can be concluded that for high activity PE, a minimum amount of CPE is necessary. In principle, changes in the polarity of the reaction medium or the stabilizing effects of CPE on the catalyst might be responsible. For **7b**/MAO, a noticeable increase in catalyst activity was also observed for E-CPE copolymerization as observed in **7a**/MAO. It also shows that with the same amount of CPE vol.-%, with increasing reaction temperature catalyst activity increased from 275 to 1265 kg·mol⁻¹·h⁻¹·bar⁻¹ (Table 3.4, entries 8, 11, 12). Increasing the amount of CPE from 3.5 vol.-% to 44 vol.-% at 50 °C, the catalyst activity increased only slightly to 385 kg·mol⁻¹·h⁻¹·bar⁻¹ compared to 275 kg·mol⁻¹·h⁻¹·bar⁻¹ (entries 8 and 9). ¹H NMR and ¹³C NMR spectra were recorded to check the amount of incorporated CPE. Surprisingly, less than 1 mol-% CPE were incorporated in all the obtained polymer poly(E)-co-poly(CPE). Despite a CPE amount of 44 vol.-% in the polymerization mixture, the incorporated CPE amount was merely up to 0.6 mol-%. HT-GPC analyses show that the molecular weights also decreased compared to CPE-free polymerization, but with a relatively narrow PDI (in the range of 1.7 < PDI < 2.5). DSC measurements show that the melting point of PE produced by **7a**/MAO was in the range of 133 to 135 °C, while the melting point of PE produced by **7b**/MAO was in the range of 131 to 135 °C. The addition of CPE not only increased catalyst activity but also decreased the PDI. For PE produced by **7b**/MAO, the melting points also increased.

Table 3.4 Ethylene and CPE copolymerization with **7a** and **7b** activated by MAO.

# ^a	cat.	CPE (vol.-%)	<i>T</i> (°C)	Activity ^b	CPE (mol%) ^c	<i>M_n</i> ^d (g/mol)	<i>M_w</i> / <i>M_n</i> ^d	<i>T_m</i> ^e (°C)
1		0	50	93	0	325,000	11	133
2		3.5	50	1050	<0.5	443,000	2.0	135
3		3.5	65	2250	<0.5	298,000	1.8	133
4	7a	3.5	80	4000	<0.5	92,000	2.3	134
5		0.8	80	3750	<0.5	104,000	2.5	134
6		0.1	80	250	<0.5	280,000	2.0	135
7		0	80	130	0	551,000	4.2	135
8		3.5	50	275	<0.5	534,000	1.6	135
9		44	50	385	0.6	180,000	1.7	131
10	7b	0	65	14	0	121,000	7.7	124
11		3.5	65	575	<0.5	240,000	1.9	132
12		3.5	80	1265	<0.5	226,000	1.7	134

^a Polymerization conditions: 500 mL autoclave, total volume of the reaction mixture 250 mL, catalyst:MAO = 1:2000, [catalyst] = 2×10^{-5} mol·L⁻¹, *p* = 4 bar of ethylene unless stated otherwise, toluene, *t* = 1 h; ^b kg·mol⁻¹·h⁻¹·bar⁻¹; ^c CPE content estimated by ¹³C NMR; ^d Determined by HT-GPC in 1,2,4-trichlorobenzene vs. PS; ^e Measured by DSC.

Figure 3.4 shows the typical ¹³C NMR spectra of poly(E)-*co*-poly(CPE) produced by the action of **7b**/MAO (Table 3.4, entry 9). Around 0.6 mol-% of CPE incorporation was detected. Apart from the signal for linear PE at δ = 29.8 ppm, the signals at δ = 26.7 (C₄), 30.9 (C_{3,5}) and 43.0 (C_{1,2}) ppm are assigned to isolated 1,2-incorporated CPE units in the E sequence. Resonances at δ = 40.8 (C_{2'}), 40.3 (C_{1',3'}), 31.9 (C_{4',5'}) ppm belong to isolated 1,3-cyclopentane units were absent in this spectra. The 1,3-substituted cyclopentane structure can be explained by isomerisation of a 1,2-substituted cyclopentane terminus as shown in Scheme 3.3.^[35-39] The mechanism is similar to the 1,3-type polymerization of propylene with some metallocene catalyst. Copolymers obtained by the system **7b**/MAO contained only 1,2-enriched CPE units. These results indicate that CPE was preferentially incorporated via 1,2-insertion.

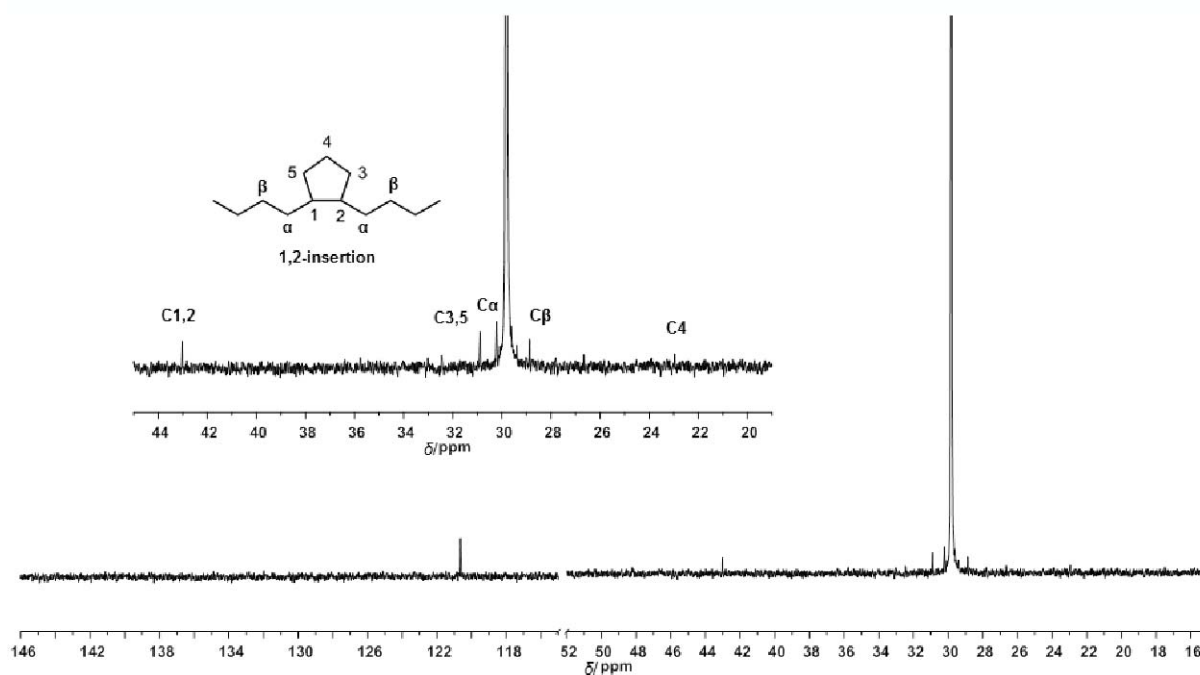
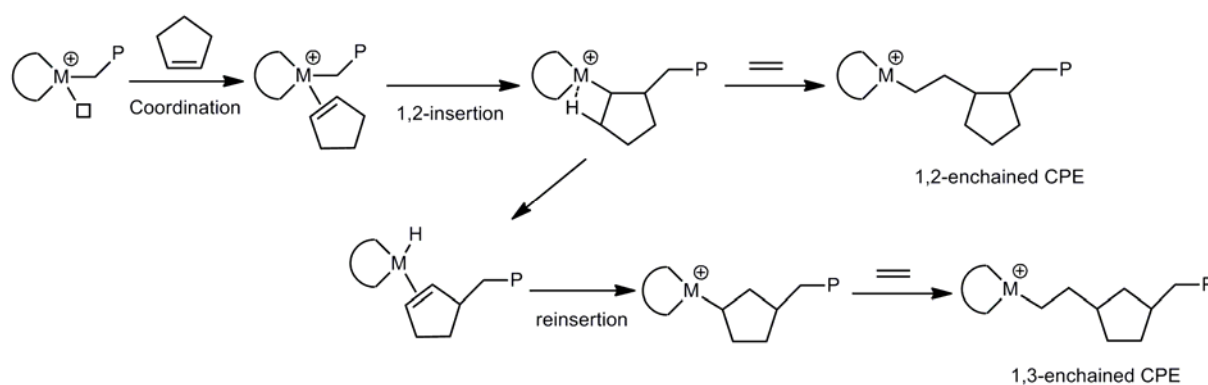


Figure 3.4 ^{13}C NMR spectra of poly(E)-co-poly(CPE) produced by the action of **7b**/MAO (Table 2, entry 9) (1,1,2,2- $[\text{D}_2]$ tetrachloroethane). The signal at $\delta = 120.64$ ppm is a solvent impurity.



Scheme 3.3 Isomerization mechanism for the generation of 1,3-enriched CPE units.

The effect of CPE on polymerization activity was less pronounced for **7a**/MAO and only minor for **7b**/MAO. Apparently, the bulky adamantyl-group in **7a** and **7b** and an additional bulky diphenylboryl-group in **7b** impede the coordination of CPE. To shed light onto the role of CPE in this copolymerization, cyclopentene-1- ^{13}C ^[40-41] was prepared and used on an 8 vol.-% level in the **7a**/MAO triggered copolymerization with E (Figure 3.5).

The above described signals for 1,2- and 1,3-incorporated CPE are both present in poly(E)-*co*-poly(CPE) where CPE was enriched by ^{13}C . These data clearly show an otherwise undetectable incorporation of CPE (< 0.5 mol-%) in the copolymerization with E even at low CPE concentrations in the reaction mixture and clearly proof the involvement of CPE in the entire polymerization process. Since CPE becomes incorporated into the polymer chain even at lower concentration and increases the activity at any volume level (Table 3.4), it must act in some way as stabilizing agent. Interestingly, in contrast to E homopolymerization, *no vinyl end groups* are visible in any of the copolymers.

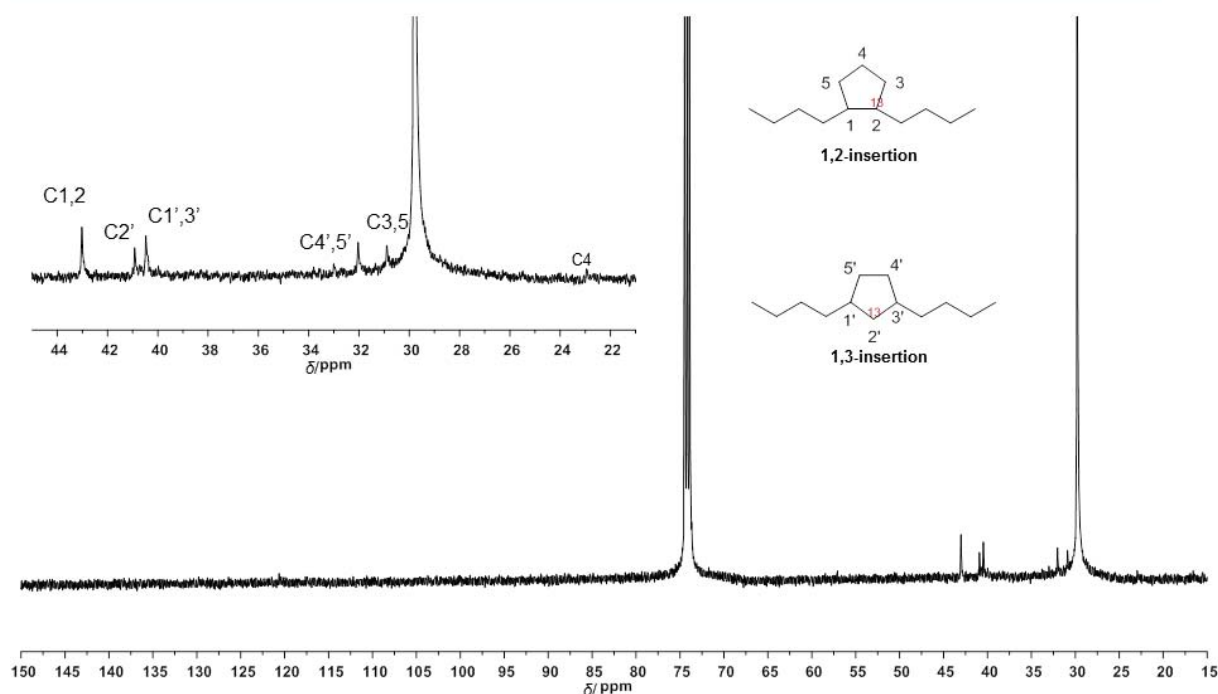
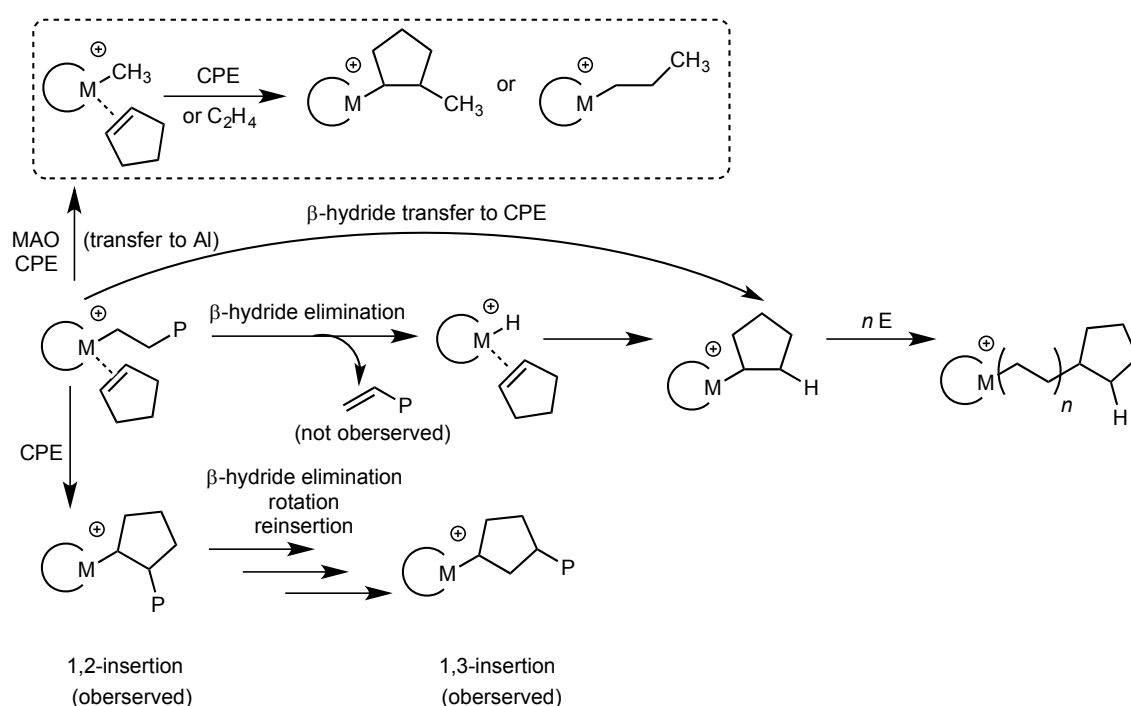


Figure 3.5 ^{13}C NMR spectra of PE-*co*-poly(CPE-1- ^{13}C) produced by the action of **7a**/MAO (8 vol.-% of CPE in the polymerization mixture) (1,1,2,2- $[\text{D}_2]$ tetrachloroethane). Signal at $\delta = 120.64$ ppm is a solvent impurity.

Scheme 3.4 shows the proposed role of CPE in the copolymerization of CPE with E. Because any β -hydride elimination or transfer to monomer would result in terminal alkenes, CPE coordination to the metal, which promotes alkyl-transfer to the aluminum of MAO is proposed. This pathway accounts for the finding that no terminal alkenes were visible in the polymer. It also explains the decrease in molecular weights with increasing CPE concentration in the polymerization mixture, which

promotes coordination of CPE to the metal center. Finally, it seems reasonable to propose such a coordination, since the concentration of CPE in toluene even at a 2 vol.-% level is already 6 times higher than the one of ethylene (ca. 0.3 M vs. 0.05 M).^[42] A simple polarity effect, caused by the polarity of CPE at high CPE concentration, can be ruled out in view of the effect of even low CPE concentrations (Table 3.4). It was additionally ruled out by running experiments with a mixture of toluene:heptane (60:40). No increase in polymerization activity was observed. Selected HT-GPC and DSC traces for poly(E)-*co*-poly(CPE) are shown in Figure 3.6 and 3.7.



Scheme 3.4 Role of CPE in the copolymerization of CPE with E. P = polymer chain.

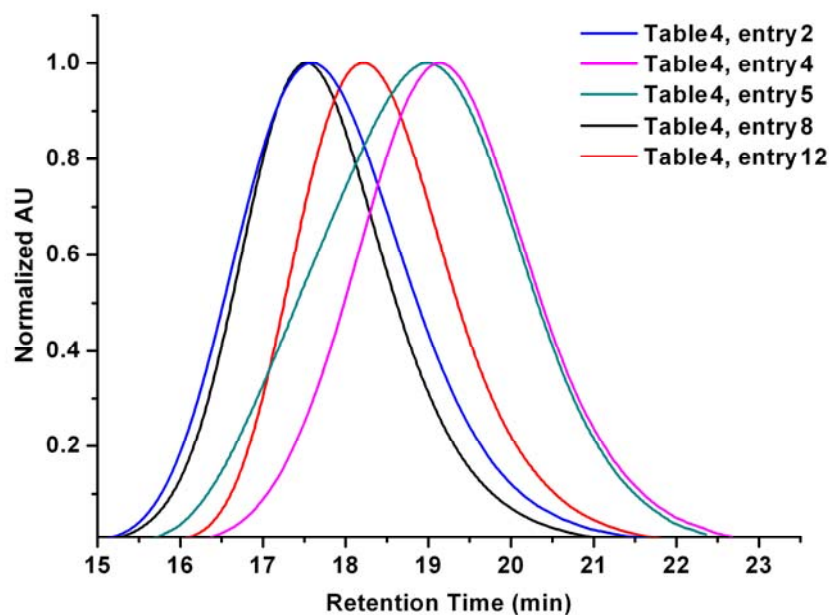


Figure 3.6 HT-GPC traces of poly(E)-co-poly(CPE) produced by **7a**/MAO and **7b**/MAO.

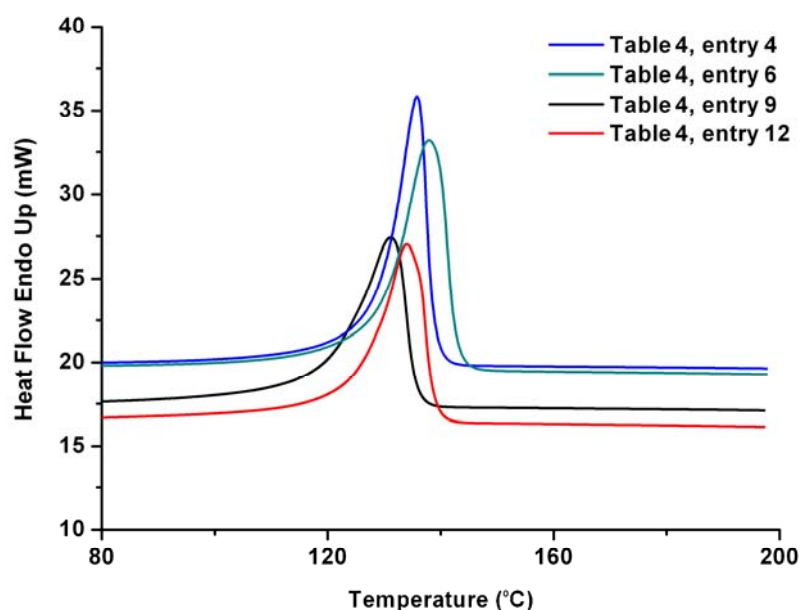


Figure 3.7 DSC curves of poly(E)-co-poly(CPE) produced by **7a**/MAO and **7b**/MAO.

3.2.4 Copolymerization of ethylene (E) with norborn-2-ene (NBE) (E-NBE)

Using a ratio of cat.:MAO:NBE = 1:2000:20000, catalyst precursor **7a** shows an increase in activity from 43 to 100 kg·mol⁻¹·h⁻¹·bar⁻¹ by increasing the temperature

from 50 °C to 80 °C (Table 3.5, entries 1, 4, 5, 7). HT-GPC analysis reveals that the molecular weight decreased from 800,000 g·mol⁻¹ to 260,000 g·mol⁻¹. When decreasing the ratio of NBE to 10000 *equiv.*, the catalyst activity increased to 75 and 140 kg·mol⁻¹·h⁻¹·bar⁻¹ at 65 °C and 80 °C (compare entries 2 to 4, 6 to 7, table 3.5). General assignments of norbornene and ethylene carbons from ¹³C NMR spectra allow for calculating the mole-percentage of norbornene incorporation in the copolymer (poly(E)-co-poly(NBE)_{VIP}). For entries 1, 4, 5 and 7, it shows that with the increase in temperature NBE incorporation increased from 4 to 11 mol-%. Decreasing the concentration of NBE to 10000 *equiv.* with respect to complex **7a** increased catalyst activity. NBE incorporation ratio increased to 18 mol-% (entry 6, Table 3.5). It is worth to mention that when 4000 *equiv.* cyclopentene (CPE) was additionally added to **7a**/MAO/NBE at 65 °C, an increase in productivity by a factor of 5 was observed (compare entries 2 and 3, Table 3.5). HT-GPC demonstrated that the polymer was monomodal and DSC revealed that this polymer possessed a melting point of 99 °C, which is lower than the one of CPE-free condition. Except for a relatively low NBE incorporation (3 vs 6 mol-%) and melting point (99 vs 120 °C), there is no big difference on the resulting polymer. A dramatic increase in activity was also found in the copolymerization of ethylene with CPE. By increasing the CPE concentration from 0 to 40 vol.-% at 50 °C, ethylene activity increased from 93 to 1050 kg·mol⁻¹·h⁻¹·bar⁻¹, which corresponds to an activation factor of > 11. E-cyclopentene-1-¹³C copolymerization revealed that CPE acts as a stabilizing agent in E-CPE copolymerization and promotes alkyl-transfer to the aluminum of MAO. This elucidated the increased activity in E-NBE reaction, and there is no detectable CPE incorporation. Complex **7b** shows the same tendency as complex **7a** at 50 °C, 65 °C and 80 °C, that is, the productivity increased with increasing temperature and went down with increasing NBE concentration, except relatively lower catalyst activity and NBE incorporation ratio. HT-GPC shows that the copolymers had a PDI in the range of 1.5 to 3.5. Melting points were in the range of 77 °C < *T_m* < 135 °C. Switching from the 6-(2-(diethylboryl)phenyl)pyrid-2-ylamido) motif in **7a** to the 6-(2-(diphenylboryl)phenyl)pyrid-2-ylamido) motif in **7b** significantly decreased catalyst activity and also lead to lower molecular weights. This is attributed to the bulky ligand in **7b**. Compared to **7a**/MAO, **7b**/MAO shows a relatively low catalyst activity towards E-NBE copolymerization.

Table 3.5 Ethylene and NBE copolymerization with **7a** and **7b** activated by MAO.

# ^a	cat. (cat:MAO:NBE)	T (°C)	Activity ^b	NBE (mol%) ^c	M _n ^d (g/mol)	M _w /M _n ^d	T _m ^e (°C)
1	7a(1:2000:20000)	50	43	4	800,000	2.0	119
2	7a(1:2000:10000)	65	75	6	330,000	2.6	122
3 ^f	7a(1:2000:10000)	65	360	3	370,000	1.5	99
4	7a(1:2000:20000)	65	55	7	400,000	1.8	121
5	7a(1:2000:20000)	70	70	8	360,000	2.0	99
6	7a(1:2000:10000)	80	140	18	300,000	2.4	120
7	7a(1:2000:20000)	80	100	11	260,000	2.0	124
8	7b(1:2000:20000)	50	5	1	400,000	1.8	133
9	7b(1:2000:10000)	65	30	4	260,000	1.7	119
10	7b(1:2000:20000)	65	10	1	340,000	1.5	133
11	7b(1:2000:10000)	80	50	3	170,000	1.8	129
12	7b(1:2000:20000)	80	35	4	300,000	2.4	135

^a Polymerization conditions: 500 mL autoclave, total volume of the reaction mixture 250 mL, catalyst:MAO = 1:2000, [catalyst] = 2×10^{-5} mol·L⁻¹, p = 4 bar of ethylene unless stated otherwise, toluene, t = 1 h; ^b kg·mol⁻¹·h⁻¹·bar⁻¹; ^c NBE content estimated by ¹³C NMR; ^d Determined by HT-GPC in 1,2,4-trichlorobenzene vs. PS; ^e Measured by DSC; ^f 4000 equiv. CPE was additionally added.

Previous studies have shown that norbornene in metallocene-catalyzed copolymerization is enchainned by *cis*-2,3-*exo* addition.^[43-44] The possible segments of an E-NBE copolymer chain where NBE units are either isolated (EE-NBE-EE), alternating (E-NBE-E-NBE), or exist in form of diads (E-NBE-NBE-E) and triads (E-NBE-NBE-NBE-E) are shown in Figure 3.8.

The configuration of C₂ and C₃ in NBE can either be R/S or S/R. The relationship of the alternating NBE sequence will either be *meso* (alternating isotactic, *alt-it*) or *racemic* (alternating syndiotactic, *alt-st*). Figure 3.9 shows typical ¹³C NMR spectra of poly(E)-*co*-poly(NBE) prepared by the action of **7a**/MAO at 65 and 80 °C using 4 bar of E. Between δ = 28 and 32 ppm, the polyethylene (E) signal overlaps with the C₅

and C₆ resonances of the NBE carbons. Signals for alternating/isolated C₅/C₆ of NBE and successive ethylene carbons show up in the range of $\delta = 29.8 - 30.4$ ppm.

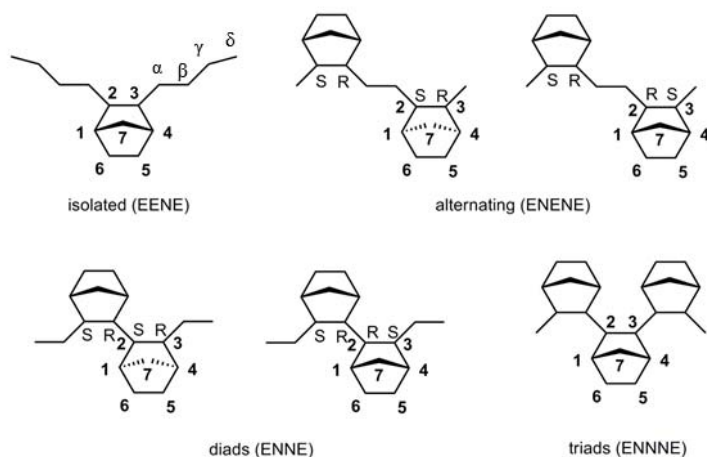


Figure 3.8 Overview of possible segments of an E-N copolymer chain where norbornene units are in isolated (EENE), alternating (ENENE), diads (ENNE) and triad (ENNNE) sequences.

The chemical shifts of the observed signals along with the integral were used for calculating the NBE content of the resulting copolymer using the following equation:^[45-48]

$$\text{mol} - \%_{\text{NBE}} = \frac{\frac{1}{3}(\int C_{2,3} + \int C_{1,4} + 2 \int C_7)}{\int CH_2} 100\%$$

Analysis of the E-NBE copolymer spectra revealed that in the spectra of copolymers with high NBE incorporation signals for *alt-it* (C₂/C₃ $\delta = 47.8$ ppm, C₁/C₄ $\delta = 42.1$ ppm), *alt-st* E-NBE sequences and/or isolated NBE sequences (C₂/C₃ $\delta = 47.2$ ppm, C₁/C₄ $\delta = 41.6$ ppm) could be observed (Figures 3.9). The isolated NBE and *alt-st* E-NBE sequences overlap and cannot be resolved. At low NBE incorporation (<5 mol-%), mainly signals for *alt-st* and/or isolated E-NBE sequences were found (Figure 3.9a). By contrast, resonances ascribed to NBE diads, i.e. E-NBE-NBE-E sequences were observed for COCs with high NBE incorporation at $\delta = 49.4, 41.1, 31.4, 30.8, 30.7$ ppm^[49-50] prepared by the action of pre-catalyst **7a**. Generally, no NBE triads (E-NBE-NBE-NBE-E sequences) were found. Notably, none of the copolymers showed signals for ROMP-derived poly(NBE), regardless of temperature, pressure, cocatalyst

ratio and NBE concentration. Demonstrated HT-GPC and DSC traces were also shown in Figure 3.10 and 3.11.

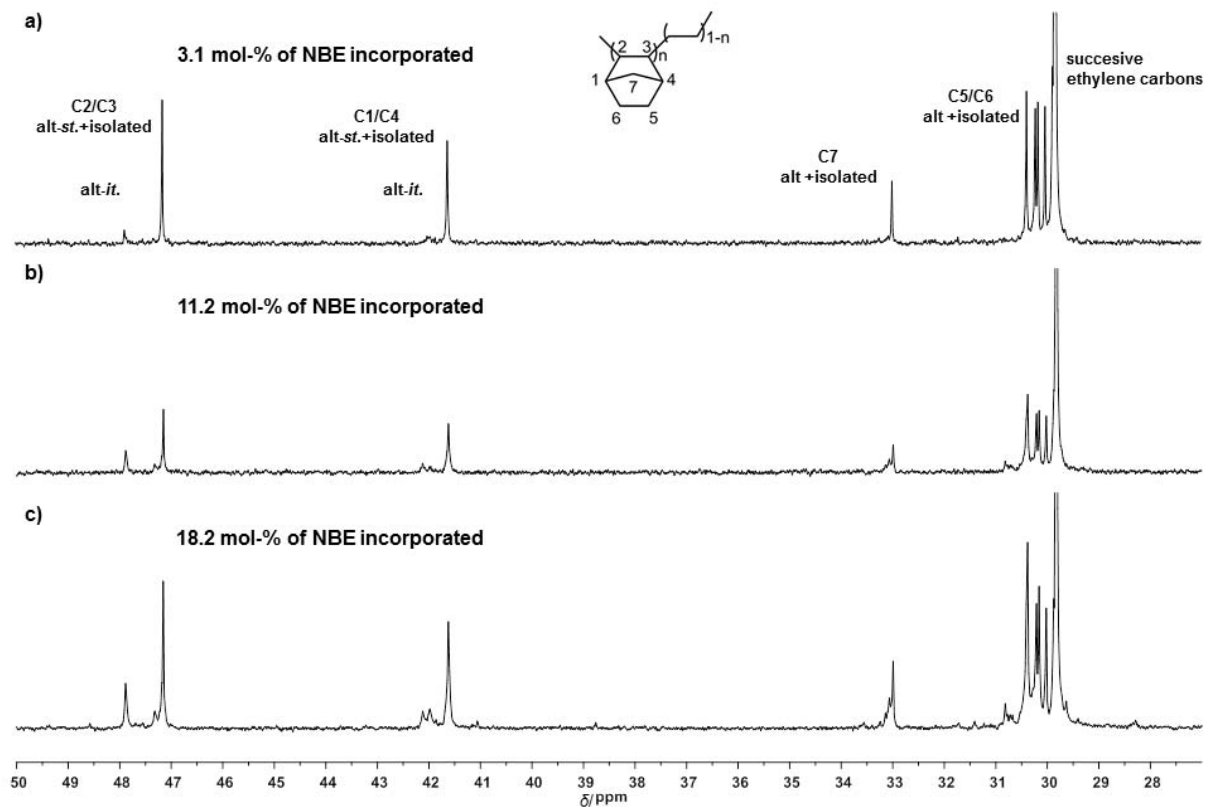


Figure 3.9 ^{13}C NMR spectra of poly(E)-co-poly(NBE)_{VIP} produced by the action of **7a**/MAO (Table 3.5, entries 1, 7 and 6) (1,1,2,2-[D₂]tetrachloroethane). alt-st.: alternating syndiotactic; alt-it.: alternating isotactic.

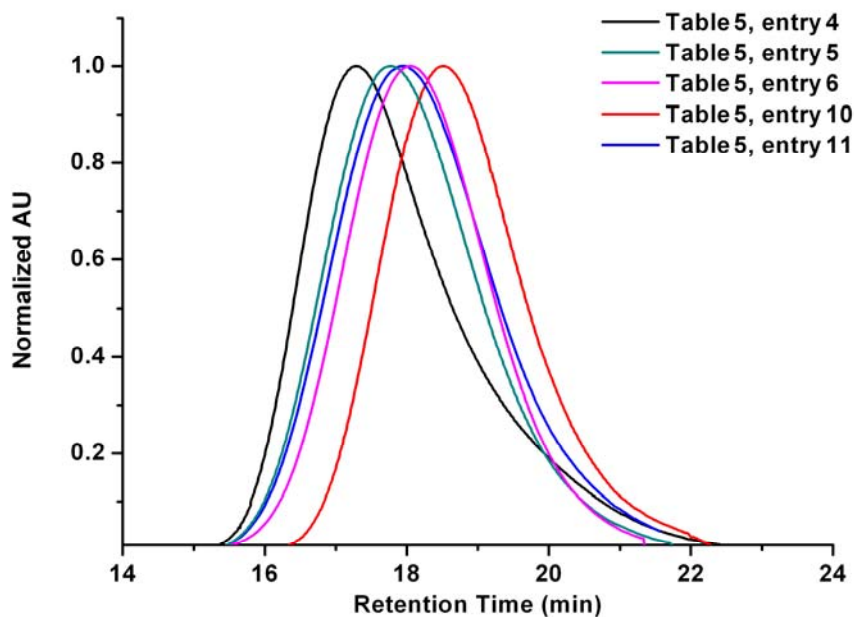


Figure 3.10 HT-GPC traces of poly(E)-co-poly(NBE) produced by **7a**/MAO and **7b**/MAO.

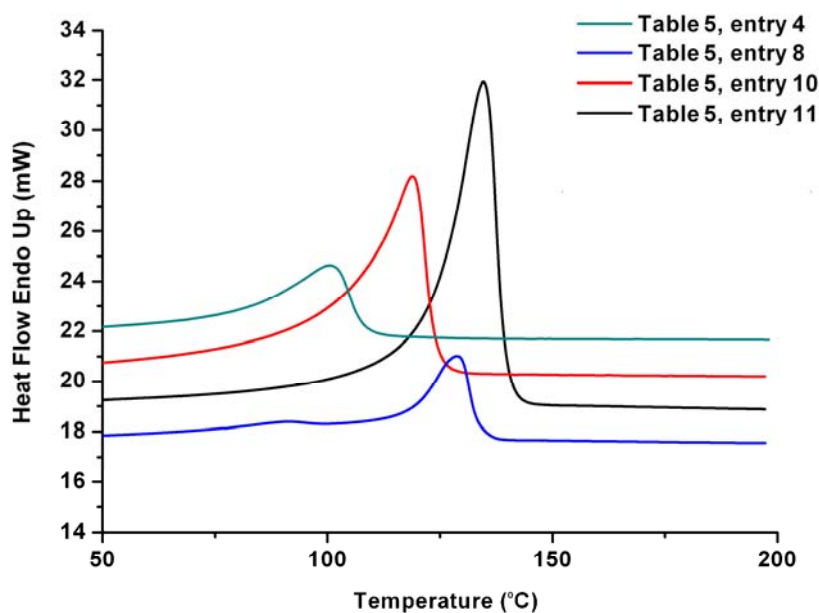
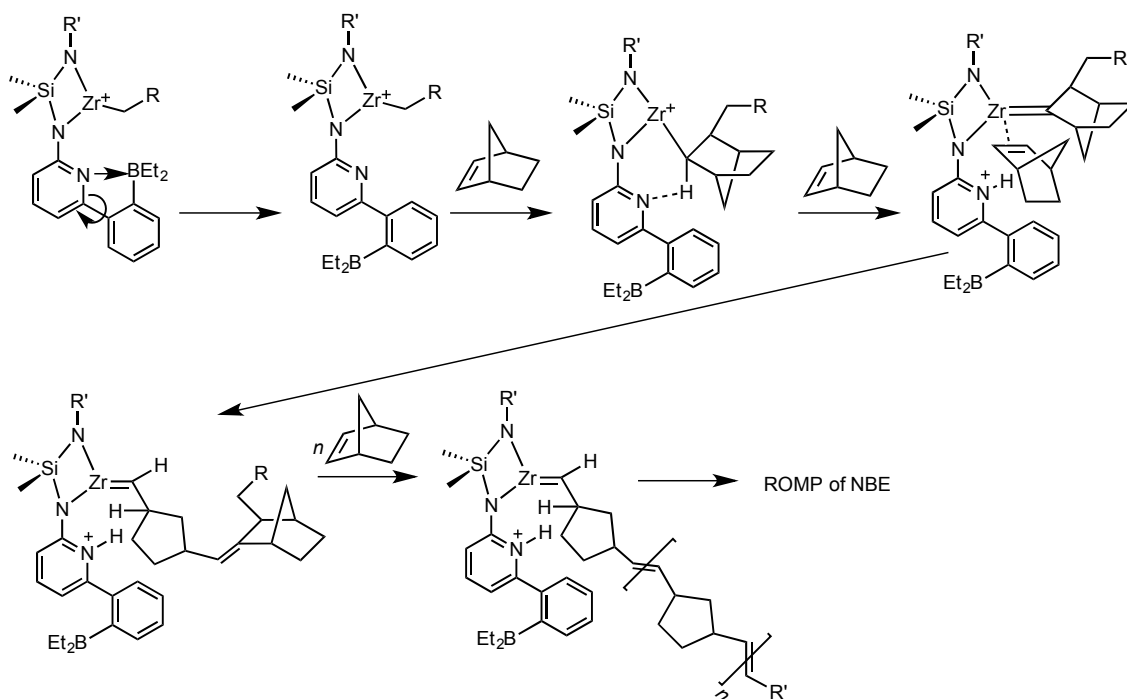


Figure 3.11 DSC curves poly(E)-co-poly(NBE) produced by **7a**/MAO and **7b**/MAO.

According to the mechanism of VIP, two consecutive monomer insertions, i.e. one insertion of NBE and E, respectively, should lead to the restoration of the initial conformation at the metal center and therefore result in *alt-it* NBE-E sequences. And in fact, signals for *alt-it* E-NBE sequences can be observed. Alongside, the signals at

$\delta = 47.2$ and 41.6 ppm are indicative for *alt-st* E-NBE sequences and/or isolated NBE sequences (*vide supra*). It is, however, reasonable to assume that the stereochemistry at the cationic Zr-center prevails, presumably stabilized by γ -agostic interactions.^[51] Consequently, we rather wish to assign the signals at $\delta = 47.2$ and 41.6 ppm to *isolated* NBE sequences than to *alt-st* E-NBE sequences, at least for low NBE content copolymers ($X_{NBE} = \leq 7$ mol-%). This is believed to be particularly true for pre-catalyst **7b**, which contains a bulky adamantyl and a bulky diphenylboron group. This pre-catalysts allow only for low NBE incorporation (≤ 4 mol-%) with no sign of *it* E-NBE sequences and most probably only *isolated* NBEs.

From these data, several conclusions with relevance to both the design of pre-catalysts capable of producing both ROMP- and VIP-derived polymers and to reaction conditions can be drawn: (i) as can be deduced from ^{13}C NMR, NBE incorporation including consecutive NBE incorporation into **Zr-1** is much easier to accomplish than with any of pre-catalysts **7a** and **7b**. Maybe the presence of two 6-(2-(diethylboryl)phenyl)pyridyl-2-yl-groups in one molecule strongly promotes α -H abstraction and consecutive formation of poly(NBE) via ROMP. (ii) in view of the high propensity of **Zr-1** to incorporate NBE, NBE-NBE sequences produced via VIP are observed, too. Vice versa, pre-catalysts that do not allow for VIP-derived NBE-NBE sequences show no propensity to switch from ROMP to VIP. This fits the proposed mechanism for the observed switch from VIP to ROMP in **Zr-1**, where NBE coordinates to MAO-activated **Zr-1** with a NBE as the last incorporated monomer (Scheme 3.5).



Scheme 3.5 Proposed switch from VIP to ROMP with **Zr-1**.

Such coordination only occurs at high NBE concentration and low E concentration (pressure), forcing NBE to preferentially coordinate over ethylene. The steric pressure that results can only be reduced by either decoordination of NBE or by switching from a tetrahedral cationic system to a square-planar Zr-alkylidene. This, however, requires α -hydrogen abstraction, which only takes place in case the 2-pyridyl motif is present and the nitrogen-lone pair is available. This in turn requires antecedent B-decoordination, which in fact occurs in the presence of MAO and at higher temperature as shown by T-dependent ^{11}B -NMR for **Zr-1**. In turn, no switch from VIP to ROMP occurs under any conditions with pre-catalysts that lack the 2-pyridyl motif since α -H abstraction is not promoted.

The answer to the question, why **Zr-1** and **Ti-1** allow for this switch from VIP to ROMP and all other pre-catalysts **7a** and **7b** do not, is currently subject of further research. Steric arguments might also apply for, e.g., **7a** or **7b** but most probably cannot describe the entire situation alone. Clearly, a very subtle ligand tuning is required to allow for a switch from ROMP to VIP. T-dependent ^{11}B -NMR measurements on both the parent and MAO-activated pre-catalysts are expected to shed more light on that issue.

3.3 Conclusions

The silicon-bridged Zr^{IV} complexes bearing the amino-borane ligands were prepared and characterized. Catalyst activity, CPE and NBE incorporation and M_n were affected by the variation of the Al/Zr ratio, temperature and catalyst concentration. In the presence of MAO, complexes **7a** and **7b** showed moderate activities of ethylene homopolymerization, E-NBE copolymerization, but high activity in E-CPE copolymerization. In most cases an increase in polymerization temperature resulted in an increase in catalytic activity and also the incorporated NBE content. By changing comonomer concentration and polymerization conditions, high incorporation ratios of CPE and NBE could be achieved up to 0.6 and 18 mol-%, respectively. All these complexes produced VIP-derived poly(E)-co-poly(CPE) and poly(E)-co-poly(NBE)_{VIP}. The microstructure of these cyclic olefin copolymers was elucidated. Though both of the complexes were not active in the reversible ROMP/VIP copolymerization, the facts observed here are important for designing effective catalyst precursors for precise olefin polymerization.

3.4 References

- [1] G. W. Coates, *Chem. Rev.* **2000**, *100*, 1223-1252.
- [2] A. C. Gottfried, M. Brookhart, *Macromolecules* **2003**, *36*, 3085-3100.
- [3] V. C. Gibson, S. K. Spitzmesser, *Chem. Rev.* **2003**, *103*, 283-315.
- [4] R. A. Stockland, S. R. Foley, R. F. Jordan, *J. Am. Chem. Soc.* **2003**, *125*, 796-809.
- [5] R. R. Schrock, *Acc. Chem. Res.* **1990**, *23*, 158-165.
- [6] T. M. Trnka, R. H. Grubbs, *Acc. Chem. Res.* **2001**, *34*, 18-29.
- [7] M. Bornand, S. Torker, P. Chen, *Organometallics* **2007**, *26*, 3585-3596.
- [8] B. K. Keitz, A. Fedorov, R. H. Grubbs, *J. Am. Chem. Soc.* **2012**, *134*, 2040-2043.
- [9] W. Spaleck, M. Antberg, J. Rohrmann, A. Winter, B. Bachmann, P. Kiprof, J. Behm, W. A. Herrmann, *Angew. Chem.* **1992**, *104*, 1373-1376; *Angew. Chem. Int. Ed.* **1992**, *31*, 1347-1350.
- [10] H. G. Alt, A. Köppl, *Chem. Rev.* **2000**, *100*, 1205-1221.
- [11] I. Tritto, L. Boggioni, D. R. Ferro, *Coord. Chem. Rev.* **2006**, *250*, 212-241.

- [12] W. Kaminsky, *Macromol. Chem. Phys.* **1996**, *197*, 3907-3945.
- [13] S. T. Yu, S. J. Na, T. S. Lim, B. Y. Lee, *Macromolecules* **2010**, *43*, 725-730.
- [14] G. M. Benedikt, E. Elce, B. L. Goodall, H. A. Kalamarides, L. H. McIntosh, L. F. Rhodes, K. T. Selvy, C. Andes, K. Oyler, A. Sen, *Macromolecules* **2002**, *35*, 8978-8988.
- [15] G. J. P. Britovsek, V. C. Gibson, D. F. Wass, *Angew. Chem.* **1999**, *111*, 448-468; *Angew. Chem. Int. Ed.* **1999**, *38*, 428-447.
- [16] N. A. Petasis, D. K. Fu, *J. Am. Chem. Soc.* **1993**, *115*, 7208-7214.
- [17] M. R. Buchmeiser, S. Camadanli, D. R. Wang, Y. L. Zou, U. Decker, C. Kühnel, I. Reinhardt, *Angew. Chem.* **2011**, *123*, 3628-3633; *Angew. Chem. Int. Ed.* **2011**, *50*, 3566-3571.
- [18] Y. L. Zou, D. R. Wang, K. Wurst, K. Kühnel, I. Reinhardt, U. Decker, V. Gurram, S. Camadanli, M. R. Buchmeiser, *Chem. Eur. J.* **2011**, *17*, 13832-13846.
- [19] T. C. Chung, H. L. Lu, C. L. Li, *Macromolecules* **1994**, *27*, 7533-7537.
- [20] G. J. Xu, D. R. Wang, M. R. Buchmeiser, *Macromol. Rapid Commun.* **2012**, *33*, 75-79.
- [21] K. Herz, D. A. Imbrich, J. Unold, G. J. Xu, M. Speiser, M. R. Buchmeiser, *Macromol. Chem. Phys.* **2013**, *214*, 1522-1527.
- [22] M. Ciftci, P. Batat, A. L. Demirel, G. J. Xu, M. Buchmeiser, Y. Yagci, *Macromolecules* **2013**, *46*, 6395-6401.
- [23] G. V. Narayana, G. J. Xu, D. R. Wang, W. Frey, M. R. Buchmeiser, *ChemPlusChem.* **2014**, *79*, 151-162.
- [24] W. Haubold, J. Herdtle, W. Gollinger, W. Einholz, *J. Org. Chem.* **1986**, *315*, 1-8.
- [25] L. Kaufmann, J. Breunig, H. Vitze, F. Schödel, I. Nowik, M. Pichlmaier, M. Bolte, H. Lerner, R. F. Winter, R. H. Herber, M. Wagner, *Dalton Trans.* **2009**, 2940-2950.
- [26] G. J. P. Britovsek, V. C. Gibson, D. F. Wass, *Angew. Chem.* **1999**, *111*, 448-468; *Angew. Chem. Int. Ed.* **1999**, *38*, 428-447.
- [27] R. R. Schrock, P. J. Bonitatebus, Y. Schrodi, *Organometallics* **2001**, *20*, 1056-1058.
- [28] A. D. Horton, K. L. von Hebel, J. de With, *Macromol. Symp.* **2001**, *173*, 123-136.

- [29] R. Baumann, W. M. Davis, R. R. Schrock, *J. Am. Chem. Soc.* **1997**, *119*, 3830-3831.
- [30] Y. M. Jeon, S. J. Park, J. Heo, K. Kim, *Organometallics* **1998**, *17*, 3161-3163.
- [31] C. H. Lee, Y. H. La, J. W. Park, *Organometallics* **2000**, *19*, 344-351.
- [32] V. C. Gibson, B. S. Kimberley, A. J. P. White, D. J. Williams, P. Howard, *Chem. Commun.* **1998**, 313-314.
- [33] S. Tinkler, R. J. Deeth, D. J. Duncalf, A. McCamley, *Chem. Commun.* **1996**, 2623-2624.
- [34] Y.-M. Jeon, J. Heo, W. M. Lee, T. Chang, K. Kim, *Organometallics* **1999**, *18*, 4107-4113.
- [35] N. Naga, Y. Imanishi, *Macromol. Chem. Phys.* **2002**, *203*, 159-165.
- [36] S. J. McLain, J. Feldman, E. F. McCord, K. H. Gardner, M. F. Teasley, E. B. Coughlin, K. J. Sweetman, L. K. Johnson, M. Brookhart, *Macromolecules* **1998**, *31*, 6705-6707.
- [37] A. R. Lavoie, M. H. Ho, R. M. Waymouth, *Chem. Commun.* **2003**, 864-865.
- [38] N. Naga, Y. Imanishi, *Macromol. Chem. Phys.* **2002**, *203*, 159-165.
- [39] A. Jerschow, E. Ernst, W. Hermann, N. Mueller, *Macromolecules* **1995**, *28*, 7095-7099.
- [40] S. D. Larsen, P. J. Vergamini, T. W. Whaley, *J. Labelled Comp.* **1975**, 325-332.
- [41] J. R. Heys, W. P. Duncan, W. C. Perry, D. A. Ebert, G. Radolovich, C. L. Haile, *J. Labelled Comp. Radiopharm.* **1979**, 295-306.
- [42] A. Sahgal, H. M. La, W. Hayduk, *Can. J Chem. Eng.* **1978**, *56*, 354-357.
- [43] W. Kaminsky, A. Bark, M. Arndt, *Macromol. Chem. Macromol. Symp.* **1991**, *47*, 83-93.
- [44] C. H. Bergström, B. R. Sperlich, J. Ruotoistenmäki, J. V. Seppälä, *J Polym. Sci. A: Polym. Chem.* **1998**, *36*, 1633-1638.
- [45] T. Rische, A. J. Waddon, L. C. Dickinson, W. J. MacKnight, *Macromolecules* **1998**, *31*, 1871-1874.
- [46] M. Arndt-Rosenau, I. Beulich, *Macromolecules* **1999**, *32*, 7335-7343.
- [47] I. Tritto, C. Marestin, L. Boggioni, L. Zetta, A. Provasoli, D. R. Ferro, *Macromolecules* **2000**, *33*, 8931-8944.
- [48] T. Hasan, T. Ikeda, T. Shiono, *Macromolecules* **2004**, *37*, 8503-8509.
- [49] X. Y. Tang, Y. X. Wang, B. X. Li, J. Y. Liu, Y. S. Li, *J Polym. Sci. A: Polym. Chem.* **2013**, *51*, 1585-1594.

[50] D. Ruchatz, G. Fink, *Macromolecules* **1998**, *31*, 4674-4680.

[51] R. H. Grubbs, G. W. Coates, *Acc. Chem. Res.* **1996**, *29*, 85-93.

**4. On the Mechanism of Tandem Ring-Opening
Metathesis/Vinyl Insertion Copolymerization of Ethylene
With Norborn-2-ene**

4.1 Introduction

Buchmeiser et al. recently reported that a series of group IV metal complexes containing the (N-(6-(2-(diethylboryl)phenyl)pyrid-2-yl)-motif are capable of copolymerizing ethylene (E) with norborn-2-ene (NBE) or *cis*-cyclooctene (COE) both via ring-opening metathesis polymerization (ROMP) and vinyl insertion polymerization (VIP). Cyclic olefin copolymers poly(NBE)_{ROMP}-co-poly(NBE)_{VIP}-co-poly(E) and poly(COE)_{ROMP}-co-poly(COE)_{VIP}-co-poly(E)^[1-3] were collected in moderate yields. Among the catalysts that display this capability (Figure 1), pre-catalyst **1** holds a prominent position.

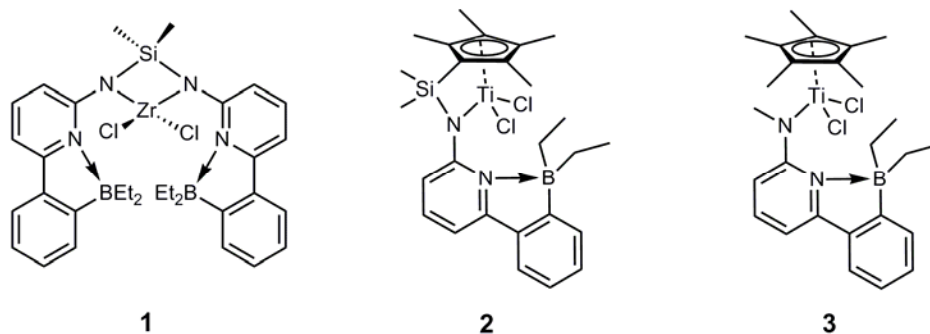


Figure 4.1 Structure of pre-catalysts **1-3**.

It was therefore of particular interest, how *exactly* this switch from ROMP to VIP or vice versa occurs. To shed light on this issue, pre-catalyst **1** and MAO-activated **1** both in the absence and presence of monomer were subjected to variable-temperature ¹H NMR and ¹¹B NMR measurements.

4.2 Results and Discussion

4.2.1 Homopolymerization of NBE and copolymerization of E with NBE

Homopolymerization of NBE by MAO-activated **1** was carried out in a Schlenk flask applying a ratio of **1**/MAO/NBE of 1:2000:20000. Pure poly(NBE)_{ROMP} ($M_n = 93,000$ g·mol⁻¹, PDI = 1.6, *cis/trans* = 15:85) was obtained at 60 °C. ¹H NMR and ¹³C NMR spectra showed the characteristic signals of poly(NBE)_{ROMP} at $\delta = 6.6, 6.5$ ppm, and 134, 133 ppm, respectively. As expected, a glass transition temperature ($T_g = 39$ °C), which is in line for a poly(NBE)_{ROMP} with 85 mol-% *trans*-configured double bonds,

was observed by differential scanning calorimetry (DSC). As reported earlier,^[1-2] the copolymerization of **E** with NBE yielded a copolymer that contained both VIP- and ROMP-derived repeat units. Thus, poly(NBE)_{ROMP-co}-poly(NBE)_{VIP-co}-poly(E)=3:13:84 ($M_n = 230,000 \text{ g}\cdot\text{mol}^{-1}$, PDI = 1.6) was obtained at 60 °C using **1**/MAO/NBE in a ratio of 1:2000:20000, $p_{\text{ethylene}} = 4 \text{ bar}$. DSC measurement revealed only a T_m at 122 °C. THF extraction experiments confirmed the absence of any free poly(NBE) in the copolymer. The monomodal molecular weight distribution in high-temperature GPC further supported the proposed polymer structure.

4.2.2 Activation process of MAO on **1**

Variable temperature measurements on **1** in toluene- d_8 were carried out in a temperature region of -60 °C to 40 °C.^[4] The protons on the aminoborane ligand were numbered from 1 to 7. The temperature dependence of the chemical shifts is shown in Figure 4.2. With an increase in temperature from -60 °C to 40 °C, the chemical shifts of protons 1 and 7 changed by 0.4 ppm, protons 2 and 6 by 0.1 ppm, protons 3 and 4 by 0.2 ppm and proton 5 by 0 ppm. ¹¹B NMR spectra of **1** in toluene- d_8 showed broad resonances. From 20 °C to 80 °C, the chemical shifts were in the range of 5.9 to 5.6 ppm (Figure 4.3), which is typical for tetracoordinated boron. Clearly and in accordance with its single crystal X-ray structure,^[1] the pyridine's nitrogen ring is bound to boron forming a Lewis acid/base pair, which does not dissociate up to 80 °C.

Upon addition of methylalumoxane (MAO) to **1** in toluene- d_8 in a molar ratio of **1**:MAO = 1:30. At -60°C, both chlorides in **1** were replaced by methyl groups and the system started to produce methane ($\delta = 0.17 \text{ ppm}$ at 20 °C, Scheme 4.1).^[5-7] The activation process and deactivation process of **1** by MAO is shown in Figure 4.4.^[8] At -20 °C, the dormant species (**III**, Scheme 4.1), which is inactive in polymerization, becomes visible in the ¹H NMR ($\delta_{\text{CH}_2} = 0.82 \text{ ppm}$ at 20°C).

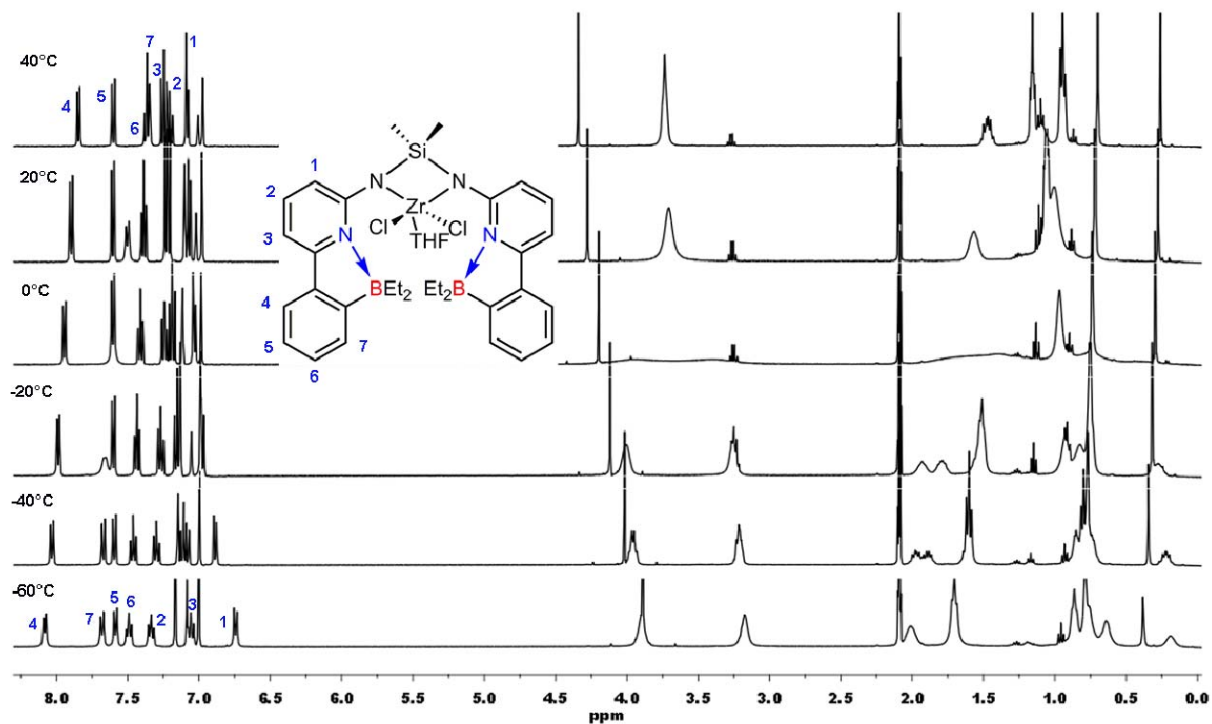


Figure 4.2 Variable-temperature ^1H NMR spectra of **1** ($\text{toluene-}d_8$).

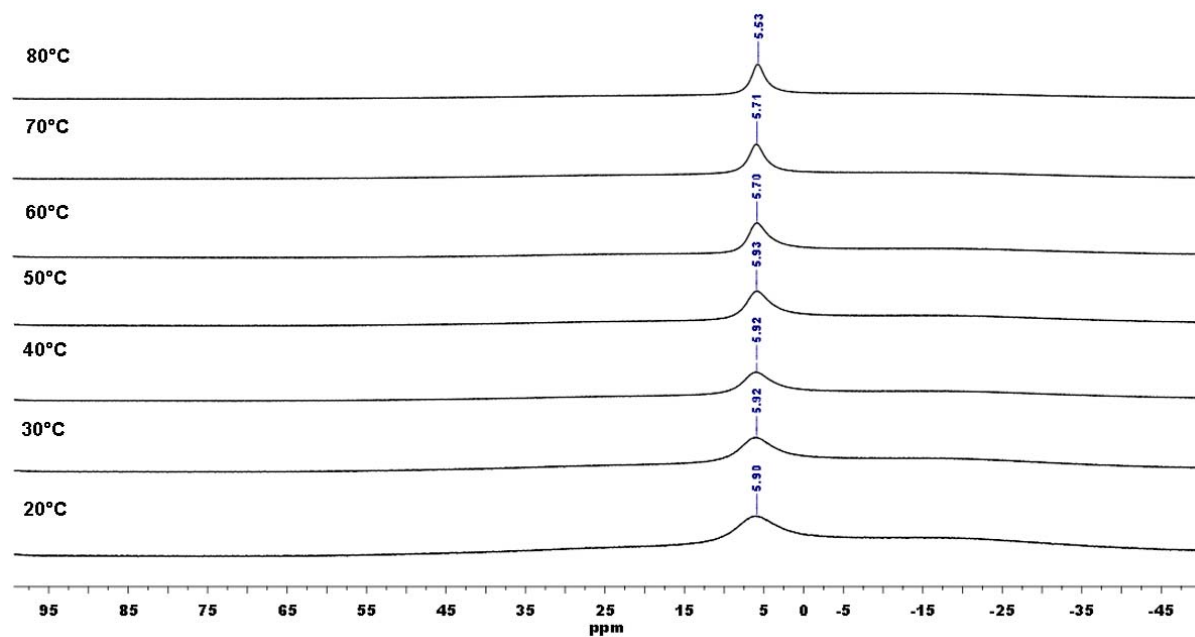
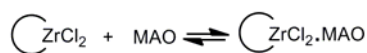
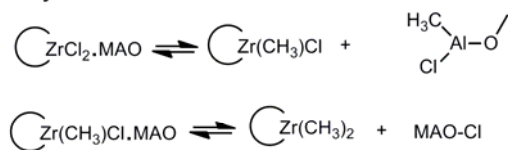


Figure 4.3 Variable-temperature ^{11}B NMR spectra of **1** ($\text{toluene-}d_8$).

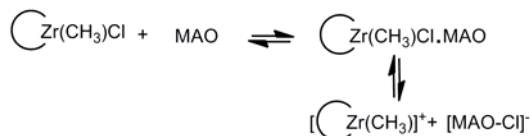
Complexation



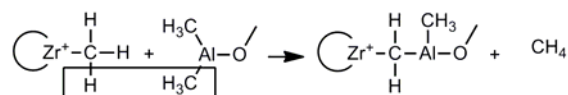
Methylation



Activation



Deactivation



Reactivation

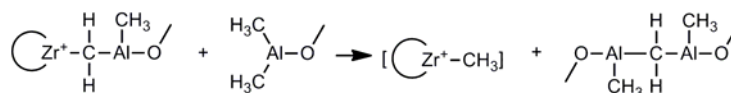
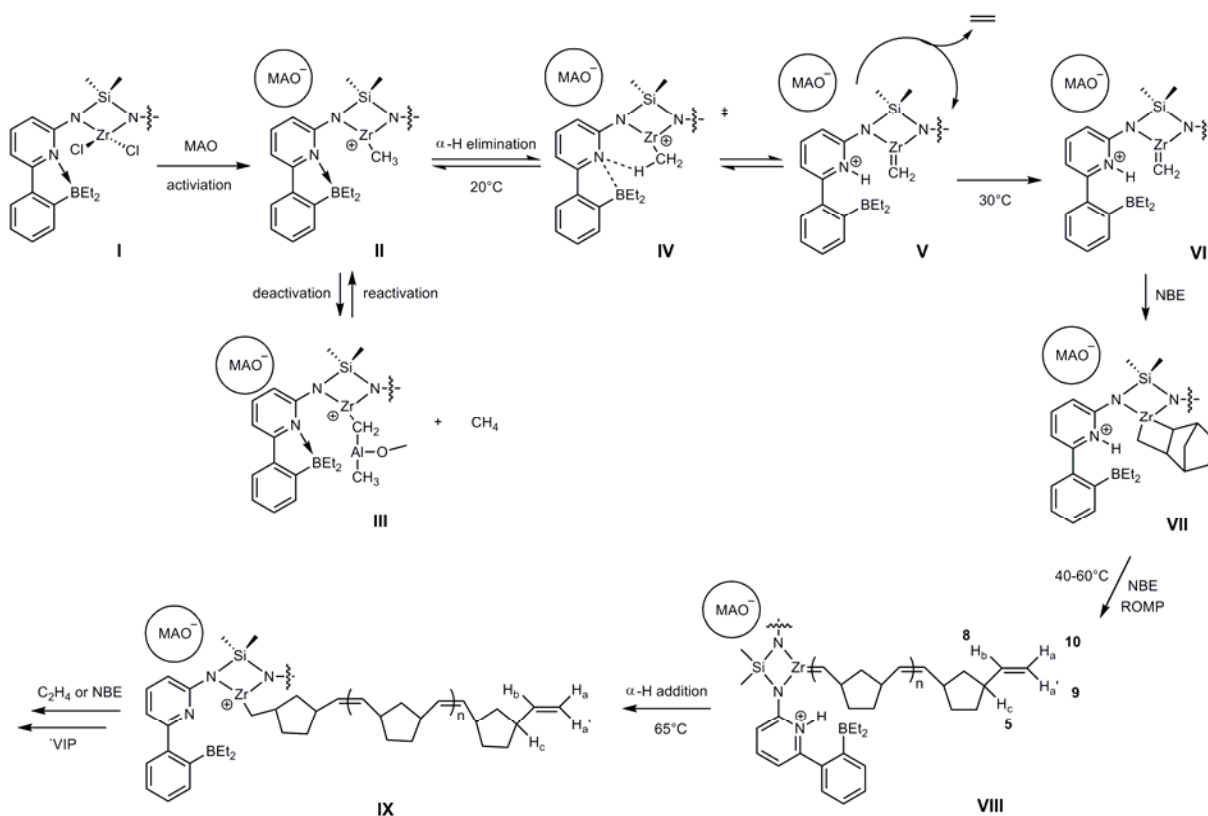


Figure 4.4 Activation process of 1.



Scheme 4.1 Proposed mechanism of NBE polymerization by MAO-activated 1.

A further increase in temperature to 20 °C resulted in α -H elimination and a ROMP-active Zr-alkylidene (**IV**, Scheme 4.1) formed as evidenced by the alkylidene signal visible at $\delta = 8.5$ ppm in the ^1H NMR (Figure 4.5).^[1, 9-11] In line with that, at 30 °C, ^{11}B NMR shows apart from the parent tetracoordinated B atom ($\delta = 2.6$ ppm) the formation of a tricoordinated species at $\delta = 86.7$ ppm indicating a dissociation of the N-B bond (Figure 4.6).^[12] This strongly suggests that the opening of the N-B bond generates a free pyridine moiety that induces α -H elimination. Since this reaction does not occur in the absence of MAO (*vide infra*), this process is both MAO- and temperature-driven. Substantial fractions of this ROMP-active Zr-alkylidene (**IV**) experience bimolecular decomposition resulting in the formation of ethylene. Thus, the signal for ethylene is clearly seen at $\delta = 5.25$ ppm in the ^1H NMR at $T \geq 30$ °C (Figure 4.5).

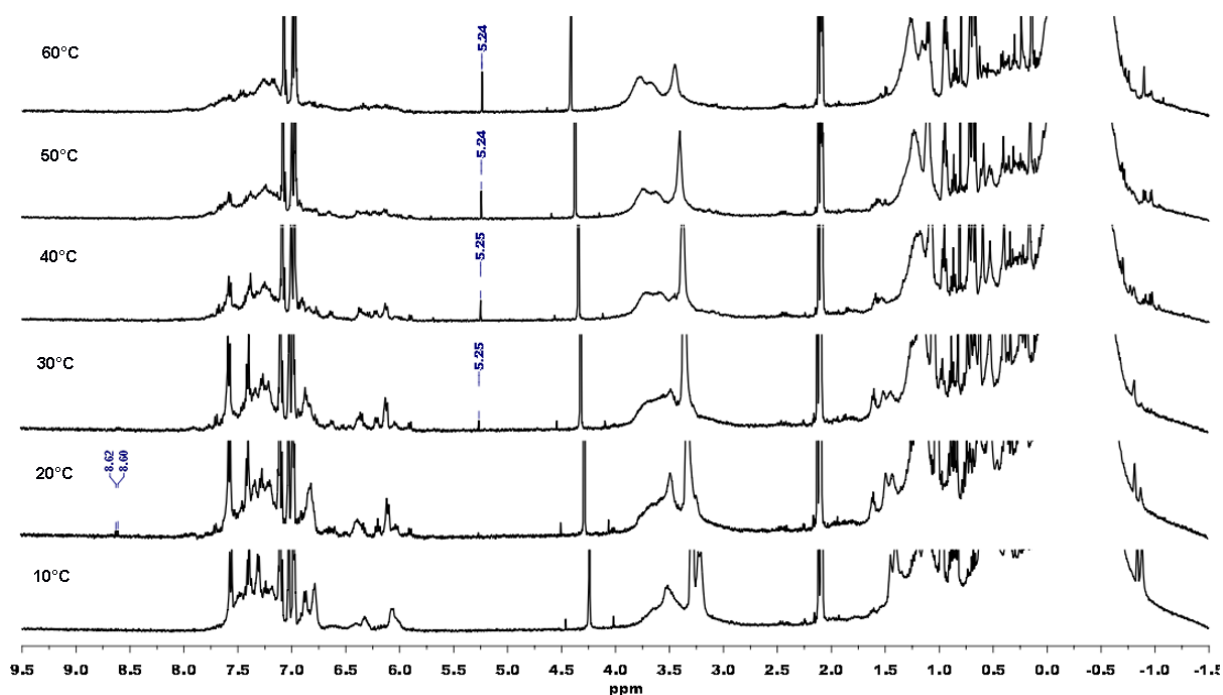


Figure 4.5 Variable-temperature ^1H NMR spectra of **1**/MAO (toluene- d_8).

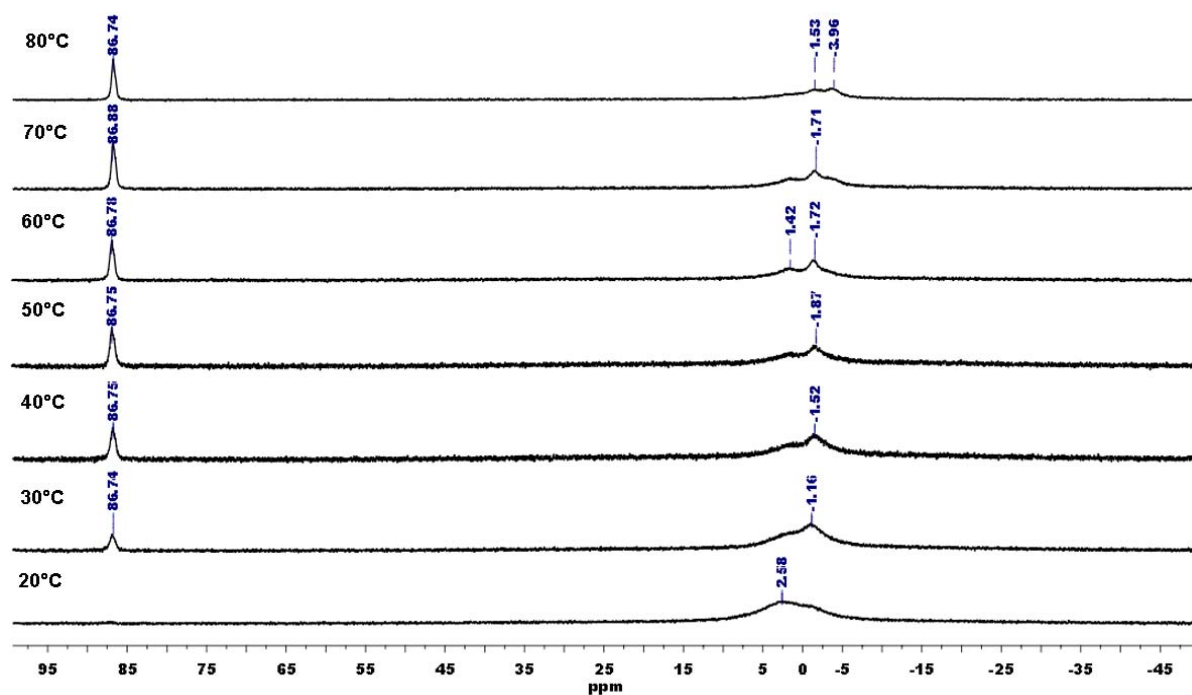


Figure 4.6 Variable-temperature ^{11}B NMR spectra of **1**/MAO (toluene- d_8).

4.2.3 Reaction of **1**/MAO with NBE

Upon addition of norborn-2-ene (NBE) to **1**/MAO (1:MAO:NBE = 1:30:10), a zirconium methylene ($\text{Zr}=\text{CH}_2$) resonance can be observed in the ^1H NMR at $\delta = 8.5$ ppm at 20 °C. This $\text{Zr}=\text{CH}_2$ again at least to some extent undergoes bimolecular decomposition resulting in the formation of ethylene at $T \geq 30$ °C ($\delta = 5.25$ ppm ^1H NMR) (Figure 4.7 and 4.8). Again, the dormant species of zirconium complex (**III**, Scheme 1) and methane can be found ($\delta = 0.82$ and 0.18 ppm at 20 °C) (Figure 4.9). At $T = 40$ °C, a vinyl end group (**VII**, Scheme 4.1) can be clearly seen in the ^1H NMR at $\delta = 4.8$ and 5.6 ppm. The corresponding coupling constants for this vinyl group were successfully assigned (Figure 4.10 and 4.11). This unambiguously shows that the initially formed $\text{Zr}=\text{CH}_2$ species do produce $\text{poly}(\text{NBE})_{\text{ROMP}}$.

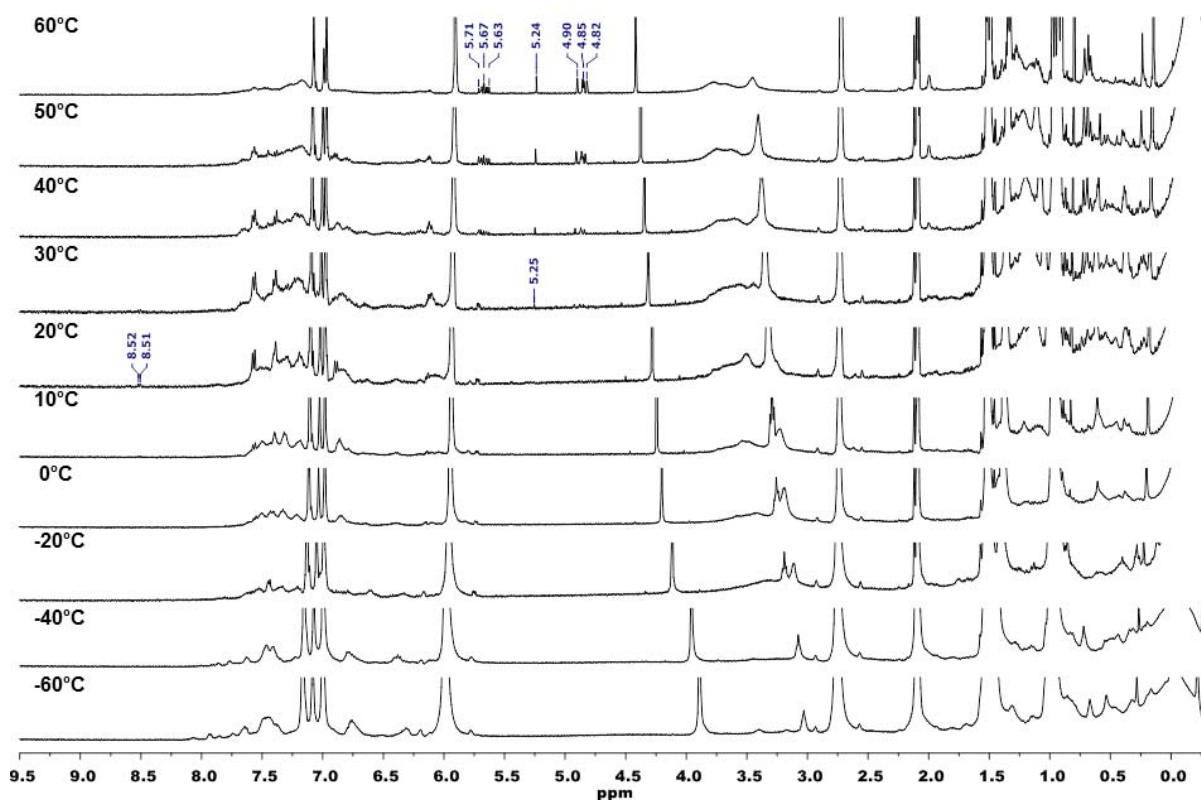


Figure 4.7 Variable-temperature ^1H NMR spectra of 1/MAO/NBE ($\text{toluene-}d_8$).

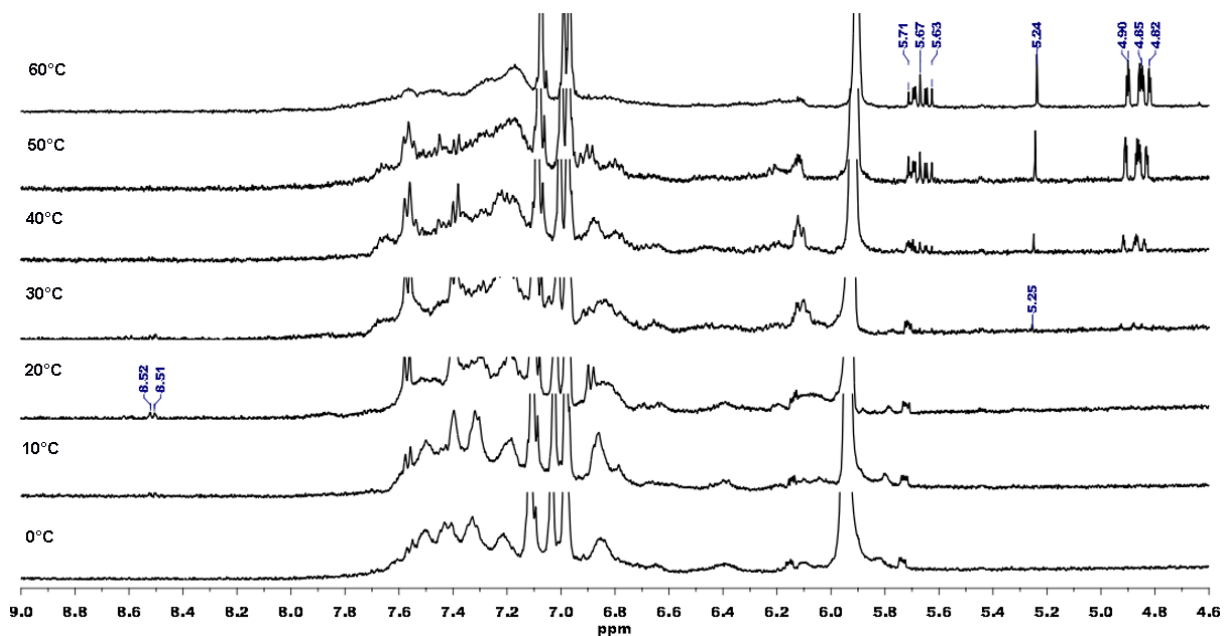


Figure 4.8 Variable-temperature ^1H NMR spectra of 1/MAO/NBE ($\text{toluene-}d_8$) (9.0-4.5 ppm).

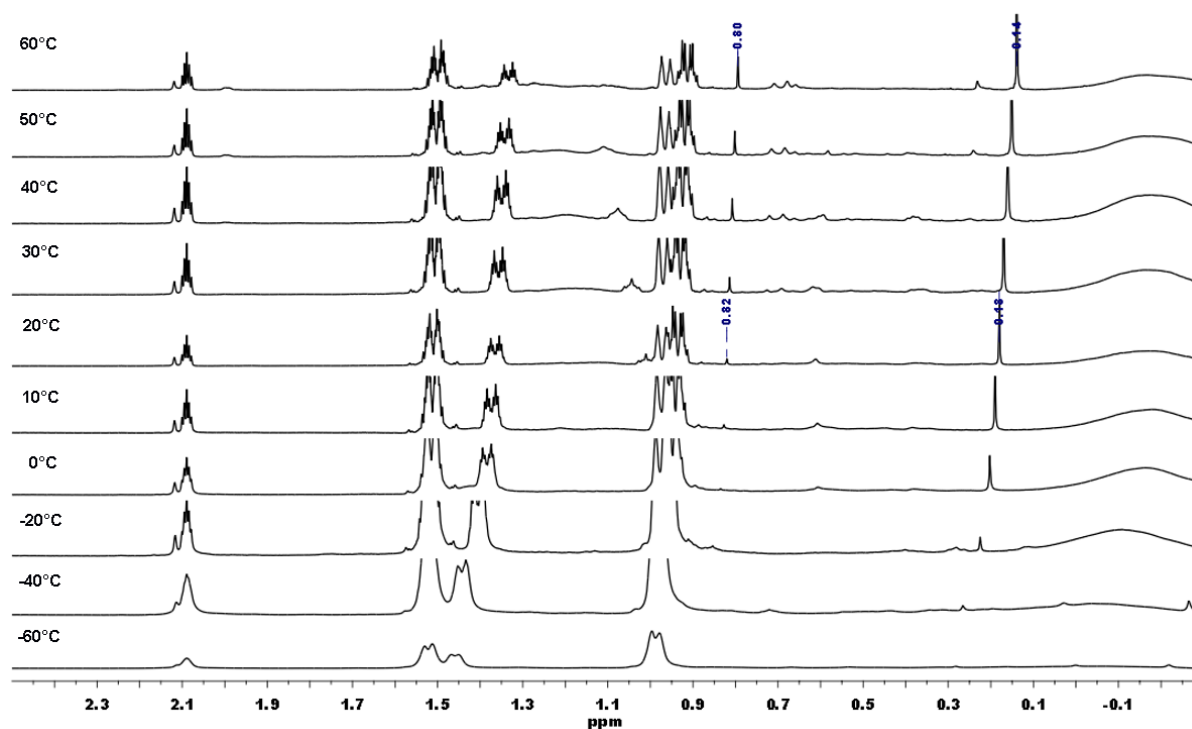


Figure 4.9 Variable-temperature ^1H NMR spectra of **1**/MAO/NBE (toluene- d_8). (2.4-0.2 ppm).

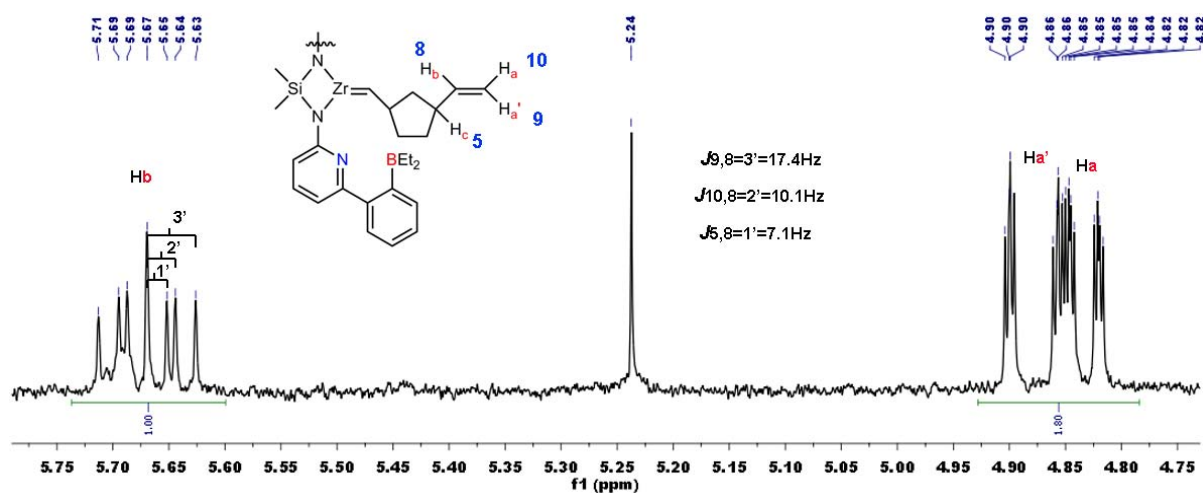


Figure 4.10 Variable-temperature ^1H NMR spectra of **1**/MAO/NBE (toluene- d_8).

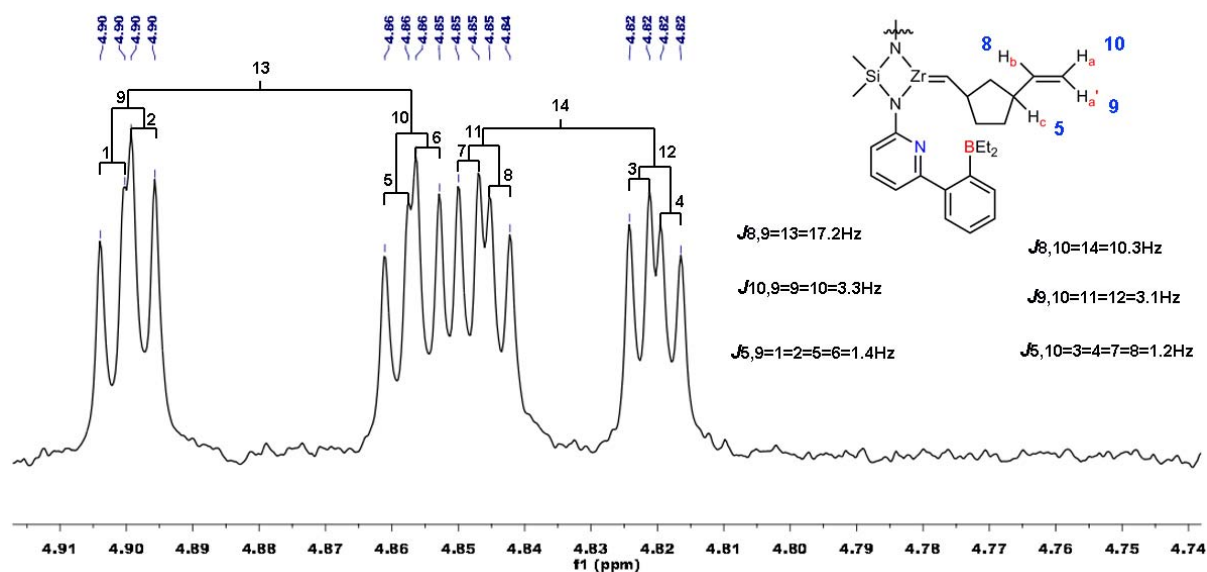


Figure 4.11 Variable-temperature ^1H NMR spectra of 1/MAO/NBE (toluene- d_8).

Concomitantly, apart from tetra-coordinated boron at $\delta = 2.8$ ppm, tri-coordinated boron can be observed by ^{11}B NMR at $\delta = 86.8$ ppm in the temperature range of 20 to 60 °C (Figure 4.12). Notably, at $T > 60$ °C, a second tricoordinated B species appears in the ^{11}B NMR at $\delta = 84.3$ ppm and grows in intensity with increasing temperature. This tricoordinated B-species might very tentatively, without any proof, be attributed to a catalyst species that experienced a switch from ROMP to VIP via α -H addition. This active species (**VIII**, Scheme 4.1) then promotes vinyl insertion polymerization. The fraction of ROMP-derived poly(NBE) in poly(NBE)_{ROMP}/poly(NBE)_{VIP}/poly(E) is, depending on the conditions between 0 and 6 mol-%. One can conclude that the introduction of ethylene, particularly at pressures > 4 bar, shifts the reaction from ROMP towards VIP. This is in line with recent findings, which show that only high NBE concentrations promote the ROMP process. The studies outlined here strongly support that the entire polymerization process indeed starts with α -H abstraction and ROMP. In view of the finding that α -H addition occurs to transform the ROMP-active species into a VIP-active one, additional switches from VIP to ROMP and vice versa can at least not be fully ruled out. Consequently, the poly(NBE)_{ROMP}/poly(NBE)_{VIP}/poly(E) copolymers can in fact be expected to contain the initially proposed multiple ROMP-derived poly(NBE) blocks.

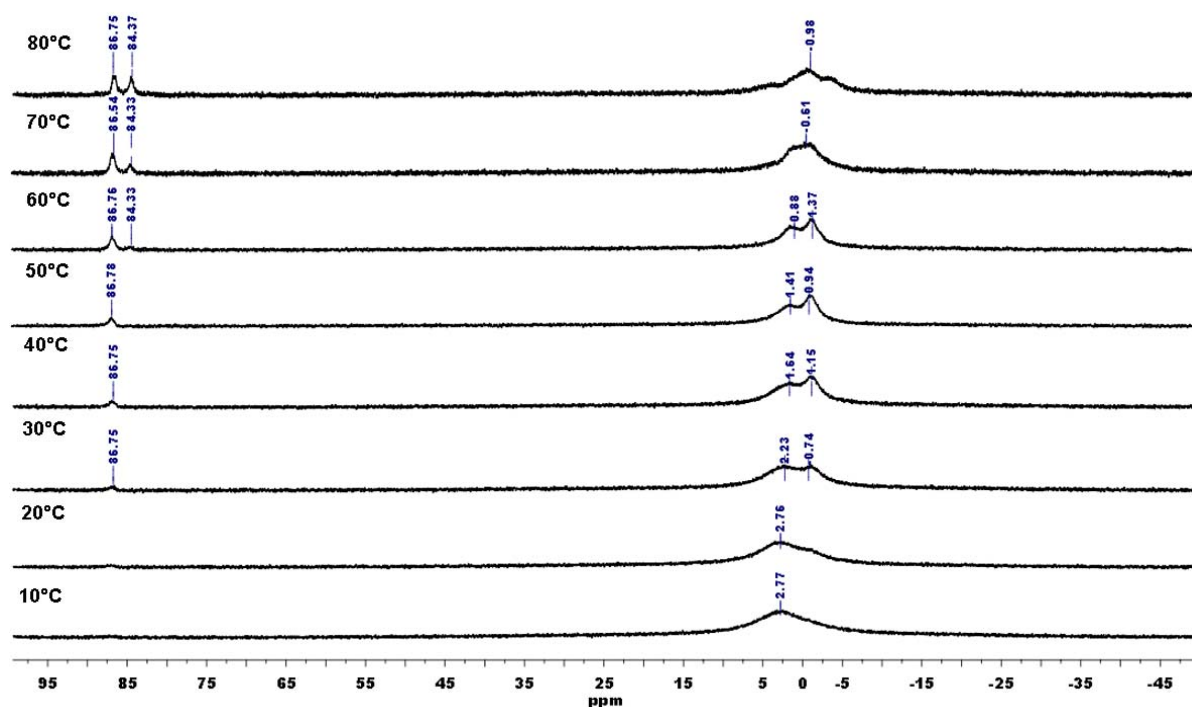


Figure 4.12 Variable-temperature ^{11}B NMR spectra of 1/MAO/NBE (toluene- d_8).

4.3 Conclusions

Both the activation process and active species in the homopolymerization of norborn-2-ene as well as in the copolymerization of ethylene with norborn-2-ene became clear. The pivotal role of the (N-(6-(2-(diethylboryl)phenyl)pyrid-2-yl)-ligand in the α -H abstraction process has been verified. The insights gained in this study, together with existing knowledge will be most helpful for the design of new catalysts suitable for tandem ROMP/VIP copolymerization.

4.4 References

- [1] Y. L. Zou, D. R. Wang, K. Wurst, K. Kühnel, I. Reinhardt, U. Decker, V. Gurram, S. Camadanli, M. R. Buchmeiser, *Chem. Eur. J.* **2011**, *17*, 13832-13846.
- [2] G. V. Narayana, G. J. Xu, D. R. Wang, W. Frey, M. R. Buchmeiser, *ChemPlusChem* **2014**, *79*, 151-162.
- [3] M. R. Buchmeiser, S. Camadanli, D. R. Wang, Y. L. Zou, U. Decker, C. Kühnel, I. Reinhardt, *Angew. Chem.* **2011**, *123*, 3628-3633; *Angew. Chem. Int. Ed.* **2011**, *50*, 3566-3571.

- [4] H. M. Möller, M. C. Baier, S. Mecking, E. P. Talsi, K. P. Bryliakov, *Chem. Eur. J.* **2012**, *18*, 848-856.
- [5] W. Kaminsky, R. Steiger, *Polyhedron* **1988**, *7*, 2375-2381.
- [6] D. Cam, U. Giannini, *Makromol. Chem.* **1992**, *193*, 1049-1055.
- [7] D. E. Babushkin, N. V. Semikolenova, V. N. Panchenko, A. P. Sobolev, V. A. Zakharov, E. P. Talsi, *Macromol. Chem. Phys.* **1997**, *198*, 3845-3854.
- [8] W. Kaminsky, *Macromol. Chem. Phys.* **1996**, *197*, 3907-3945.
- [9] J. Schwartz, K. I. Gell, *J. Organomet. Chem.* **1980**, *184*, C1-C2.
- [10] M. D. Fryzuk, S. S. H. Mao, *J. Am. Chem. Soc.* **1993**, *115*, 5336-5337.
- [11] M. D. Fryzuk, P. B. Duval, S. S. S. H. Mao, M. J. Zaworotko, L. R. MacGillivray, *J. Am. Chem. Soc.* **1999**, *121*, 2478-2487.
- [12] <http://www.chemistry.sdsu.edu/research/BNMR/#summary>.

5. Experimental and Spectroscopic Data

5.1 General Remarks

All manipulations were performed in a LabMaster 130 glove box (MBraun Garching, Germany) or by standard Schlenk techniques under a nitrogen atmosphere unless specified otherwise. CH_2Cl_2 , THF, diethyl ether, toluene and pentane were purchased from J. T. Baker (Devender, Netherlands) and were dried by using an MBraun SPS-800 solvent purification system with alumina drying columns. CDCl_3 , CD_2Cl_2 , $\text{C}_2\text{D}_2\text{Cl}_4$, toluene- d_8 , were dried over calcium hydride, freeze-pump-thaw degassed and stored inside the glove box. C_6D_6 was dried over Na/benzophenone, distilled, and degassed prior to use.

NMR spectra were recorded on a Bruker Avance III 400 spectrometer in the indicated solvent at 25 °C and data are listed in parts per million (ppm) downfield from tetramethylsilane (TMS) as an internal standard.

FT-IR spectra were measured on an ALPHA spectrometer (Bruker) using ATR technology.

GC-MS data were obtained by using an Agilent Technologies 5975C inert MSD with triple-axis detector, a 7693 autosampler, and a 7890A GC system equipped with a SPB-5 fused silica column (34.13 m x 0.25 mm x 0.25 μm film thickness). The injection temperature was set to 150 °C. The column temperature ramped from 30 to 250 °C within 8 min, and was then held for further 5 min. The column flow was set to 1.05 $\text{mL}\cdot\text{min}^{-1}$.

Elemental analysis was done in a Carlo Erba elemental analyzer (1106) at the Institute of Organic Chemistry, University of Stuttgart, Germany.

DSC data were recorded by heating under a nitrogen atmosphere on a SC 7 Perkin-Elmer differential scanning calorimeter.

The number-average molecular weights (M_n), weight-average molecular weights (M_w), and polydispersity indices of polymers were determined either by gel permeation chromatography (GPC) using a Waters 2414 refractive-index detector

and a Waters UV/visible detector vs. polystyrene standards ($800 < M_n < 650000$ $\text{g}\cdot\text{mol}^{-1}$) and CHCl_3 or THF as eluent at a flow rate of $1.0 \text{ mL}\cdot\text{min}^{-1}$ or on a polymer standards high temperature gel permeation chromatography (HT-GPC) system with triple detection (concentration, light-scattering at 15° and 90° , viscosity) using three consecutive Waters Styragel HR 4 4.6×300 mm columns in 1,2,4-trichlorobenzene at 145°C , the flow rate was set to $1 \text{ mL}\cdot\text{min}^{-1}$. Narrow polystyrene standards in the range of $162 < M_n < 6035000$ $\text{g}\cdot\text{mol}^{-1}$ (Easi Vial-red, yellow and green) were purchased from Polymer Labs.

5.2 Functional Polyolefins by Post-polymerization Modification

Materials

$\text{RuCl}_2(\text{PCy}_3)_2(\text{CHPh})$ (**G1**) (PCy_3 = tricyclohexylphosphine), *cis*-cyclooctene (COE), 3-chloroperbenzoic acid (*m*CPBA), 9-borabicyclo[3.3.1]nonane solution 0.5M in THF (9-BBN), hydrogen peroxide (H_2O_2) 30 wt.-%, hydrogen bromide (HBr) (33 wt.-% solution in acetic acid), sodium hydroxide (NaOH), N,N,N',N'',N''-pentamethyldiethylenetriamine (PMDETA), Cu(I)Br, *tert*-butyl acrylate (*t*BA) and 1,2-dichloroethane (anhydrous, 99.8 %) were obtained from Aldrich Chemical Co. (Karlsruhe, Germany). *cis*-4-octene was purchased from Alfa Aesar (Karlsruhe, Germany). *cis*-COE, PMDETA and *t*BA were dried over CaH_2 and distilled under N_2 then degassed by repeated freeze-pump-thaw cycles. Purchased starting materials and other chemicals or reagents were used without further purification unless specified.

Synthesis of Poly(COE)^[1]

($[\text{COE}]_0:[\text{G1}]_0:[\text{CTA}]_0 = 800:1:6$) A solution of **G1** (8.3 mg, 0.010 mmol,) in 1 mL of CH_2Cl_2 was added to a solution of COE (0.88 g, 8 mmol, 800 equiv.) and CTA (8.4 mg, 0.060 mmol) in 30 mL CH_2Cl_2 under vigorous stirring. The reaction mixture was allowed to stir for 8 h at room temperature. After 8 h, the reaction was terminated by the addition of ethyl vinyl ether (2.0 mL) and the polymer was precipitated by the dropwise addition of the solution into methanol. The precipitated polymer was collected by filtration, washed with excess methanol and dried *in vacuo*. Yield: 0.80 g.

¹H NMR (400.133 MHz, CDCl₃, δ in ppm) 5.39-5.32 (m, 2H), 1.97-2.02 (m, 4H), 1.29 (m, 8H) ppm. **¹³C NMR** (100.623 MHz, CDCl₃, δ in ppm) 130.5, 130.0, 32.8, 29.9, 29.8, 29.3, 29.2, 27.4. **FT-IR** (ATR, cm⁻¹): 3003 (m), 2917 (vs), 2849 (vs), 1462 (s), 1070 (w), 964 (s), 720 (s).

Synthesis of Poly(COE-O)

*m*CPBA (0.48 g, 2.8 mmol) was added to a solution of poly(COE) (0.30 g, *M_n* = 118400 g/mol) in dichloromethane (20 mL) under nitrogen at 0 °C. The reaction was gradually warmed to room temperature and stirred for 10 h. The polymer was precipitated from methanol and dried *in vacuo*. Yield: 0.51 g of a white solid. **FT-IR** (ATR, cm⁻¹): 2923 (vs), 2852 (vs), 1463 (s), 1256 (m), 1071 (m), 882 (s), 723 (m).

Synthesis of Poly(COE-OH)^[2-3]

2.2 mL 9-BBN (0.5 M in THF) was added to a 2 wt.-% solution of the poly(COE) (*M_n* = 118400 g/mol, PDI = 1.56) in THF in a Schlenk flask. The flask was placed into a 60 °C oil bath for 16 h. After that the polymer solution was cooled in an ice water bath. The required amounts of aqueous 6 M NaOH solution (1.3 mol/borane) and 30 wt.-% aqueous solution of H₂O₂ (3.9 mol/borane) were added to the reaction solution. Then the solution was allowed to warm to room temperature and was placed into a 60 °C oil bath for 20 h. The polymer was isolated by pouring the solution into water and was washed several times with water. It was redissolved in a THF-methanol mixture, precipitated in water, washed several times with acetone, and dried *in vacuo*. Yield: 95 %. **FT-IR** (ATR, cm⁻¹): 3324 (s), 2917 (vs), 2849 (vs), 1460 (s), 1120 (m), 1031 (s), 719 (m).

Synthesis of Poly(COE-Br)

HBr (1.1 mL, 33 wt.-% solution in acetic acid, 5.9 mmol) was added to a solution of poly(COE) (0.50 g, 0.012 mmol) in 60 mL 1,2-dichloroethane in a pressure tube under nitrogen. The reaction solution was heated to 100 °C and refluxed for 48 h. After that the polymer was precipitated by the dropwise addition of the solution into methanol. The precipitated polymer was collected by filtration, washed with excess

methanol and dried *in vacuo*. Yield: 0.62 g. $^1\text{H NMR}$ (400.133 MHz, CDCl_3 , δ in ppm) 3.97-4.07 (m), 1.72-1.81 (m), 1.29-1.53 (m). $^{13}\text{C NMR}$ (100.623 MHz, CDCl_3 , δ in ppm) 59.1, 39.1-39.3, 29.4-29.6, 29.1-29.2, 27.5-27.7. **FT-IR** (ATR, cm^{-1}): 2924 (s), 2852 (s), 1459 (s), 1305 (m), 1238 (m), 724 (m), 613 (m), 530 (m).

Synthesis of PE-g-PtBA^[4]

Graft copolymerization was carried out in a Schlenk tube. In a typical reaction, poly(COE-Br) (0.10 g, 0.0019 mmol) was placed in a Schlenk tube and 2.8 mL of toluene were added. The mixture was stirred vigorously to get a homogeneous solution. The catalyst, CuBr (0.075 g, 0.52 mmol) and PMDETA (0.091 g, 0.52 mmol) were then added, then the tube was sealed with a silicone rubber septum and purged with nitrogen for 20 min. Then, tBA (3.4 g, 26 mmol) was transferred to the tube with a continuous purge of nitrogen. Afterwards, the Schlenk tube was placed into an oil bath at 90 °C. After a given time, the reaction mixture was cooled to room temperature. The polymerization was terminated by opening the flask to air. Then, the resulting polymer solution was passed through a short alumina column. Finally, the polymer was precipitated by slowly adding the polymer solution to cold pentane. The precipitate was filtered and washed with pentane, then dried *in vacuo*. Yield: 0.27 g. $^1\text{H NMR}$ (400.133 MHz, CDCl_3 , δ in ppm) 4.00-4.05 (m), 2.22 (m), 1.80 (m), 1.25-1.60 (m). $^{13}\text{C NMR}$ (100.623 MHz, CDCl_3 , δ in ppm) 174.3, 80.5, 59.0, 42.5, 42.2, 42.0, 39.3, 37.6, 36.3, 29.5-29.1, 28.1-28.3, 27.7. **FT-IR** (ATR, cm^{-1}): 2975 (m), 2930 (m), 1723 (s), 1478 (m), 1450 (m), 1390 (m), 1366 (s), 1141 (s), 844 (m), 751 (w).

5.3 Bis(diamido)silylene Zirconium^{IV} Complexes Containing the Bromoborane Motifs in Vinyl Insertion Polymerization: On the Role of Cyclopentene

Materials

Boron tribromide, trimethyl(phenyl)silane, methoxytrimethylsilane, *n*-butyllithium solution 1.6 M in hexanes, dichlorodimethylsilane, zirconium(IV) chloride tetrahydrofuran complex (1:2) ($\text{ZrCl}_4 \cdot 2\text{THF}$), cyclopentanol-1- ^{13}C (99 atom-%), bicyclo[2.2.1]hept-2-ene (99 %), cyclopentene were purchased from Sigma-Aldrich

Co. (Karlsruhe, Germany). 1-Adamantylamine was purchased from abcr. phosphoric acid (85 %), potassium pyrosulfate were obtained from Merk (Karlsruhe, Germany). 2-(2-Bromophenyl)-6-(2,2,5,5-tetramethyl-1,2,5-azadisilolidin-1-yl)pyridine (**2**) was synthesized according to literature.^[5] Methylalumoxane (MAO) solution (10 wt.-% in toluene) was purchased from Aldrich Chem. Co. Trimethylaluminum was removed from commercial MAO via drying in *vacuo* (8 h, 70 °C) and the obtained solid MAO was re-dissolved in toluene to prepare a 2.0 M solution, which was stored inside the glove box. Ethylene (Air Products) was dried by passing through columns filled with a Cu-based catalyst (BASF catalyst R3-11) and then through molecular sieves (3 Å) before use. Cyclopentene (95 %, Fluka) was dried over calcium hydride, vacuum transferred and stored in the glove box. Purchased chemicals were used without further purification.

Synthesis of Diphenylmethoxyborane (L1)^[6-7]

In a 100 mL Schlenk flask, PhSiMe₃ (25 g, 0.17 mol) was added dropwise to BBr₃ (20.8 g, 0.08 mol) under nitrogen at 0 °C. After the addition, it was gradually warm to room temperature and then placed into a preheated oil bath at 125 °C which was slowly heated to 200 °C, and refluxed for 16 h. During this time bromotrimethylsilane was coming out through a 30 cm Vigreux column. At last fractionated distillation was applied, and after a by-product dibromophenylborane (10 %) was separated, diphenylbromoborane was collected in a yield of 80 % (11 g). **¹H NMR** (400.133 MHz, CDCl₃, δ in ppm) 7.52 (m, 4H), 7.64 (m, 2H), 8.02 (m, 4H). **¹³C NMR** (100.623 MHz, CDCl₃, δ in ppm) 128.0, 133.2, 137.6. **GC-MS** (EI, 70 eV): *m/z* calcd. for C₁₂H₁₀BBr: 244.92, found: 244.1.

A solution of methoxytrimethylsilane (4.68 g, 4.50 mmol) in toluene (8 mL) was added dropwise with stirring at -78 °C to a solution of diphenylbromoborane (11 g, 4.50 mmol) in toluene (20 mL). The reaction mixture was slowly warmed to room temperature and stirred over night. All volatiles were removed from the reaction mixture *in vacuo* and the crude oily product was extracted into hexane. Yield of diphenylmethoxyborane (**L1**) is 7.1 g (81 %). **¹H NMR** (400.133 MHz, C₆D₆, δ in ppm) 7.24 (m, 6H), 7.66 (m, 4H). **¹³C NMR** (100.623 MHz, C₆D₆, δ in ppm) 128.4, 130.5, 134.7. **GC-MS** (EI, 70 eV): *m/z* calcd. for C₁₃H₁₃BO: 196.05, found: 196.1.

Synthesis of N-Adamantylchlorodimethylsilylamine (L2)^[8]

A solution of *n*-BuLi (1.6 M in hexanes 22 mL, 34.68 mmol) was slowly added to a solution of 1-adamantylamine (5.0 g, 33.05 mmol) in pentane (100 mL) at -60 °C. A large amount of white precipitate formed during the addition. The reaction mixture was warmed to room temperature and stirred for 4 h. The resulting precipitate was collected on a frit, washed with cold *n*-pentane (10 mL) and dried in *vacuo* to give pure lithium 1-adamantylamide (5.0 g, 99 %), which was used for the next reaction without any analysis.

Dichlorodimethylsilane (10.25 g, 79.49 mmol) was stirred in THF (75 mL), lithium-1-adamantylamide (5.0 g, 31.79 mmol) in THF (50 mL) was added slowly and the resulting reaction mixture was allowed to stir for 2.5 h at room temperature. Then, all volatiles were removed in *vacuo* and the residue was extracted with *n*-pentane and evaporated under reduced pressure to isolate **L2** as white solid (6.0 g, 75 %). **¹H NMR** (400.133 MHz, CD₂Cl₂, δ in ppm) 0.45 (s, 6H), 1.34 (br, 1H), 1.62 (s, 6H), 1.73 (s, 6H), 2.03 (s, 3H). **¹³C NMR** (100.623 MHz, CD₂Cl₂, δ in ppm) 4.9, 30.7, 36.8, 47.1, 50.0 ppm. **GC-MS**: *m/z* calcd. for C₁₂H₂₂CINSi: 243.1; found.243.1 (M⁺); **Elemental anal.** calcd. for C₁₂H₂₂CINSi: C 59.11; H 9.09; N 5.74; found C 58.86; H 8.96; N 5.62.

Synthesis of 6-[2-(Diphenylboryl)phenyl]pyridine-2-amine (3b)

n-Butyllithium (1.6 M in hexane, 9.6 mL, 15.3 mmol) was added to a solution of **2** (5.0 g, 12.8 mmol) in diethyl ether (50 mL) at -78 °C and the mixture was stirred for 2 h at this temperature. Diphenylmethoxyborane (**L1**, 2 M in THF, 10 mL, 10 mmol) was then added and the resulting mixture was stirred for a further 1 h at -78 °C. The mixture was allowed to warm to room temperature overnight and then poured into iced water and stirred for 15 minutes. The organic phase was isolated and the water phase was extracted twice with ethyl acetate. The combined organic phases were washed with brine and dried over MgSO₄. After removal of the solvents, the residue was subjected to chromatography on silica gel eluting with EtOAc/pentane (1:10, containing 3 drops of triethylamine per 1000 mL of eluent). Yield: 3.1 g (73 %). **¹H NMR** (400.133 MHz, CDCl₃, δ in ppm) 4.95 (s, 2H), 6.42 (d, ³J_{HH} = 8.3 Hz, 1H), 7.16

(m, 2H), 7.22 (m, 5H), 7.35 (m, 5H), 7.52 (d, $^3J_{\text{HH}} = 7.1$ Hz, 1H), 7.74 (t, $^3J_{\text{HH}} = 7.9$ Hz, 2H). ^{13}C NMR (100.623 MHz, CDCl_3 , δ in ppm) 106.2, 108.5, 121.2, 125.8, 125.9, 127.7, 130.0, 130.1, 133.5, 136.2, 141.3, 154.8, 157.1. FT-IR (ATR, cm^{-1}): 3502 (s), 3397 (s), 3060 (s), 1636 (s), 1496 (s), 1425 (s), 1305 (m), 1174 (s), 863 (m), 805 (m), 757 (s), 702 (s). ESI-MS: m/z calcd. for $\text{C}_{23}\text{H}_{19}\text{BN}_2$: 334.22, found: 334.2.

Synthesis of N-Adamantyl-N¹-(6-(2-(diethylboryl)phenyl)pyridin-2-yl)-1,1'-dimethylsilyldiamine (5b)

n-Butyllithium (1.6 M in hexanes, 2 mL, 3.1 mmol) was added to a solution of **3b** (1 g, 3 mmol) in diethyl ether at -37 °C. The pale-yellow solution was allowed to warm to room temperature and then stirred for another 1 h. The precipitate was collected by filtration, washed with cold diethyl ether/pentane (1:10, v/v), and dried *in vacuo* to give a pure yellow Li salt of **5** (Yield 1.1 g, 92 %) which was used without further analysis.

N-Adamantylchlorodimethylsilylamine (**L2**, 0.66 g, 2.7 mmol) was added to a suspension of the lithium salt of **3b** (1.1 g, 2.7 mmol) in diethyl ether at -37 °C. The solution was allowed to warm to room temperature and stirred for 4 h. Afterwards, the solution was filtered over celite and washed with diethyl ether. The volatiles were removed *in vacuo* and the crude product was recrystallized from diethyl ether/pentane. Yield 1.2 g, 86 %. ^1H NMR (400.133 MHz, CD_2Cl_2 , δ in ppm) -0.03 (s, 3H), 0.91 (s, 1H), 1.15 (t, $^3J_{\text{HH}} = 7.0$ Hz, 6H), 1.37 (d, $^3J_{\text{HH}} = 2.5$ Hz, 6H), 1.44 (d, $^3J_{\text{HH}} = 11.2$ Hz, 3H), 1.53 (d, $^3J_{\text{HH}} = 12.1$ Hz, 3H), 1.86 (s, 3H), 3.43 (q, $^3J_{\text{HH}} = 7.0$ Hz, 4H), 5.19 (s, 1H), 6.99 (d, 1H, $^3J_{\text{HH}} = 8.5$ Hz), 7.10 (m, 2H), 7.17 (m, 4H), 7.28 (m, 6H), 7.34 (d, $^3J_{\text{HH}} = 7.5$ Hz, 1H), 7.48 (d, $^3J_{\text{HH}} = 6.8$ Hz, 1H), 7.77 (m, 2H). ^{13}C NMR (100.623 MHz, CD_2Cl_2 , δ in ppm) 0.3, 15.7, 30.5, 36.6, 46.9, 50.4, 66.2, 106.3, 110.9, 121.5, 126.1, 126.2, 127.9, 129.6, 130.8, 133.7, 137.4, 141.1, 156.7, 157.2. FT-IR (ATR, cm^{-1}): 3120 (s), 3080 (w), 2905 (s), 1626 (s), 1569 (s), 1493 (s), 1454 (m), 1382 (m), 1305 (m), 1261 (m), 1171 (s), 1140 (s), 1097 (m), 1034 (s), 1005 (m), 877 (s), 836 (s), 760 (s), 731 (s), 703 (s). ESI-MS: m/z calcd. for $\text{C}_{35}\text{H}_{40}\text{BN}_3\text{Si}$: 541.61, found: 541.32.

Synthesis of {Me₂Si[(NAd)(6-(2-(diphenylboryl)phenyl)pyridyl-2-yl-N)]ZrCl₂} (7b)

A solution of *n*-butyllithium (1.6 M in hexanes, 1.7 mL, 2.8 mmol) was added to a solution of **5** (0.6 g, 1.1 mmol) in pentane (15 mL) at -37 °C. The reaction mixture was warmed to room temperature and stirred for 3 h. The resulting precipitate was collected on a frit, washed with cold pentane and dried *in vacuo* to give a pure Li salt of **5** (0.57 g, 73 %) which was used without any further analysis.

The Li salt of **5b** (0.57 g, 0.8 mmol) was dissolved in tetrahydrofuran (10 mL) and added dropwise to a solution of ZrCl₄·2THF (0.31 g, 0.8 mmol) in tetrahydrofuran (20 mL) at -37 °C and the resulting reaction mixture was allowed to stir at room temperature for 6 h. After removal of the solvent, toluene was added and the mixture was stirred for half an hour. It was then filtered through celite and the filtrate was concentrated *in vacuo*. The obtained oily product was recrystallized from dichloromethane/pentane at -37 °C to give a colorless powder. Crystals suitable for single crystal X-ray analysis were obtained via recrystallization from dichloromethane/diethylether/pentane. Yield 0.2 g, 31 %. ¹H NMR (400.133 MHz, CD₂Cl₂, δ in ppm) 0.68 (s, 3H), 1.16 (t, ³J_{HH} = 7.0 Hz, 3H), 1.56 (s, 6H), 1.82 (d, ³J_{HH} = 3.0 Hz, 6H), 1.97 (s, 3H), 3.44 (q, ³J_{HH} = 7.0 Hz, 2H), 6.72 (d, ³J_{HH} = 8.4 Hz, 1H), 7.19 (t, ³J_{HH} = 7.5 Hz, 1H), 7.26 (t, ³J_{HH} = 7.3 Hz, 1H), 7.38 (d, ³J_{HH} = 7.5 Hz, 1H), 7.42-7.45 (m, 6H), 7.61-7.68 (m, 2H), 7.93-7.98 (m, 5H). ¹³C NMR (100.623 MHz, CD₂Cl₂, δ in ppm) 3.6, 15.7, 31.0, 36.6, 46.4, 61.0, 66.3, 107.3, 113.7, 122.0, 126.9, 128.9, 131.2, 132.0, 132.1, 136.0, 136.4, 142.6, 157.4, 159.7. **Elemental anal.** calcd. for C₃₅H₃₈BCl₂N₃SiZr·0.5C₄H₁₀O·0.5CH₂Cl₂: C 57.65, H 5.69, N 5.38; found C 57.84, H 5.84, N 5.36.

Cyclopentene-1-¹³C [9-10]

Cyclopentanol-1-¹³C (10 g, 0.12 mol), phosphoric acid 85 % (44 g), potassium pyrosulfate (27 g), and a stirring bar were placed in a 100 mL pear-shaped flask. The flask was fitted with a small condenser connected to a receiving vessel, which was immersed in a liquid nitrogen bath. Cyclopentene-1-¹³C began to distil at 50 °C, and after initial frothing had subsided the temperature of the contents was raised from 90 °C to 140 °C. The cyclopentene-1-¹³C distillate (6.0 g, 76 % yield) was dried over calcium hydride, and kept in refrigerator. ¹H NMR (400.13 MHz, CDCl₃, δ in ppm)

1.83 (m, 2H), 2.32 (m, 4H), 5.73 (m, 1H), 5.76 (m, 1H). ^{13}C NMR (100.62 MHz, CDCl_3 , δ in ppm) 22.9, 32.5, 130.8. **GC-MS** (EI, 70eV) m/z calcd. for C_5H_8 : 69.12, found: 69.1, $t_R = 1.92$ min.

General Procedure for Ethylene Homo/Copolymerization ^[11]

The homopolymerization of ethylene or copolymerization of ethylene with cyclopentene or NBE was carried out in a 500 mL Büchi glass autoclave with a Type I glass pressure vessel. Temperature was adjusted with a heat jacket connected to a thermostat, which allowed adjustment of the polymerization temperature with an accuracy of ± 0.5 °C. During polymerization runs, the ethylene pressure was kept constant using a pressure controller. Ethylene consumption was monitored with a Büchi press flow gas controller bpc 6010 GC. For a typical copolymerization, the reactor was evacuated at 100 °C for 2 h. It was then flushed with argon several times while the temperature was equilibrated to 30 °C within 30 min. The reactor was charged with a solution of monomer in toluene, toluene, a solution of MAO in toluene, and ethylene up to a total volume of 240 mL. The polymerization was started by injection of the corresponding pre-catalyst in toluene. After 1 h, the reaction was quenched by addition of methanol (20 mL).

After discharge and cleaning, the reactor was evacuated at 100 °C for the next polymerization cycle. The polymer was precipitated upon pouring the whole reaction mixture into methanol (200 mL) to which concentrated hydrochloric acid (20 mL) had been added. The polymer was collected by filtration, washed with methanol and then dried *in vacuo* at 40 °C until the weight remained constant.

Copolymerization of Ethylene with Cyclopentene-1- ^{13}C

Copolymerization of ethylene with cyclopentene-1- ^{13}C was carried out in a 50 mL pressure tube equipped with an oil bath, vacuum lines and pressure gauge. A mixture of the catalyst:MAO:CPE = 1:2000:4000 in 5 mL of toluene was introduced into a pressure tube inside glove box. The pressure tube was removed from the glove box and charged with ethylene gas. Polymerization was stopped by closing the ethylene valve and introducing methanol (10 mL) into the pressure tube. The polymer

was precipitated from methanol (50 mL) to which concentrated hydrochloric acid (2 mL) had been added. The polymer was collected by filtration, washed with methanol and then dried *in vacuo* at 40 °C overnight.

5.4 On the Mechanism of Tandem Ring-Opening Metathesis/Vinyl Insertion Copolymerization of Ethylene With Norborn-2-ene

Materials

Complex **1** was synthesized according to the literature.^[5] Bicyclo[2.2.1]hept-2-ene (99 %), methylaluminoxane (MAO) solution (10 wt.-% in toluene) were purchased from Sigma-Aldrich Co. (Karlsruhe, Germany). Trimethylaluminum was removed from commercial MAO via drying *in vacuo* (8 h, 70 °C) and the obtained solid MAO was re-dissolved in toluene to prepare a 2.0 M solution, which was stored inside the glove box. Ethylene (Air Products) was dried by passing through columns filled with a Cu-based catalyst (BASF catalyst R3-11) and then through molecular sieves (3 Å) before use. Purchased starting materials and other chemicals or reagents were used without further purification unless specified. ¹¹B NMR was measured in a quartz tube.

Homopolymerization of NBE

The homopolymerization of NBE was carried out in Schlenk flask and all preparations were carried out in a glove box. The freshly NBE and a defined amount of MAO were dissolved in toluene 45 mL in a Schlenk flask. After the mixture was stirred for 5 min it was quickly transferred to the indicated temperature while a defined amount of pre-catalyst **1** in toluene 5 mL was added. The reaction was kept at 60 °C for 1 h and was then quenched by the addition of 10 mL methanol. The polymer was precipitated upon pouring the whole reaction mixture into methanol (200 mL) to which concentrated hydrochloric acid (20 mL) had been added. The polymer was collected by filtration, washed with methanol and then dried *in vacuo* at 40 °C over night.

Copolymerization of Ethylene with NBE ^[11]

The copolymerization of ethylene with NBE was carried out in a 500 mL Büchi glass autoclave with a Type I glass pressure vessel. Temperature was adjusted with a heat jacket connected to a thermostat, which allowed adjustment of the polymerization temperature with an accuracy of ± 0.5 °C. During polymerization runs, the ethylene pressure was kept constant using a pressure controller. Ethylene consumption was monitored with a Büchi press flow gas controller bpc 6010 GC. For a typical copolymerization, the reactor was evacuated at 100 °C for 2 h. It was then flushed with argon several times while the temperature was equilibrated to 30 °C within 30 min. The reactor was charged with a solution of NBE in toluene, toluene, a solution of MAO in toluene, and ethylene up to a total volume of 240 mL. The polymerization was started by injection of the pre-catalyst **1** in toluene. After 1 h, the reaction was quenched by addition of methanol (20 mL).

After discharge and cleaning, the reactor was evacuated at 100 °C for the next polymerization cycle. The polymer was precipitated upon pouring the whole reaction mixture into methanol (200 mL) to which concentrated hydrochloric acid (20 mL) had been added. The polymer was collected by filtration, washed with methanol and then dried *in vacuo* at 40 °C until the weight remained constant.

Prepared Sample for Variable-Temperature ^1H NMR on 1/MAO/NBE ^[12]

Manipulations were done inside glove box under a nitrogen atmosphere. 1:MAO:NBE = 1:30:10, $[\mathbf{1}] = 8 \times 10^{-3} \text{ mol}\cdot\text{L}^{-1}$. MAO and NBE were dissolved in toluene- d_8 and kept in an NMR tube, after cooling at -37 °C for 4 h, a chilled solution of **1** in toluene- d_8 was added to the NMR tube. The total volume of the solution was 0.6 mL. The NMR tube was sealed with Teflon and cooled with liquid nitrogen prior to measurements.

Prepared Sample for Variable-Temperature ^{11}B NMR on 1/MAO/NBE

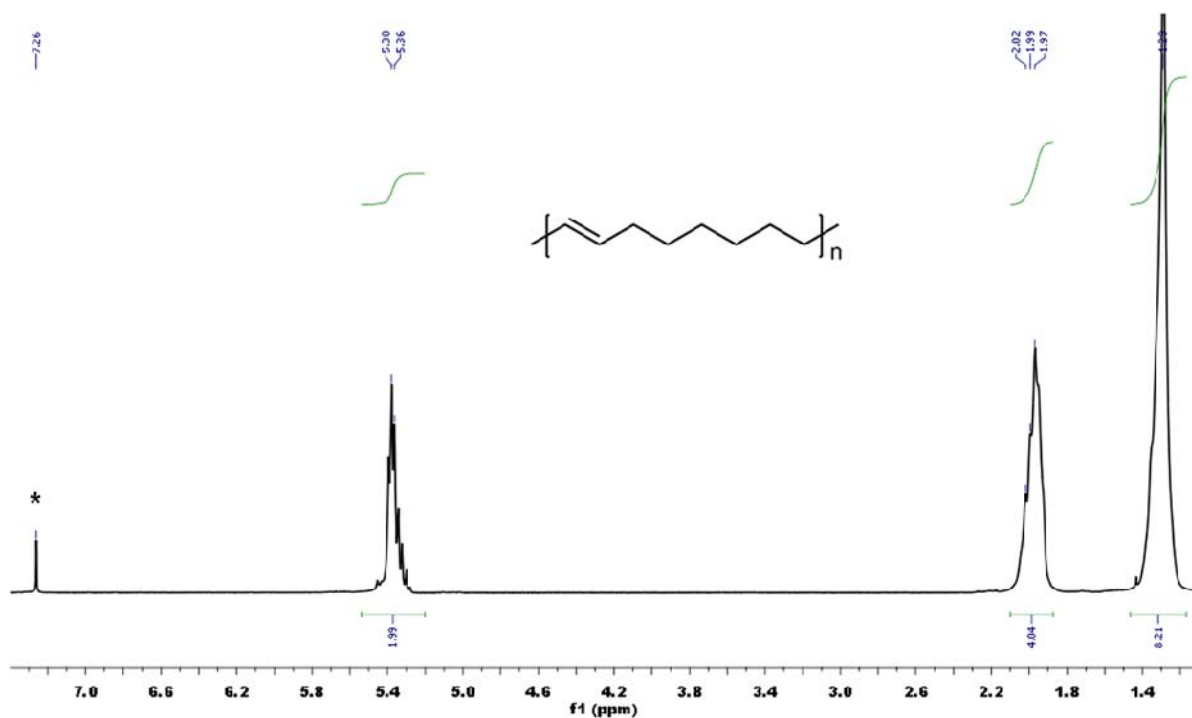
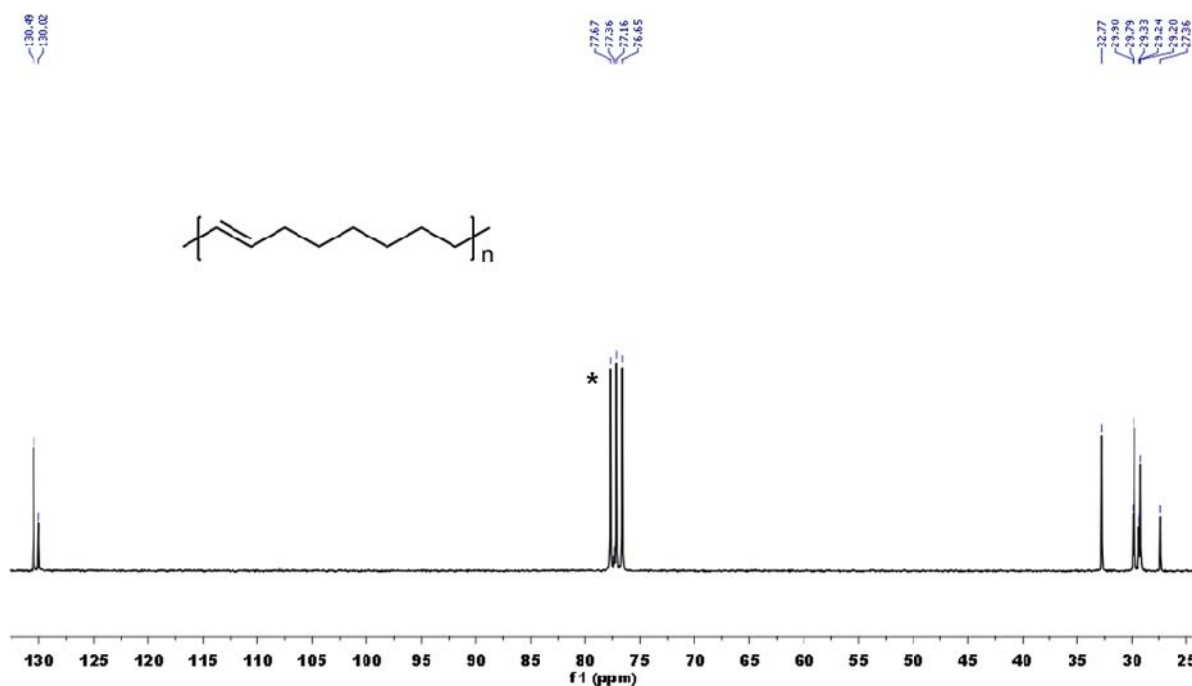
Manipulations were done inside glove box under a nitrogen atmosphere. 1:MAO:NBE = 1:30:10, $[\mathbf{1}] = 40 \times 10^{-3} \text{ mol}\cdot\text{L}^{-1}$. MAO and NBE were dissolved in toluene- d_8 and kept in an NMR tube, after cooling at -37 °C for 4 h, a chilled solution of **1** in toluene- d_8 was added to the NMR tube. The total volume of the solution was 0.6 mL. The NMR tube was sealed with Teflon and cooled with liquid nitrogen prior to measurements.

5.5 References

- [1] R. Walker, R. M. Conrad, R. H. Grubbs, *Macromolecules* **2009**, *42*, 599-605.
- [2] S. Ramakrishnan, *Macromolecules* **1991**, *24*, 2753-3759.
- [3] T. C. Chung, M. Raate, E. Berluce, D. N. Schulz, *Macromolecules* **1988**, *21*, 1903-1907.
- [4] D. J. Haloi, K. Naskar, N. K. Singha, *Macromol. Chem. Phys.* **2011**, *212*, 478-484.
- [5] Y. L. Zou, D. R. Wang, K. Wurst, K. Kühnel, I. Reinhardt, U. Decker, V. Gurram, S. Camadanli, M. R. Buchmeiser, *Chem. Eur. J.* **2011**, *17*, 13832-13846.
- [6] W. Haubold, J. Herdtle, W. Gollinger, W. Einholz, *J Org. Chem.* **1986**, *315*, 1-8.
- [7] L. Kaufmann, J. Breunig, H. Vitze, F. Schödel, I. Nowik, M. Pichlmaier, M. Bolte, H. Lerner, R. F. Winter, R. H. Herber, M. Wagner, *Dalton Trans.* **2009**, 2940-2950.
- [8] G. V. Narayana, G. J. Xu, D. R. Wang, W. Frey, M. R. Buchmeiser, *ChemPlusChem* **2014**, *79*, 151-162.
- [9] S. D. Larsen, P. J. Vergamini, T. W. Whaley, *J. Labelled Comp.* **1975**, 325-332.
- [10] J. R. Heys, W. P. Duncan, W. C. Perry, D. A. Ebert, G. Radolovich, C. L. Haile, *J. Labelled Comp. Radiopharm.* **1979**, 295-306.
- [11] J. Kiesewetter, W. Kaminsky, *Chem. Eur. J.* **2003**, *9*, 1750-1758.
- [12] H. M. Möller, M. C. Baier, S. Mecking, E. P. Talsi, K. P. Bryliakov, *Chem. Eur. J.* **2012**, *18*, 848-856.

6. Appendix

6.1 Functional Polyolefins by Post-polymerization Modification

Figure 6.1.1 ^1H NMR spectra of poly(COE) (CDCl_3).Figure 6.1.2 ^{13}C NMR spectrum of poly(COE) (CDCl_3).

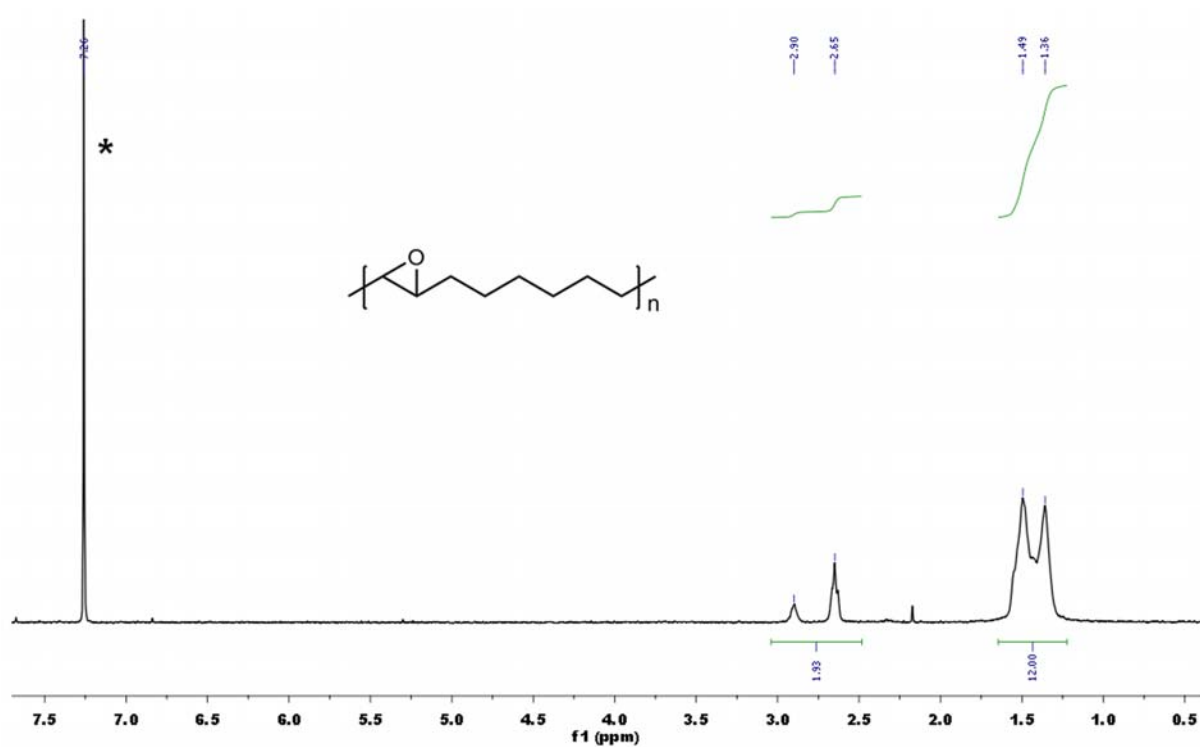


Figure 6.1.3 ^1H NMR spectrum of poly(COE-O) (CDCl_3).

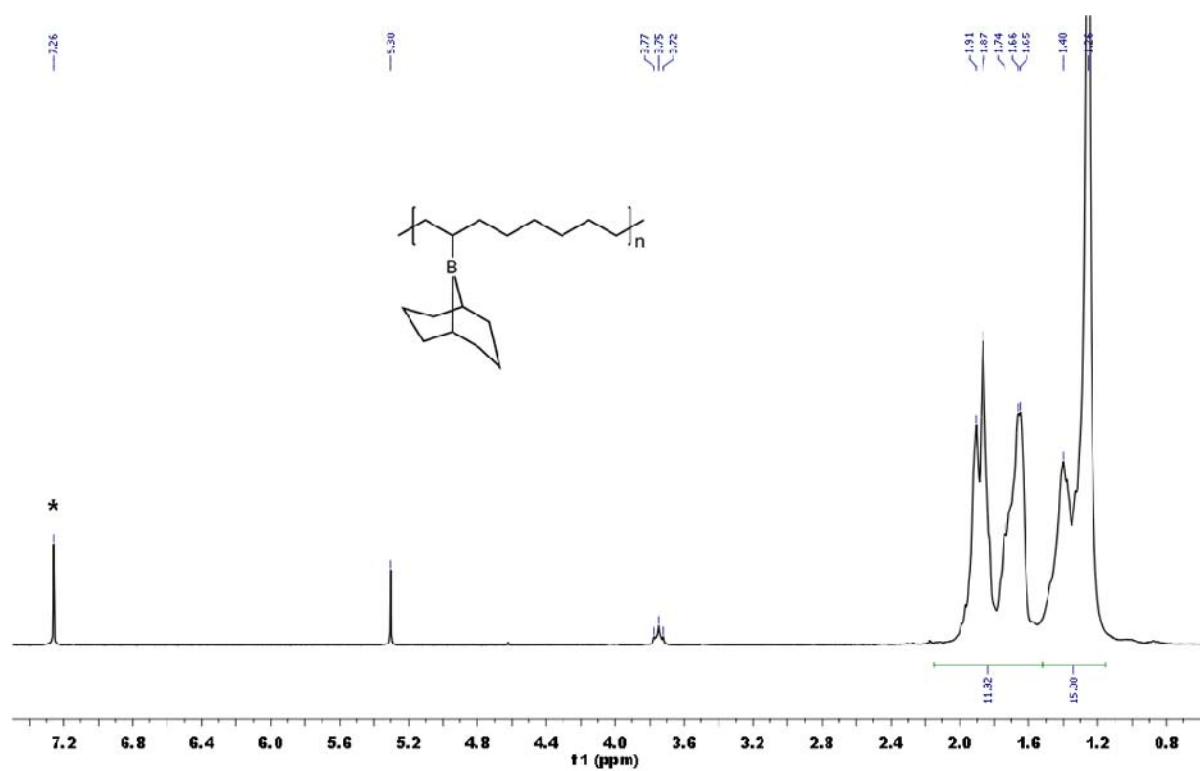


Figure 6.1.4 ^1H NMR spectrum of poly(COE-9-BBN) (CDCl_3).

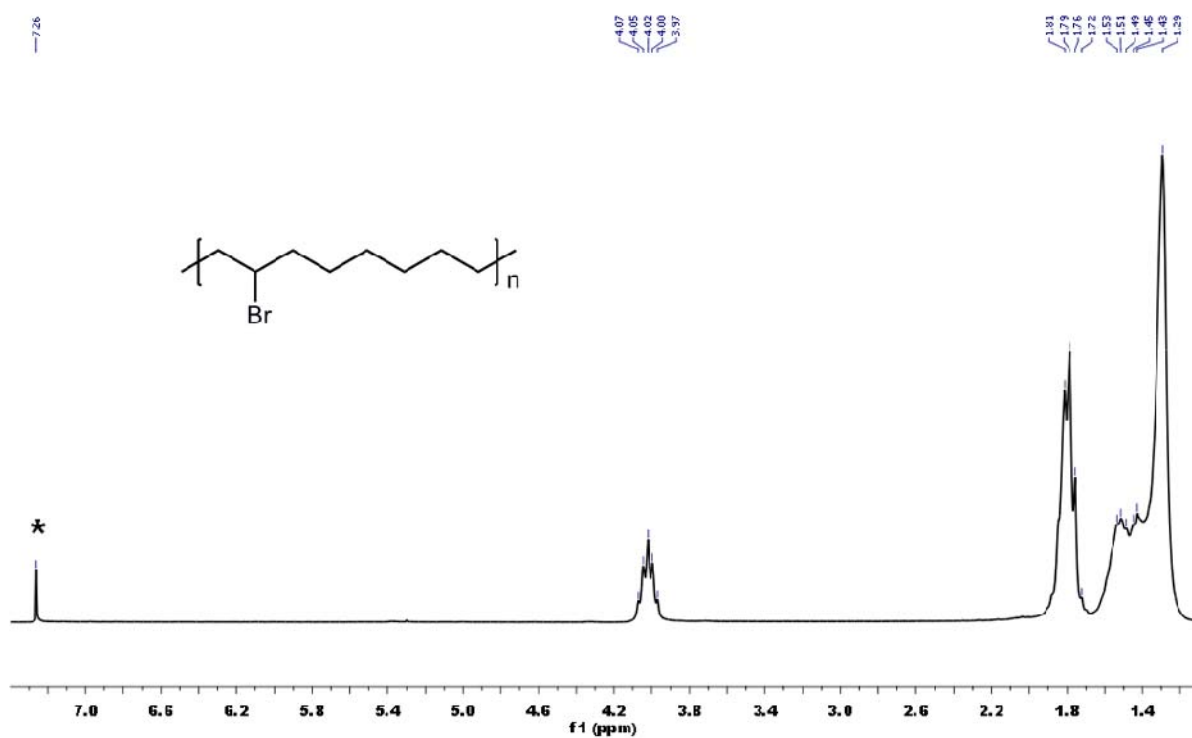


Figure 6.1.5 ^1H NMR spectrum of poly(COE-Br) (CDCl_3).

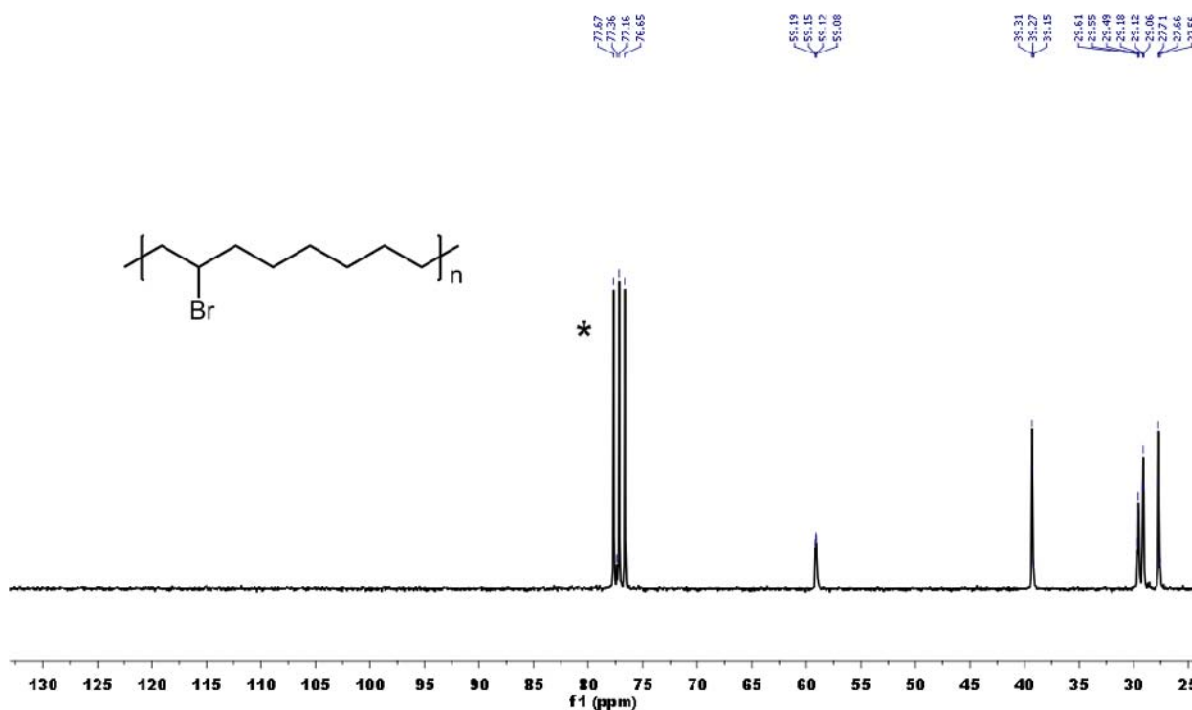


Figure 6.1.6 ^{13}C NMR spectrum of poly(COE-Br) (CDCl_3).

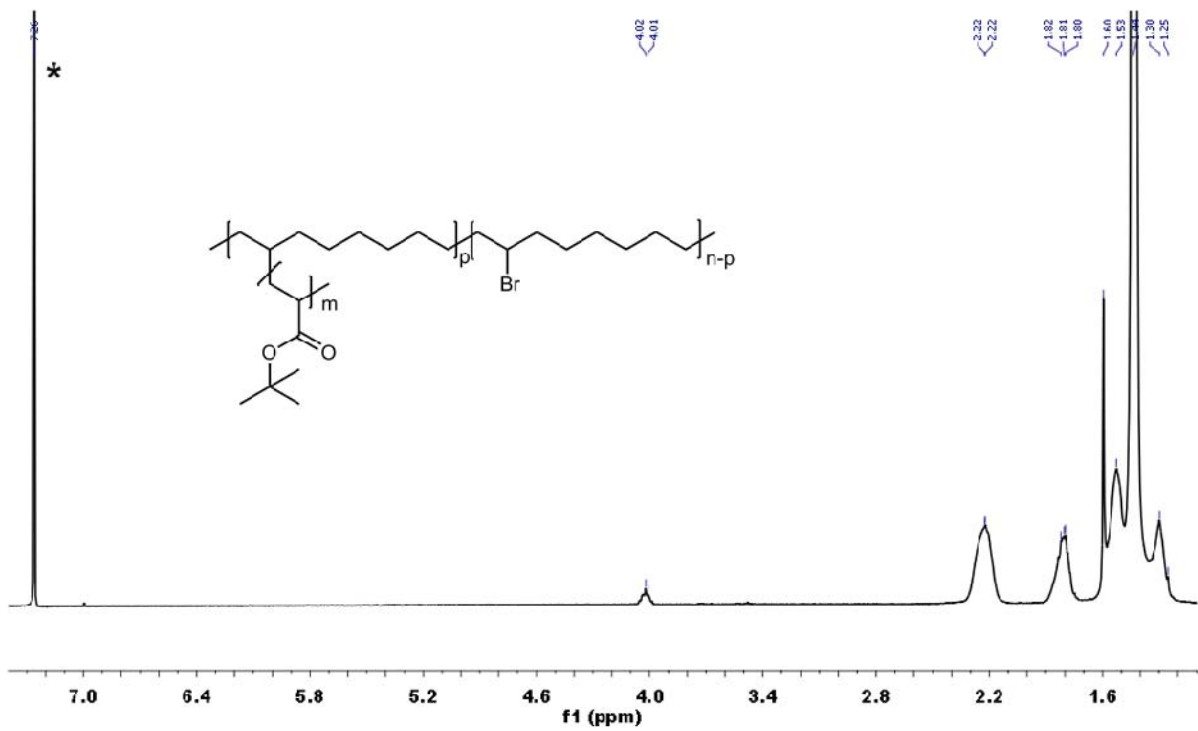


Figure 6.1.7 ^1H NMR spectrum of PE-g-PtBA (CDCl_3).

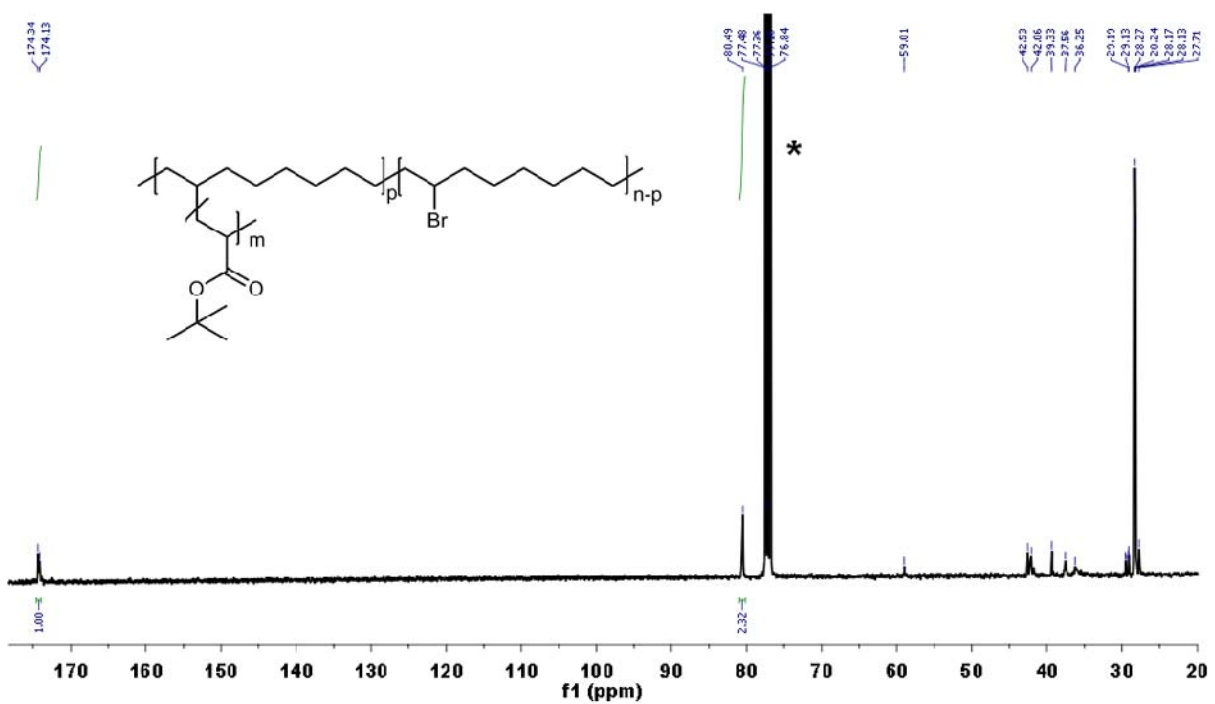


Figure 6.1.8 ^{13}C NMR spectrum of PE-g-PtBA (CDCl_3).

6.2 Bis(diamido)silylene Zirconium^{IV} Complexes Containing the Bromoborane Motifs in Vinyl Insertion Polymerization: On the Role of Cyclopentene

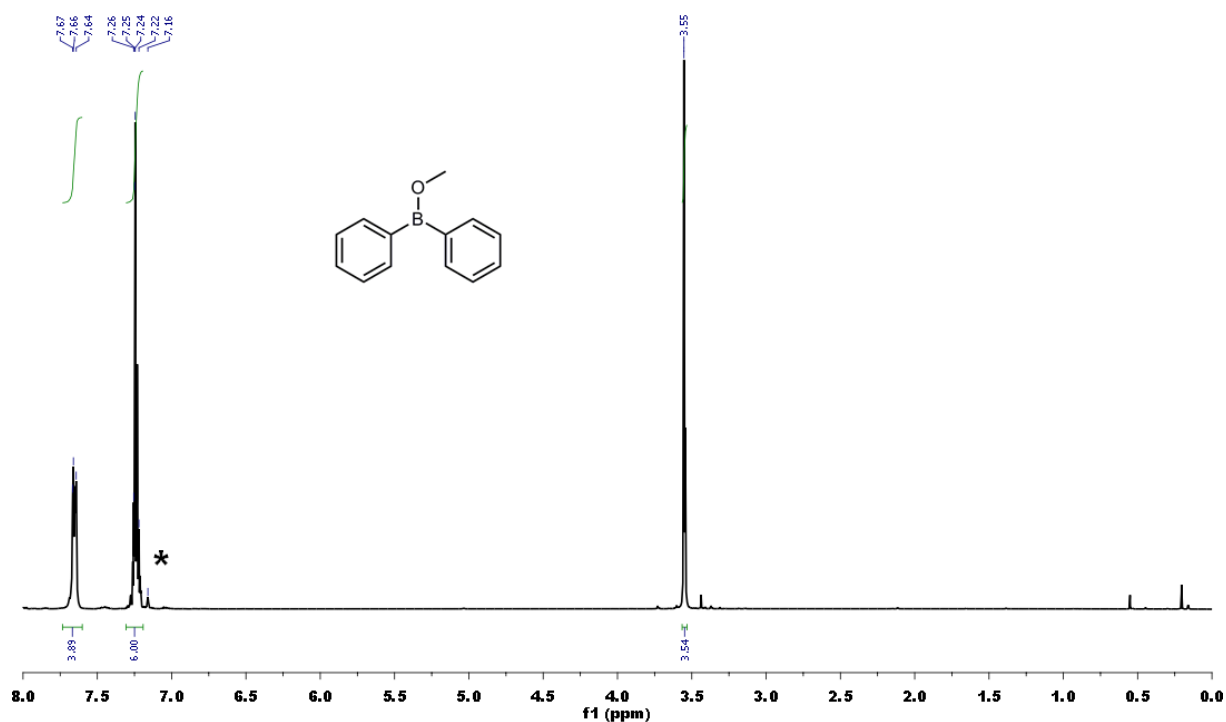


Figure 6.2.1 ¹H NMR spectrum of L1 (C₆D₆).

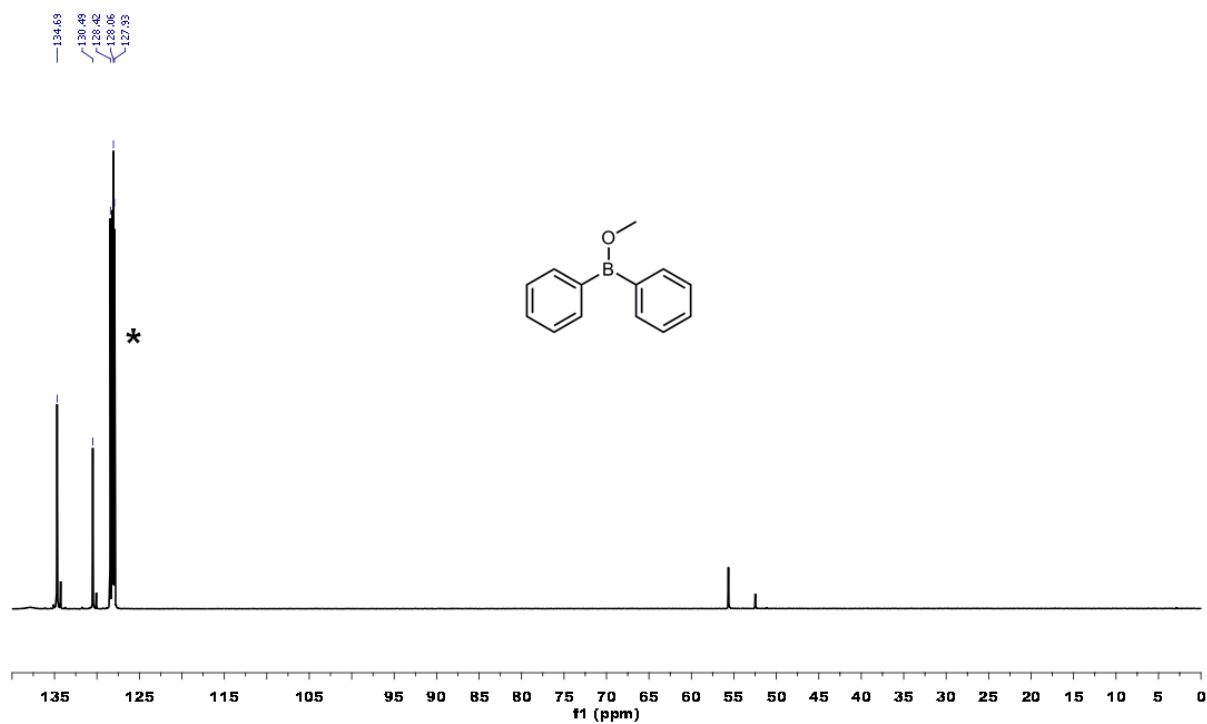
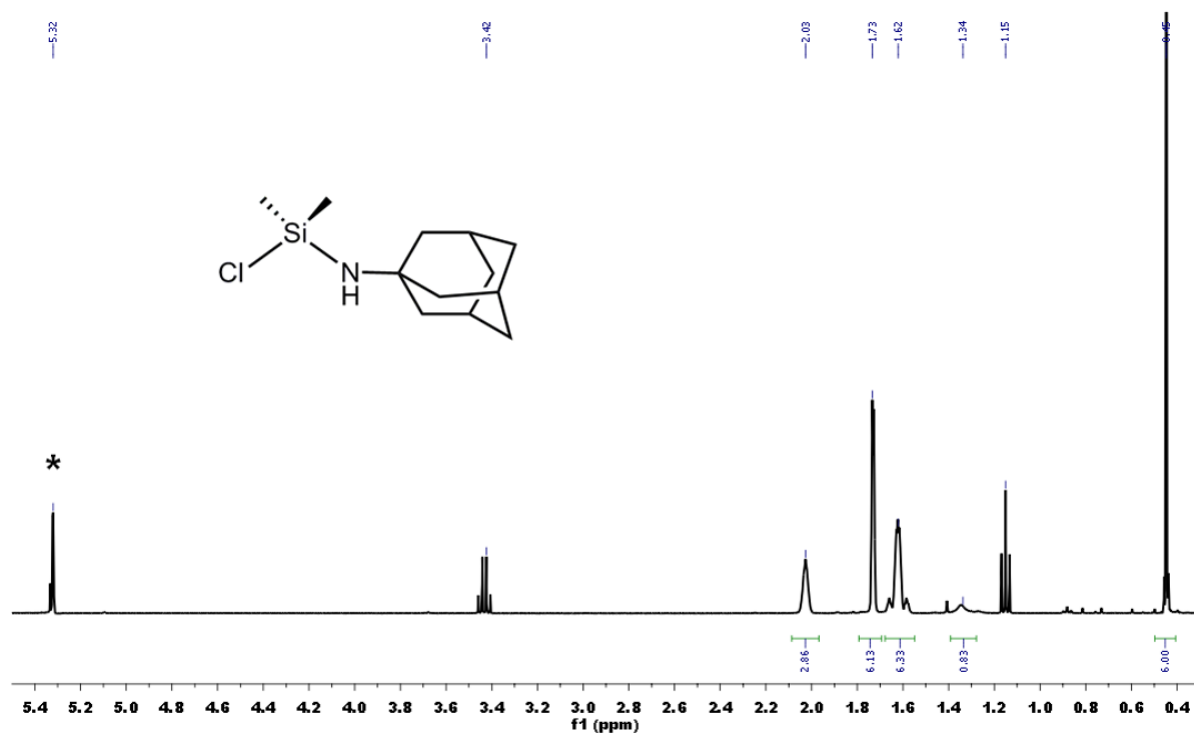
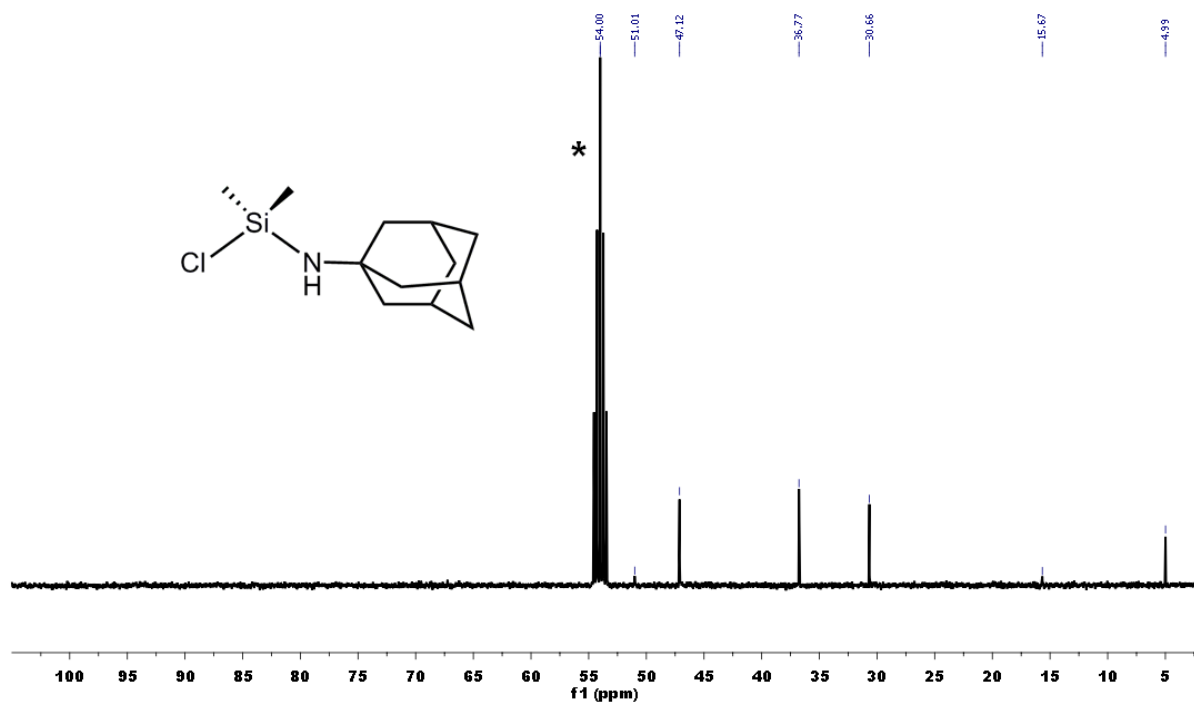
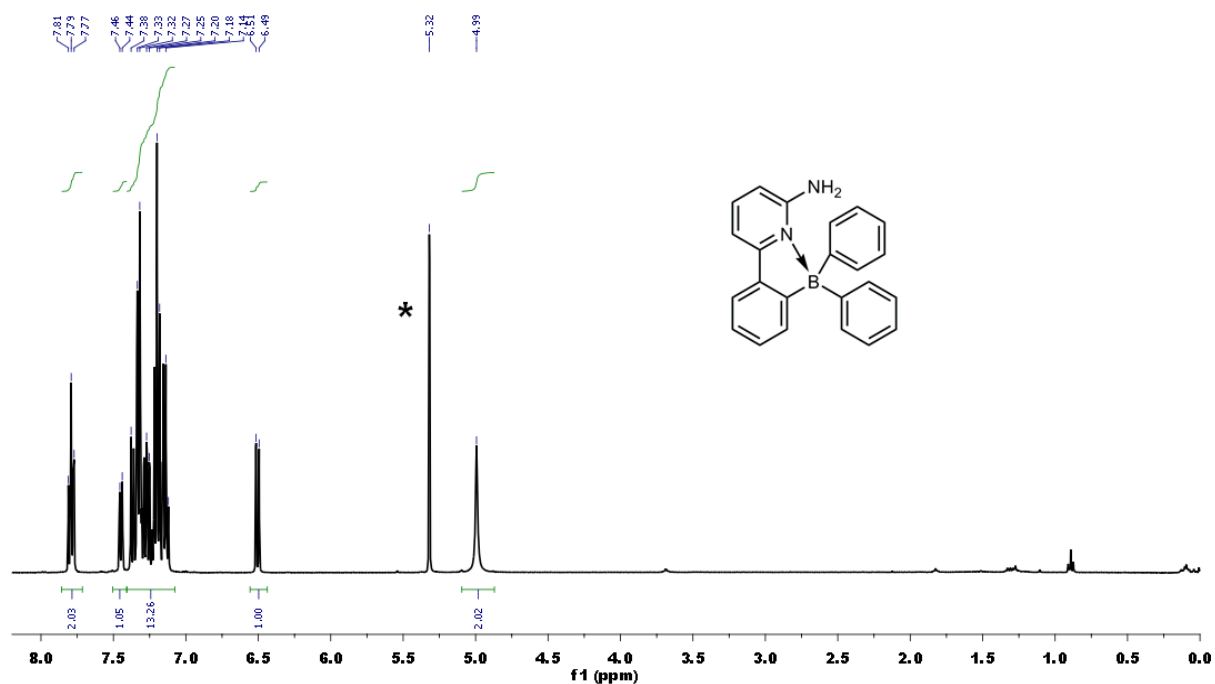
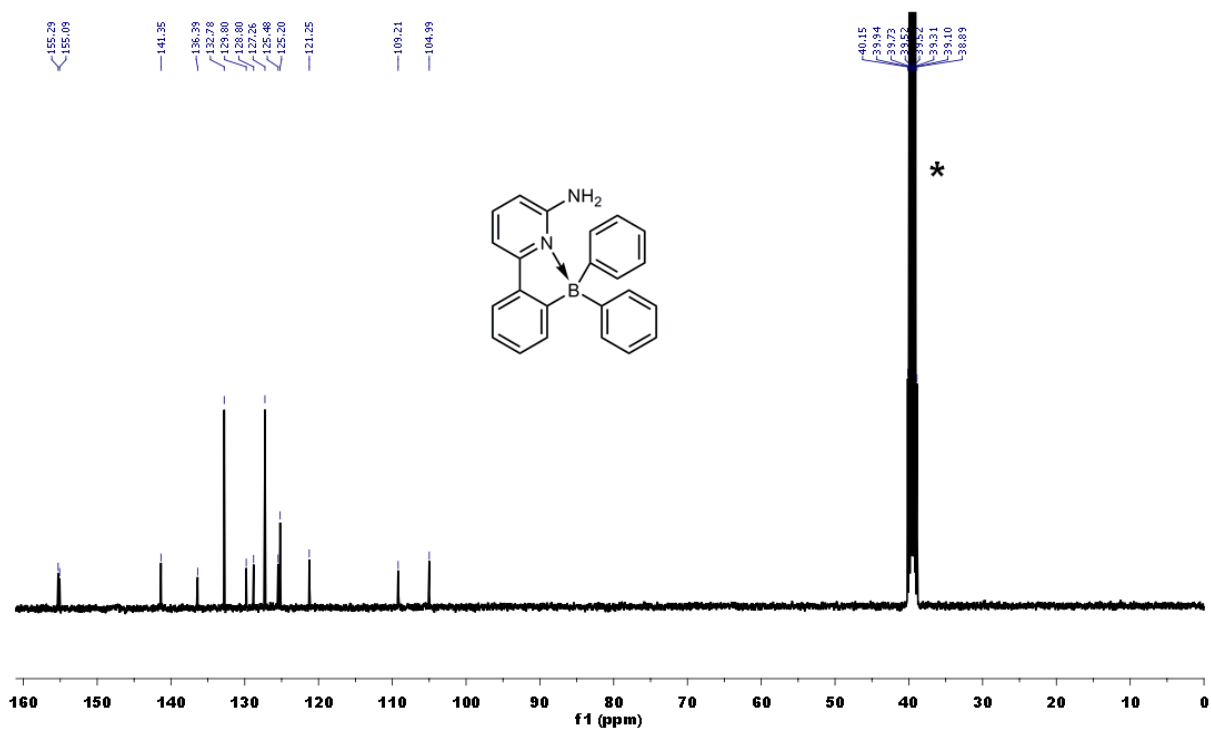


Figure 6.2.2 ¹³C NMR spectrum of L1 (C₆D₆).

Figure 6.2.3 ^1H NMR spectrum of L2 (CD_2Cl_2).Figure 6.2.4 ^{13}C NMR spectrum of L2 (CD_2Cl_2).

Figure 6.2.5 ^1H NMR spectrum of **3b** (CD_2Cl_2).Figure 6.2.6 ^{13}C NMR spectrum of **3b** (CD_2Cl_2).

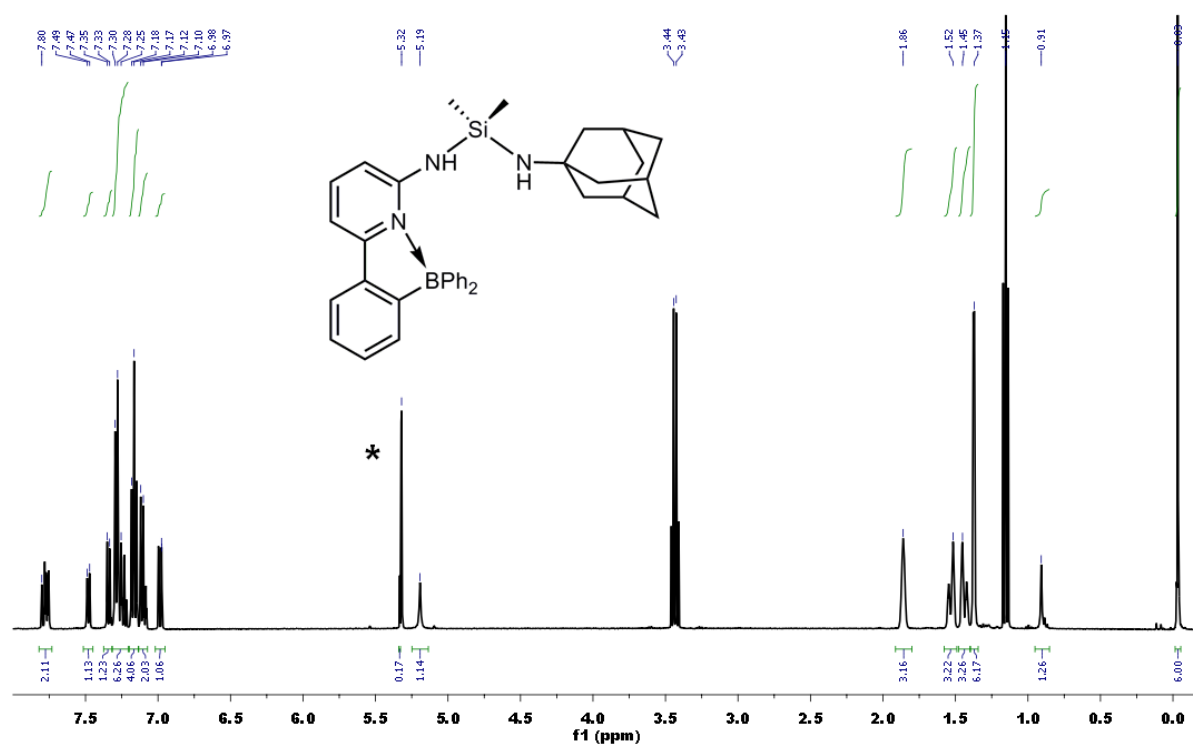


Figure 6.2.7 ^1H NMR spectrum of **5b** (CD_2Cl_2).

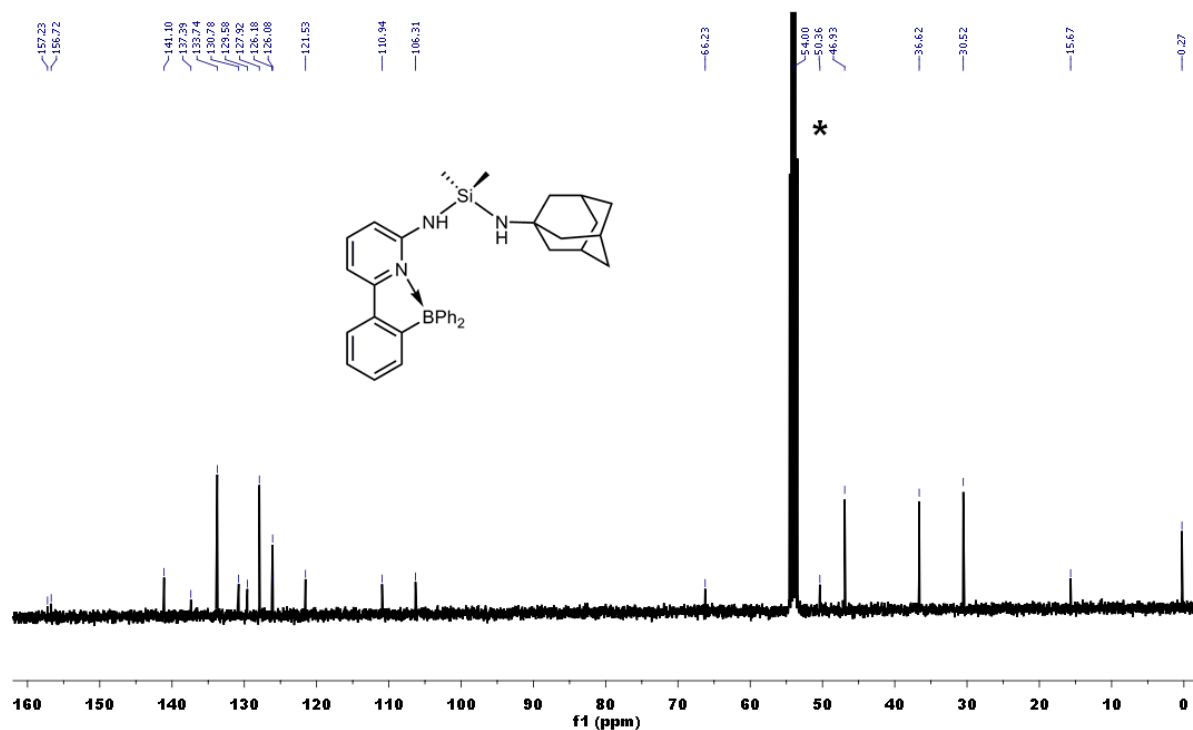
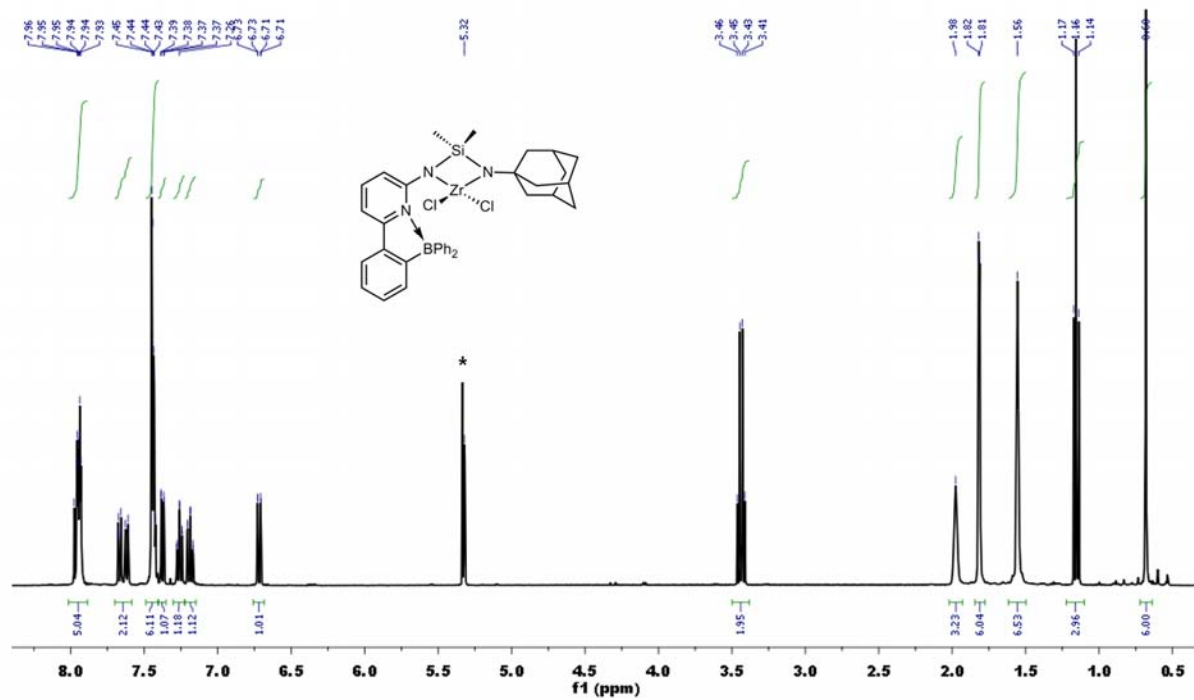
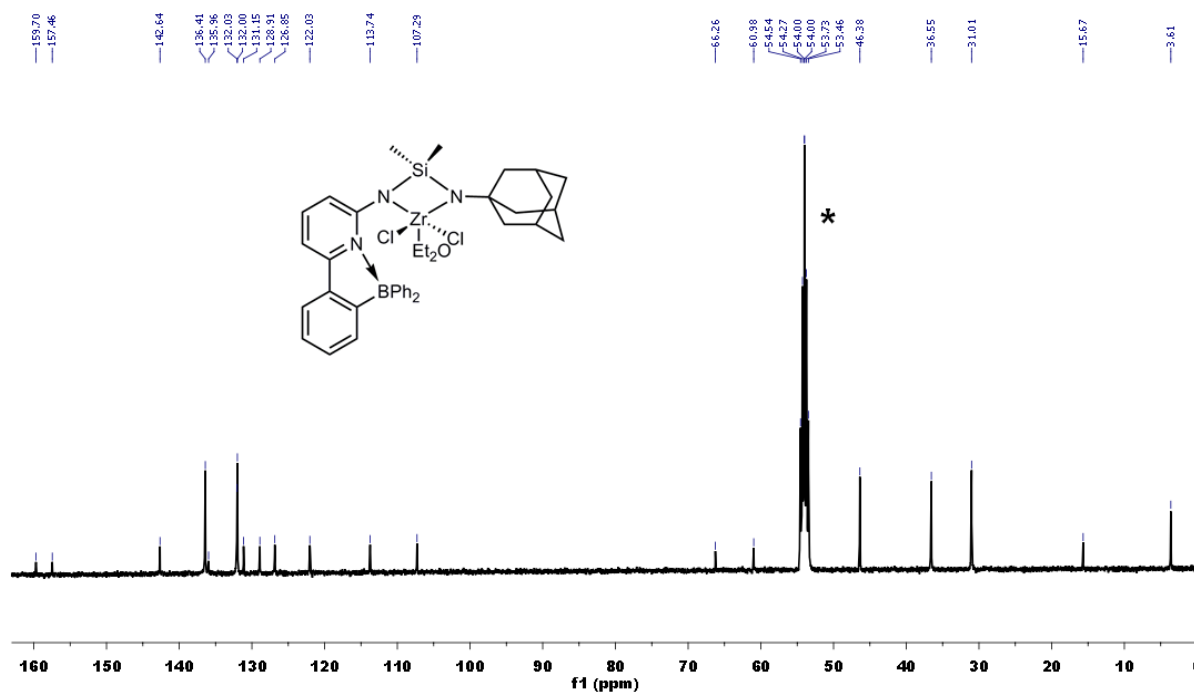


Figure 6.2.8 ^{13}C NMR spectrum of **5b** (CD_2Cl_2).

Figure 6.2.9 ^1H NMR spectrum of 7b (CD_2Cl_2).Figure 6.2.10 ^{13}C NMR spectrum of 7b (CD_2Cl_2).

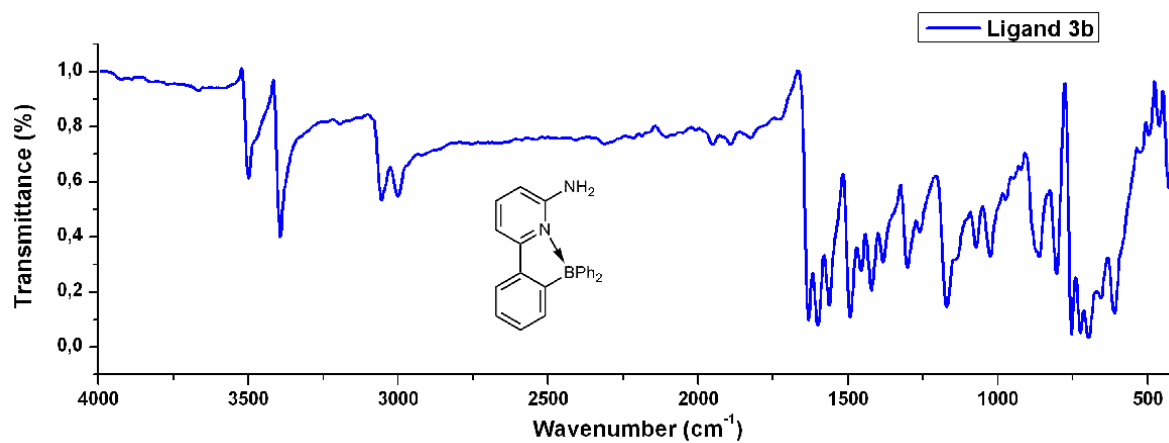


Figure 6.2.11 IR spectrum of ligand 3b.

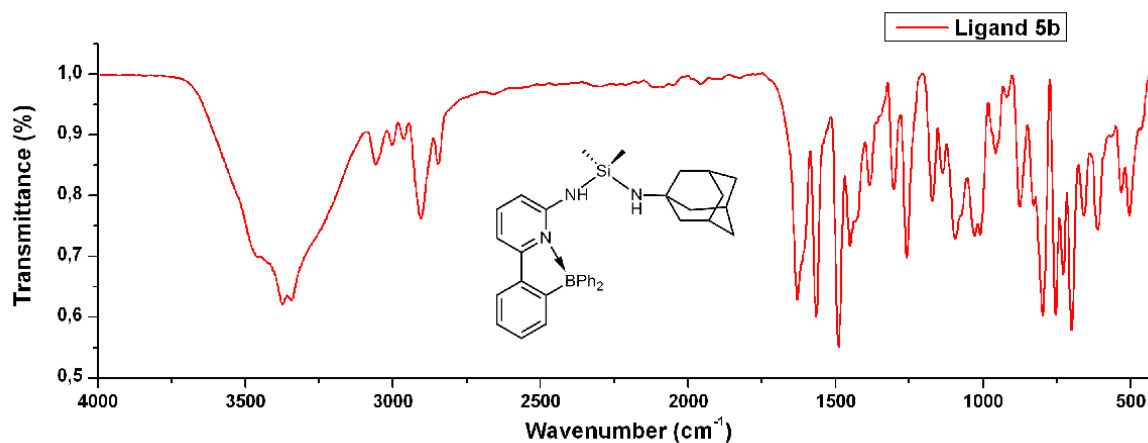


Figure 6.2.12 IR spectrum of ligand 5b.

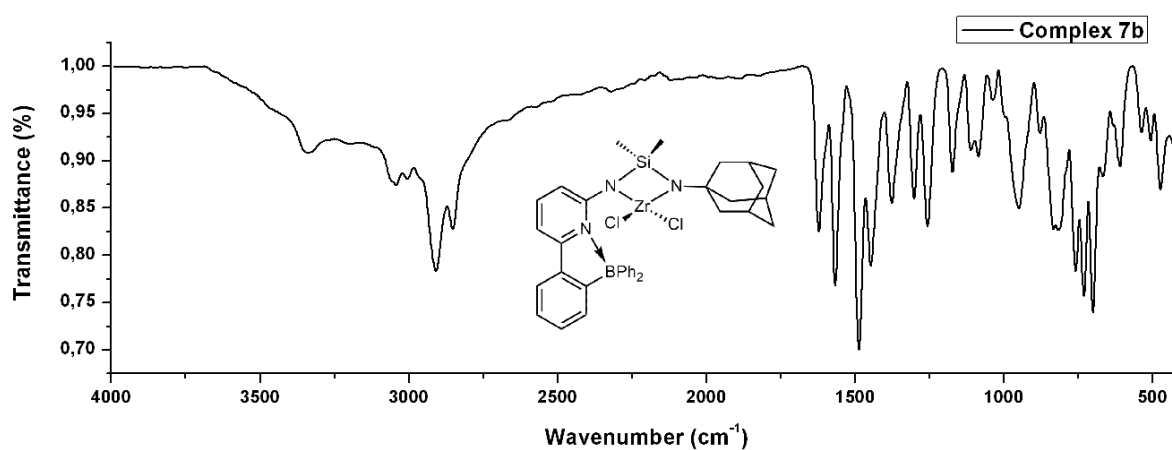


Figure 6.2.13 IR spectrum of complex 7b.

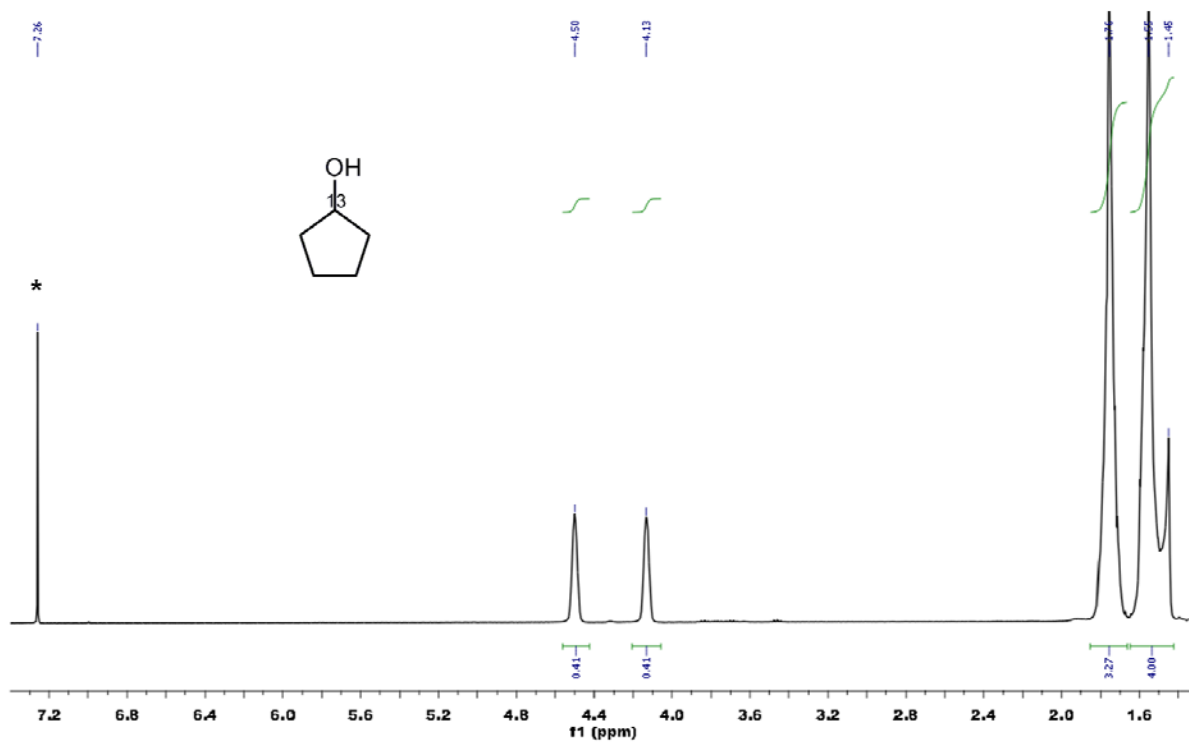


Figure 6.2.14 ^1H NMR spectrum of cyclopentanol-1- ^{13}C (CDCl_3).

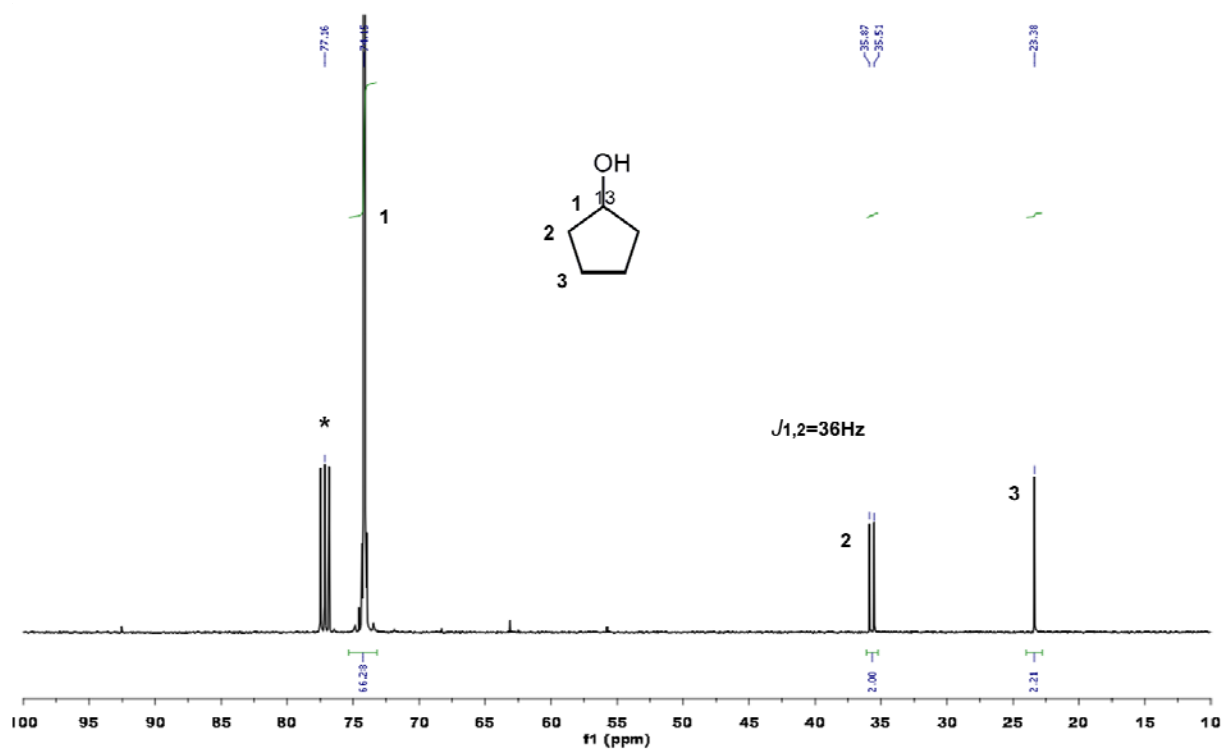


Figure 6.2.15 ^{13}C NMR spectrum of cyclopentanol-1- ^{13}C (CDCl_3).

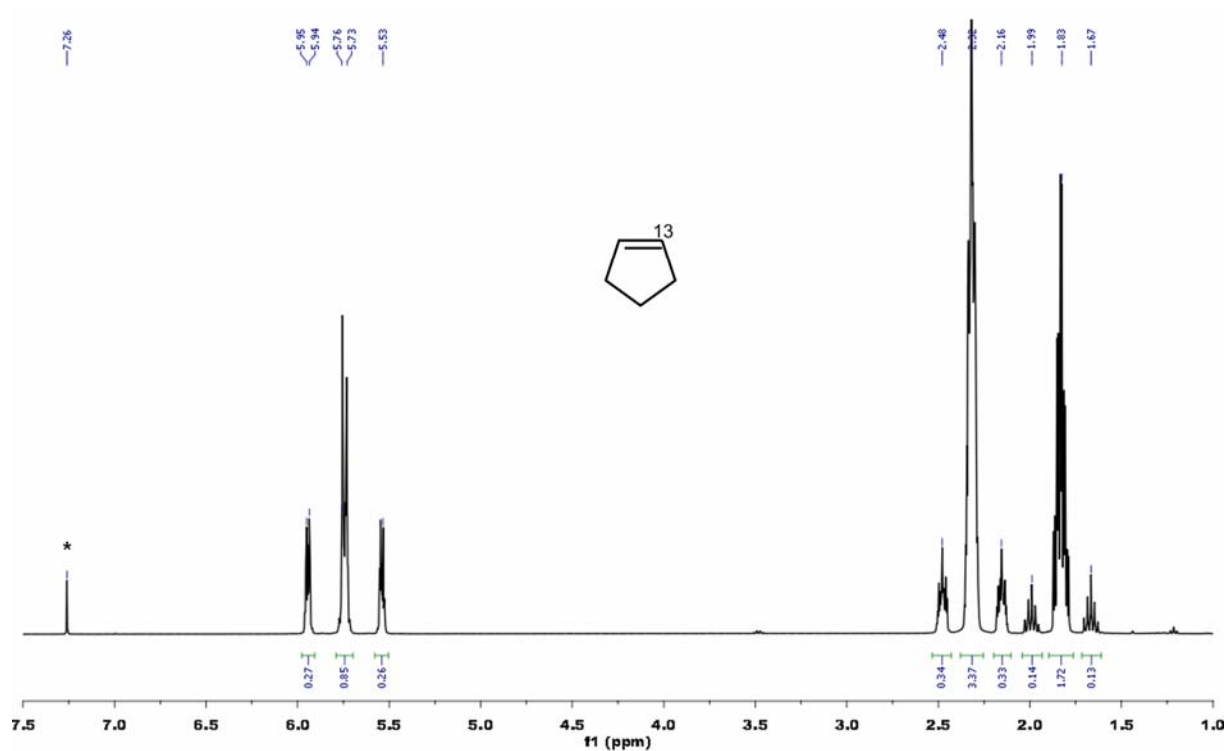


Figure 6.2.16 ^1H NMR spectrum of cyclopentene-1- ^{13}C (CDCl_3).

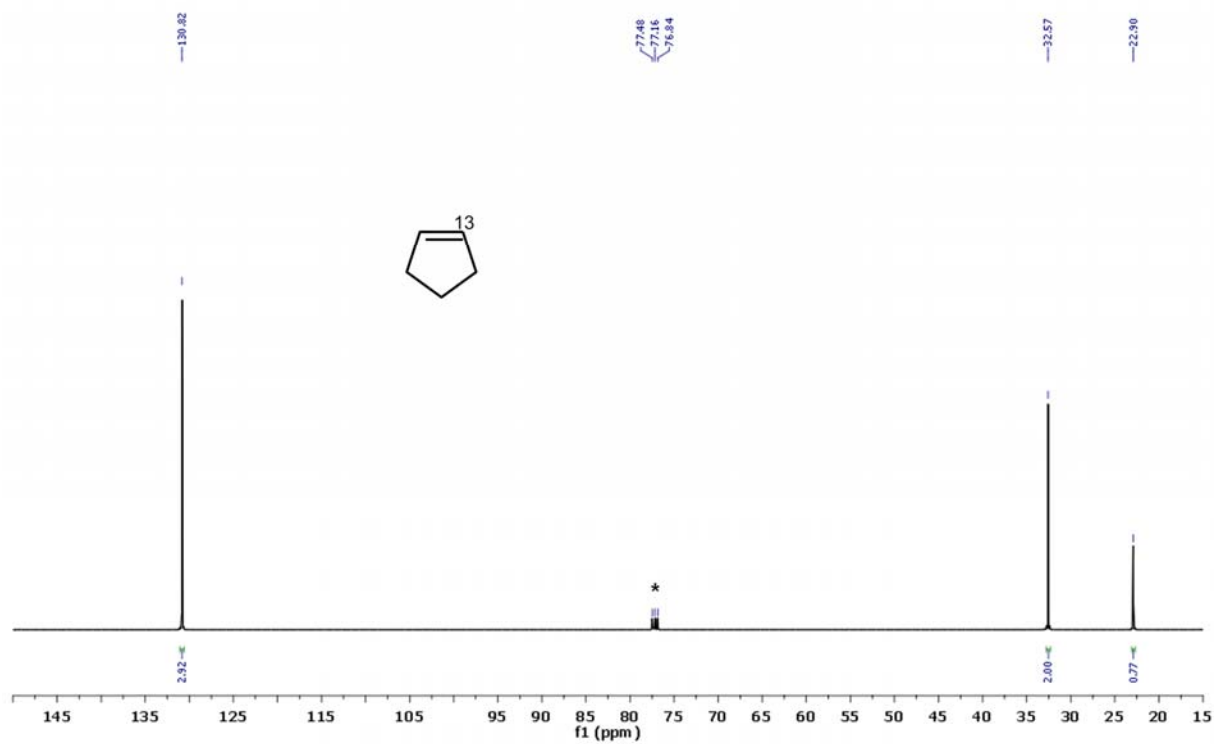


Figure 6.2.17 ^{13}C NMR spectrum of cyclopentene-1- ^{13}C (CDCl_3).

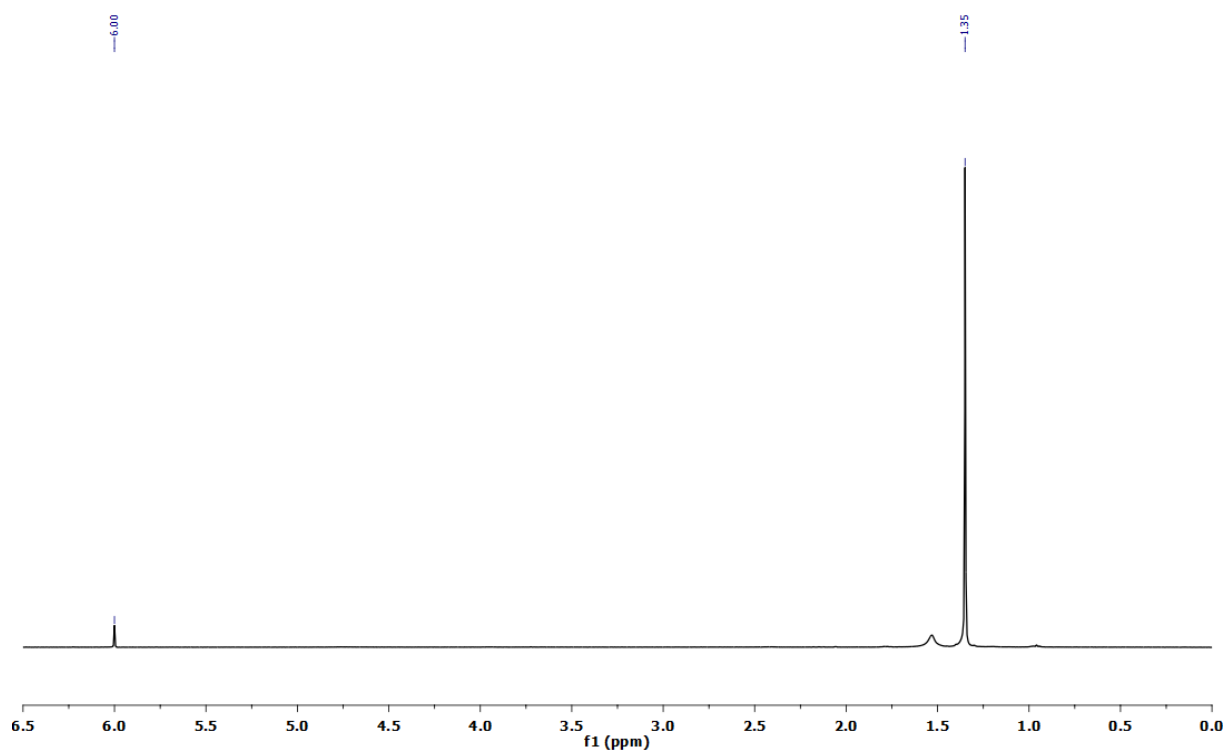


Figure 6.2.18 ^1H NMR spectrum of poly(E) produced by the action of **7a**/MAO (Table 3, entry 2) (1,1,2,2- $[\text{D}_2]$ tetrachloroethane).

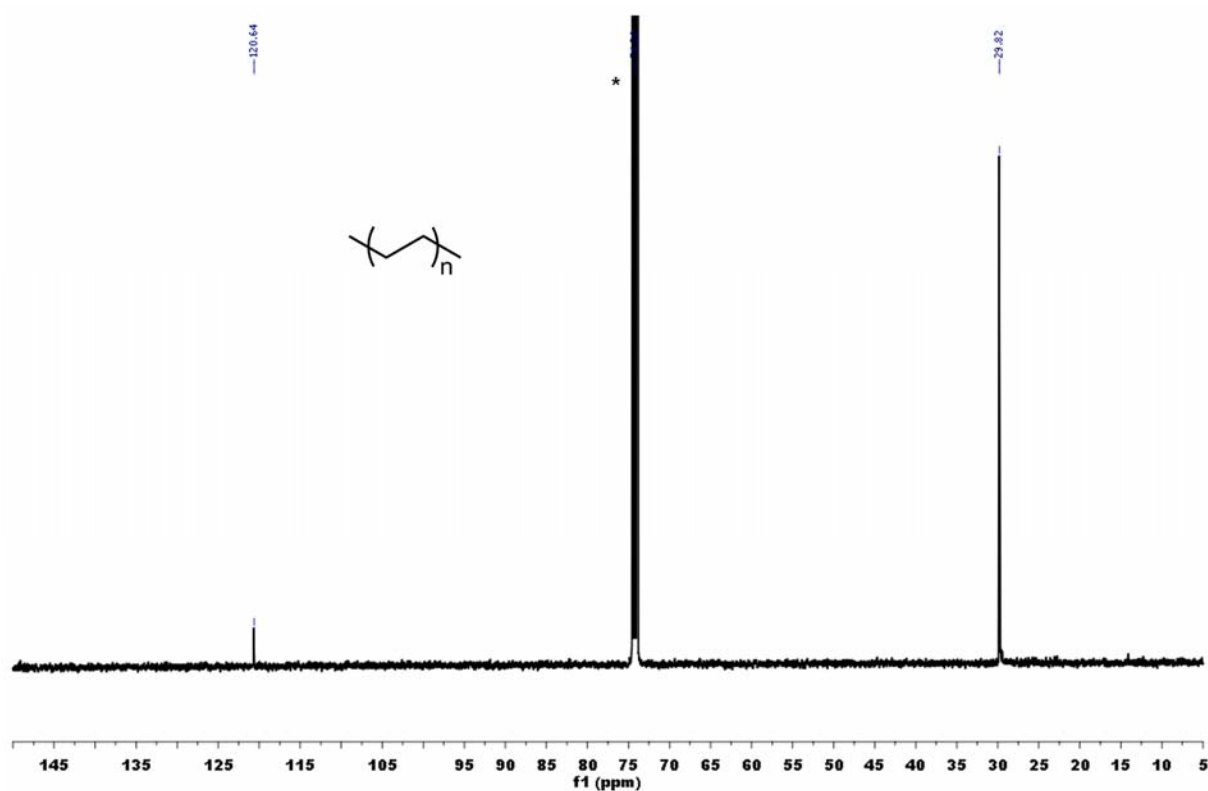


Figure 6.2.19 ^{13}C NMR spectrum of poly(E) produced by the action of **7a**/MAO (Table 3, entry 2) (1,1,2,2- $[\text{D}_2]$ tetrachloroethane). The signal at $\delta = 120.6$ ppm stems from C_2Cl_4 (impurity).

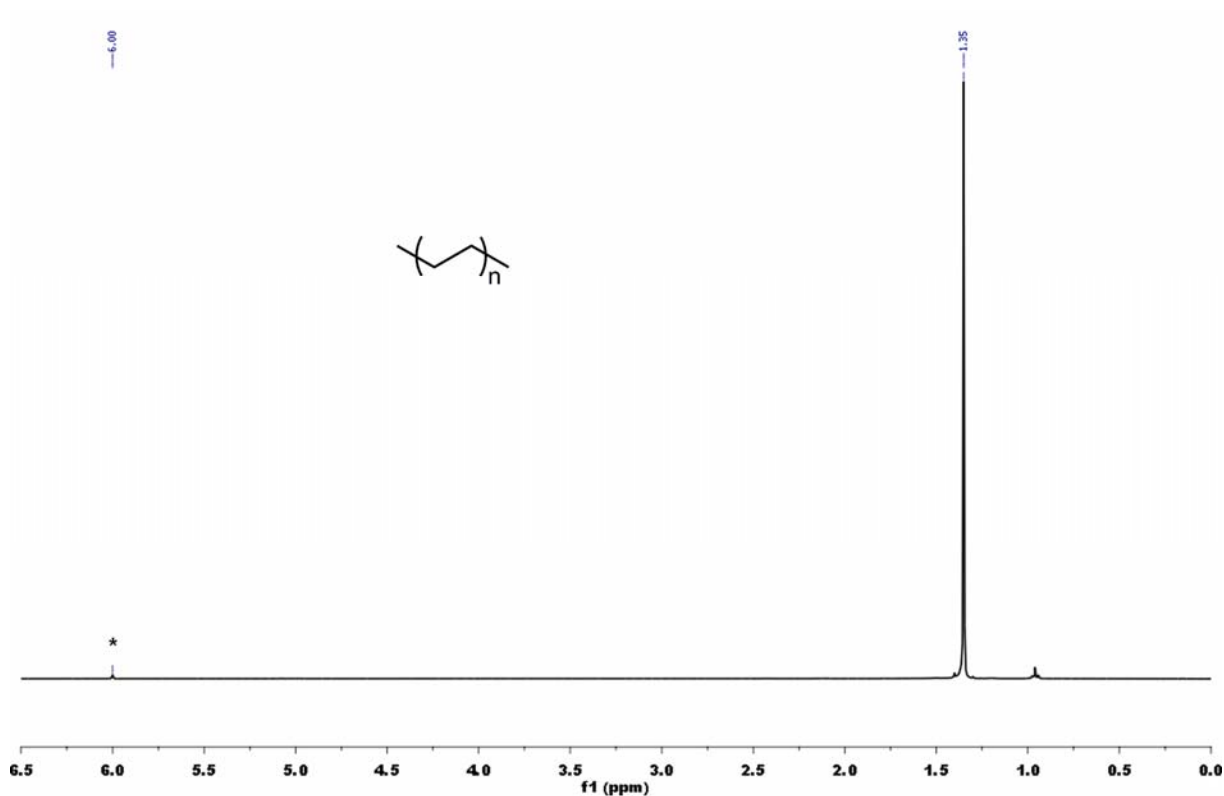


Figure 6.2.20 ^1H NMR spectrum of poly(E) produced by the action of **7b**/MAO (Table 3, entry 6) (1,1,2,2- $[\text{D}_2]$ tetrachloroethane).

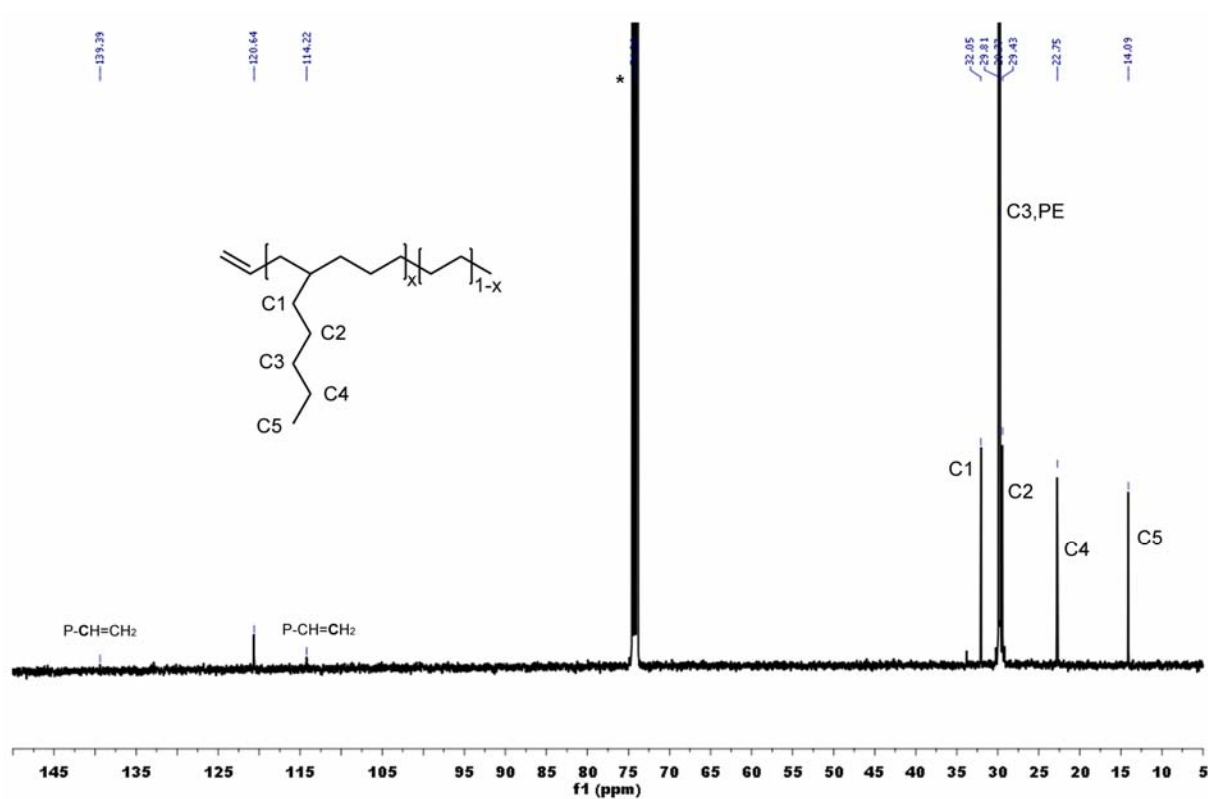


Figure 6.2.21 ^{13}C NMR spectrum of poly(E) produced by the action of **7b**/MAO (Table 3, entry 6) (1,1,2,2- $[\text{D}_2]$ tetrachloroethane). The signal at $\delta = 120.6$ ppm stems from C_2Cl_4 (impurity).

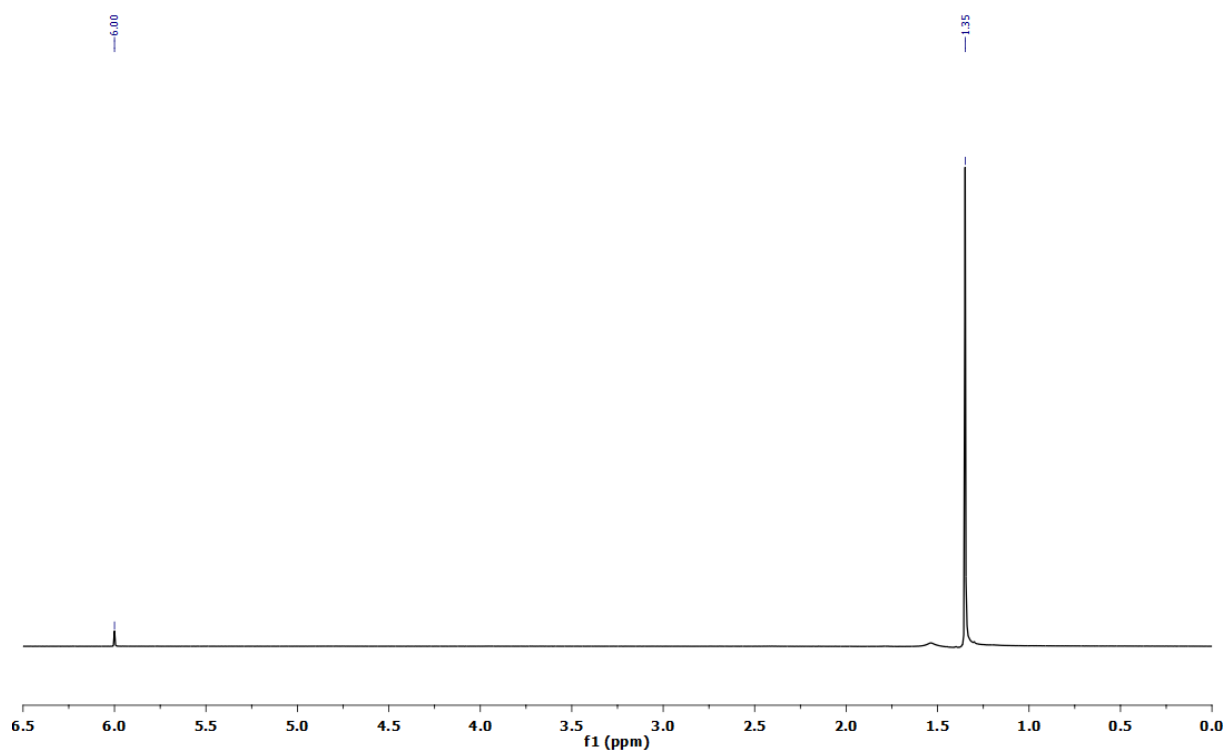


Figure 6.2.22 ^1H NMR spectrum of poly(E)-co-poly(CPE) produced by the action of **7a**/MAO (Table 4, entry 2) (1,1,2,2- $[\text{D}_2]$ tetrachloroethane).

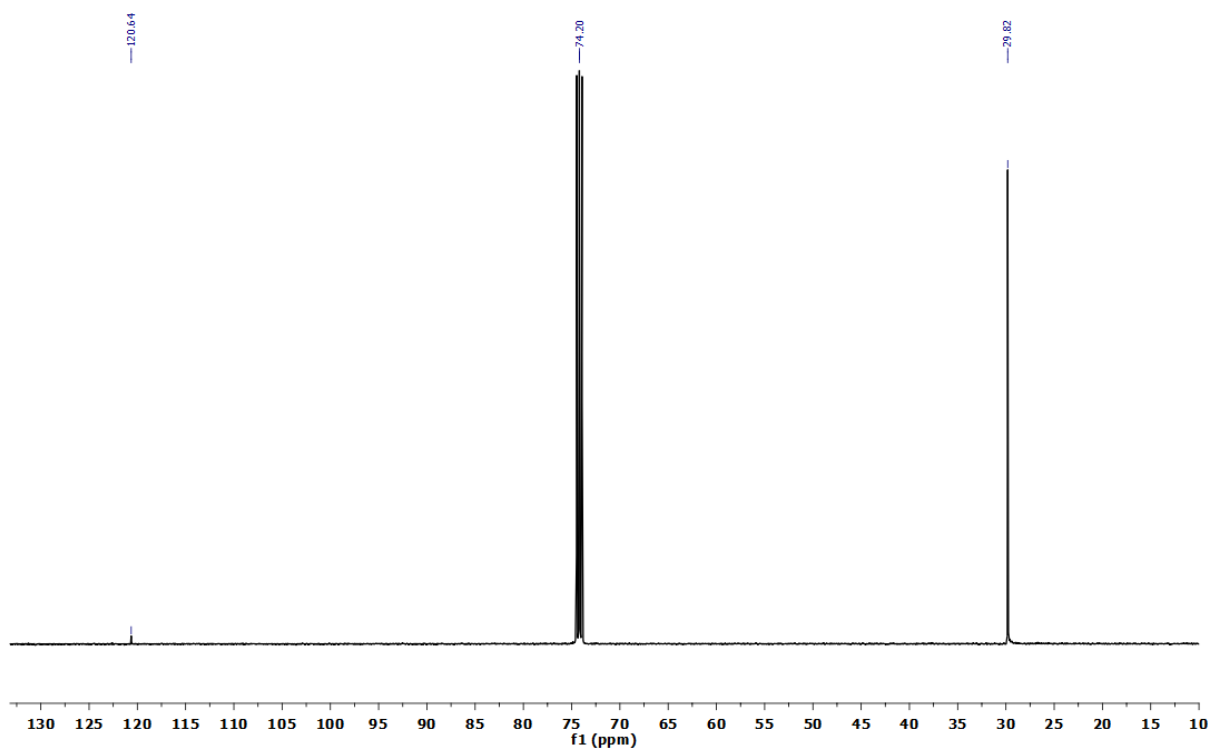


Figure 6.2.23 ^{13}C NMR spectrum of poly(E)-co-poly(CPE) produced by the action of **7a**/MAO (Table 4, entry 2) (1,1,2,2- $[\text{D}_2]$ tetrachloroethane). The signal at $\delta = 120.6$ ppm stems from C_2Cl_4 (impurity).

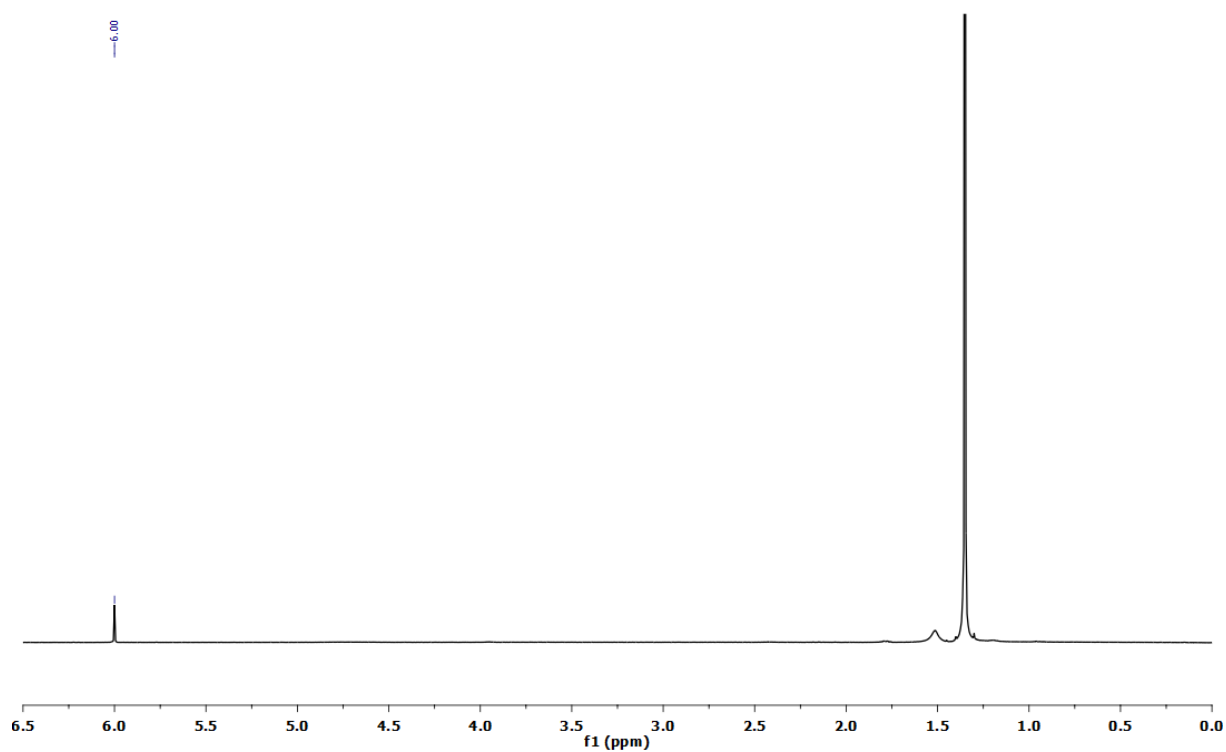


Figure 6.2.24 ¹H NMR spectrum of poly(E)-co-poly(CPE) produced by the action of **7a**/MAO (Table 4, entry 4) (1,1,2,2-[D₂]tetrachloroethane).

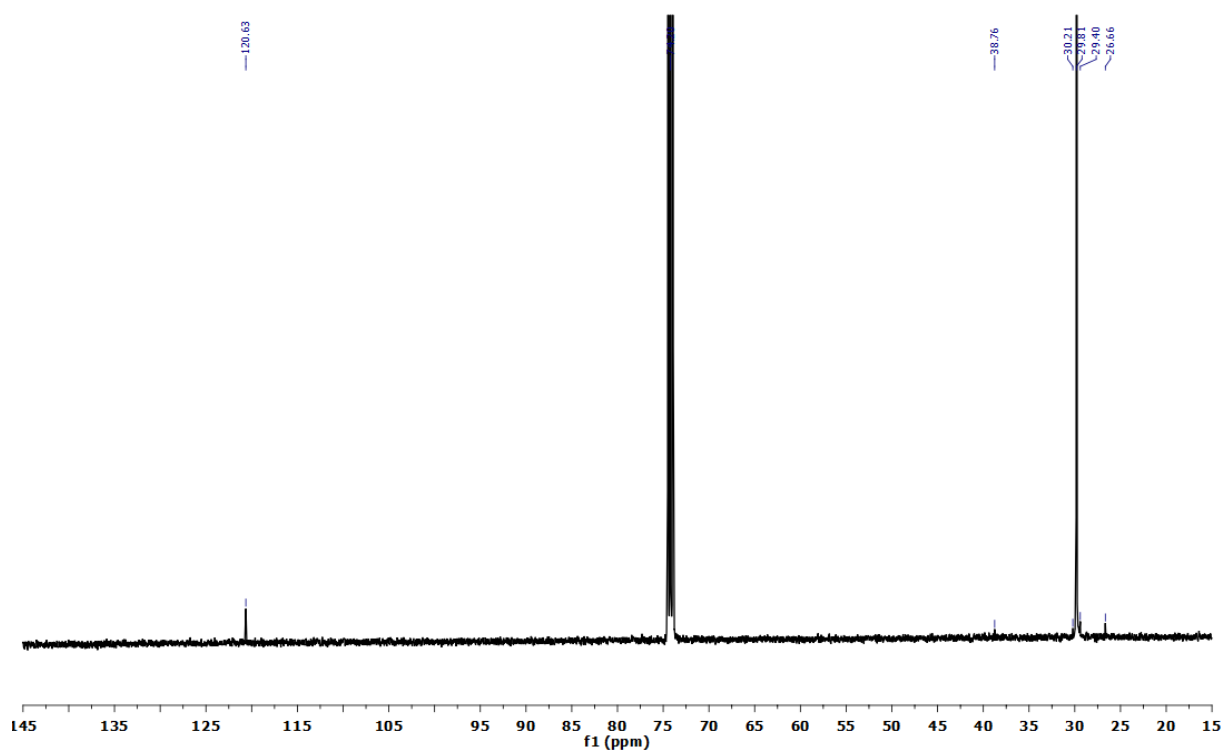


Figure 6.2.25 ¹³C NMR spectrum of poly(E)-co-poly(CPE) produced by the action of **7a**/MAO (Table 4, entry 4) (1,1,2,2-[D₂]tetrachloroethane). The signal at $\delta = 120.6$ ppm stems from C₂Cl₄ (impurity).

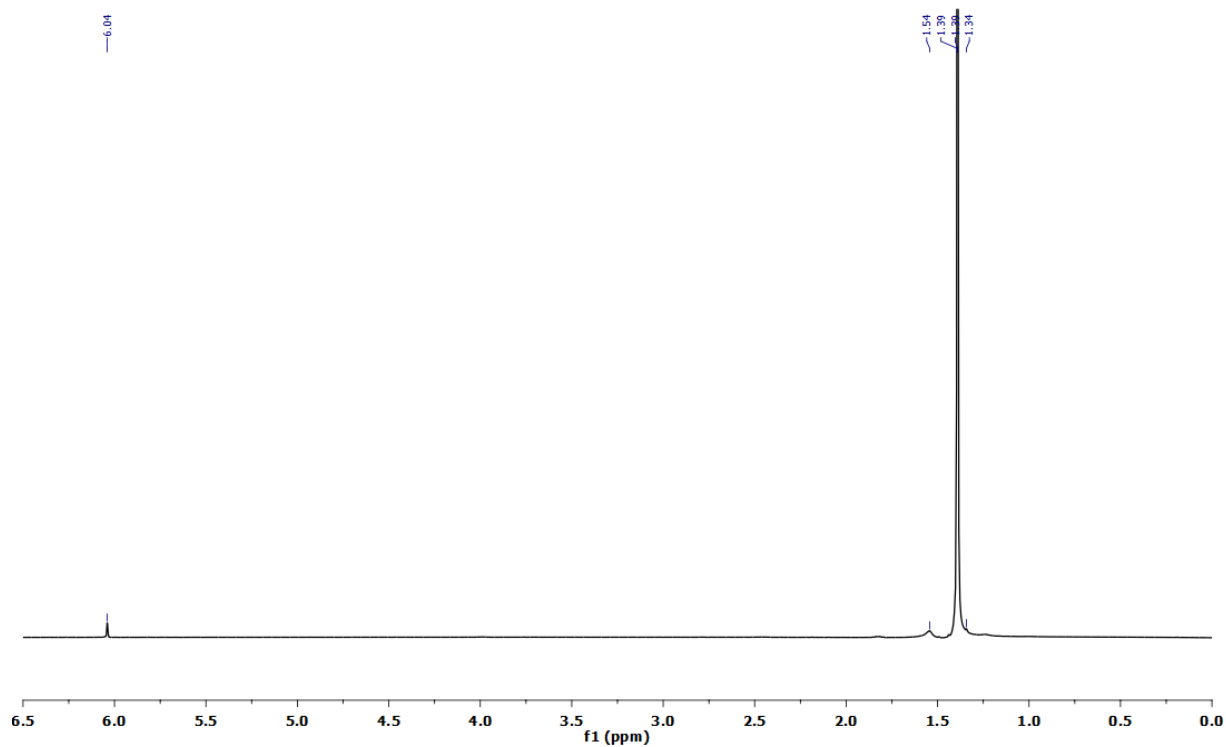


Figure 6.2.26 ^1H NMR spectrum of poly(E)-co-poly(CPE) produced by the action of **7a**/MAO (Table 4, entry 6) (1,1,2,2- $[\text{D}_2]$ tetrachloroethane).

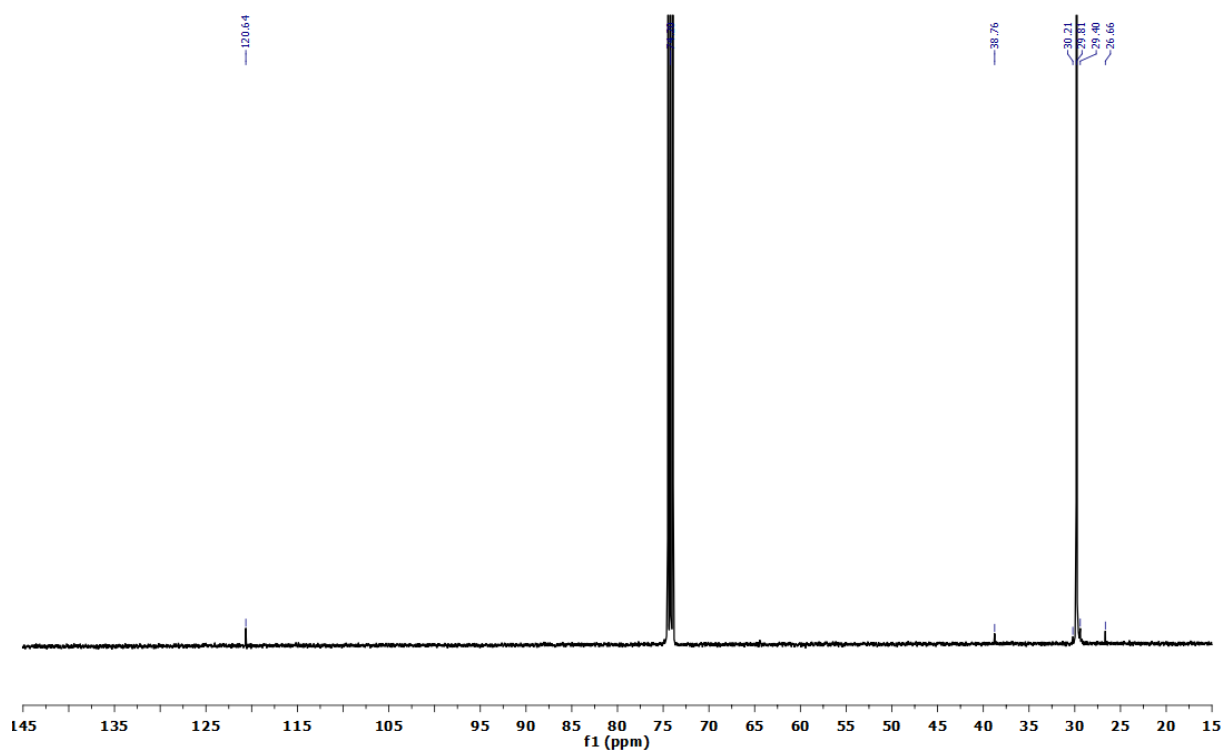


Figure 6.2.27 ^{13}C NMR spectrum of poly(E)-co-poly(CPE) produced by the action of **7a**/MAO (Table 4, entry 6) (1,1,2,2- $[\text{D}_2]$ tetrachloroethane). The signal at $\delta = 120.6$ ppm stems from C_2Cl_4 (impurity).

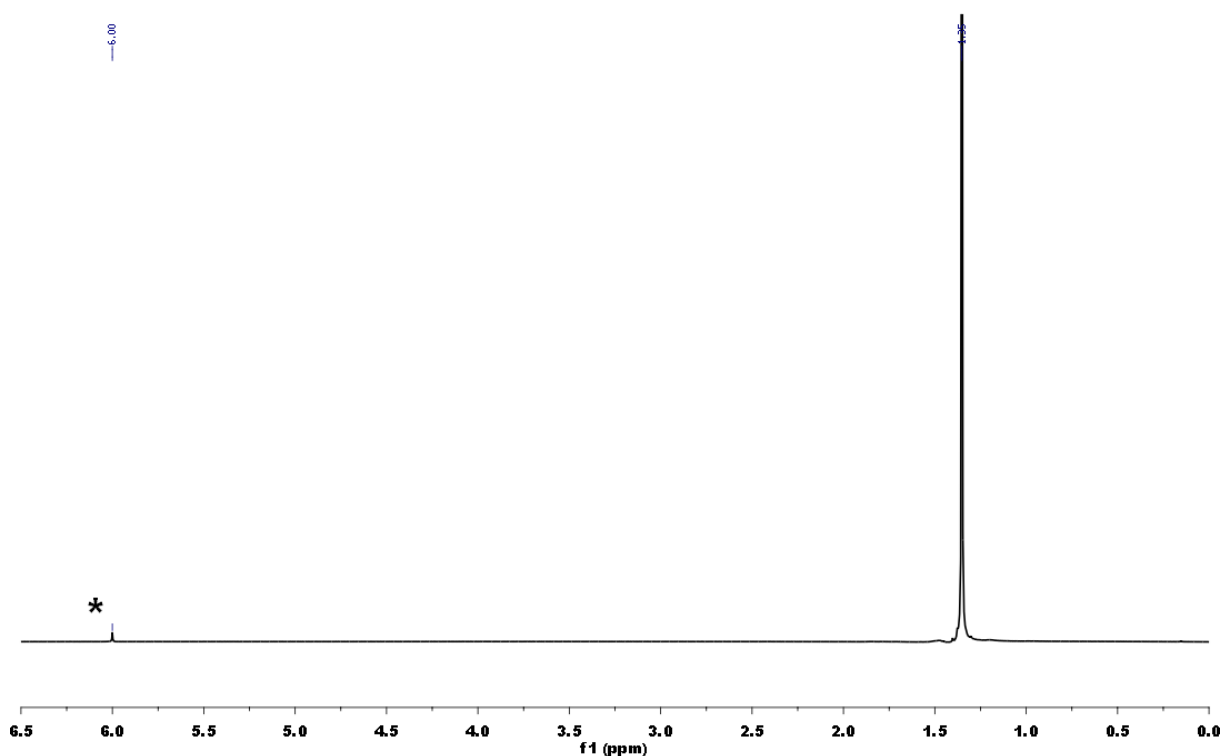


Figure 6.2.28 ^1H NMR spectrum of poly(E)-co-poly(CPE) produced by the action of **7b**/MAO (Table 4, entry 9) (1,1,2,2- $[\text{D}_2]$ tetrachloroethane).

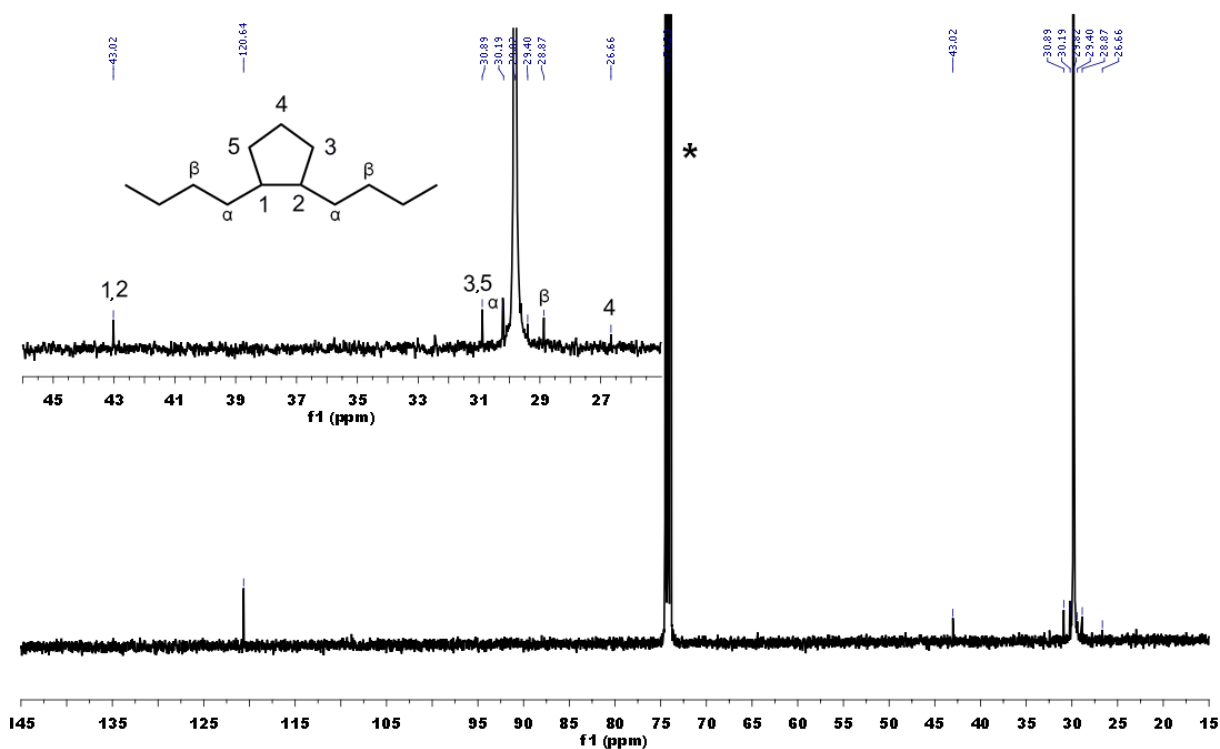


Figure 6.2.29 ^{13}C NMR spectra of poly(E)-co-poly(CPE) produced by the action of **7b**/MAO (Table 4, entry 9) (1,1,2,2- $[\text{D}_2]$ tetrachloroethane). The signal at $\delta = 120.6$ ppm stems from C_2Cl_4 (impurity).

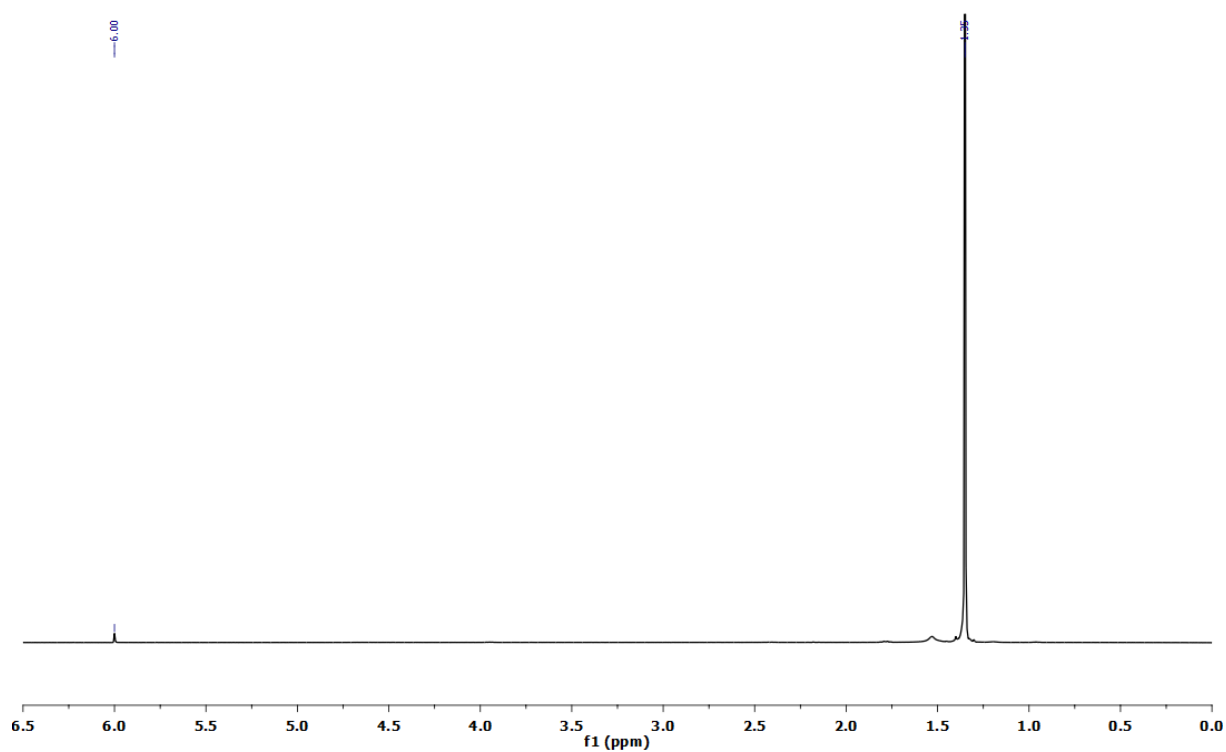


Figure 6.2.30 ^1H NMR spectrum of poly(E)-co-poly(CPE) produced by the action of **7b**/MAO (Table 4, entry 12) (1,1,2,2- $[\text{D}_2]$ tetrachloroethane).

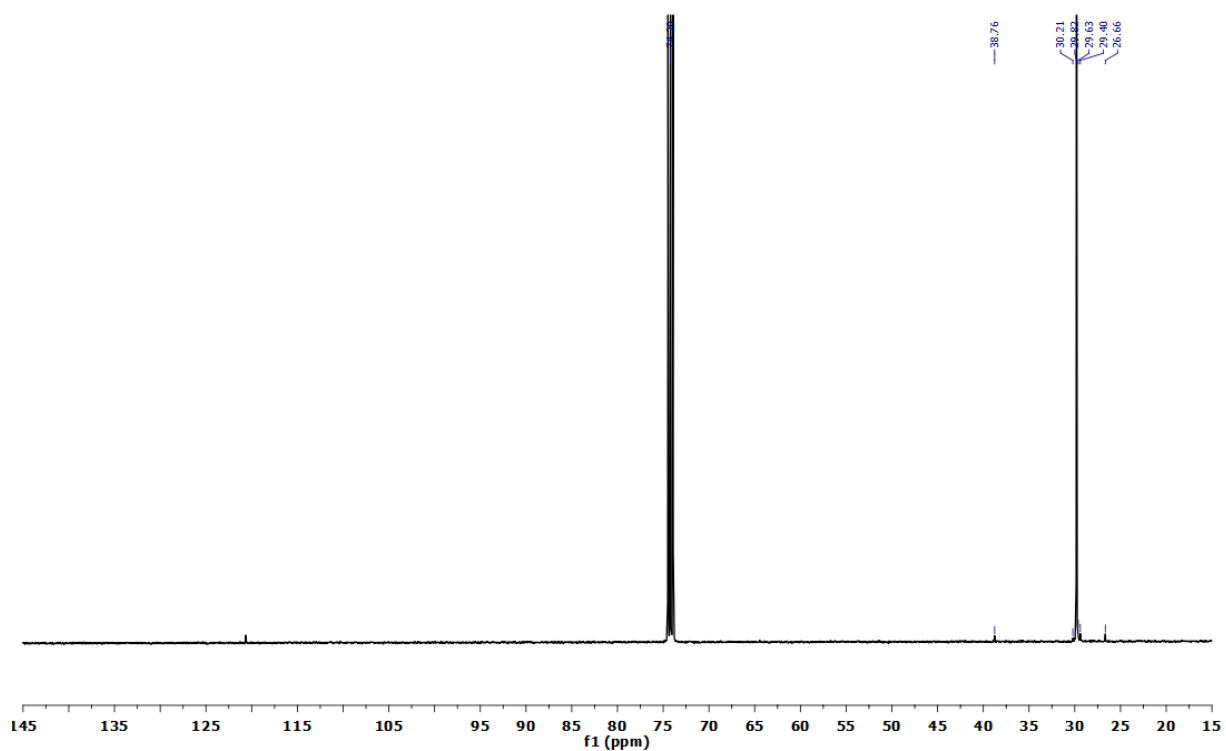


Figure 6.2.31 ^{13}C NMR spectrum of poly(E)-co-poly(CPE) produced by the action of **7b**/MAO (Table 4, entry 12) (1,1,2,2- $[\text{D}_2]$ tetrachloroethane). The signal at $\delta = 120.6$ ppm stems from C_2Cl_4 (impurity).

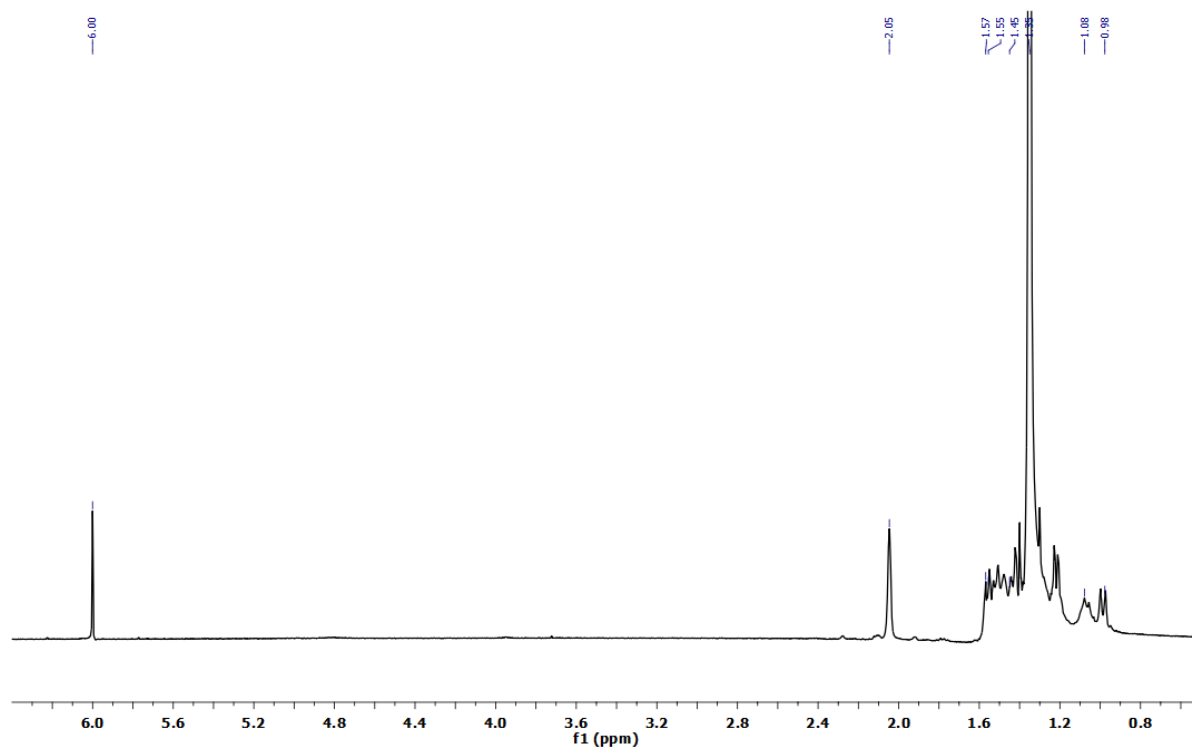


Figure 6.2.32 ¹H NMR spectrum of poly(E)-co-poly(NBE)_{VIP} produced by the action of **7a**/MAO (Table 5, entry 4) (1,1,2,2-[D₂]tetrachloroethane).

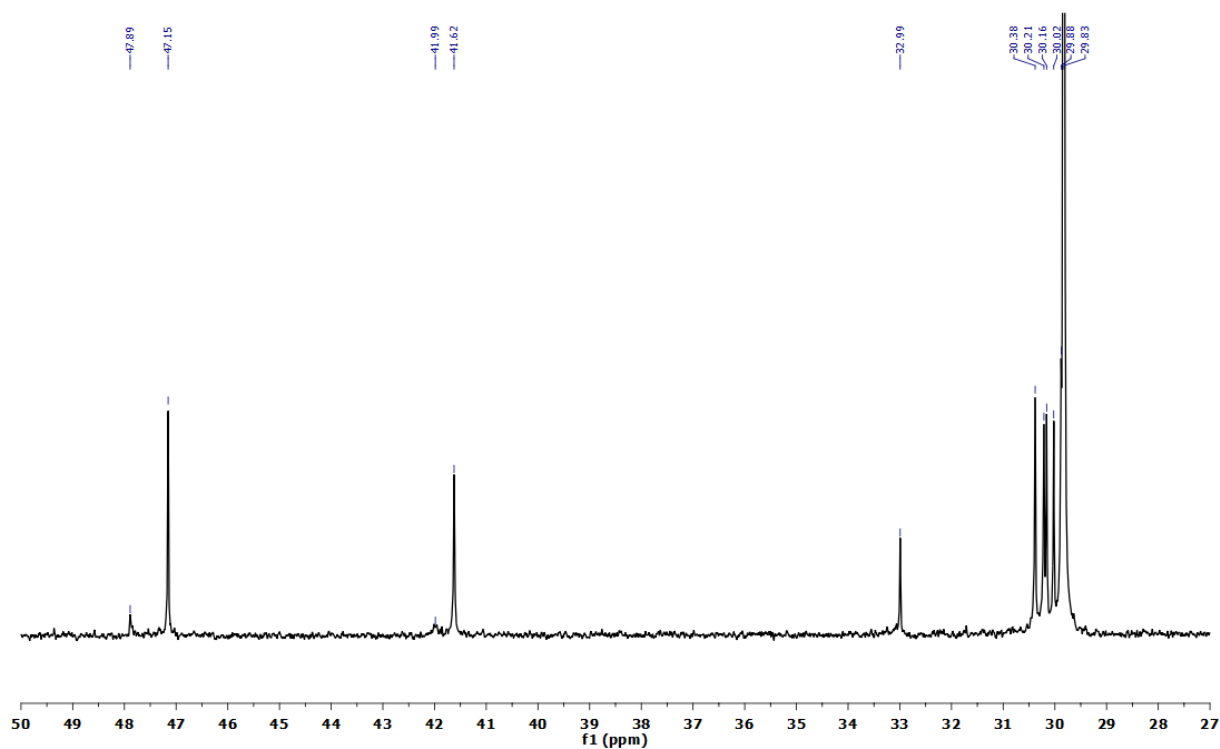


Figure 6.2.33 ¹³C NMR spectrum of poly(E)-co-poly(NBE)_{VIP} produced by the action of **7a**/MAO (Table 5, entry 4) (1,1,2,2-[D₂]tetrachloroethane).

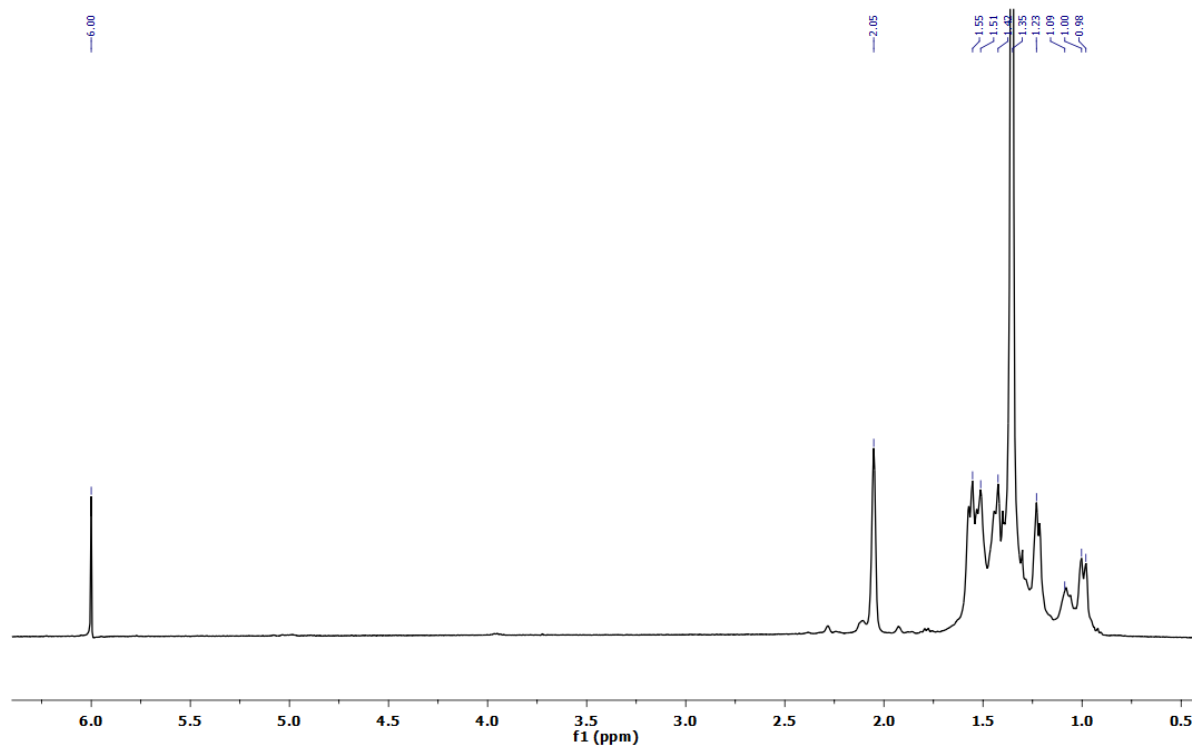


Figure 6.2.34 ^1H NMR spectrum of poly(E)-co-poly(NBE)_{VIP} produced by the action of **7a**/MAO (Table 5, entry 7) (1,1,2,2-[D₂]tetrachloroethane).

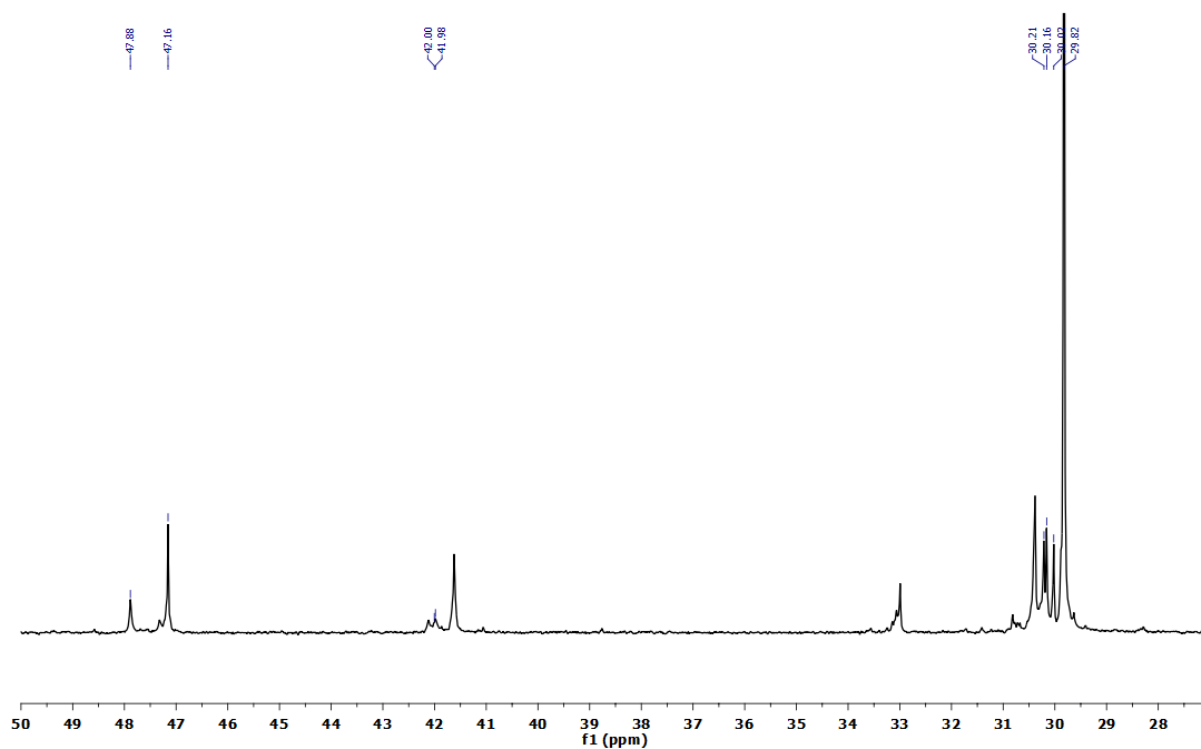


Figure 6.2.35 ^{13}C NMR spectrum of poly(E)-co-poly(NBE)_{VIP} produced by the action of **7a**/MAO (Table 5, entry 7) (1,1,2,2-[D₂]tetrachloroethane).

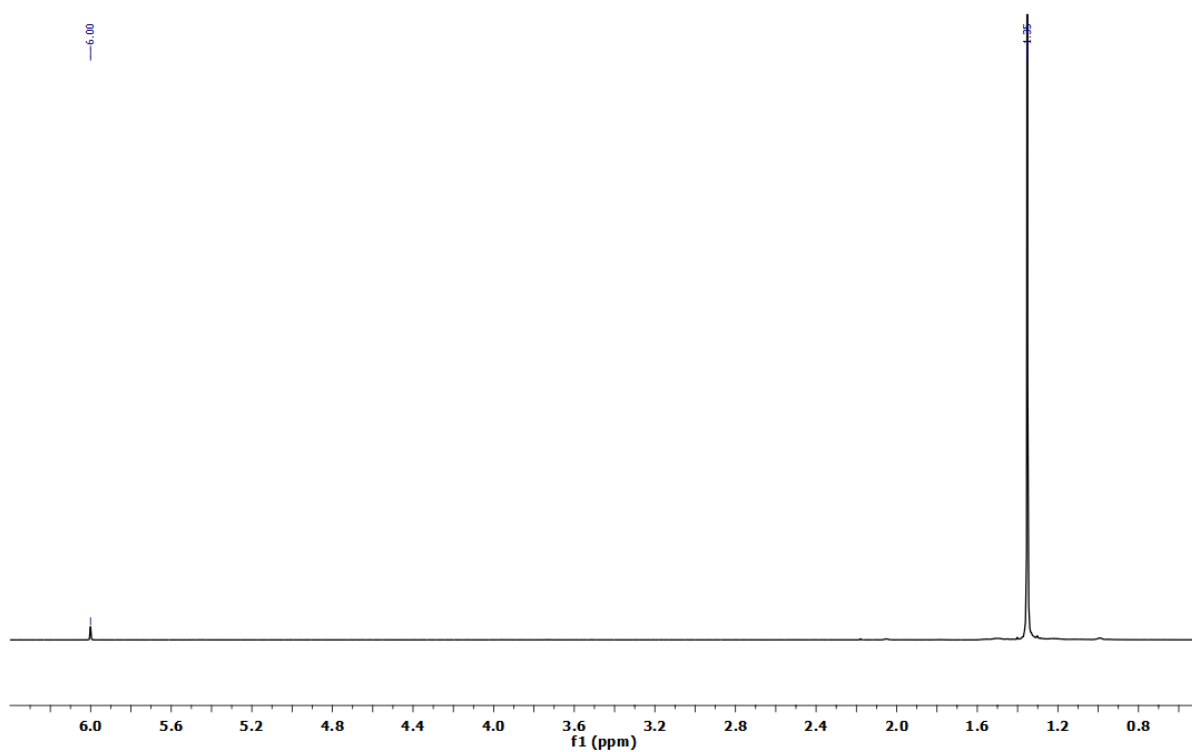


Figure 6.2.36 ^1H NMR spectrum of poly(E)-co-poly(NBE)_{VIP} produced by the action of **7b**/MAO (Table 5, entry 10) (1,1,2,2-[D₂]tetrachloroethane).

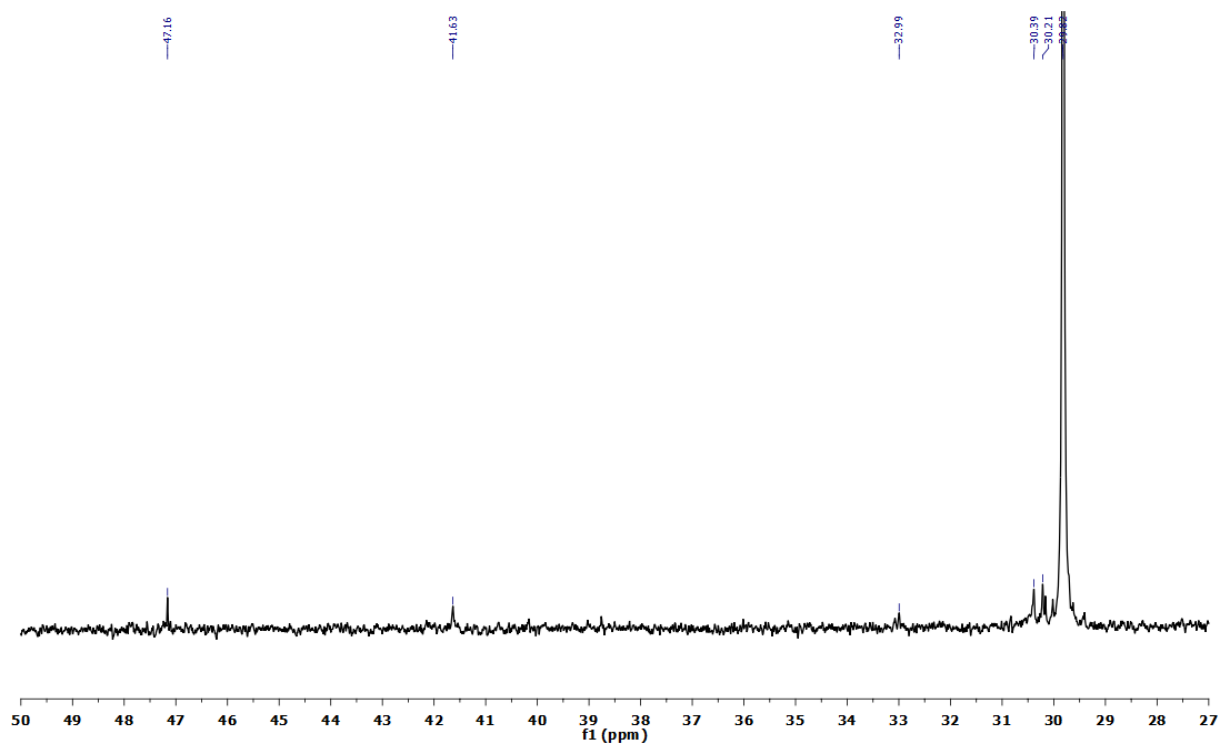


Figure 6.2.37 ^{13}C NMR spectrum of poly(E)-co-poly(NBE)_{VIP} produced by the action of **7b**/MAO (Table 5, entry 10) (1,1,2,2-[D₂]tetrachloroethane).

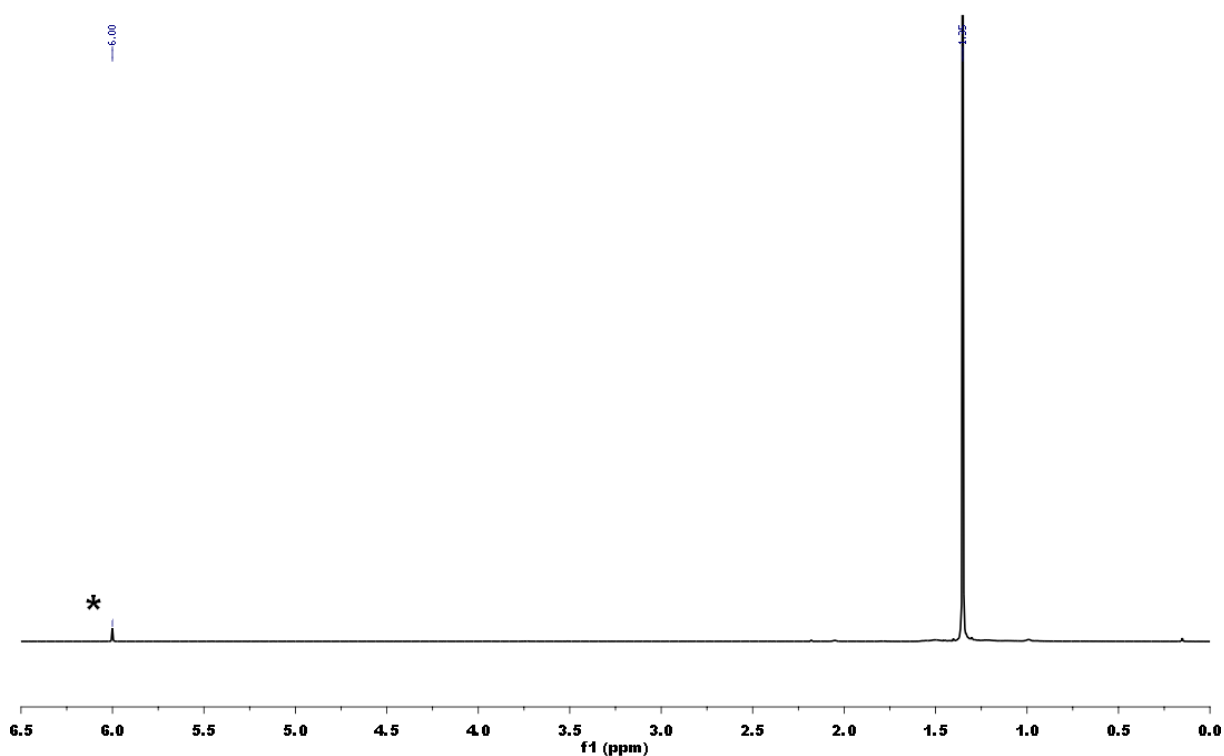


Figure 6.2.38 ^1H NMR spectrum of poly(E)-*co*-poly(NBE)_{VIP} produced by the action of **7b**/MAO (Table 5, entry 11) (1,1,2,2-[D₂]tetrachloroethane).

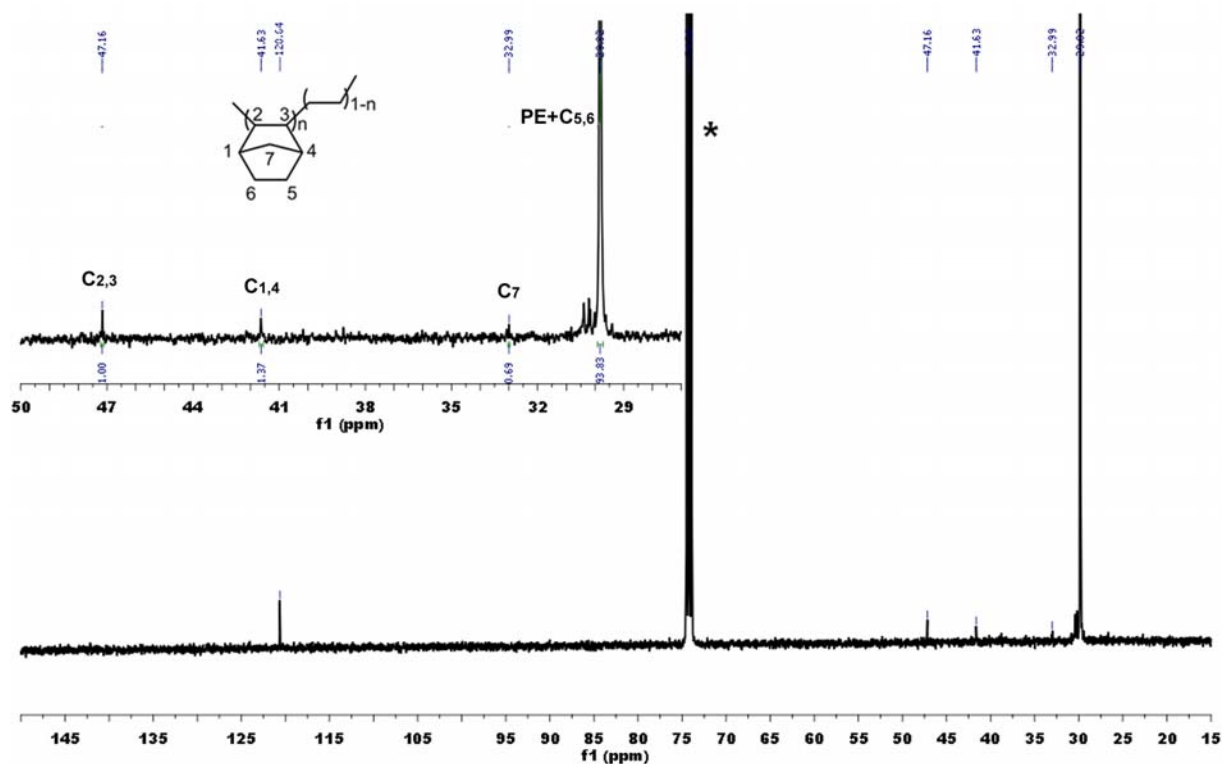


Figure 6.2.39 ^{13}C NMR spectra of poly(E)-*co*-poly(NBE)_{VIP} produced by the action of **7b**/MAO (Table 5, entry 11) (1,1,2,2-[D₂]tetrachloroethane). The signal at $\delta = 120.6$ ppm stems from C_2Cl_4 (impurity).

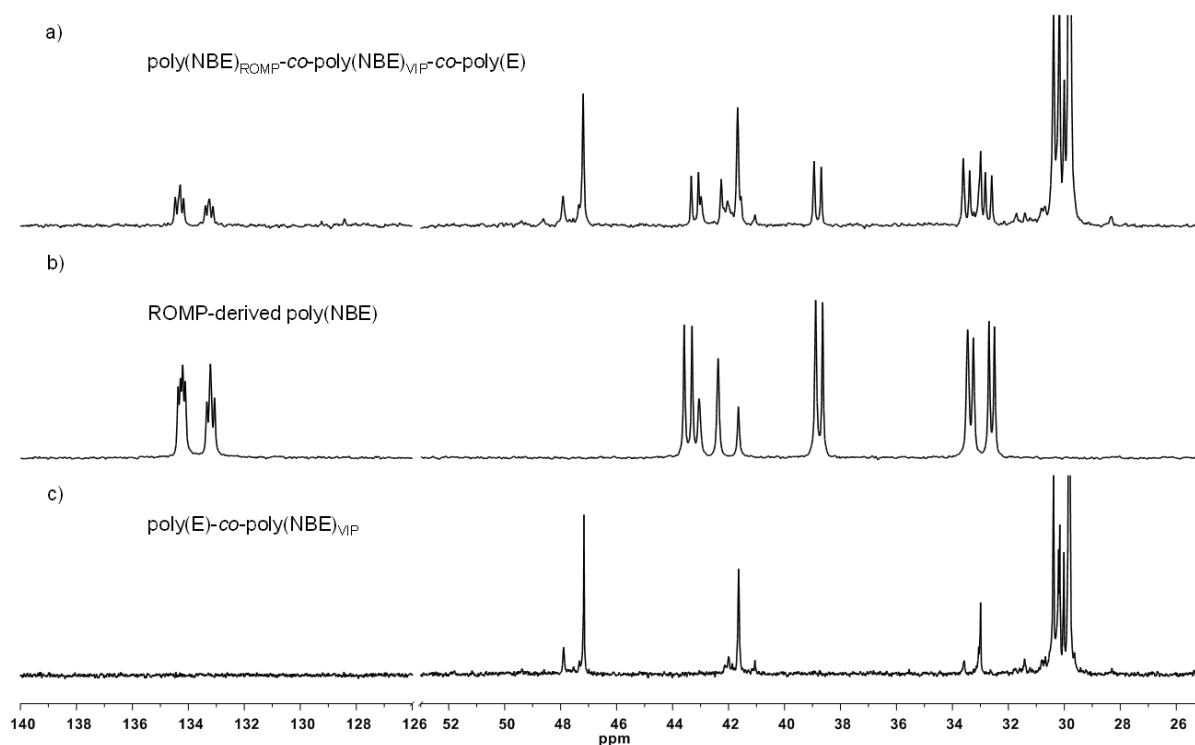


Figure 6.2.40 ^{13}C NMR spectra of a) poly(NBE)_{ROMP}-co-poly(NBE)_{VIP}-co-poly(E), b) poly(NBE), and c) poly(E)-co-poly(NBE)_{VIP} produced by the action of **7a**/MAO (Table 5, entry 7) (1,1,2,2-[D₂]tetrachloroethane).

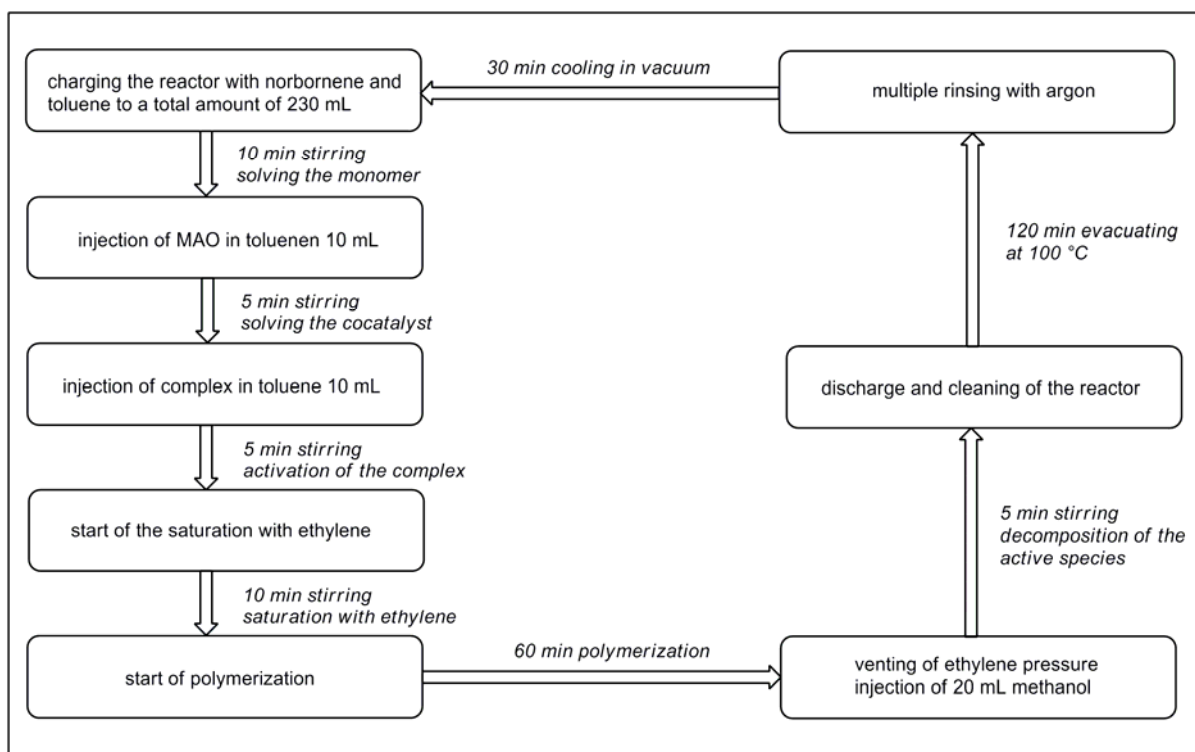


Figure 6.2.41 Standard polymerization sequence.

6.3 On the Mechanism of Tandem Ring-Opening Metathesis/Vinyl Insertion Copolymerization of Ethylene With Norborn-2-ene

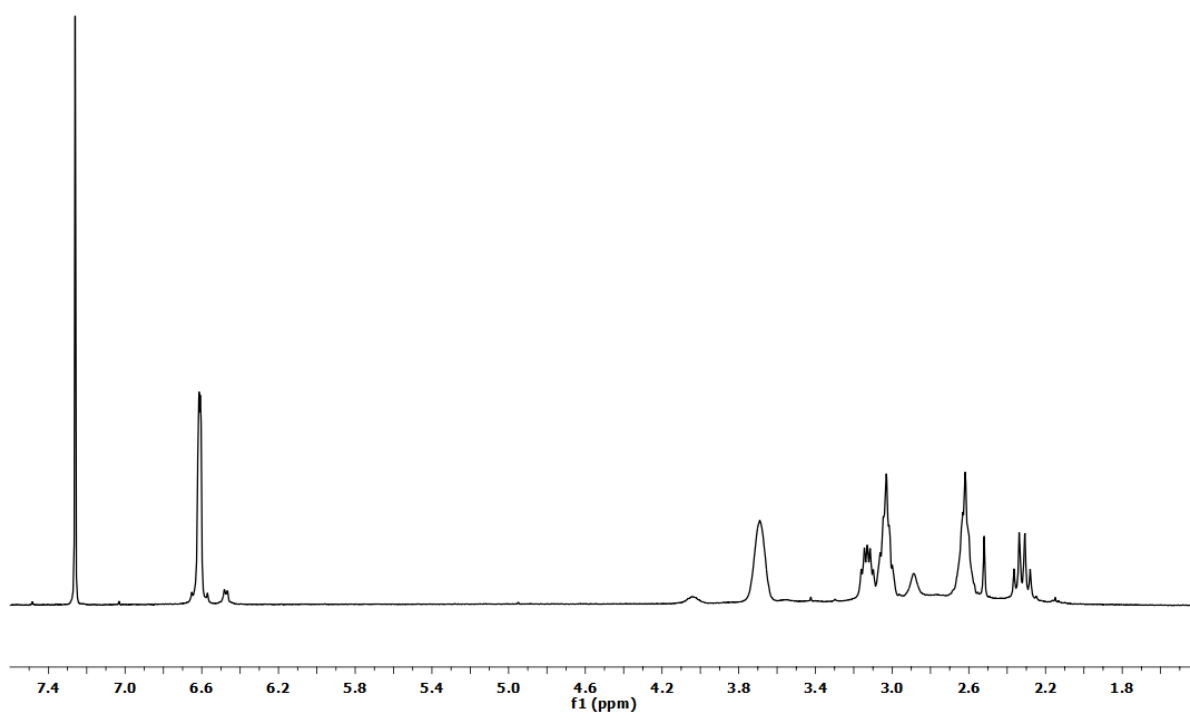


Figure 6.3.1 ^1H NMR spectrum of poly(NBE)_{ROMP} produced by the action of **1**/MAO (CDCl_3).

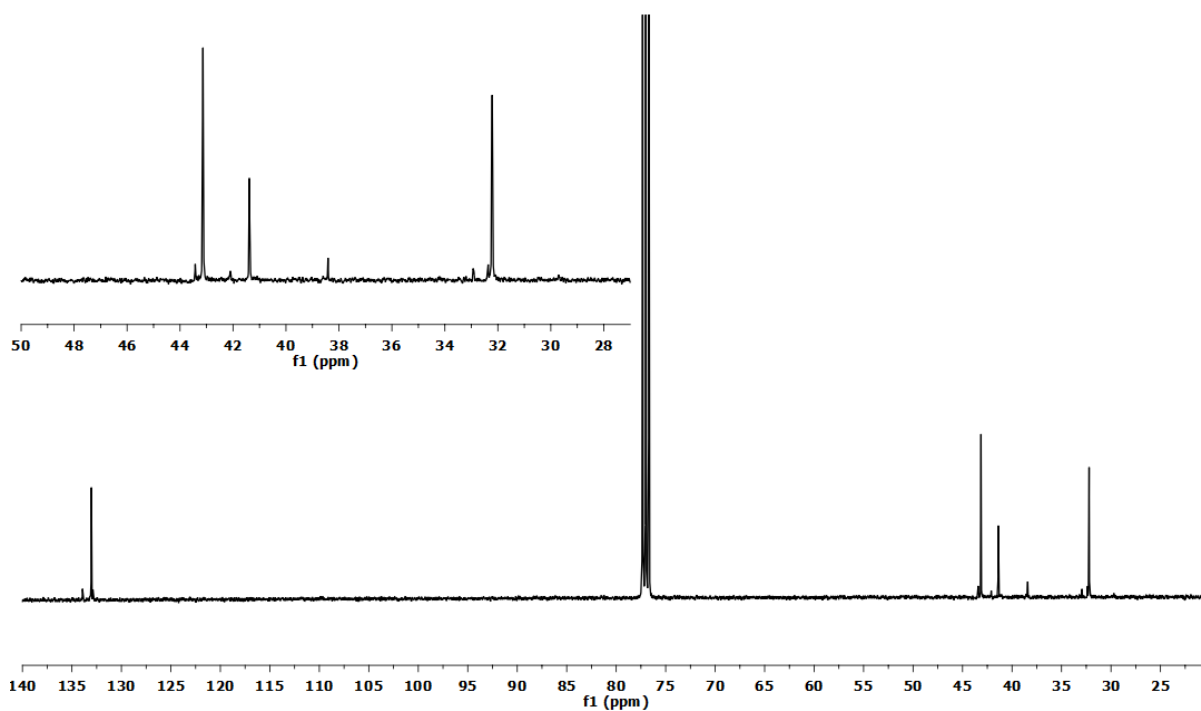


Figure 6.3.2 ^{13}C NMR spectra of poly(NBE)_{ROMP} produced by the action of **1**/MAO (CDCl_3).

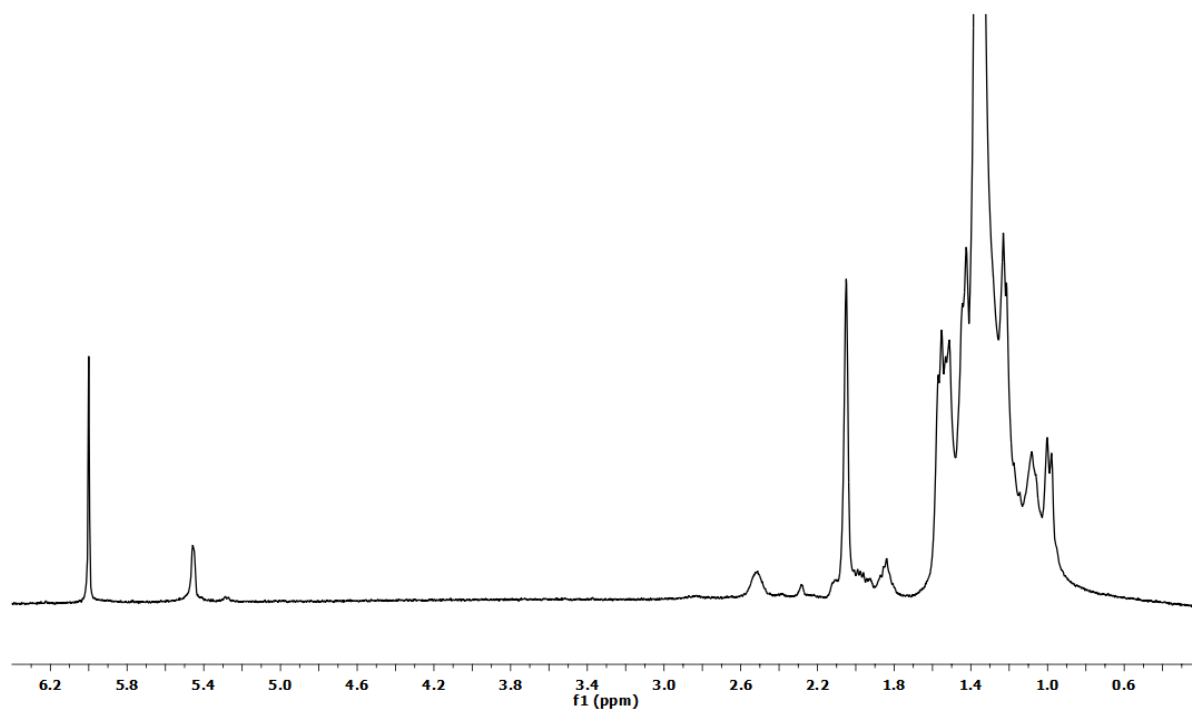


Figure 6.3.3 ¹H NMR spectrum of poly(NBE)_{ROMP}-co-poly(NBE)_{VIP}-co-poly(E) produced by the action of 1/MAO (1,1,2,2-[D₂]tetrachloroethane).

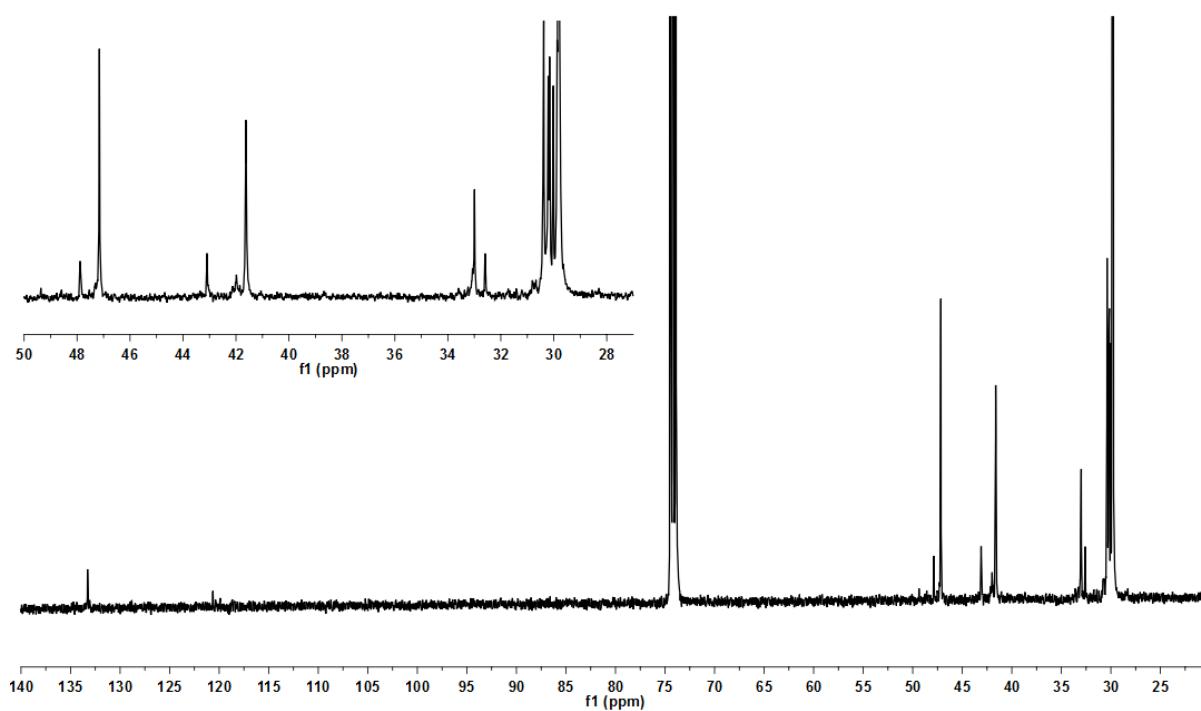


Figure 6.3.4 ¹³C NMR spectra of poly(NBE)_{ROMP}-co-poly(NBE)_{VIP}-co-poly(E) produced by the action of 1/MAO (1,1,2,2-[D₂]tetrachloroethane). The signal at $\delta = 120.64$ ppm is a solvent impurity.

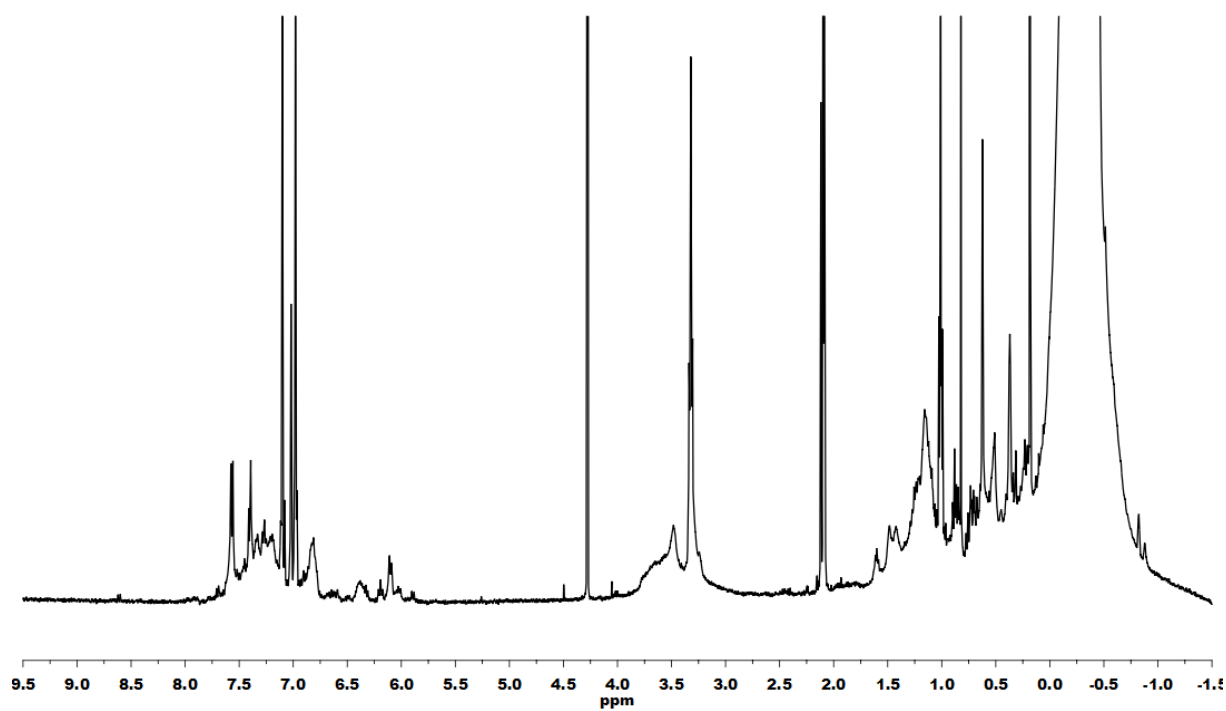


Figure 6.3.5 ^1H NMR spectrum of 1/MAO (toluene- d_8 , 20 °C).

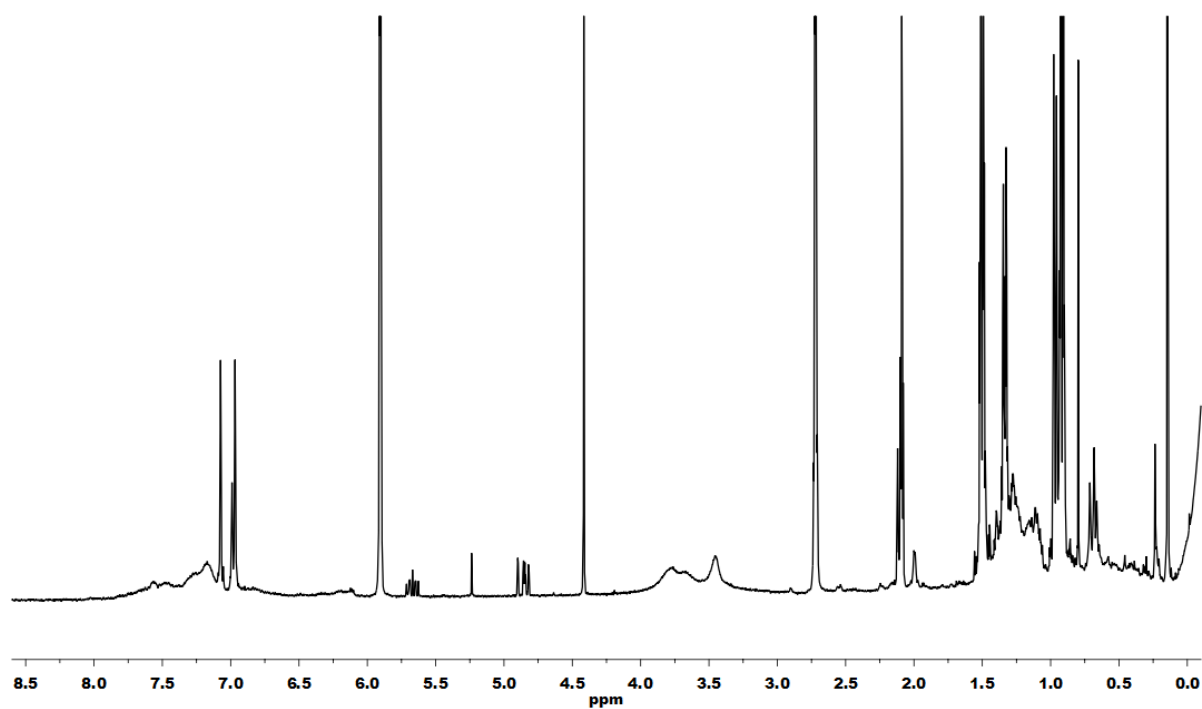


Figure 6.3.6 ^1H NMR spectrum of 1/MAO/NBE (toluene- d_8 , 60 °C).

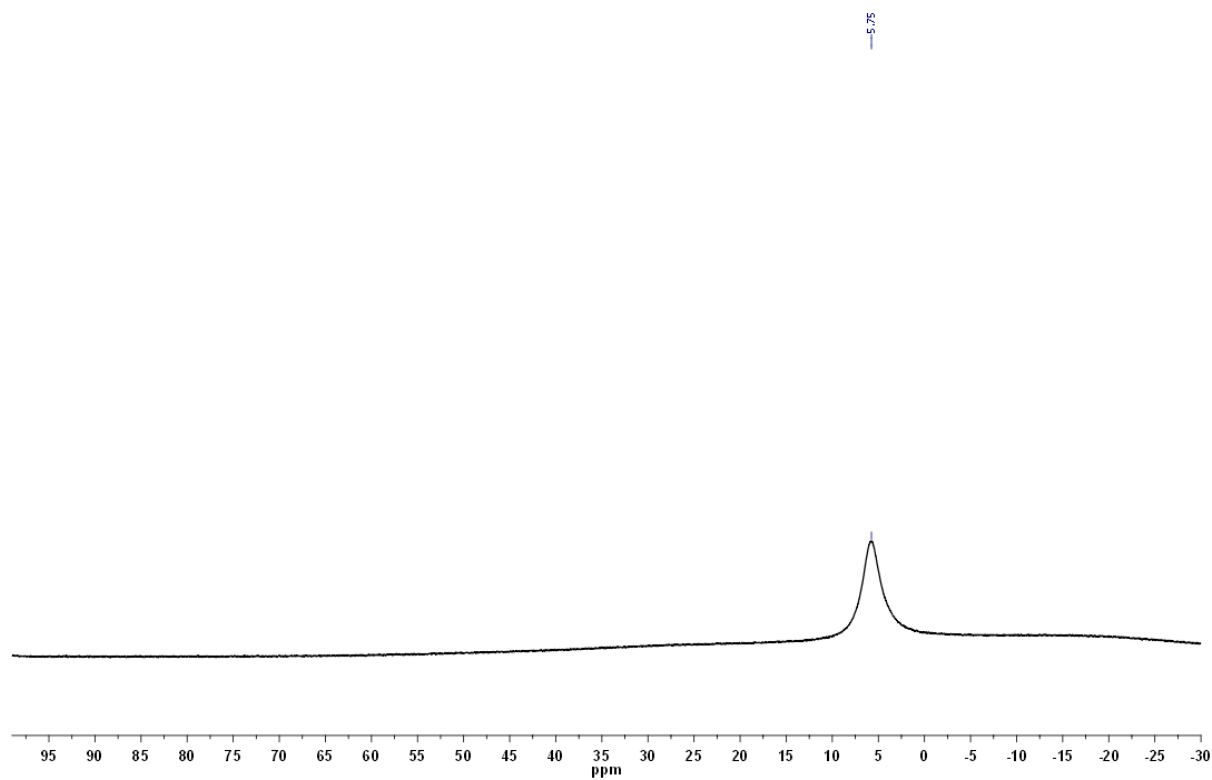


Figure 6.3.7 ^{11}B NMR spectrum of **1** (toluene- d_8 , 70 °C).

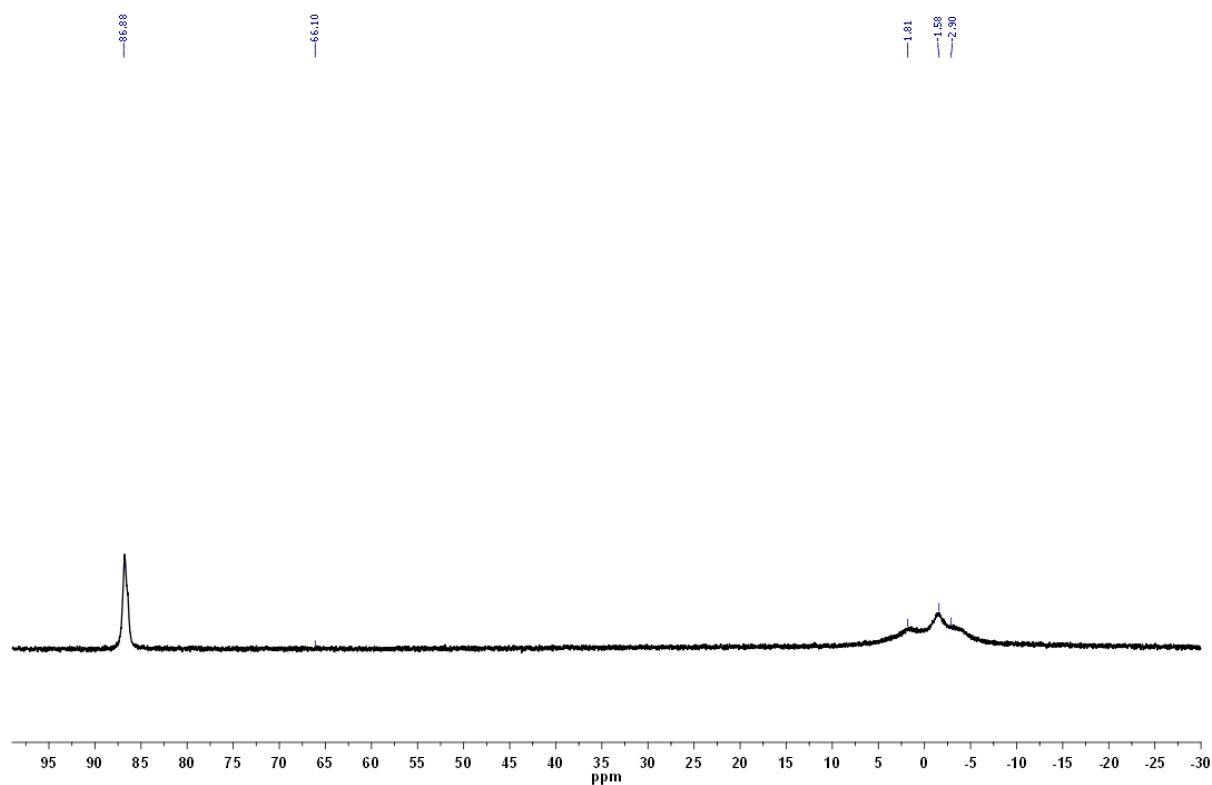


Figure 6.3.8 ^{11}B NMR spectrum of **1/MAO** (toluene- d_8 , 70 °C).

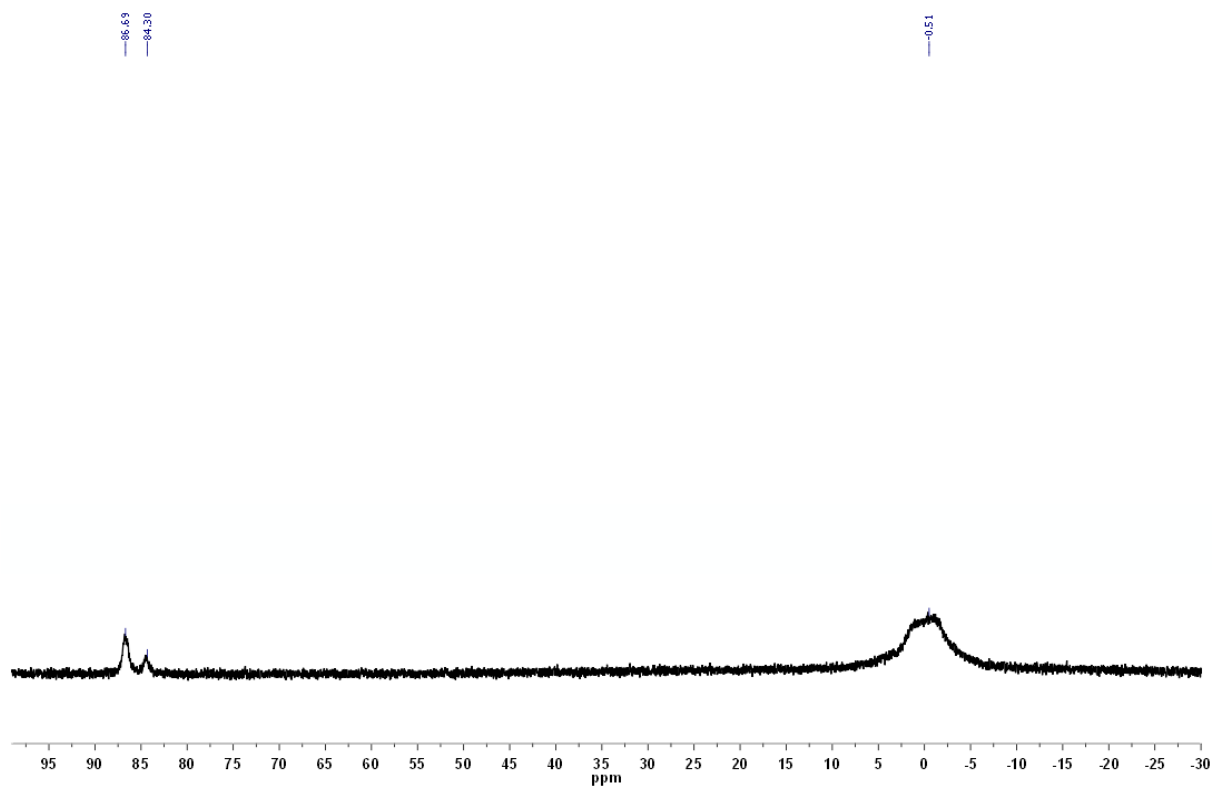


Figure 6.3.9 ^{11}B NMR spectrum of 1/MAO/NBE (toluene- d_8 , 70 °C).

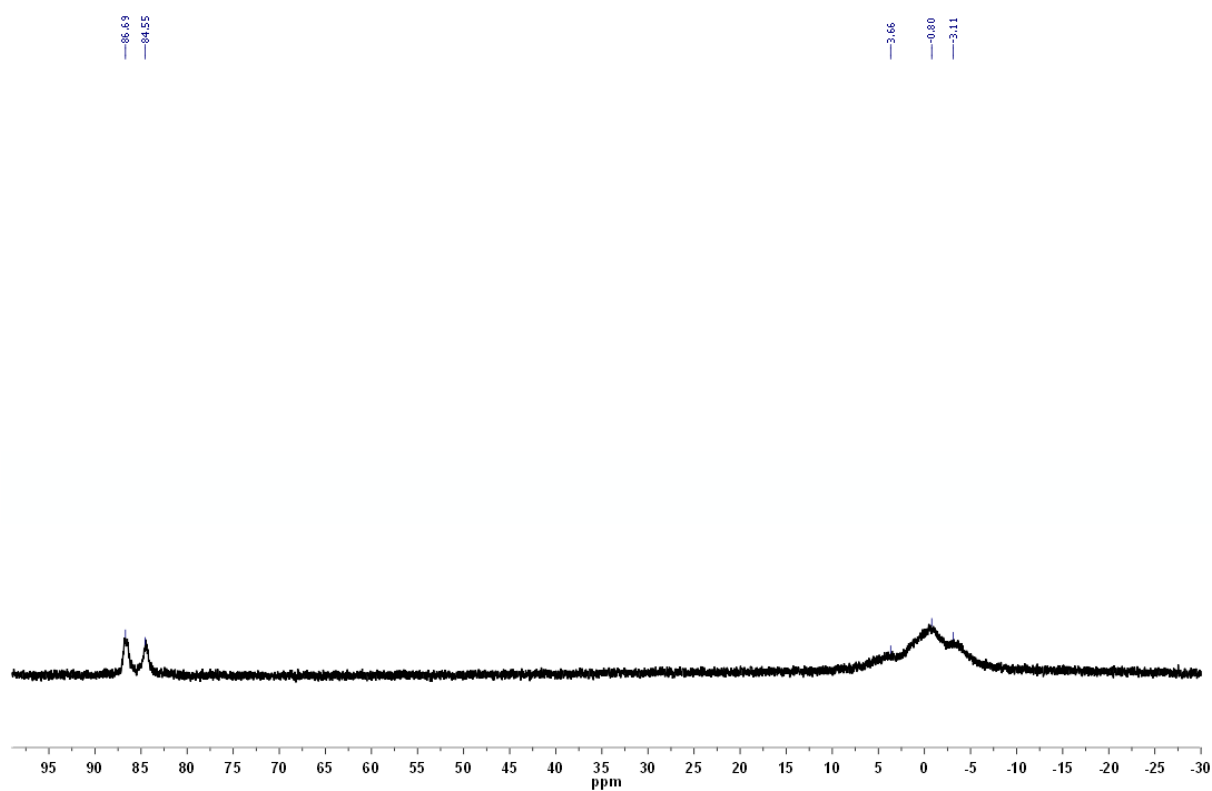


Figure 6.3.10 ^{11}B NMR spectrum of 1/MAO/NBE (toluene- d_8 , 80 °C).

7. Curriculum Vitae

Date of Birth September 14th, 1983
Nationality P. R. China
Address Nanningnan 78, Heping district, Shenyang, 110013,
 P. R. China
E-mail guangjuan.xu@gmail.com, gjx1019@163.com

Education

2010/08-Present Institute of Polymer Chemistry, University of Stuttgart
 Supervisor: Prof. Dr. Micheal R. Buchmeiser
2007/09-2010/07 Institute of Physical Chemistry, Northeast Normal University
 Master of Science
 Supervisor: Prof. Zhongmin Su
2003/09-2007/07 Dept. of Chemistry, Beihua University
 Bachelor of Science

Main Publications

1. Poly(ethylene)-co-Poly(norborn-2-ene) Prepared by Group IV Bisamido and Half-Sandwich Amido Complexes with Pendant Aminoborane Groups: Vinyl Insertion vs. Ring-Opening Metathesis Polymerization. G. J. Xu, G. V. Narayana, M. Speiser, D. R. Wang, M. R. Buchmeiser, *Macromol. Chem. Phys.* **2014**, *215*, 893-898.
2. Stereospecific Styrene Polymerization by Methylalumoxane-Activated Ti (IV) N-Trimethylsilylamido-Complexes Bearing the N-Biphenyl or N-(6-(2-(Diethylboryl)phenyl)-Pyrid-2-yl) Motif. G. V. Narayana, G. J. Xu, D. R. Wang, M. Speiser, W. Frey, M. R. Buchmeiser, *Macromol. Chem. Phys.* **2014**, DOI: 10.1002/macp.201300764.
3. Methylalumoxane-Activated Group-4 Bisamido-Complexes Bearing the 6-(2-(Diethylboryl)phenyl)-Pyrid-2-ylamido Motif: Access to Ultra-High Molecular Weight Poly(ethylene) and Activity Boost in the Presence of Cyclopentene. G.

- V. Narayana, G. J. Xu, D. R. Wang, W. Frey, M. R. Buchmeiser, *ChemPlusChem* **2014**, *79*, 151-162.
4. Visible Light-Induced Grafting from Polyolefins. M. Ciftci, P. Batat, A. Demirel. G. J. Xu, M. R. Buchmeiser, Y. Yagci, *Macromolecules* **2013**, *46*, 6395-6401.
 5. Functional Ring-Opening Metathesis Polymerization-Derived Poly(cyclopentene)s. K. Herz, D. A. Imbrich, J. Unold, G. J. Xu, M. Speiser, M. R. Buchmeiser, *Macromol. Chem. Phys.* **2013**, *214*, 1522-1527.
 6. Functional Polyolefins: Poly(ethylene)-*graft*-Poly(*tert*-butyl acrylate) *via* Atom Transfer Radical Polymerization From a Polybrominated Alkane. G. J. Xu, D. R. Wang, M. R. Buchmeiser, *Macromol. Rapid Commun.* **2012**, *33*, 75-79.
 7. A new 2D 5-connected coordination polymer based on 3,4-bis(pyridin-4-ylmethoxy)benzoic acid ligand. G. J. Xu, Y. H. Zhao, K. Z. Shao, Y. Q. Lan, P. Li, Z. M. Su, *Inorg. Chem. Commun.* **2010**, *13*, 932-934.
 8. A novel luminescent 3D metal–organic framework possessing 4-fold interpenetrating (3,4)-connected net. G. J. Xu, Y. H. Zhao, K. Z. Shao, G. Yuan, Z. M. Su, L. K. Yan, *Inorg. Chem. Commun.* **2009**, *12*, 969-971.
 9. Syntheses and characterizations of five coordination polymers constructed by 3,5-bis(pyridin-3-ylmethoxy)benzoic acid ligand. G. J. Xu, Y. H. Zhao, K. Z. Shao, G. S. Yang, Y. Q. Lan, X. L. Wang, Z. M. Su, L. K. Yan, *Polyhedron* **2009**, *28*, 3155-3161.
 10. Three novel 3D (3,8)-connected metal–organic frameworks constructed from flexible-rigid mixed ligands. G. J. Xu, Y. H. Zhao, K. Z. Shao, Y. Q. Lan, X. L. Wang, Z. M. Su, L. K. Yan, *CrystEngComm.* **2009**, *11*, 1842-1848.

Posters and International Conferences

1. Poly(ethylene)-*graft*-Poly(*tert*-butyl acrylate) *via* Atom Transfer Radical Polymerization: Functional Polyolefins From Polybrominated Alkanes. G. Xu, M. R. Buchmeiser, The 4th EuCheMS Chemistry Congress, August 26-30, **2012**, Prague, Czech Republic.

Erklärung über die Eigenständigkeit der Dissertation

Ich versichere, dass ich die vorliegende Arbeit mit dem Titel:

„Functional Polyolefins Prepared by Group 4 Diamide Complexes Through Tandem Ring-Opening Metathesis/Vinyl Insertion Polymerization”

selbstständig verfasst und keine anderen als die angegebenen Quellen und Hilfsmittel benutzt habe; aus fremden Quellen entnommene Passagen und Gedanken sind als solche kenntlich gemacht.

Declaration of Authorship

I hereby certify that the dissertation entitled:

„Functional Polyolefins Prepared by Group 4 Diamide Complexes Through Tandem Ring-Opening Metathesis/Vinyl Insertion Polymerization”

is entirely my own work except where otherwise indicated. Passages and ideas from other sources have been clearly indicated.

Name/Name: _____

Unterschrift/Signed: _____

Datum/Date: _____